MODELLING WATER QUALITY DYNAMICS BY INTEGRATING PYWR, CLIMATE CHANGE, AND LAND-COVER SCENARIOS:

A CASE STUDY IN THE GROOTDRAAI DAM CATCHMENT, UPPER VAAL, SOUTH AFRICA

A thesis submitted in fulfilment of the requirements for the degree of

MASTER OF SCIENCE

RHODES UNIVERSITY

By

SOFIA LAZAR

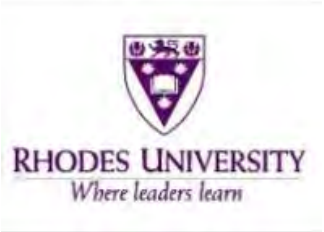

April 2024

ABSTRACT

Water resource management faces global challenges in allocation, quality, and sustainability. Despite extensive focus on quantity, water quality remains neglected, especially in developing nations, owing to data scarcity and funding issues. Water quantity modelling is more advanced, leaving water quality modelling lagging, as it requires finer spatiotemporal scales. Global water quality models, including those used in South Africa, encounter complexity and data requirements, and some proprietary models limit access. In South Africa, a water quality model is integrated with the less accessible Water Resources Yield Model (WRYM). However, WRYM's spatial lumping may not suffice for water quality assessment, emphasising the need for improvement. This study aims to address the gap in water quality modelling by transitioning from lumped, proprietary, and monthly time-step models applied in South Africa to more spatially distributed, user-friendly, transparent, fast models and daily time-step models, using the Grootdraai Dam Catchment in the Upper Vaal as a study region. The study examines providing water quality simulation for various variables under different tested scenarios, including (i) land-use scenarios (e.g., urbanisation, industrialisation, population growth and expansion in agricultural areas); (ii) mixed scenarios (e.g., climate change, mine closure, and demand increase). The study proposed a framework shifting from the WRYM to a Python water resources (Pywr) model, linked with the Water Quality Systems Assessment Model (WQSAM) in the Grootdraai Dam Catchment. This integration, the Python water resources-Water Quality (Pywr-WQ) model, was developed by the Water Research centre (WRc) in the United Kingdom. The study employed multiple regression models to develop land-use models, the outcomes of which were integrated into the Pywr-WQ model for medium and long term land-use scenario predictions. The study resulted in the following findings: (1) significant patterns emerge concerning the impacts of urbanisation, mining, and agricultural expansion on water quality; (2) urban areas exhibit elevated levels of nitrate plus nitrite and ammonium over the long term associated with human activities and infrastructure development; (3) increased cultivation leads to heightened phosphate levels, indicative of agricultural runoff and potential high fertiliser usage, while the expansion of mining activities results in elevated concentrations of sulphate and Total Dissolved Solids (TDS), attributed to the discharge of mine effluents; (4) noticeable declines in the concentrations of TDS and sulphate are evident in the medium to long term when compared to the baseline simulations. However, the worst-case scenario (i.e., a 70% abstraction increase) exhibits elevated peaks and concentrations compared to scenarios with more probable demand increases (e.g., a 5% increase).

DEDICATION

In loving memory of my dear father, Hocine Lazar, and my esteemed grandfather, Yahia Battache, whose spirits dance among the stars, illuminating my path with eternal love and wisdom, this thesis is dedicated.

ACKNOWLEDGEMENTS

I express my sincere gratitude to Sasol, Eskom, the Department of Water and Sanitation (DWS), and the Water Research Commission (WRC) for their financial support, which played a pivotal role in the successful execution of this study. Additionally, I extend my appreciation to the DWS and Rand Water for granting access to data resources.

I extend my heartfelt appreciation to Dr Neil Griffin, and Dr Andrew Slaughter, for their exceptional guidance, mentorship, and continuous support throughout every phase of this study. Their invaluable supervision, profound insights, and expertise have been instrumental in shaping the trajectory of this study and nurturing its development. I am profoundly grateful for their mentorship and encouragement, which have significantly contributed to my personal and professional growth. Special thanks to Dr Frank Akamagwuna for his guidance, and to Prof Oghenekaro Nelson Odume for his support.

I express my gratitude to the staff and students, both past and present, of the Institute for Water Research (IWR), whose generous assistance has been invaluable throughout this journey.

I extend my heartfelt gratitude to my beloved family members, my mother, brothers, uncles, and aunts, for their continuous support and encouragement.

Above all, I offer my deepest thanks to God, whose guidance and presence have sustained me through every challenge. The promise to never leave nor forsake has been a steadfast source of comfort and assurance.

TABLE OF CONTENTS

LIST OF TABLES

LIST OF FIGURES

LIST OF APPENDICES

LIST OF ABBREVIATIONS

AQUATOOL	A Generalized Decision-Support System For Water-Resources Planning And Operational Management
C2Vsim	The California Department Of Water Resources Central Valley Groundwater-Surface Water Simulation Model
CSIR	Council For Scientific And Industrial Research (South Africa)
CWatM	The Community Water Model
DMRE	Department Of Mineral Resources And Energy (South Africa)
DWAF	Department Of Water Affairs And Forestry (South Africa)
DWS	Department Of Water And Sanitation (South Africa)
FAO	Food And Agriculture Organization
GSFLOW	GSFLOW-Coupled Groundwater And Surface-Water FLOW Model
IWQM	Integrated Water Quality Management
MIKE	Model-Based And Incremental Knowledge Engineering
MODSIM	Decision Support System For Integrated River Basin Management
PCC	Presidential Climate Commission
Pywr	Python Water Resources Model
Pywr-WQ	Python Water Resources – Water Quality Model
RQOs	Resources Quality Objectives
SWAT	Soil And Water Assessment Tool
TDS	Total Dissolved Solids
UNEP	United Nations Environment Programme
WEAP	Water Evaluation And Planning System
WQSAM	Water Quality System Assessment Model
WRIMS	Water Resource Integrated Modelling System
WRYM	Water Resources Yield Model
WEF	Water-Energy-Food Nexus
WEFE	Water-Energy-Food-Environment Nexus
WWTW	Wastewater Treatment Works

CHAPTER 1: GENERAL INTRODUCTION AND LITERATURE REVIEW

1.1 Introduction

Global water quality is on a continual decline (Ayana, 2019; Blanchon, 2003; Bouleau & Pont, 2014; Cariou, 2015; Moyen-Orient & du Nord, 2007; Verdier & Viollet, 2015), primarily attributed to various human-induced factors such as urbanisation, industrialisation (Akamagwuna, 2021; Odume, 2011, 2014, 2017, 2020), and the expanding human population (Cropper & Griffiths, 1994; Cullis et al., 2018). In the next five decades, varied global scenarios are anticipated, including the potential for stagnation or decline in developed regions and continued rapid growth in less developed areas (Bongaarts, 2009). The human population growth will require increased food production, agricultural activities, and intensified land-use, which will, in turn, affect water health (Davis et al., 2015; FAO, 2006). Urbanisation has emerged as a factor contributing to the loss of biodiversity, increased eutrophication, and changes in aquatic biological communities which impact water quality and increase potential risks to public health (House et al., 1993). Climate, land-use, population density, and landscaping exert a significant influence on pollutant concentration, resulting in variable impacts (Bradford, 1977; House et al., 1993; Pitt, 1979). Soil and water degradation are accelerated by inputs of nutrients, organics, and other forms of pollutants, including sediments and metals, into the stream and riverine ecosystems (Dickinson, 2003; Gwapedza et al., 2020; Wong, 2003; Zhu et al., 2013). For instance, mining activities pose a rising challenge to water quality management, negatively impacting the water environment by elevating suspended solids, mobilising minerals, and reducing the pH of the receiving water (Ochieng et al., 2010). Within the context of South Africa, mining activities are considered to be the major mobilizer of toxic metals in environmental landscapes (Okereafor et al., 2020).

Models play a central role in managing water quantity and quality owing to their effectiveness in investigating future scenarios and the associated impacts on water resources, and in monitoring and supporting decision-making processes (Andreu et al., 1996; Cortés et al., 2003; Roberts, 2003). These models exhibit variations in structure, time-step, accessibility, and methodologies (Xu & Singh, 1998, 2004). The ongoing development of models remains an active process, with new models and versions emerging annually. In the context of developing countries like South Africa, data scarcity presents a growing challenge for both research and practical applications in various industries (Baisch, 2009; Dinku, 2019). This scarcity underscores the need to establish

effective communication between the scientific community and policymakers, with models serving as crucial tools in facilitating this exchange. Consequently, leveraging existing models in these regions for improvement and adaptation is more efficient and feasible than developing a model from the ground up.

The Water Resources Yield Model (WRYM) has been utilised in Southern African countries for over two decades (Juízo & Lidén, 2010; Nkwonta et al., 2017) and is frequently employed as a national water resource allocation tool in South Africa. Initially designed for water resource allocation, the WRYM has also been applied to generate water quantity data for water quality modelling in a previous study (e.g., Slaughter et al., 2018). The WRYM operates at a monthly time-step and is characterised as a black-box model as users do not have open access to the underlying code. Past application of WYRM to catchments in South Africa has adopted a lumped spatial structure as this has been deemed adequate for water quantity management. Consequently, while existing WRYM models may be effective for visualising the water operating system and for water quantity modelling, their structures may not be sufficiently detailed for the intricacies of water quality modelling. Water quality models require more intricate, distributed structures that consider both point and non-point pollution inputs from various water users (e.g., agricultural, industrial, and domestic) (Rode et al., 2010), including return flows, potential leakage, abstractions, and potential sewage, as well as land-uses, such as mining and agriculture. Since water quality processes also take place at fine temporal scales, water quality modelling should be conducted at a daily time-step as a minimum. At the same time, the existing WRYM model applications can continue to be of use for water quality modelling, despite the shortcomings mentioned above (Juízo & Lidén, 2010). Therefore, some way of converting them to a more distributed structure and operating at a finer temporal scale should be identified rather than creating new model applications from scratch.

This study aims to establish a framework facilitating the shift from a monthly lumped model (i.e., WRYM) to a daily distributed model named the Python water resources (Pywr) model (Tomlinson et al., 2020). While previous applications of the Water Quality System Assessment Model (WQSAM) have read inflow data from the WRYM as input data, this study chose to use the Python water resources-Water Quality (Pywr-WQ) model : an adaptation in Pywr in which the water quality processes of WQSAM (Slaughter et al., 2012; Slaughter & Mantel, 2017) are dynamically integrated into Pywr. There are two advantages to this approach: (1) the time taken to transfer flow data from the yield model to WQSAM is avoided, which was of benefit, given the large number of scenarios investigated in this study; (2) while only touched on briefly in this

study, the dynamic integration allows water quality to inform water allocation in the Pywr model, which has several considerable advantages for future work, as discussed later (section 4.4.2).

The rest of this chapter is devoted to a literature review. It is important to note that each subsequent chapter will include an in-depth literature review tailored to its specific focus and objectives. It commences with an exploration of water resource models in developing countries, specifically focusing on South Africa, and then proceeds to an examination of the National Water Resources Strategy (NWRS) version 1 and 2. The review delves into the drivers of water quality degradation, with an evaluation of both sources and impacts of pollutants. The concluding part of this chapter captures the rationale behind this study, articulates the study questions, and outlines the study's aim and objectives. An overview of the overall thesis structure is also provided.

1.2 Water Resources Models

Simulation models have historically played a crucial role in water resources management and planning applications. Previous studies have primarily focused on assessing the influence of water systems on economic development and designing efficiency (Maass et al., 1962; Loucks et al., 1981). System dynamics rely significantly on the integration of both quantitative and qualitative data to delineate feedback loops within complex systems (Forrester, 1968). These water resources models serve to enhance our current qualitative comprehension by incorporating supplementary quantitative information as highlighted by Loucks & van Beek (2017). Several simulation models have been developed by various authors and institutions (Andreu et al., 1996; Jha & Das Gupta, 2003; Draper et al., 2004; Sieber & Purkey, 2007; Sulis & Sechi, 2013), models that portray the water system network through the representation of edges and nodes as described by Tomlinson et al. (2020).

There are two types of simulation models distinguished by their approach to water allocation. Shrestha et al. (1996) emphasise the significance of rules-based models in aiding decision-making processes within water resource management. These models assist in prioritising allocation and identifying optimal strategies. Rules-based models can be integrated with optimisation to enhance their capacity for providing comprehensive solutions to complex challenges. In contrast, the second type of simulation model utilises mathematical programming to simulate water allocation in the resource network, transforming the water system representation into a mathematical optimisation problem as defined by Tomlinson et al. (2020). Simulation models such as Pywr exemplify the integration of simulation with optimisation. Pywr employs linear programming to minimise penalties at each time-step, illustrating the fusion of

simulation and optimisation to iteratively identify optimal solutions according to defined objectives and constraints (Tomlinson et al., 2020).

Simulation models have faced challenges in incorporating parametric adjustments and alternative objectives, such as power capacity maintenance, into optimisation models for water resource systems (e.g., Labadie, 2004; Wurbs, 2005). Water allocation systems differ across simulation models. A wide range of such models has been developed, including Model based and Incremental Knowledge Engineering (MIKE) (Angele et al., 1992), the water balance network model (MODSIM) (Labadie, 2003), the Water Resources Integrated Modelling System (WRIMS) (Draper et al., 2004), and the Water Evaluation and Planning (WEAP) (Sieber & Purkey, 2007). These computational models demonstrated the capability to project hydrological parameters, encompassing river flows, reservoir storage, water abstractions, return flows, and related variables (Adgolign et al., 2016; Neubert, 1993). This projection incorporates inflow dynamics and operational regulations. In general, these models have utilised a node-link structure, where nodes represent various elements like reservoirs, boundary inflows, water demands, return flows, and reservoir discharge, while links represent connections such as river reaches and transfers. Most of these models facilitate the redistribution of water within a depicted system by assigning priority levels to various water allocations (Azevedo et al., 2000; Nabinejad et al., 2017; Yates et al., 2005). This prioritisation is mathematically formulated as the minimisation of a penalty, typically achieved through the application of linear programming algorithms (Can & Houck, 1984; Momoh et al., 1999). Water resource systems, characterised by their inherent complexity, are influenced by a myriad of qualitative and quantitative factors that collectively govern the availability of water resources (Raju & Pillai, 1999). In the context of transboundary river basins, water allocation can become a contentious issue, potentially leading to political sensitivities among countries sharing these resources. For example, disagreements among developing countries, such as South Africa, Swaziland, and Mozambique, regarding transboundary catchment management aspects like water allocation, environmental flow releases, and inter-basin transfers have persistently surfaced as a significant concern (Nkomo & van der Zaag, 2004). Furthermore, in the face of climate change, reservoir and resource management has become increasingly crucial, with research highlighting the challenges and issues prevalent in South Africa's water resource management (Savenije & van der Zaag, 2008).

Lumped models based on the black-box approach have been commonly employed in hydrological studies according to Xu & Singh (2004). Black-box models are characterised by their ability to use inputs and outputs to generate useful information, without revealing the

internal workings of the model (Maeda et al., 2021). For instance, the WRYM is a process-based model that incorporates operating rules. Despite representing processes, it remains a black-box model because users cannot access its internal workings. The Pywr model is also process-based; however, Pywr distinguishes itself as an open-source platform, allowing users to access and understand how processes are represented within the model.

Many of these models use the storage concepts as discussed in Fleming (1975). These lumped models have undergone substantial development over the past few decades, encompassing time-steps from monthly to less than a day. For instance, monthly models such as the T-model (Thornthwaite, 1955), the abcd-model (Thomas Jr, 1981), and the P-model (Alley, 1984; Palmer, 1965) conceptually describe hydrologic processes occurring on land, which are spatially averaged or lumped (Xu & Singh, 1998). In addition, daily lumped models have emerged in recent decades in Europe, the United States of America, Canada, and Asia, such as the Hydrologiska Byråns Vattenbalansavdelning (HBV) model (Bergström, 1992), the daily version of the Monash rainfall-runoff (HYDROLOG) model (Porter & McMahon, 1971) and the Xinanjiang model (Zhao, 1992). Nonetheless, notable challenges confronting monthly or daily lumped and distributed models are the scarcity, unavailability, and insufficiency of meteorological data (e.g., precipitation, temperature) (Baisch, 2009; Dinku, 2019), as these models depend heavily on such data to estimate hydrological parameters. These lumped models serve diverse purposes such as flood prediction, water resources assessment, studies on the impact of climate change, and water resources management, as outlined by Xu & Singh (2004).

Within the context of Southern African countries, the WRYM has played a pivotal role as the primary tool in official joint water resources studies, as confirmed by Juízo & Lidén (2010). However, it is essential to recognise that water resources infrastructure alone may not be the sole determinant of water availability and equitable allocation between nations and various users within a shared river basin (Juízo & Lidén, 2010). Remarkably, WRYM has served as the cornerstone of water resources management in the region for over two decades, as documented by Nkwonta et al. (2017). It is imperative to acknowledge that a country's development is intricately intertwined with its management of water resources (Casey et al., 2017). Nevertheless, the prevailing reliance on the WRYM tool has resulted in a shift in the focus of discussions. Instead of primarily centring on strategies to enhance water resource allocation among Southern African countries, the conversation has transitioned towards an in-depth examination of the tool's inherent characteristics and limitations (Juízo & Lidén, 2010). This shift in emphasis may have contributed to the emergence of trust issues among Southern African countries engaged in

collaborative river-basin projects. The transparency and user-friendliness of the models are important factors in water resource allocation models (Horlitz, 2007; Juízo & Líden, 2008; Wurbs, 1993), with these two characteristics lacking in the most utilised water resource management model in Southern Africa.

Previous study has underscored the significance of factors beyond technical complexity when evaluating the efficacy of water resource allocation models within shared river basins (Juízo & Líden, 2008). These factors include the integrity and transparency of the model developer, as well as the principles guiding allocation and prioritisation specific to the river basin in question. Within this context, it becomes evident that the WRYM poses certain challenges. The model's intricate nature and limited transparency often hinder stakeholders' comprehension and trust in the outcomes it produces. Furthermore, trust issues have arisen between the predominantly South African model developers and other governments acting as stakeholders in shared river basins (Juízo & Lidén, 2010). It is important to note that the utilisation of the WRYM requires authorisation, as it operates under licensing restrictions for water resource projects and research. The ensuing controversies regarding the model's performance can potentially spill over into disputes surrounding system analysis results (Juízo & Líden, 2008). Moreover, according to Xu & Singh (2004), in a lumped approach to runoff modelling, the catchment is regarded as a spatially singular entity with the role of converting rainfall excess into an outflow hydrograph, utilising a black-box approach to model various hydrological processes. The optimisation operation of the WRYM utilises a black-box approach as it considers the water wastage as outflows from the system (Nkwonta et al., 2017). Hence, in various instances (e.g., Arnold & Orlob, 1989; Paredes & Lund, 2006), water resource management tends to disregard the aspects related to water quality, often treating them exclusively as constraints rather than integral components of the management framework (Paredes-Arquiola et al., 2010). Lumped models, exemplified by the WRYM model, tend to route runoff directly to the catchment outlet without explicit consideration of interactions among runoff from diverse areas. The oversight of how these interactions impact solute export introduces uncertainties, with the spatial representation of the catchment being a notable concern, as highlighted by Neumann et al. (2007). This limitation could serve as a barrier to achieving sustainable and equitable water management and planning, particularly concerning water quality, a critical aspect, especially in developing countries. Hence, developing countries should consider implementing distributed daily models capable of reflecting water quantity dynamics and easily integrating with water quality models such as the Pywr model.

According to Tomlinson et al. (2020), Pywr is a computational library that enables modellers to construct water resource models and conduct multi-objective assessments. The modular model's architecture facilitates smooth deployment in high-performance and cloud computing environments. The Pywr algorithm operates with two key loops in simulations: an outer loop, progressing through time-steps (e.g., monthly, weekly, daily), and an inner loop, exploring scenarios within each time-step. The Pywr model uses directed graphs with core nodes like "input", "output", "storage" and "links", and the Pywr library provides essential tools for modelling, organising, executing, and analysing resource systems.

This versatile tool not only bridges the gap in cross-sectoral approaches to investment strategies but also facilitates an objective conceptualisation of the Water-Energy-Food (WEF) nexus (e.g., Gabriel & Palma, 2021). Moreover, Pywr's potential extends to guiding sustainable development by facilitating the design, operation and optimisation of Water-Energy-Food-Environment (WEFE) resource systems. Within the Volta River Basin, particularly in the context of Ghana (Gonzalez et al., 2021), Pywr served as a valued tool for analysing the consequences of proposed infrastructure development and operational strategies on the existing water supply system, ecosystem services, and conflicts among stakeholders. The flexibility of the Pywr model, coupled with its adaptability to simulate power systems in developing countries, as exemplified in the case study of Ghana (Gonzalez et al., 2021), has emerged as an instrumental factor in addressing the longstanding challenges identified in previous studies. In its application to a river basin in Chile (Vicuña et al., 2019), Pywr served as an essential tool in analysing various interventions, such as infrastructure development and policy changes. In the context of climate change, the Pywr model has proved its efficiency in evaluating and optimising adaptation measures for water supply, including storage infrastructure and water market extensions, with a specific application to the City of Santiago, Chile (Ricalde et al., 2022).

The Pywr model has an excellent computational speed, with the time taken to run 160 scenarios only approximately four times that to run a single scenario (Tomlinson et al., 2020). Past studies showed that running multiple scenarios in one simulation is more efficient than running each scenario in separate parallel processes that do not share memory (e.g., Hybinette & Fujimoto, 2001; Pinho et al., 2012; Tomlinson et al., 2020). Pywr was also employed in the optimisation of a land-cover design in a catchment area with multiple objectives, including flood propensity, total annual runoff volume, solar power potential, food production, and ecosystem health (Janus et al., 2023).

1.3 National Water Resources Strategy (NWRS)

In South Africa, the development of water policy has been influenced by political and technical factors, leading to the establishment of the National Water Act (NWA) in 1998 (de Coning, 2006), and the Water Services Act (No. 108 of 1997) (DWAF, 1997). The NWA and WSA aim to ensure equitable access to water for all South Africans ending all racial, class, and gender discrimination, protecting the environment, and promoting sustainable water management practices. Additionally, the WSA deals with the provision of water supply, sanitation services, and how to price water within the context of a municipal financing policy.

Resource Directed Management (RDM) was developed by the Department of Water Affairs and Forestry (DWAF) in 2006 to ensure the sustainable management and protection of water resources, considering ecological, social, and economic considerations. Although the NWA does not explicitly mention RDM, it still recognizes the principle that water resources should not be exploited to the detriment of future users. RDM involves implementing strategies and actions aimed at managing factors that contribute to negative effects on water quality, guided by Resource Quality Objectives (RQOs) according to DWAF (2006). This includes Source Directed Control (SDC) to address the root causes of water quality issues. As part of RDM, Catchment Management Strategies (CMS) are developed, incorporating a water quality framework plan and a water quality allocation plan aligned with Resource Water Quality Objectives (RWQOs) to achieve RQOs (DWAF, 2006). According to DWA (2011), RDM measures are applied to address water quality issues in the Grootdraai Dam Catchment to mitigate the impact of urban, mining, and industrial areas, as well as dryland agriculture, and to protect the water quality in the dam.

The NWA mandated the creation of the National Water Resources Strategy (NWRS), the inaugural version of which was released in 2004, followed by the second edition (NWRS2) in 2013. The NWRS2 outlines various key aspects, including objectives, challenges, and proposed actions, as described by DWS (2013). However, some areas might be critical and need further exploration. While the NWRS2 underscores the importance of involving stakeholders in the decision-making process concerning water resources management and planning, such as local communities, industries, and environmental groups, a structured procedure, or tools, to facilitate this objective is not clearly defined. For instance, previous studies have identified this shortcoming as a barrier to achieving sustainable and equitable water resource management (Adom & Simatele, 2022; Anokye, 2013; Conallin et al., 2017; Megdal et al., 2017; Sigalla et al., 2021). In addition, DWS (2013) affirmed that, in the majority of instances, deficiencies in water supply can be attributed not to inadequacies in water resources availability, but rather to

deficiencies in the management of water supply systems. For instance, there is an urgent need to improve water management practices and infrastructure maintenance to ensure more efficient and sustainable water resource management (Mothetho, 2018; Ruiters & Matji, 2015). The NWRS2 acknowledges that South Africa faces challenges related to climate change impacts, pollution, and poor governance, but the complex interaction between changes in water quantity and quality, along with their combined impacts, remains largely unexplored in South Africa (Schulze, 2010). Research into the influence of climate change on water quality remains in its nascent stage and requires further development (Ngcobo, 2013). Currently, there is limited integration of climate change scenarios into water quality modelling, and the capacity for conducting comprehensive assessments of climate change is insufficient (Ziervogel et al., 2014). Consequently, a critical gap exists in fully incorporating water quality considerations into long term planning to ensure water supply and quality security in South Africa, particularly under changing conditions.

1.4 Key Drivers of Water Quality Degradation in South Africa

South Africa grapples with water scarcity as the demand for and utilisation of water surpasses the natural resources available in various river basins (UNEP, 2009). Since 1994, the substantial increases in South Africa's population across multiple provinces have posed a substantial challenge, triggering concerns for water scarcity and security and leading to water quality-related risks to human health (Tempelhoff, 2009). Several factors contribute to water quality degradation, among them: (i) changes in land-use and land-cover; (ii) inadequate and unsuitable irrigation practices; (iii) lack of wastewater treatment; (iv) effluent from mines; (v) climate change. For instance, salinisation remains an ongoing water quality concern in South Africa, primarily attributed to the discharge of municipal and industrial effluents, the return flows from irrigation, urban stormwater runoff, the mobilisation of pollutants from mines and businesses, and seepage from waste disposal sites (Dikio, 2010; du Plessis, 2017; Lerotholi et al., 2004; Williams et al., 2003). In addition, unsustainable abstraction may contribute to water quality problems, leaving less water available for dilution. Chapman (2021) demonstrated the evolving significance of water quality issues from the 1850s to the post-1980s era, emphasising concerns such as organic pollution, metal pollution, eutrophication, nitrate pollution, and acid rain. These water quality issues may be caused by high population growth, economic development, and an increase in infrastructure development that induces changes in catchment hydrological response, such as dams or transfer schemes.

According to the DWA (2011), various water quality issues were identified within the Upper Vaal water management area including eutrophication, salinisation, turbidity, toxicants, and acid mine drainage. These issues primarily stem from factors such as Wastewater Treatment Works (WWTW), intensive agriculture, fertiliser application, and urban sewage, as well as operational and abandoned mines. In 2011, DWA warned that without effective mine water management, Grootdraai Dam's long term water quality is at risk, particularly during closures. Furthermore, the water quality in the Vaal River at Schmidtsdrift, which is upstream of Grootdraai Dam, was found to be unacceptable owing to high levels of salts and nutrients, especially high levels of ammonia.

1.5 Rationale and Significance of the Study

The Vaal River Catchment, particularly the Grootdraai Dam Catchment, plays a pivotal role in South Africa's socio-economic well-being (du Plessis et al., 2015). It serves as a crucial pillar for various industries, including manufacturing, mining, agriculture, tourism, and petrochemical production, all vital for the country's economic development (DWAF, 2004). These sectors heavily rely on the raw water supply from the Vaal and the Grootdraai Dam catchments to sustain their operations. Nonetheless, water quality in the catchment has shown a concerning decline over time (du Plessis et al., 2015). This deterioration has been attributed to a multitude of factors, encompassing non-point sources (Ncube, 2015; Ntshalintshali, 2019), like runoff from agricultural lands, and point sources, such as inadequately treated or untreated effluents discharged from municipal WWTW (du Plessis et al., 2015). The compounding effect of variable and evolving climate patterns, changes in land-use, and a lack of predictive tools for informed scenario analysis collectively contribute to the complex challenge. The catchment encompasses the upper Vaal River, its tributaries, and several smaller streams, receiving inflows from transfer schemes like Heyshoop and Zaaihoek, while also transferring water out to the Vaal-Olifants transfer scheme (Pitman et al., 2002).

The poor raw water quality can escalate the cost of treating the abstracted water to meet industrial standards. This, in turn, may increase operational expenses for industries, potentially leading to job losses and endangering the sustainability of raw-water-dependent operations in the catchment. Ecologically, water quality degradation may result in increased biodiversity loss, reduced species diversity, and wetland degradation in the catchment (Akhtar et al., 2021).

Addressing this issue requires technical solutions and decision-making frameworks to assist in informed decision-making which is currently lacking and one of the key drivers of poor water resource management, among which a predictive model can fulfil the crucial need to forecast

water quality changes. This study aligns with the broader framework of water quality management in South Africa, providing a contribution to academic research in the field. Hence, this study's contributions are presented in three pillars: (i) application of the open-source, free Pywr model, validated against the licensed, commonly employed WRYM for water quantity modelling, and the Pywr-WQ model for water quality modelling; (ii) examination of the dynamics in water quality under various scenarios (i.e., climate change, changes in land-use, and water use changes) over the medium and long term; (iii) development of water quantity-quality modelling frameworks for sustainable and equitable water resource management.

1.6 Aim and Objectives

1.6.1 Aim

This study aimed to predict current and future water quality changes in the Grootdraai Dam Catchment due to various natural and anthropogenic factors, including land-use and land-cover changes, climate change, and planned demand increases, across medium and long term scenarios identified by stakeholders as possible.

1.6.2 Objectives

The study questions that prompted the specific objectives are as follows:

i. What is the applicability and effectiveness of the Pywr model, known for its distributed structure, compared to the previously employed WRYM, within the Grootdraai Dam Catchment?
ii. How well does the Pywr-WQ model perform in simulating and predicting water quality based on historical data in the Grootdraai Dam Catchment?
iii. How do alterations in land-use and land-cover affect water quality in the medium and long term, and how can predictive input parameters derived from multiple regression models be integrated into the Pywr-WQ model to better understand these effects?
iv. What are the implications of changes in water usage patterns, mine closures, and climate change scenarios for water quality in the Grootdraai Dam Catchment over the medium and long term?

The overall aim of this study was achieved through the following objectives:

i. To implement the Pywr model, followed by an assessment of its applicability through a rigorous validation process against the previously utilised WRYM, within the Grootdraai Dam Catchment. This is crucial to address the specific need for a more distributed model in this catchment area.

ii. To apply Pywr-WQ model, encompassing model calibration and subsequent validation against historical water quality datasets derived from the study area Grootdraai Dam Catchment.

iii. To investigate the influence of alterations in land-use on water quality, particularly over the medium and long term.

iv. To assess modifications in water usage patterns in conjunction with scenarios involving mine closure and climate change on water quality in the Grootdraai Dam Catchment over the medium and long term.

1.7 Thesis Design

Chapter 1: This chapter comprises the study's introduction and literature review. It encompasses the rationale and significance of this study, along with a detailed presentation of the study's aims and objectives.

Chapter 2: This chapter introduces the pressing concern of water quality in the Grootdraai Dam Catchment, emphasising its importance to stakeholders. It delves into the geological, soil, and land-use characteristics of the region, highlighting their roles in water quality dynamics.

Chapter 3: The Pywr model is introduced as an alternative to the WRYM for the Grootdraai Dam Catchment. The effectiveness and flexibility of Pywr are evaluated, showing its potential for enhanced water resource modelling when compared to WRYM.

Chapter 4: This chapter directly addresses the critical global issue of water quality degradation by introducing the Pywr-WQ model, which seamlessly integrates water quality mechanisms from WQSAM. The Pywr-WQ model is dynamically linked to the Pywr model. With a focus on the Grootdraai Dam Catchment, the strategic objectives include catchment setup in the Pywr-WQ model; the statistical separation of baseflow; and the detailed calibration and validation of the Pywr-WQ model using historical data.

Chapter 5: This chapter provides a study of water quality dynamics in the Grootdraai Dam Catchment. It highlights the challenges faced in water quality modelling, driven by limited data, technical gaps, and financial constraints. Using the Pywr-WQ model, the study focuses on improving non-point load modelling through the evaluation of land-use models and regression

analysis. The chapter aims to enhance our understanding of the relationship between land-cover and water quality.

Chapter 6: The chapter delves into the consequences of a future scenario of increased abstraction, climate change, and decreased coal mining (or mining impacts) in the Grootdraai Dam Catchment. Amidst South Africa's prominence as a mining hub, exists a delicate balance between economic prosperity and sustainable development. To address these concerns, the study employs the Pywr-WQ model for a comprehensive assessment of how mining cessation affects water quality. It also probes the viability of this strategy against the backdrop of shifting climate patterns and rising water demands.

Chapter 7: This chapter serves as the culmination of the study, offering a comprehensive discussion of the results, an in-depth critical evaluation of the study frameworks, and the implications within the water quality scientific community in South Africa. The chapter not only highlights the significance of the findings but also provides recommendations for addressing the challenges identified throughout this study.

CHAPTER 2: STUDY AREA BACKGROUND

2.1 Introduction

The study area has been an ongoing cause of concern for investigators and stakeholders (industries, government, and civil society) alike because of the varying water quality that poses a significant threat to industries, agricultural activities, public health, and ecological systems. that rely on it for water supplies. The Grootdraai Dam Catchment was selected for its socioeconomic and ecological importance (du Plessis et al., 2015). The location is under three different environments of contamination: air (Braune et al., 1987), soil, and water pollution (Ncube, 2014). This significant degradation of ecosystems in the area is due to human activities (Pörtner et al., 2021), and as a result, the economic weight is one of the essential factors for site selection because it is associated with multiple and different actions related to the economy and generates serious degradation of water quality (du Plessis, 2017). This chapter focuses on these subject areas: i) geology and soil, ii) land-use, and iii) hydrology and climate of the Grootdraai Dam Catchment.

2.2 Study Area Description

The Grootdraai Dam Catchment is in the Mpumalanga Province (Figure 2.1), South Africa (Simpson et al., 2019), bounded by Limpopo Province to the north, Mozambique, and Swaziland to the east, KwaZulu-Natal and Free State provinces to the south, and Gauteng Province to the west. The Grootdraai Dam is situated northeast of the Upper Vaal, Gauteng Province, South Africa. As stated by Jeleni & Mare (2007), the Upper Vaal WMA has an advanced position of industrialisation and development with a high population density. It represents a significant WMA within South Africa in terms of water resource management compared to the Orange-Vaal WMAs. Jeleni & Mare (2007) affirmed that the Grootdraai Dam, Vaal Dam, Sterkfontein Dam, and Bloemhof Dam comprise the main Vaal system. The Grootdraai Dam Catchment is composed of twelve quaternary catchments and eleven towns, namely: Standerton, Bethal, Ermelo, Amersfoort, Volksrust, Davel, Breyten, Morgenzon, Perdekon, Thuthukani, and Camden. In this context, a quaternary catchment, classified as the fourth order in a hierarchical system, serves as a primary water management unit in South Africa, attempting to facilitate effective water resource management (DWS, 2011). Most of South Africa's coal-fired power stations are in Mpumalanga, strategically situated near the mines that supply coal (Simpson et al., 2019). There are four mines located upstream of the Grootdraai Dam, namely, the Vunene coal mine, Umlabu Colliery, Golfview mine, and Spitzkop mine. In addition, there are three mines located on the catchment boundaries: Penumbra Coal Mine, Thutsi Colliery, and New Denmark Colliery. In

addition, the Grootdraai Dam Catchment includes three power stations, namely the Camden, Majuba, and Tutuka power stations.

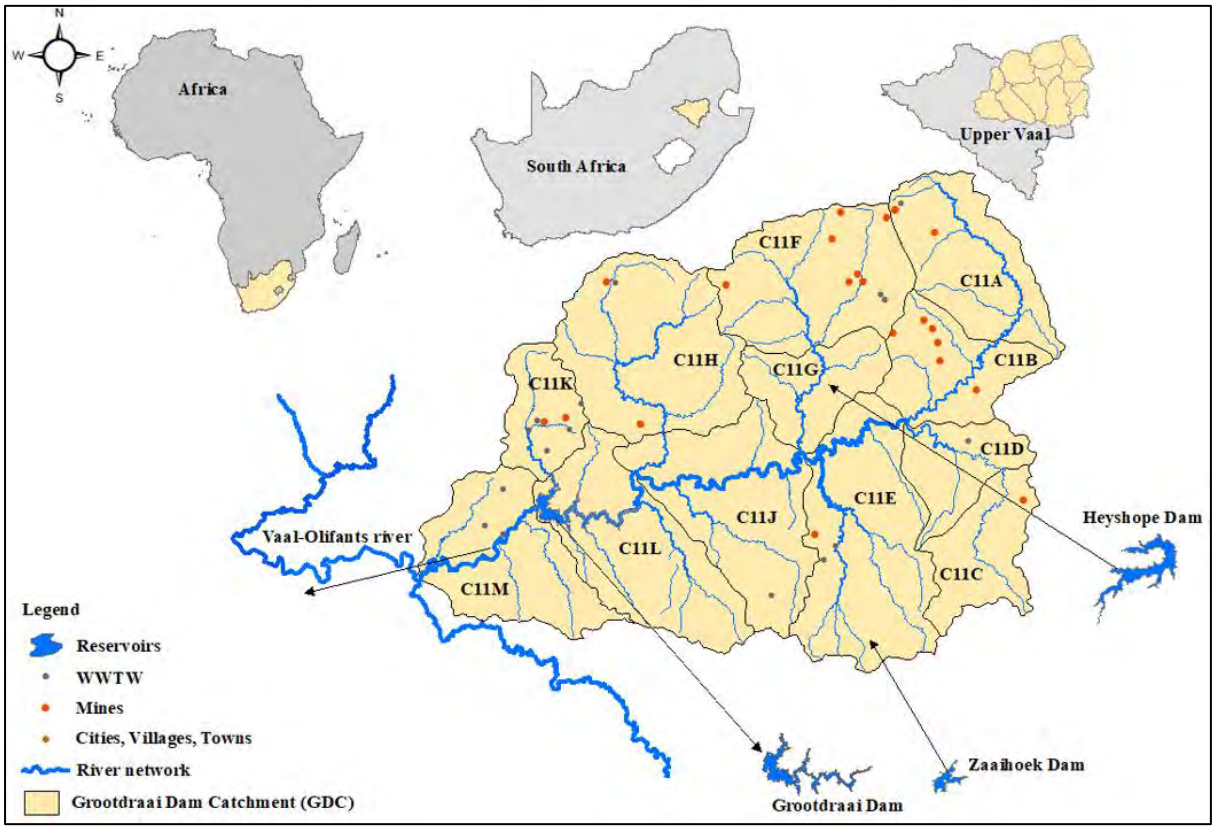

Figure 2.1: Map displaying the geospatial location of the Grootdraai Dam Catchment within the broader Upper Vaal Catchment, South Africa.

2.3 Geology and Soil of the Grootdraai Dam Catchment

The geology of Mpumalanga Province is rich owing to its historical significance, which led to extensive mining activity in the region. Mining operations in Mpumalanga extract a range of minerals and commodities, including coal, ferrochrome, ferromanganese, gold, iron ore, nickel, and platinum (Utembe et al., 2015). The Grootdraai Dam Catchment geology is underlain by four sub-groups: Volksrust, Beaufort, Karoo, and Vryheid. The Volksrust and Beaufort dominate the southeast part of the catchment, whereas the Vryheid is dominant in the northeast part of the catchment, and the Karoo Dolorite dominates most parts, as presented in Figure 2.2. Thus, the lithological characteristics of the catchment are composed of two main groups, intercalated arenaceous and, principally, argillaceous strata. This type of lithology is mainly composed of clay layers (Durmishyan, 1974), and it is known for its ability to absorb and retain water (Carretero, 2002), and its capacity to adsorb pollutants such as organic or inorganic nutrients, heavy metals, and other types of pollutants (Uddin, 2017). The movement of water flow through strata pores

may facilitate the mobilisation of contaminants, leading to water quality degradation on a wide-reaching scale across groundwater and surface-water bodies.

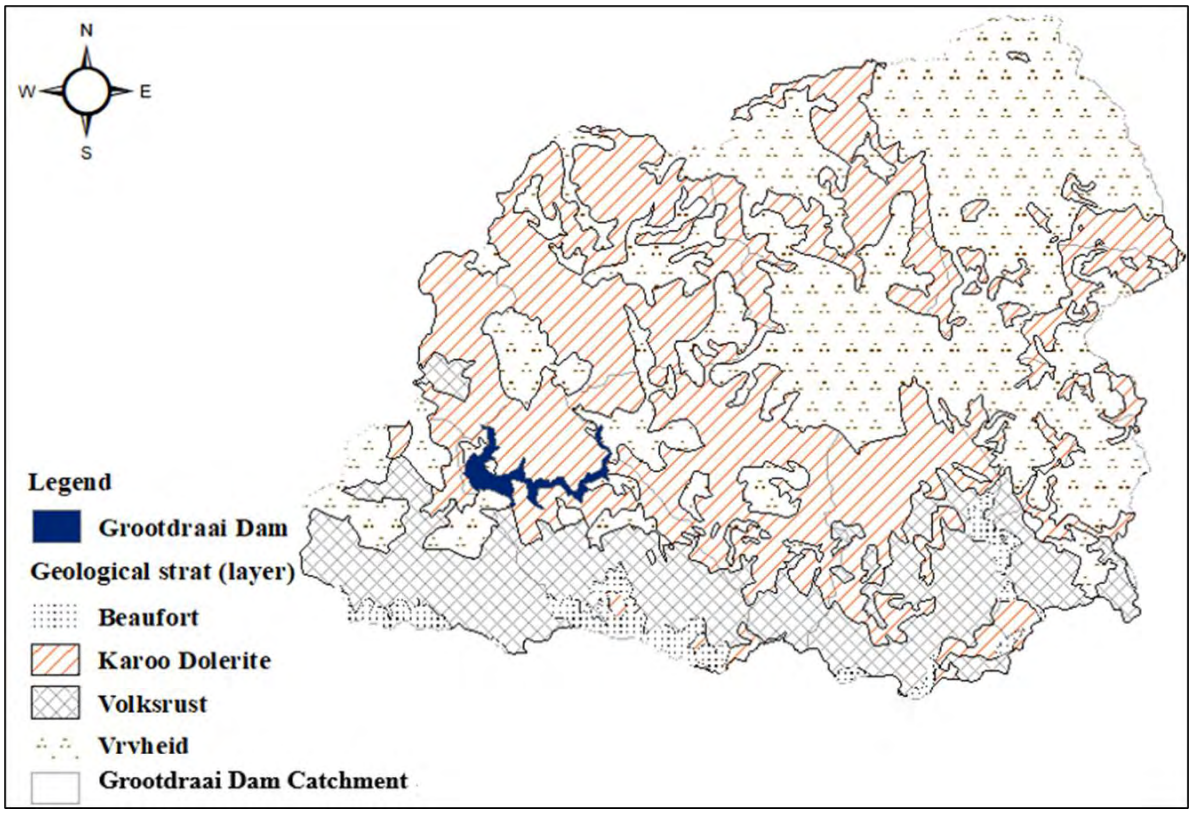

Figure 2.2: Map displaying geological layer classification for the Grootdraai Dam Catchment within the broader Upper Vaal Catchment, South Africa.

The soil data for the study was obtained from the Soil and Terrain Database for Southern Africa (SOTERSAF), a database hosted on Food and Agriculture Organisation (FAO) Africa soils, (https://library.mcmaster.ca/maps/geospatial/soil-and-terrain-database-southern-africa-sotersaf). The soil type in the Grootdraai Dam Catchment, being a subset of Mpumalanga Province, is expected to exhibit similar characteristics as the broader region, which consists of varying ratios of clay, sand, and loam. According to DCOGTA (2019), there are various types of soil in the area, including soils with reddish colouration, soils with yellow colouration, soils classified as vertic and melanic, pedologically young soil, and exposed rock covering about 18.7%, 0.9%, 17.7%, 22.0%, and 6.9% of the area, respectively. Loam soil dominates approximately 65% of the area, while sandy and clay soils account for 21.4% and 12.8%, respectively (Figure 2.3). Similar types of soil are observed in the catchment with varying percentages and distribution (Table 2.1). Sandy clay to clay soil is the dominant type, particularly downstream and towards the centre of the catchment. Sandy loam soil represents the second most prevalent type, with loamy sand to sandy loam, which is mostly found in the northeast of the

catchment. Poor land management, land-use change, and climate change may cause soil loosening, transport, and relocation, contributing to water quality degradation (Issaka & Ashraf, 2017). The dominant type of soil has a strong adsorption capacity for phosphate, heavy metals, and organics (Song et al., 2021). Soil erosion may contribute to clay sediment relocation to water bodies, causing nutrients and heavy metal loading to waterbodies and wetlands, resulting in water eutrophication and disturbance of the aquatic environment (Issaka & Ashraf, 2017).

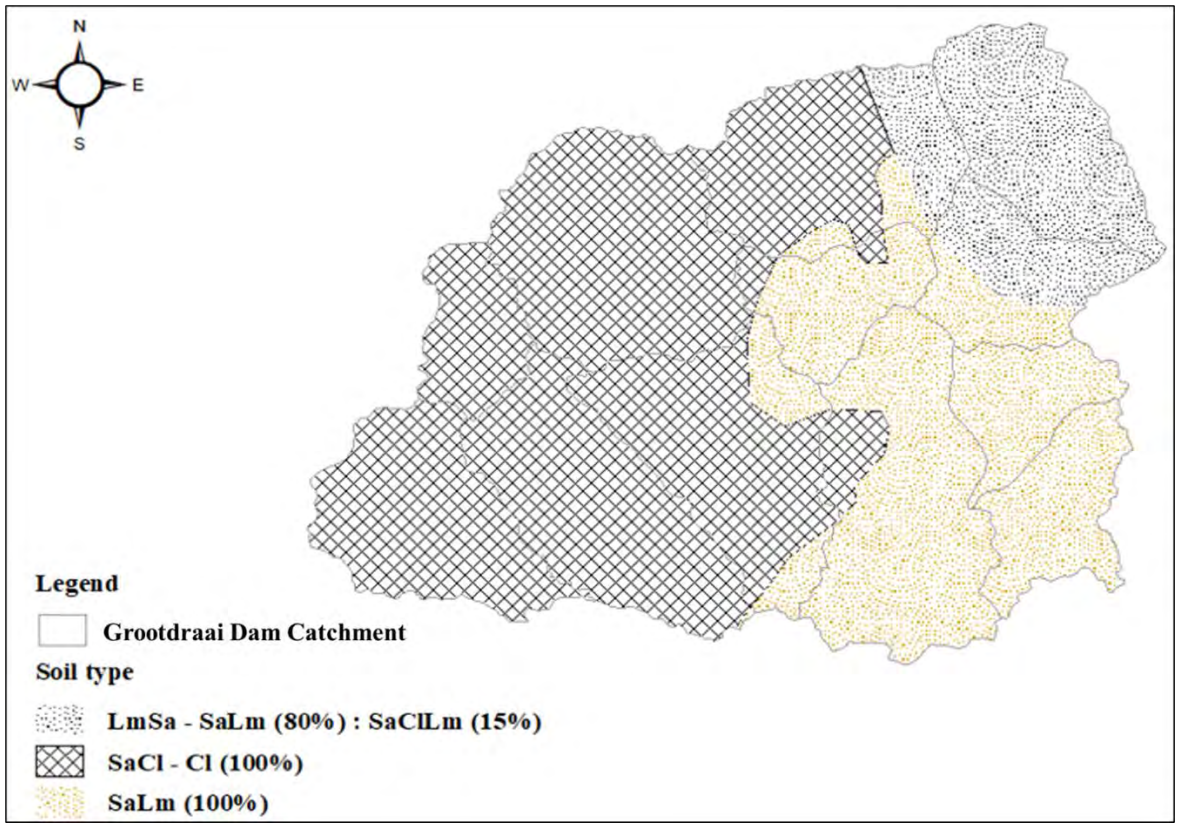

Figure 2.3: Map displaying soil type classification for the Grootdraai Dam Catchment within the broader Upper Vaal Catchment, South Africa. In this map, "Lm" denotes loam, "Sa" signifies sand, and "Cl" represents clay.

2.4 Land-Use of the Grootdraai Dam Catchment

According to the land-cover distribution proportion for the year 2009, the Grootdraai Dam Catchment was dominated by cultivated land estimated to be more than 82%, with the remainder consisting of natural land, water bodies, mining, and forest (du Plessis et al., 2015). Figure 2.4 provides a land-use and land-cover map for the year 2020 presenting different land-use classes such as urban areas, grassland, cultivated land, bare land, and water bodies (reservoirs, wetlands). The Landsat images were provided by the Southern African National Land-Cover SANLC programme for the year 2020 [https://egis.environment.gov.za/]. The predominant land-cover class in the area is grassland, accounting for approximately 49% of the total land-cover. The

second dominant land-use category is agricultural activity, including cultivated land, which accounts for 42% of the total land-cover and is mainly found in the northeast of the watershed, gradually extending downstream throughout the catchment. There is also a small portion estimated to be 5% of water bodies (i.e., dams and wetlands) and mining areas that form approximately less than 0.4% of the catchment landscape. Altogether urban and mining areas present a small fraction of land-use, less than 6% of the total land-cover (Table 2.1). Although mining areas present a small fraction (approximately less than 0.4% of the total land-cover), their effect on water quality may eventually be significant owing to their influence on the production of acid mine drainage (du Plessis et al., 2015).

Table 2.1: Percentage composition of land-use and land-cover sub-features, and soil types in the Grootdraai Dam Catchment.

Features	**Sub-features**	**Area (Km^2)**	**% Grootdraai Dam Catchment**
Land-Cover and Land-Use classes	Forest	128.5	1.45
	Shrub land	< 1	< 1
	Grassland	4163.9	47.4
	Cultivated land	3750.5	42.7
	Barren land	17.9	0.21
	Urban built-up	163.1	1.85
	Water bodies	95.8	1.09
	Wetlands	435.9	4.97
	Mines-Quarries	29.4	0.33
Soil	Loamy sand	1271.2	14.4
	Sandy clay	4785.2	54.5
	Sandy loam	2728.6	31.1

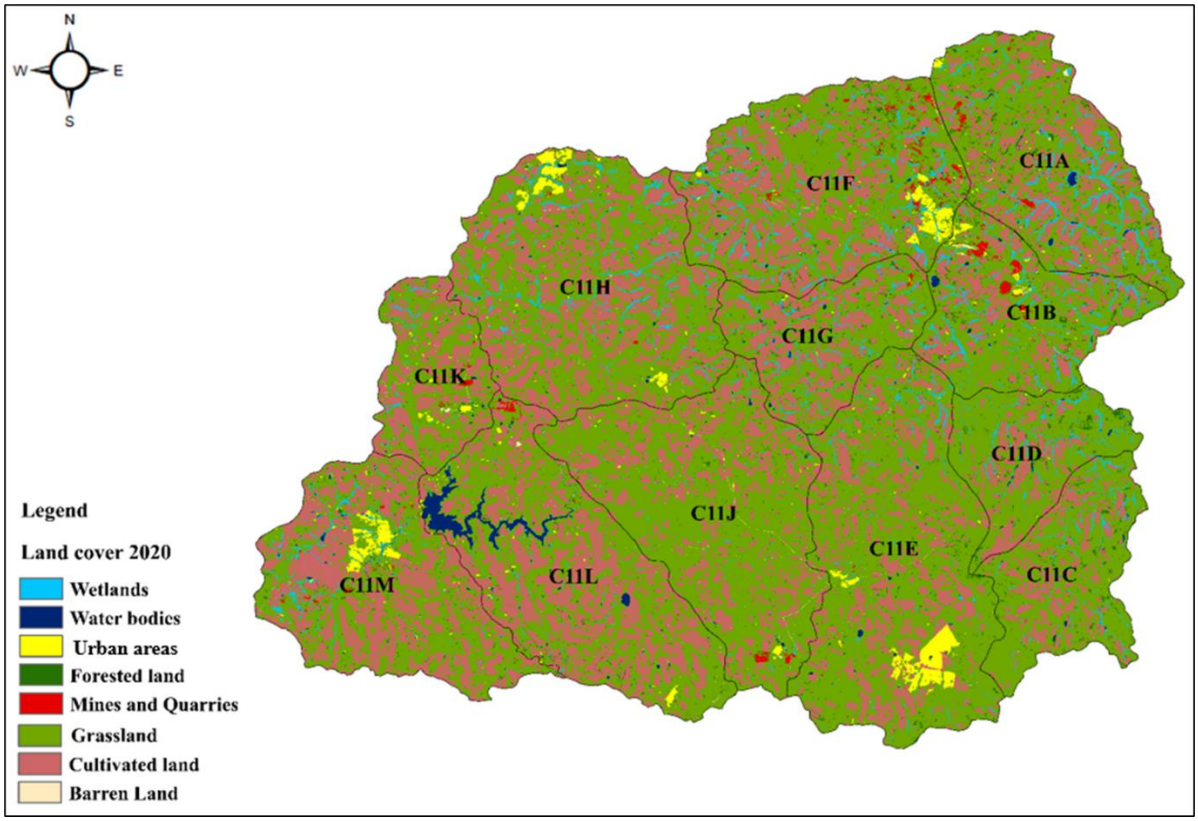

Figure 2.4: Map displaying land-use and land-cover classification for the Grootdraai Dam Catchment within the broader Upper Vaal Catchment, South Africa.

2.5 Hydrology and Climate of the Grootdraai Dam Catchment

The Grootdraai Dam Catchment is situated in the C1 secondary catchment in the Vaal River Catchment areas. It comprises eleven quaternary catchments (i.e., C11M, C11L, C11K, C11G, C11J, C11E, C11H, C11A, C11B, C11C, C11D) with an area of about 8785 km^2 and a perimeter length of 1532 km (Figure 2.5). The primary river stretches approximately 163.4 km in length. The study area has a low elevation band differences value ranging from 1500 m to 2029 m, decreasing from the southeast gradually towards the downstream of the catchment (Figure 2.5).

The study area is characterised by a sub-humid climate (van Wyk, 2010), where the rainfall varies from 603 mm to 903 mm per annum (Figure 2.6). Climate variability may be considered one of the factors influencing water quality (Nazari-Sharabian et al., 2018; Ziervogel et al., 2014), but a study conducted by du Plessis et al. (2015) found that rainfall, evaporation, and water flow variability may not significantly contribute to water quality degradation in the Grootdraai Dam Catchment.

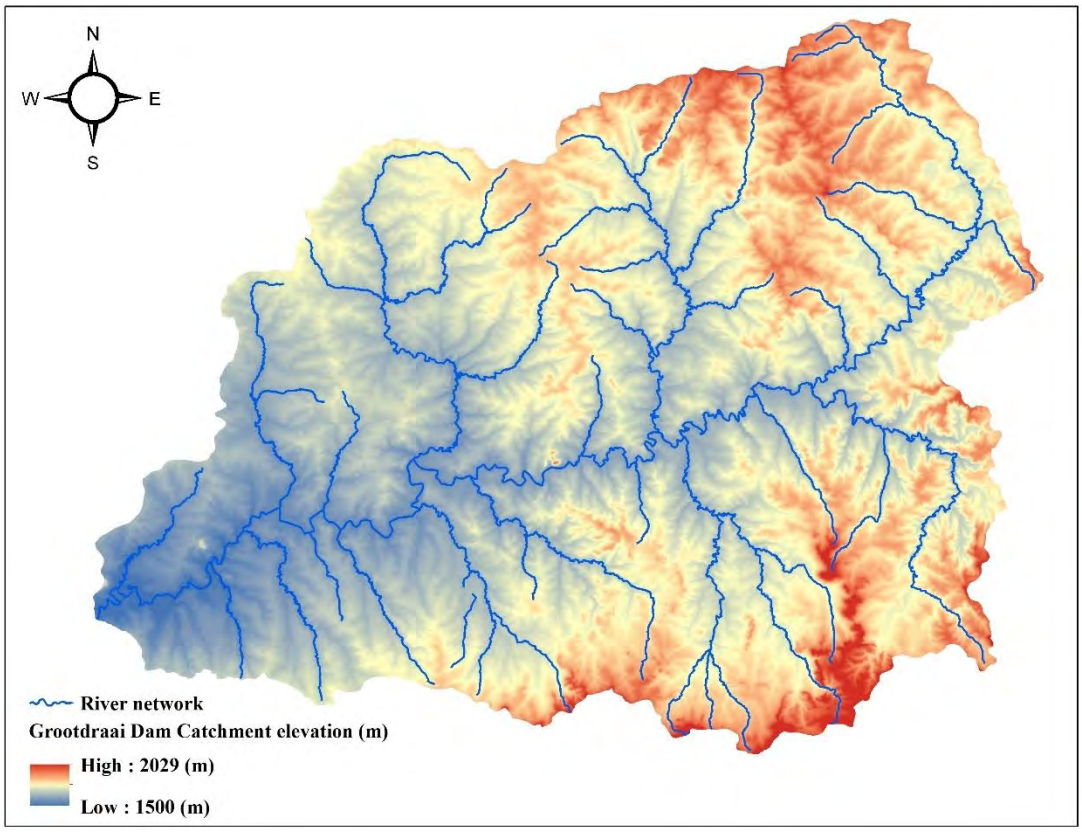

Figure 2.5: Map displaying the river network and elevation of the Grootdraai Dam Catchment within the broader Upper Vaal Catchment, South Africa.

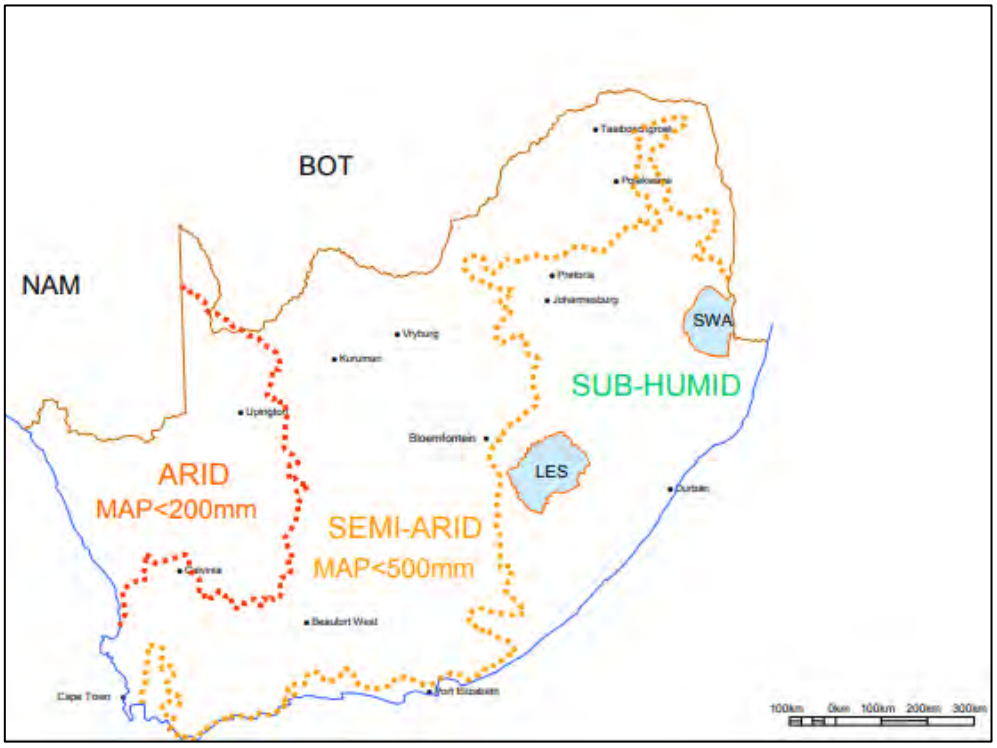

Figure 2.6: Boundaries of the major climate zones in Southern Africa (Van Wyk, 2010).

The Grootdraai Dam Catchment is a critical area with diverse geological, soil, and land-use characteristics. The catchment's complexity, from its mineral geology to its soil types and land uses, highlights the challenges and importance of effective water resource management. The region's hydrology and climate further influence its water quality dynamics. Understanding the interaction between water quantity and quality is important for comprehending the structure and functioning of the water system in the catchment. Additionally, exploring how these quantity-quality relationships behave under anticipated scenarios, such as land-cover and land-use changes, climate change, and increased demand, are addressed in the upcoming chapters.

CHAPTER 3: PYWR, AN ALTERNATIVE MODEL TO THE WRYM: A CASE STUDY FOR THE GROOTDRAAI DAM CATCHMENT, UPPER VAAL, SOUTH AFRICA

3.1 Introduction

Water resource models are crucial tools for planning, managing, and governing water resources, and it is imperative to assess the extent to which these models can effectively address a diverse array of challenges (e.g., water quantity allocation). These models can act as informed decision-making tools for effective water resource management. Nkwonta et al. (2017) described a water resource model as an environment to assess several scenarios and test the impact of implemented management operations, infrastructures, and policy measures. In addition, these models operate as useful tools to back up qualitative understanding with quantitative data (Loucks & van Beek, 2017).

In water resource management, a diverse array of approaches and models has been utilised globally, contributing to extensive research and evolving strategies for sustainable water management. Examples include the *ad hoc* approach (Rule-based) (Cetinkaya et al., 2008); algorithms like the 'out-kilter' algorithm that are applied for an efficient solution (Fulkerson, 2006); and REALM (REsource Allocation Model) that allows users to develop specific water allocation models for various types of water supply systems (Perera et al., 2005). However, according to Ilich (2009), these approaches (e.g., mathematical optimisation algorithms) may cause problems, and caution is crucial when using this type of approach, including for handling flow constraints. These approaches may depend on expert input (Rizzo et al., 2016), which would constrain their use within a developing country such as South Africa, which contends with a deficiency in institutional capabilities and financial resources (Viljoen & van der Walt, 2018). Over time, different kinds of water allocation models, such as AQUATOOL (Andreu et al., 1996), Water Evaluation and Planning (WEAP) (Yates et al., 2009), and others have been developed and used. These models shaped the development of water management and planning by introducing a new approach to decision-making, namely Decision Making under Deep Uncertainty (DMDU) (Tomlinson et al., 2020). Yet the application of the approach of integrating only one or two different scenarios with similar data seems to be inefficient as it does not capture the full range of uncertainties, potentially leading to inefficient and inaccurate decision-making (Tomlinson et al., 2020). Another difficulty resides in the sensitivity or robustness metrics (Herman et al., 2015).

The WRYM, which is part of the Water Resources System Model (WRSM) (Mallory et al., 2011), is a model used for yield analysis, and it has been considered a tool for managing South Africa's water resource for more than 20 years (Nkwonta et al., 2017). The WRYM is not an Open-Source model as the legal custodian of the WRYM is the Department of Water and Sanitation (DWS). Various critical uncertainties have been associated with the WRYM, among them, (1) assumptions that depend on the user; (2) the accuracy of the result is data-dependent; and (3) modelling software may not be user-friendly as it requires experts for configuration, interpretation, and testing (Nkwonta et al., 2017). In addition, Nkwonta et al. (2017) affirmed that the WRYM spatially lumped. For instance, the model cannot simulate evaporation losses accurately due to undefined relationships between surface area and storage volume for lumped storage units. The reliance on proprietary models such as WRYM in South Africa has led to capacity challenges due to limited training opportunities and associated costs. Many existing WRYM applications, dating back to the 2010s, are outdated and require urgent updates (Juízo & Lidén, 2010). In addition, in regions in which these models have been applied, a spatially lumped representation of a catchment has, historically, generally been sufficient for water quantity management requirements. However, with increasing emphasis on water quality management, there is an urgent need to generate more spatially distributed simulations of water quantity to drive water quality simulations.

A recent water resource simulator was developed in a Python environment called Pywr (Tomlinson et al., 2020). The model used a linear programming approach and implemented advanced Decision-making under Deep Uncertainty (DMDU) by incorporating a many-scenario simulation methodology. Distinctive features set Pywr apart from other DMDU models (Tomlinson et al., 2020). These features include:

i. Time-stepping optimisation;
ii. Multi-scenario simulation;
iii. Cross-platform compatibility (e.g., it allows users to develop models on one operating system and run large simulation studies on another);
iv. Clear separation of computational and interface layers (e.g., its deployment in high-performance computing and cloud environments).

Pywr is an Open-Source, free model, which makes it accessible to different stakeholders (academia and non-academic), the model is user-friendly and has flexibility in the spatiotemporal scale at which it is applied. Pywr gives the user access to add developing infrastructure to the

water supply and to investigate its impact on the water system. Thus, the model can aid stakeholders in reaching a common understanding of the water system and any system changes. The model promotes the use of advanced multi-criteria analysis, which means that its structure has an extension to apply climate change, climate adaptation, and climate mitigation scenarios for long term impact for a specific water system.

This chapter aims to develop a daily time-step, spatially distributed water allocation model for the Grootdraai Dam Catchment based on an existing monthly-time-step, spatially lumped representation of the same catchment. The objectives of this chapter are to:

i. Establish a Pywr spatially distributed and daily time-step water resource model of the Grootdraai Dam Catchment.
ii. Calibrate and validate the Pywr model by comparing flow simulations against those of the WYRM.

3.2 Methods and Materials

3.2.1 Overview of the study area

The Grootdraai Dam is part of the Grootdraai Dam Catchment (as illustrated in Figure 2.1 in Chapter 2) and forms an integral part of the Upper Vaal Catchment, South Africa. The reservoir, completed in 1982 with a capacity of 350 million cubic meters (DWAF, 2009), was originally built to fulfil the water requirements of the Sasol coal-to-liquid plant in Secunda, a critical facility in the region's energy sector. The dam also plays a crucial role in supporting industries, such as electricity generation by Eskom at its Tutuka, Majuba, and Camden power stations, as well as coal mines. Spanning approximately 8785 km², the Grootdraai Dam Catchment is linked to inflowing transfer schemes, such as Heyshope and Zaaihoek, and the Vaal-Olifants outflow transfer scheme.

3.2.2 Description of the lumped, monthly-time-step WRYM model for the Grootdraai Dam Catchment

Figure 3.1 illustrates the monthly lumped model structure utilised within the WRYM in a previous project by Aurecon (2020). The WRYM represents water resource supply and demands through a flow network, using nodes and links, with natural monthly flows as its primary input (DWS, 2006). The WRYM model also represents water resource system behaviour, generating historical monthly inflow sequences to reservoirs and nodal points (Nkwonta et al., 2017). The WRYM facilitates system simulation and stochastic streamflow sequence generation for planning analyses (Coleman et al., 2007; Maass, 2017). Moreover, the model advocates for the

equitable utilisation of interdependent water resources, fostering sustainable water resource management within a catchment area and facilitating subsequent ecological assessments. Figure 3.1 represents a systems diagram of the Grootdraai Dam Catchment representation in the WRYM. Figure 3.1 is taken from the larger representation of the Upper Vaal River Catchment in the study by Aurecon (2020).

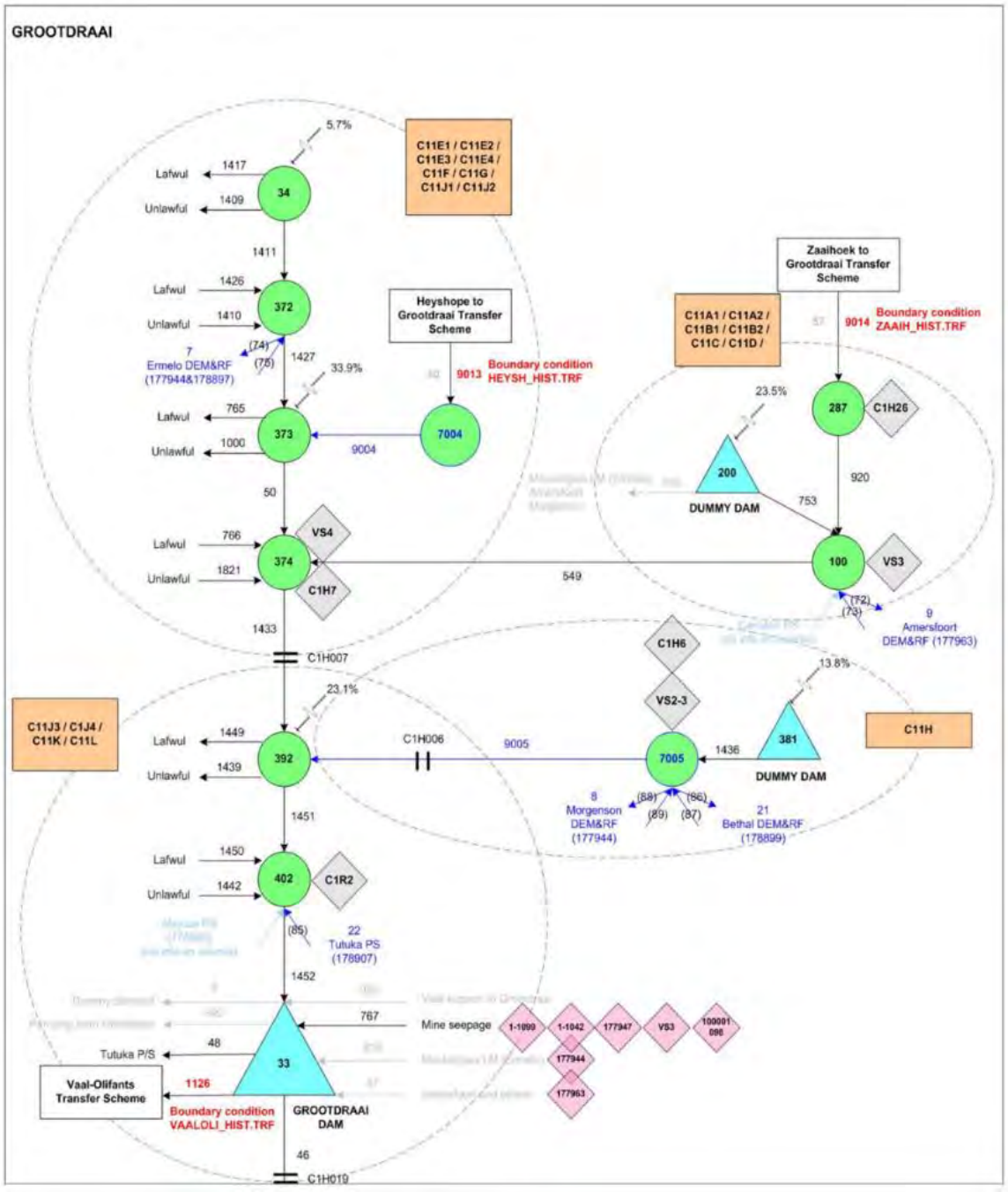

Figure 3.1: Water system diagram of the WRYM for the Grootdraai Catchment, Upper Vaal Catchment, South Africa, taken from the study by Aurecon (2020).

The WRYM has a node link structure, represented as circles connected by lines in Figure 3.1. Arrows with a central wave-shaped interruption represent natural inflow into the system, such as the example shown entering node 34. Node 34 accumulates natural inflow from specific quaternary catchments, including C11E, C11J, C11G, and C11F, as depicted in Figure 3.1. Return flows and demands are represented as arrows pointing to and away from nodes, respectively; for example, node 372 displays one arrow indicating demand (outward) and another indicating return flow (inward). These inward flows may originate from potential sewage, WWTW, or industrial activities in the vicinity. Water storage is represented as blue triangles. Apart from established reservoirs in the catchment, such as the Grootdraai Dam, the WRYM also represents the cumulative storage of multiple small dams used in agriculture and industry as 'dummy dams', for example, dummy dam 200 in Figure 3.1. The WRYM adopts a lumped spatial structure. In this regard, circles around particular branches of the systems diagram, along with associated orange boxes, represent the quaternary catchments falling within that branch. The diamond shapes in Figure 3.1 represent gauges measuring return flow and in-stream river flow, which were used to establish return flows in the model and to validate the results of the WRYM, respectively. Transfers in and out are labelled in Figure 3.1 and depicted as arrows emanating from nodes. For instance, at the blue triangle labelled 'GROOTDRAAI DAM', an arrow extends outward into a box labelled 'Vaal-Olifants Transfer Scheme', indicating a transfer out of the catchment. Conversely, at node 7004, an arrow enters the node from a box representing a transfer from Heyshope Dam into the Grootdraai Dam Catchment. Additionally, the transfer into the catchment is illustrated at node 287, where an arrow arrives from a box denoting a transfer from Zaaihoek Dam into the Grootdraai Dam Catchment.

3.2.3 Description of the daily time-step Pywr model for the Grootdraai Dam Catchment

3.2.3.1 Data used

Daily infilled rainfall data were obtained from a Water Research Commission product (Lynch, 2004) for October 1920–September 2010. Water quantity data for October 1920–September 2010 at a monthly time-step, including natural inflow, water demands, return flows, transfers in and out, and reservoir rainfall and evaporation were obtained from the established WRYM employed in a previous study (Aurecon, 2020). Locations of return flow in the catchment were obtained from the South African Department of Water and Sanitation (DWS) Resource Quality Information Services (RQIS) website (https://www.dws.gov.za/iwqs/report.aspx). These return flow locations were used to distribute lumped return flows from the WRYM to the distributed Pywr model. Table 3.1 displays flow gauges and their coordinates representing return flows

included in the distributed Pywr water system model of the Grootdraai Dam Catchment. The return flows included in the Pywr model based on gauged return flows shown in Figure 3.1 were reconciled with the lumped return flows included in the WRYM model. The flow from a lumped return flow in the WRYM model encompassing multiple return flows in the distributed Pywr model was evenly allocated among the distributed return flows. Unfortunately, while the DWS gauges provide an indication of the position and water quality of return flow gauges, measured flows for these gauges are not publicly available. Therefore, the redistribution of return flows from a lumped to a distributed structure represents a source of uncertainty in the present study.

Table 3.1: Summary of return flow gauges managed by the South African Department of Water and Sanitation and their coordinates within the Grootdraai Dam Catchment.

Node	Longitude	Latitude	Quat.	DWS gauge	Node description
RR_1	29.77	−26.59	C11F		Lawful leakage
RR_2	29.77	−26.60	C11F		Unlawful leakage
RR_3	29.79	−26.61	C11F	177944/177897	Ermelo S/W final effluent to Klein Drinkwater Spruit (GDDC07)/SESW
RR_4	29.64	−26.91	C11J	178890	Eskom Majuba WWTW effluent to Geelklipspruit
RR_5	29.65	−26.92	C11J		
RR_6	29.32	−26.80	C11K		Denmark colliery effluent
RR_7	29.33	−26.82	C11K	178902	Rand Water TUTU
RR_8	29.35	−26.84	C11K	178907	Tutuka S/W to Leeuspruit
RR_9	29.33	−26.97	C11L	1-1042/177963	Mine seepage
RR_10	29.84	−26.82	C11G	177963	Amersfoort WWTW
RR_11	29.53	−26.69	C11H	177944	Ermelo S/W final effluent to Klein Drinkwater Spruit (GDDC07)
RR_12	29.57	−26.70	C11H	178899	The effluent at Bethal WWTW to Blesbokspruit

*Quat. refers to the quaternary catchment.

While the WRYM showed return flows linked to specific nodes, the absence of corresponding DWS gauges suggests that not all return flows are captured by the monitoring network. The DWS

gauges may not capture every single return flow due to potential resource constraints. In this case, the return flow from the WRYM was assigned to an equivalent node in the Pywr model representation.

3.2.3.2 Preparation of daily flow data for input into the Pywr model

The Pywr model can create rapid, flexible, and accurate models that reflect the reality of a water system in a specific area [https://www.waterstrategy.org/]. The model is considered a tool that can improve the understanding of the operating water system and convert that into a network of interconnected nodes and links (Figure 3.2). In Figure 3.2, input nodes are depicted in green, output nodes in orange, junction nodes in black, and storage-reservoir nodes in blue. The model operates in a time-step approach, where each iteration generates changes in a certain node.

The state (volume at the level of nodes) is modified after each daily time-step iteration (Equation 3.1), where $Q^{int}_i - Q^{out}_i$ is the net flow, V_i is the volume stored in a storage node, V_{i+1} is the updated storage volume for subsequent time-step Δt_i.

$$\boldsymbol{V_{i+1} = V_i + \left(Q_i^{int} - Q_i^{out}\right) \Delta t_i} \qquad (\mathbf{3.1})$$

The model integrates the mass balance approach, which considers input and output for each node to simulate the behaviour of the water system. For this reason, it is crucial to understand the overall structure of the model, where the most important items to consider are the nodes and the edges. The node can be identified by two main properties: its name and type [https://pywr.github.io/pywr/]. Two types of nodes are recognised in the Pywr model, i) non-storage nodes, and ii) storage nodes.

There are three different sub-types of non-storage nodes such as input, output, and link nodes where these nodes have two prior parameters that need to be included, namely maximum flow and cost. However, storage nodes have additional and different properties such as maximum, minimum, and initial volume, and other properties, including input (rainfall), and output (evaporation).

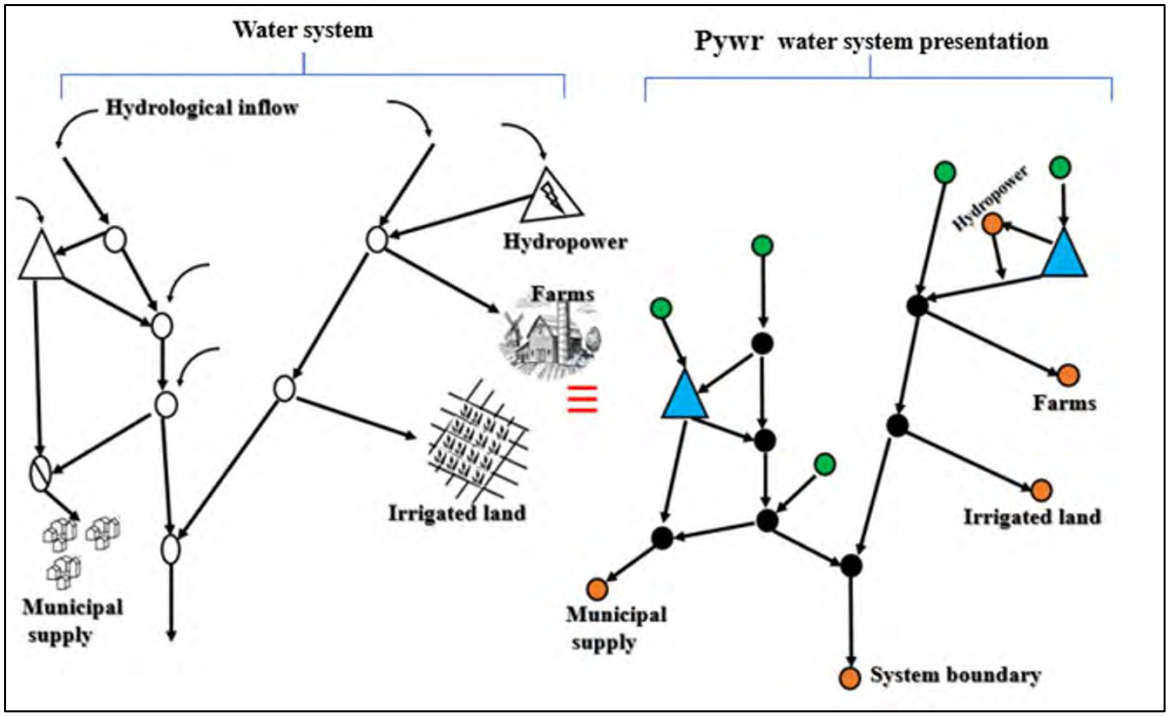

Figure 3.2: Visualisation of the water system in the Pywr environment (Tomlinson et al., 2020).

Another significant property is cost, also known as penalty, which determines the node's importance to the water system. This property is assigned a negative or positive value; a high negative value indicates critical importance to the water system's functionality. Secondly, the links are used to describe the different connections that exist between nodes, defined by the names of nodes in order of flow direction.

The creation of a daily time-step Pywr model for the Grootdraai Dam Catchment requires daily flow data, including natural flow, demand, and return flows, transfers in and out of the catchment, and reservoir rainfall and evaporation. This data is essential for accurately modelling and managing the water resource within the catchment, ensuring that the model reflects the dynamic interactions and variations in water availability.

An important flow input is the natural flow into the catchment. Natural flow inputs into the WRYM are at a monthly time-step and are generally generated separately through hydrological models such as the Pitman Model (Pitman, 1973). Since the WRYM adopts a spatially lumped structure, natural flows are input at an aggregated catchment level (Figure 3.1). Generating natural flows for input into daily time-step Pywr required (1) disaggregation of the spatially lumped natural flow inputs of WRYM from monthly to daily, and (2) further separation of the daily spatially lumped natural flows to a finer, distributed spatial scale representative of a quaternary catchment level. In this context, a quaternary catchment, classified as the fourth order

in a hierarchical system, serves as a primary water management unit in South Africa, facilitating effective water resource management (DWS, 2011).

For the first step, the method by Slaughter et al. (2015) was used to disaggregate monthly natural flows into daily. The process followed six steps, during which data were adjusted for variations, daily rainfall was converted to antecedent rainfall, and volume equivalence between disaggregated daily flow and monthly flow was ensured. The current study does not go into the finer details of this process and readers should refer to Slaughter et al. (2015) for more information. The study utilised rain gauges situated within the catchment boundary (e.g., 441593W, 0441596A, and 0441596W). The values of parameters used in the disaggregation are listed in Table 3.2.

Table 3.2: Optimised parameters and NSE values for the monthly to daily flow disaggregation process.

Rain gauge weights			**Antecedent rainfall**		**FDC parameters**		
1	**2**	**3**	**RT (mm)**	**K**	**A**	**B**	**C**
1	1	1	10	0.99	1	−0.9	0.6

*FDC refer to Flow Duration Curve; RT refer to rainfall threshold; K refer to simple recession

Each quaternary catchment was attributed an inflow node reflecting natural runoff, and the computation of the new fraction of runoff, named the surface ratio formula, was applied for each inflow node. Widely utilised in dam construction and network design for estimating runoff, this formula also finds application in designing hydrotechnical structures in ungauged areas. An underlying assumption is the requirement for homogenous and uniform rainfall distribution across the drained area, as indicated in previous studies (Guillot, 1967, 1981; Guillot & Duband, 1980).

The surface ratio physical formula is presented in Equation 3.2:

$$\frac{R_1}{S_1} = \frac{R_2}{S_2} = \frac{R_3}{S_3} = \ldots\ldots\ldots\ldots = \frac{R_{n-1}}{S_{n-1}} = \frac{R_n}{S_n} = \frac{R_{n+1}}{S_{n+1}} \qquad (3.2)$$

where R signifies the runoff (Million m^3/day), S designates the draining area (in Km^2), and n stands for the number of adjacent basins.

The diagram in Figure 3.1 provides insight into three different nodes presented as dummy dam 200, node 373, and node 392. These nodes were addressed for the runoff distribution process because the other nodes such as dummy dam 381 have been assigned to receive runoff only from

C11H, and node 34 will also receive runoff only from C11F. This study concentrated on delineating the drainage area associated with runoff accumulation in specified nodes and reservoirs, as depicted by the circles with boxes in Figure 3.1. These drained surfaces were allocated to each node or reservoir receiving natural flow, as shown in Figure 3.1. The runoff fraction for new nodes responsible for channelling water to the original node was computed using the surface ratio formula. For example, the runoff fraction for the new node named 'node 1', intended to divert water from C11A to dummy dam 200 node, was determined through Equation 3.3 as follows:

$$\boldsymbol{R_{node\,1} = \frac{R_{dummy\,dam\,200}}{S_{eq}} \times S_{C11A}} \qquad (\mathbf{3.3})$$

Where, $R_{node\ 1}$ denotes the runoff fraction for node 1 (%), $R_{dummy\ dam\ 200}$ represents the accumulated runoff fraction at the dummy dam 200 (%), S_{C11A} signifies the draining area for node 1 (in square kilometres), and S_{eq} designates the cumulated area responsible for draining water to dummy dam 200 (in square kilometres).

Other monthly flow inputs from the WRYM required disaggregation to daily for input into the Pywr model, namely demands, return flows, transfers in and out, reservoir rainfall, and evaporation. The current study adopted a simplified approach in which these monthly flows were disaggregated evenly across the month to daily, that is, under a 30-day month, the flow for each day in that month was the monthly flow divided by 30. Among the disaggregated flows, the mean demand flows range from 0.0018 to 0.029 Mm^3/day, with corresponding standard deviations of 0.00016 to 0.0066 Mm^3/day; means of transfers in and out of the study area data vary from 0.033 to 0.37 Mm^3/day, with standard deviations of 0.017 to 0.043 Mm^3/day.

3.2.3.3 Setup of the daily time-step, distributed Pywr model representation of the Grootdraai Dam Catchment

Pywr is a practical water resource modelling tool designed as a node-link model. Within the Pywr environment, inflows and outflows are treated as nodes, facilitating a comprehensive representation of the system. The model definition is structured in a JavaScript Object Notation (JSON) file, allowing a clear separation of model elements, such as nodes, links, parameters, and recorders. Notably, Pywr provides flexibility in handling model data; data can either be embedded directly in the JSON file or called from external data files. This modularity, coupled with the ability to specify time-steps and simulation windows that can be either a Million cubic

meters or litres per day, week, month, and year renders Pywr an efficient and adaptable tool for building water resource models (Tomlinson et al., 2020).

Inflow nodes and rainfall into reservoirs are visually represented in Figure 3.3 as green circles; the directed interconnections between proximate nodes, appropriately designated as 'edges', are represented as orange lines; demands and evaporation out of reservoirs are represented as outflows, depicted as orange circles; return flows are depicted as red circles and have the prefix 'RR'; storage, including established single dams and dummy dams, are represented as blue triangles; links in the model representing junctions between nodes are depicted as black circles; transfers in and out of the catchment are labelled in Figure 3.3.

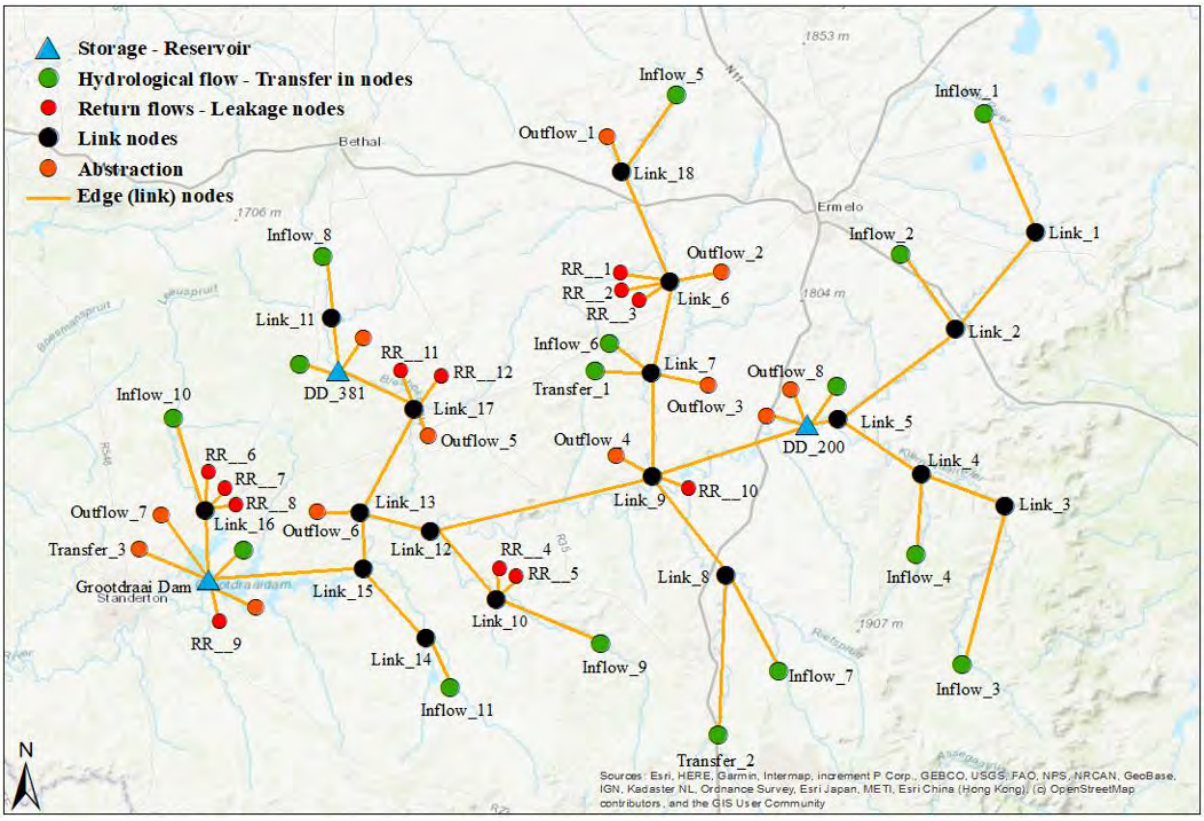

Figure 3.3: Representation of the Grootdraai Dam Catchment within the broader Upper Vaal catchment in South Africa. The map provides geospatial coordinates for the nodes incorporated in the Pywr model.

The current study used the online interface provided by Water Strategy (www.waterstrategy.org) to construct the distributed, daily time-step Pywr model. The platform allows model nodes and links to be georeferenced, and they can be easily dragged and dropped onto a map in the platform. The constructed Pywr model for the Grootdraai Dam Catchment following the system's structure is shown in Figure 3.4.

While the Water Strategy online interface allows model parameters and inflow data to be specified, as well as the model to be run, the current study chose to export the model definition file, after which these aspects of the model were performed locally, facilitating the incorporation of input data from external files, exploration of various scenarios, and generation of more sophisticated graphs than those available in the online interface. During this process, the model inflow data were established in external comma-separated (CSV) text files. The WRYM data are represented as m^3/s, as is the standard for water resources modelling in South Africa. However, a feature of Pywr is that input data into the model must be at a rate consistent with the time-step of the model. Therefore, a monthly-, weekly-, and daily time-step Pywr model would need inflow data with units specified per month, per week, and per day, respectively. The current study therefore had to convert the m^3/s data to a daily rate. The unit of Million m^3/day was chosen.

Python scripts were then created to update the model definition file for (i) defining model parameters; (ii) linking to the external model input files; (iii) defining model recorders, which record the model simulations of interest; (vi) the simulation time-step and simulation period.

The Pywr model incorporates a penalty system in which penalties are assigned to water allocation nodes. During the model run, these penalties are activated if the water allocation takes place. In the Pywr model, large negative penalties are given to allocations that are deemed to be very important, such as allocations to important demand centres, or to allocations that must occur, such as evaporation from a reservoir. In contrast, large positive penalties are given to allocations that are deemed to be less optimal, such as a spill from a reservoir. The linear programme sums the penalties during model runtime, intending to minimise the total penalty (Tomlinson et al., 2020). Within the Pywr model of the Grootdraai Dam Catchment, each allocation to a demand centre was given a penalty of −500, whereas evaporation from reservoirs was assigned a penalty of −10000 (Tomlinson et al., 2020). This penalty system ensures that critical water needs are prioritized, thereby ensuring equitable allocation and distribution of water. Moreover, to verify the model output, this study conducted a check to ensure that allocations were accurately executed. The reservoirs were configured to act as overtopping spill reservoirs, thereby eliminating the need for a reservoir release curve.

3.2.3.4 Verification of the distributed Pywr model representation of the Grootdraai Dam Catchment against that of the lumped WRYM representation

The Pywr model was run locally, with recorded model simulations depicted as time series and frequency distribution graphs in Jupyter Notebooks. The current study restricted verification of

Pywr simulations against that of the WRYM simulations for the Grootdraai Dam. This is because no sensible comparison between the two models could be achieved for a run-of-river node since the WRYM adopted a lumped structure and the Pywr model adopted a distributed structure.

The current study assessed the model simulations of Grootdraai Dam quantity using key performance indicators, including:

- Percent Bias (PBIAS) (Gupta et al., 1999; Seong et al., 2015) that measures the average tendency of the Pywr model to overestimate or underestimate the corresponding observed data (i.e., WRYM data), where a value of zero indicates no overall bias and positive or negative (±) values indicate over- and under-estimation bias, respectively.
- Nash-Sutcliffe Efficiency (Nash & Sutcliffe, 1970) that evaluates the performance of a hydrological model's relative residual variances, expressed in a range from negative infinity to 1.
- R-square (Nagelkerke, 1991) measures the correlation between observed and simulated data.
- Root Sum Square Error (RSSE) (Chu & Shirmohammadi, 2004; Seong et al., 2015; Singh et al., 2005) used to simplify the relative comparison of RMSE values produced for estimations in different units and scales by normalising RMSE with the observed data's standard deviation.

3.3 Results

3.3.1 Runoff distribution

The runoff percentages distribution for the Pywr model distributed structure (Figure 3.3), is presented in Table 3.3, with their position in the Grootdraai Dam Catchment. Table 3.3 reveals that inflows with higher surface area ratios tend to have higher runoff percentages. In addition, inflow nodes linked to quaternary catchments C11E and C11K have the highest runoff percentages (10.11% and 11.13% respectively), showing that these nodes contribute significantly to the overall runoff. Inflow nodes for quaternary catchments C11F and C11J, with the lowest surface area ratios, also have the lowest runoff percentages.

Table 3.3: Runoff distribution for draining quaternary nodes.

Node	Quat.	Surface ratio (Km^2/Km^2)	Runoff percentage (%)
Inflow 1	C11A	0.346	8.15

Node	Quat.	Surface ratio (Km^2/Km^2)	Runoff percentage (%)
Inflow 2	C11B	0.25	6.05
Inflow 3	C11C	0.179	4.21
Inflow 4	C11D	0.216	5.08
Inflow 5	C11F	0.148	3.43
Inflow 6	C11G	0.413	9.56
Inflow 7	C11E	0.437	10.11
Inflow 8	C11H	0.264	8.96
Inflow 9	C11J	0.122	4.16
Inflow 10	C11K	0.328	11.13
Inflow 11	C11L	0.284	9.65

*Quat. refer to the quaternary catchment.

3.3.2 Pywr model setup

The model's structure encompasses a network of nodes, including catchment, extraction, return-flow, reservoirs, and links, interconnected by edges. Table 3.4 provides insights into links/reservoir nodes. Notably, abstraction nodes and return-flow nodes are maintained from Aurecon (2020), as illustrated in Figure 3.1. Figure 3.4 illustrates the typology of the distributed daily time-step Pywr model for the Grootdraai Dam Catchment within https://www.waterstrategy.org/ environment.

Table 3.4: Original nodes in the WRYM against Pywr model nodes.

Vaal Barrage diagram	Pywr model
34	Link_18
372	Link_6
373	Link_7
7004	Transfer_1
374	Link_12
287	Transfer_2
100	Link_9
200	DD_200
381	DD_381
7005	Link_17

Vaal Barrage diagram	Pywr model
392	Link_13
402	Link_16
Grootdraai Dam	Grootdraai Dam

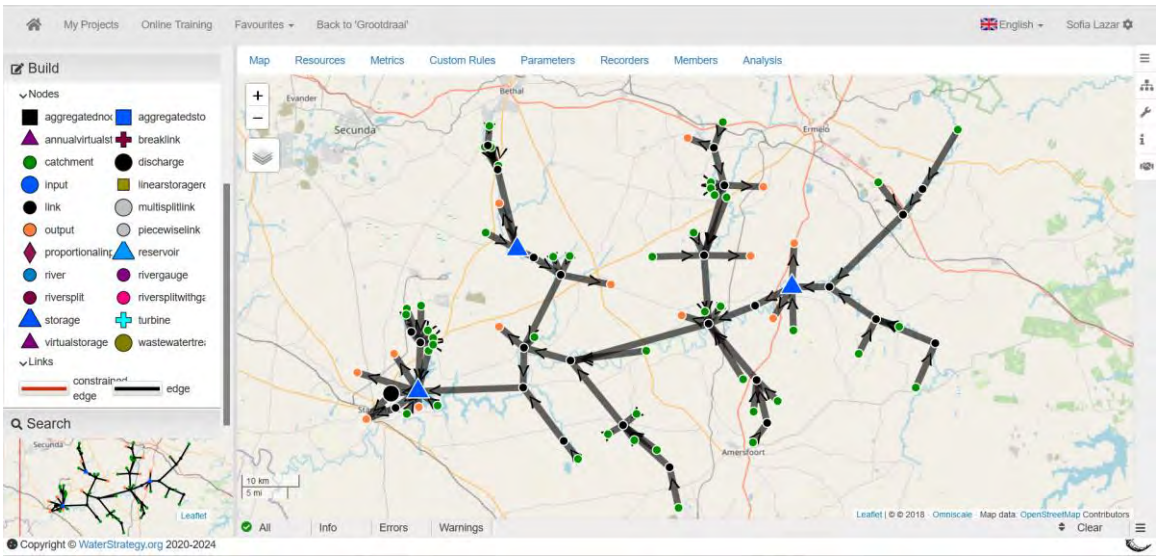

Figure 3.4: Python water resource model for the operating system in the Grootdraai Dam Catchment (GDC). https://hydra.org.uk/

3.3.2.1 Inputs of flow data from WRYM to Pywr model

Figure 3.5 depicts the breakdown of monthly flow data, originally derived from the WRYM as outlined by Aurecon (2020) into daily flow data by utilizing rainfall datasets accessible within the study area. Both the flow and rainfall datasets spanned the entire simulation period (1920–2010) and were instrumental in determining specific parameters (referenced in Table 3.2) that facilitated the conversion from monthly to daily variations in the flow dataset. Subsequently, these resulting flow datasets were redistributed across the quaternary catchment nodes. This graph displays a subset of the disaggregation process within the Grootdraai Dam from 1956 to 1966.

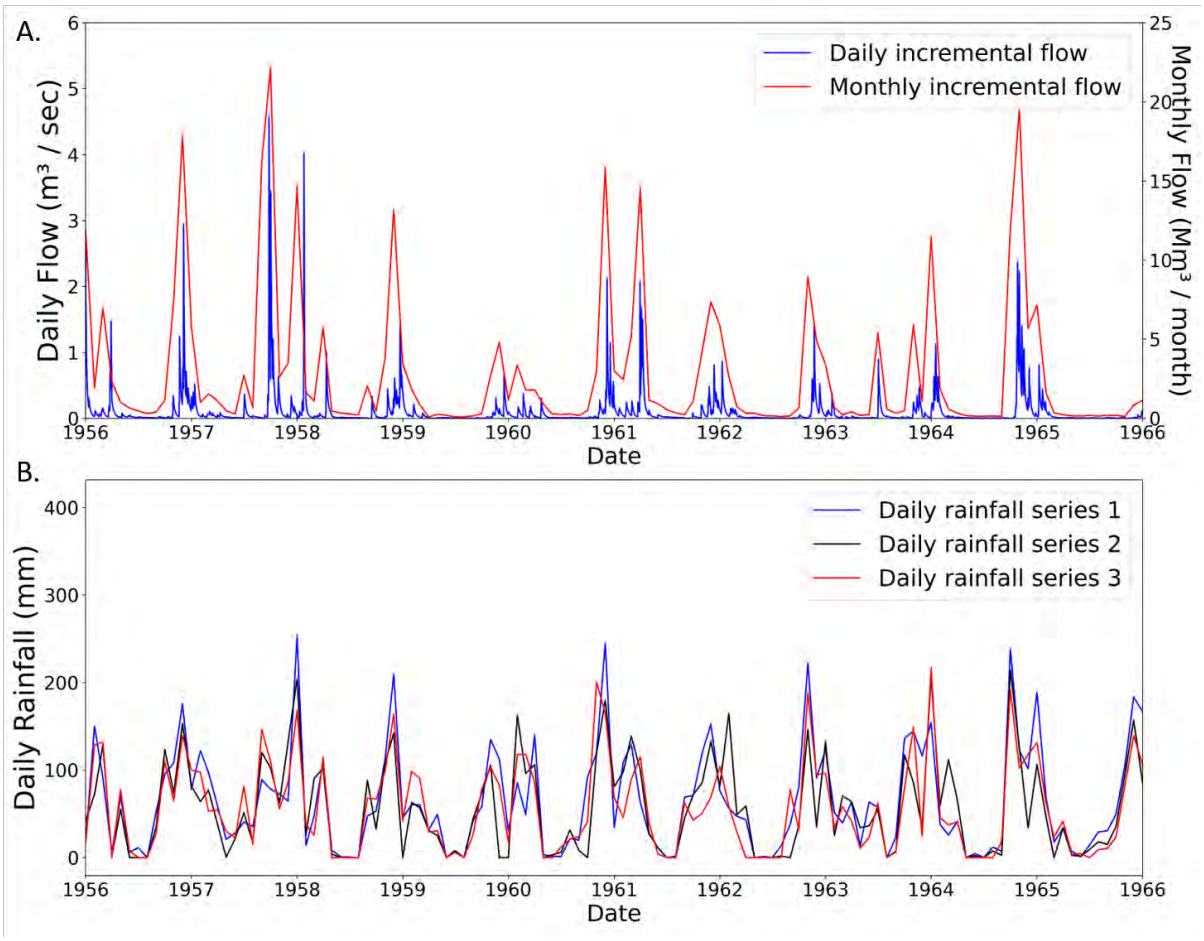

Figure 3.5: Disaggregation of monthly natural flows for the Grootdraai Dam Catchment to daily using the method developed by Slaughter et al. (2015). (A) presents a comparison between daily simulated incremental flow and monthly simulated incremental flow, while (B) displays the daily rainfall series employed for driving the disaggregation process.

3.3.2.2 Storage variation in the WRYM and Pywr model for the Grootdraai Dam Catchment

Figure 3.6 depicts the Grootdraai reservoir storage simulations conducted by both the WRYM and Pywr models, employing distinct time-steps of monthly and daily, respectively. The visual representation spans the entire simulation period from 1920 to 2010, along with a focused subset from 1980 to 2008.

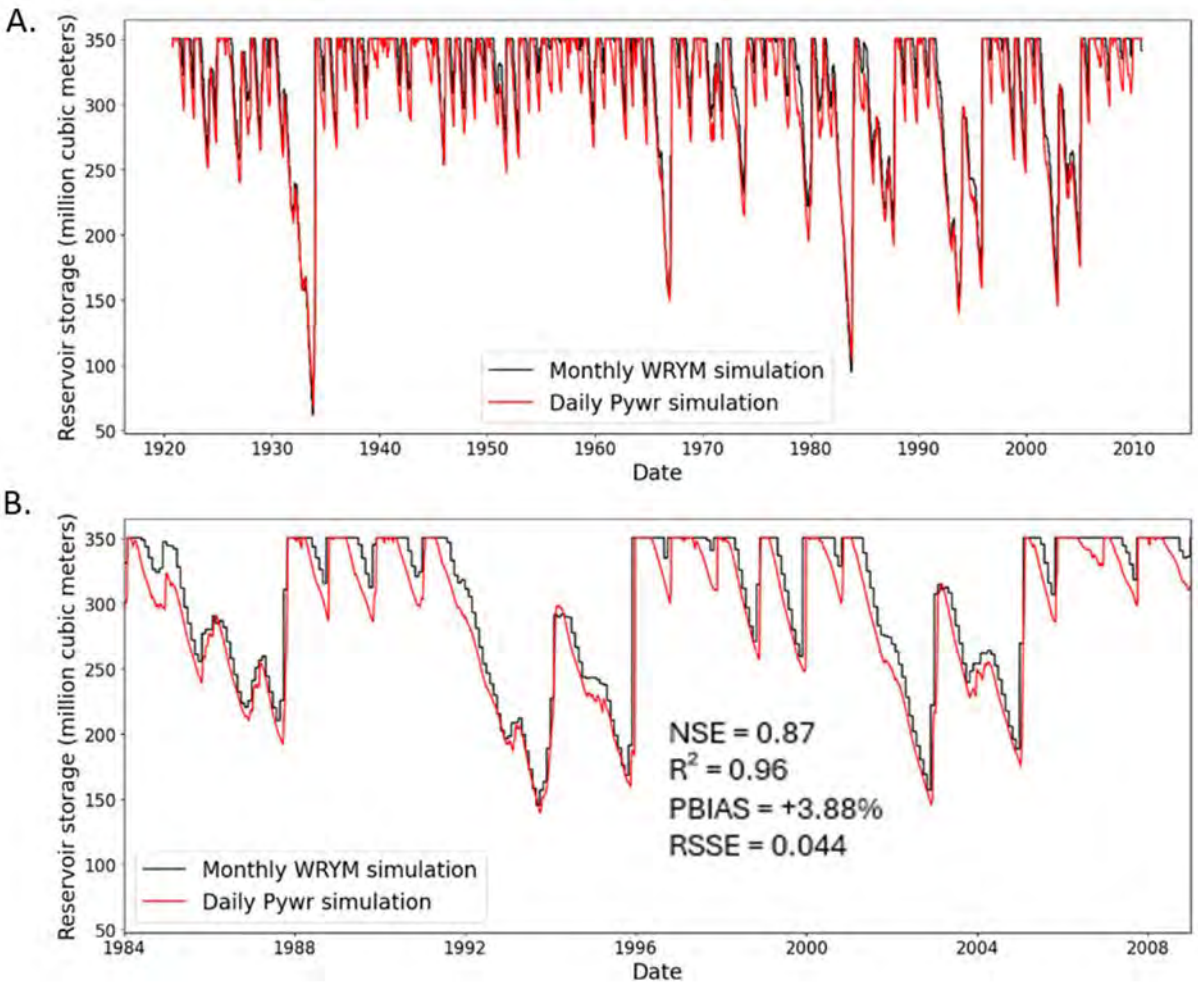

Figure 3.6: Simulated monthly storage of the Grootdraai Reservoir by the WRYM versus simulated daily storage by the Pywr model. (A) displays simulation over the complete simulation period (1920–2010). (B) displays simulations over a specific segment of the simulation period (1984–2008).

Figure 3.6 illustrates the comparison between the daily simulated data and the monthly simulated data generated by the WRYM. It is noteworthy that the Pywr model simulations demonstrate greater variability than the WRYM simulations. This heightened variability has the potential to significantly impact the goodness-of-fit statistics, thereby influencing the evaluation of model performance. The model exhibits a notably high NSE estimated at 0.87, alongside an excellent coefficient of determination (R^2) estimated at 0.96. Moreover, there is significant agreement between the simulated reservoir volume under the Pywr and WRYM outcomes. However, it is worth mentioning that the Pywr model slightly overestimates the storage, albeit to a minor extent.

3.4 Discussion

The aim of Chapter 3 was to establish Pywr model for the Grootdraai Dam Catchment and evaluate its potential as an alternative to the WRYM. This was achieved in a three-step process: (1) establishing a Pywr model to reflect the topography of the catchment; and (2) validating the

Pywr model simulation for historical conditions against that of the WRYM. The validation results indicate a strong alignment between the Pywr model and WRYM datasets, suggesting Pywr is an effective alternative to WRYM. The Pywr model's daily time-step and spatially distributed nature allow for more detailed modelling of water quality within the catchment (Tomlinson et al., 2020). The transition from a spatially lumped to a distributed structure of the water system, including individual return flows, each represented with distinct water qualities, sufficiently captures water quality processes and simulates the complex dynamics within the catchment.

The active involvement of stakeholders in decisions made by model developers is crucial. In certain models, like WRYM, where yield analysis may be influenced by user actions, transparency can be compromised. Trust becomes a pivotal factor when transparency or understanding is lacking (Chapman et al., 1995). In situations where stakeholders may not possess sufficient knowledge to comprehend the system, the lack of transparency raises concerns about the credibility and quality of WRYM's predictions. Despite being the sole model used in official water resources system analyses and junction projects in South Africa (Juízo & Lidén, 2010), uncertainties surrounding WRYM's results are significant due to the considerable freedom granted to the model user.

This chapter underscores the considerable advantages of Pywr as a viable alternative to WRYM, extending beyond its efficacy in South Africa. Pywr's flexibility, open-source accessibility, and cost-effectiveness render it a valuable tool for water resource management worldwide, particularly in regions with limited resources like many developing countries. The transition from traditional spatially lumped models to more sophisticated, spatially distributed ones holds significant importance in enhancing water management practices. This study not only highlights the applicability of Pywr within the South African context but also serves as a guide for water managers, academic scholars, and industry stakeholders, on transitioning from monthly, spatially lumped models to spatially distributed models operating on a daily time-step. This study offers a pathway toward more effective, transparent, and sustainable water resource management within the context of developing countries.

When implementing a distinct penalty system approach in diverse water simulation models, it is essential to recognise that variations in predicted data may arise. For example, differences between WRYM and Pywr simulations can be attributed to variances in their penalty system approaches, structural disparities, level of spatial resolution, and the time-step employed.

3.5 Conclusion

The results of this Chapter highlight the Pywr model's ability to provide robust simulations for the Grootdraai Dam Catchment. Through the application of a more distributed and detailed structure compared to the lumped structure used in the WRYM, the Pywr model effectively simulates daily datasets (i.e., flow, demands, and return flow). Additionally, the validation process demonstrated a strong alignment between the Pywr model and WRYM datasets, indicating Pywr's potential as a viable alternative to traditional models.

Furthermore, the active involvement of stakeholders in decision-making processes is emphasised as crucial for ensuring transparency and trust in water resource management projects. Stakeholders can access and utilise the Pywr interface, allowing them to identify their activities within the model's structure and observe the penalties assigned to specific nodes associated with those activities. This ensures that stakeholders direct their attention towards the model's outcomes rather than questioning its capabilities, thus fostering greater trust in the model.

The considerable advantages of Pywr, such as its flexibility, open-source accessibility, and cost-effectiveness make it a valuable tool for water quantity management projects. The findings presented here contribute to advancing the understanding and implementation of water resource management models, highlighting the potential of the Pywr model to address complex challenges in water resource management.

CHAPTER 4: APPLICATION OF PYWR-WQ MODEL: A CASE STUDY FOR THE GROOTDRAAI DAM CATCHMENT, UPPER VAAL, SOUTH AFRICA

4.1 Introduction

Global water quality is currently a pressing environmental concern, particularly due to issues such as eutrophication (Khan & Mohammad, 2014), contamination from heavy metals (Ali et al., 2021; Bharti & Sharma, 2022), salinisation (Cañedo-Argüelles et al., 2013), plastics contamination (Bhateria & Jain, 2016), and inadequate wastewater treatment (Edokpayi et al., 2017). Heavy metal contamination is potentially caused by mining and industrial activities (Guan et al., 2014) as well as irrigation runoff (Su, 2014). In addition, ongoing population growth, socioeconomic growth, rural-urban migration, and urbanisation collectively exert detrimental impacts on water health, leading to the degradation of water quality, disturbance of aquatic ecosystems, and the loss of aquatic species. It can also contribute to water scarcity due to less water being available of a suitable quality. Contaminants of ecosystems primarily originate from point sources, such as discharge pipes and industrial effluent, as well as non-point sources, such as runoff from agricultural fields, which carry pesticides and fertilizers, and leakage from sewerage pipes, which introduces untreated sewage into the environment. Contaminants can include organic pollutants and inorganic pollutants, such as heavy metals. For example, over half of the larger reservoirs in South Africa are currently eutrophic or hypertrophic (Griffin, 2017; van Ginkel, 2011), which indicates severe nutrient pollution and poses significant risks to water quality, aquatic life, and human health.

Efficient and sustainable management of water resources is essential for preserving both water quantity and quality. Yet, in South Africa, water management faces numerous challenges, including political and racial dynamics, limited resources, and a growing population (Molobela & Sinha, 2011). Water quality models have been employed by researchers to investigate water quality in numerous countries, for example, MIKE21 (Chapman, 1996) in South Korea and China (Jang, 2021; Xu et al., 2012), QUAL2K (Fang et al., 2008) in Iran, the United States (USA), India and Portugal (Burigato Costa et al., 2019; Idris et al., 2016; Oliveira et al., 2012; Rafiee et al., 2014), WASP6 (Artioli et al., 2005) in Italy, and SWAT (Grizzetti et al., 2003) in Europe (Abbaspour et al., 2015). However, certain models, such as QUAL2E (Brown & Barnwell, 1987), Mike 11 (Tsakiris & Alexakis, 2012), and SIMCAT (Jacobs, 2007), exhibit some limitations, such as the omission of the denitrification process during their operation, as noted by Olowe & Kumarasamy (2018). SWAT possesses the capability to simulate the in-stream fate and transport

of a diverse range of pollutants (Ejigu, 2021), and, while SWAT is widely used, its reliability depends on extensive calibration and validation data, often posing challenges in regions with limited monitoring data (Qi & Grunwald, 2005), such as many developing countries. This limitation highlights a broader issue inherent in complex models: their reliance on extensive observed data inputs. Consequently, there is an increasing demand for models that prioritise simplicity and concentrate on representing fundamental water quality processes. Adopting a simplified approach that encompasses these essential processes can enable models to maintain effectiveness while requiring fewer observed data inputs. Furthermore, SWAT exhibits notable inaccuracies in predicting baseflow discharge, sediment, and soluble phosphorus and nitrate loadings in regions with substantial winter snow cover (Qi et al., 2016).

Hence, according to Slaughter & Mantel (2017), research and modelling in the field of water quality in South Africa are not extensively developed. Water quality management tools in South Africa have remained in an immature state owing to various constraints, including a lack of observed data, and technical modelling expertise (Griffin et al., 2014; Pitman, 1973). The existing water quality models mentioned above, commonly developed in countries like the USA, are known for their complexity and their high demand for observed data for calibration and validation. However, in regions with limited data availability, such as South Africa, there is a pressing need for a model that prioritises simplicity and focuses solely on representing the key processes driving observed variations in water quality. The Water Quality Systems Assessment Model (WQSAM) (Hughes & Slaughter, 2016; Slaughter et al., 2015) is a water quality model used in South Africa for water quality investigation and management. The model was designed to address the challenge of limited observed data and has been utilised in multiple projects (Slaughter & Mantel, 2018; Slaughter et al., 2014). The WQSAM possesses several key characteristics. Firstly, it focuses solely on representing processes that contribute to the majority of observed variations in water quality, such as nitrification and denitrification. This emphasis on simplicity allows for a clear focus on essential water quality processes. Furthermore, the WQSAM seamlessly integrates with the WRYM, which is routinely used for water quantity modelling in South Africa (Juízo & Lidén, 2010).

The Pywr model (Tomlinson et al., 2020), an Open-Source model, is a Python-based generalised network resource allocation model which offers flexibility and swift run times. The Pywr model's inherent flexibility, user-friendliness, transparency, and capacity for seamless integration with other models, including water quality models, render it a compelling choice for water quantity-quality modelling. The Water Research centre (WRc) in the United Kingdom has integrated the

water quality processes of WQSAM into Pywr in a model called Pywr-WQ. This model is Open-Source and freely available on Github.com at: https://github.com/WRC-Digital/pywr-wq.

This chapter aims to represent the Grootdraai Dam Catchment in Pywr-WQ based on the Pywr representation of the catchment developed in Chapter 3 and to calibrate the model simulations of water quality for historical conditions. This chapter has several objectives: (1) to separate natural flow into flow fractions: surface flow, interflow, and groundwater flow; (2) to calibrate the model simulations of water quality against available monitoring data (baseline scenario), and (3) to evaluate the performance of the calibrated model.

4.2 Methods and Materials

4.2.1 Structure of the Pywr-WQ model representation of the Grootdraai Dam Catchment

The Pywr-WQ model employed in this study implements dynamic water allocation-water quality modelling. In the modelling framework of Pywr-WQ, the system is characterised by the network structure resembling that of the Pywr representation (Figure 4.1).

In this configuration, the model utilises flows generated by the Pywr model to simulate water quality. Nodes representing sub-catchments and reservoirs are distributed throughout the catchment, interconnected by links and edges, which are categorised into input and output nodes. Each node type corresponds to specific flows, such as hydrological flow, return flow, or reservoir releases. This categorisation enables the Pywr-WQ model to differentiate between various flow types and understand their respective impacts on water quality within the catchment.

The conceptual structure of Pywr-WQ is visually depicted in Figure 4.2 for clarity.

The first tier (A in Figure 4.2) focuses on the breakdown of daily simulated incremental flow generated from the Pywr model into three flow fractions: surface water flow (SF), interflow (IF), and groundwater flow (GWF) in the Pywr-WQ model. This is achieved through a statistical baseflow separation method developed by Hughes et al. (2003). The method allows for differentiating between different flow fractions and their respective impacts on water quality, as each flow may be influenced by specific sources of pollution, such as groundwater flow influenced by aquifer lithology and chemical characteristics of rocks.

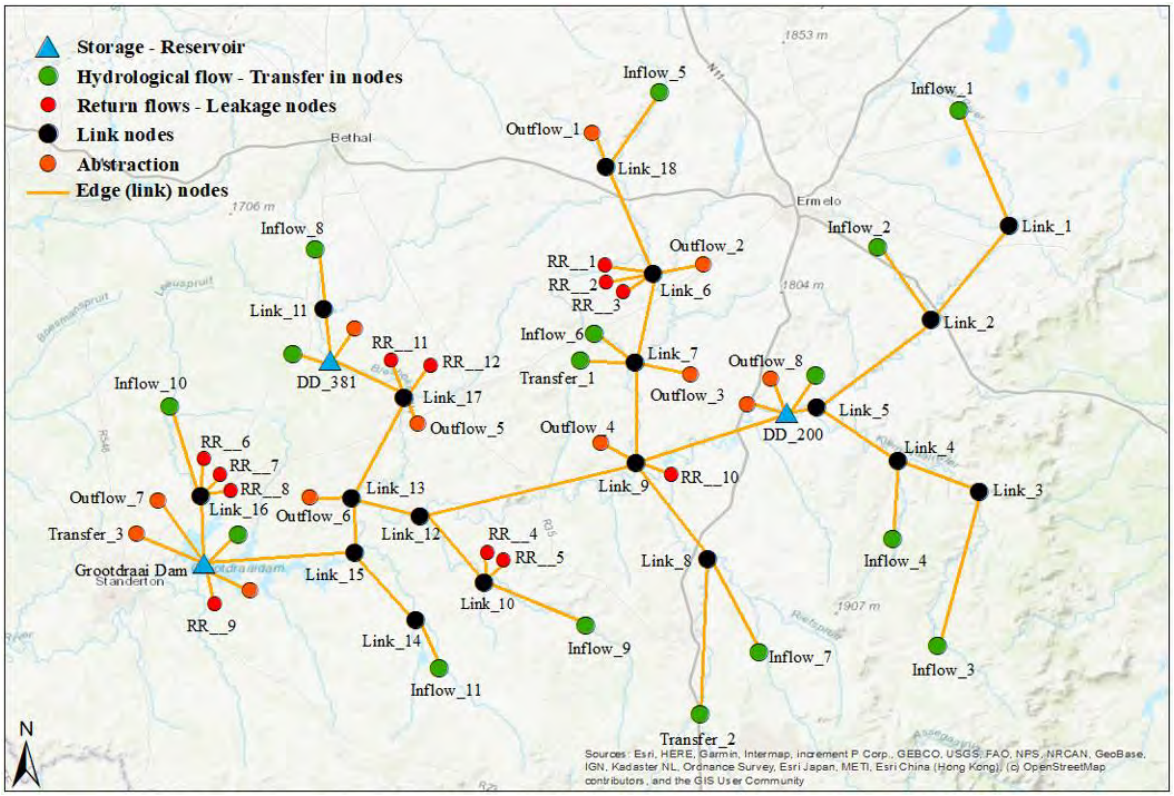

Figure 4.1: Representation delineating the Grootdraai catchment within the Upper Vaal Catchment, South Africa. The map illustrates the georeferenced positions of nodes in the Pywr environment.

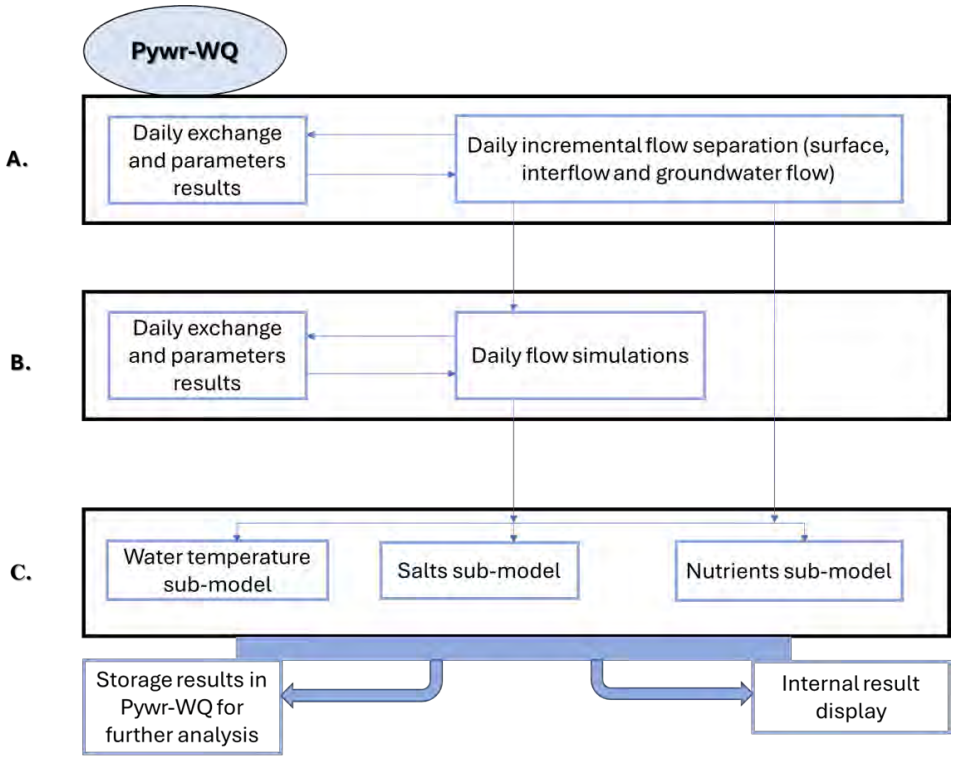

Figure 4.2: Conceptual representation of the Pywr-WQ model.

The second tier (B in Figure 4.2) involves the simulation of daily separated flows, representing the dynamic allocation of water resource and management actions within a single time-step. This includes reservoir releases, reservoir storages, wastewater return flows, and reservoir evaporation. Daily flow simulation and water allocation are central to this tier. The final tier (C in Figure 4.2) represents the actual water quality simulation process within the Pywr-WQ model, occurring within a single time-step. Here, the model dynamically generates simulations based on the inputs and processes described in the previous tiers. This stage allows for the assessment of water quality dynamics within the modelled system, providing insights into the temporal variations and interactions between water quantity and quality.

In the Pywr-WQ model, the simulation of non-point source and point source loads involves attributing water quality signatures to flow fractions, specifically surface flow, and interflow and groundwater flow fractions, across incremental flow. According to Slaughter et al. (2015), incremental flow is the monthly increase in streamflow or runoff produced by a hydrological model, representing the added flow from sub-catchments for each month rather than the total cumulative flow. When generating non-point loads, it is crucial to consider the characteristics of the surface, with a greater emphasis on surface flow for non-point nutrient loads and groundwater flow for non-point salt loads. Conversely, when addressing point sources, attention should be given to the signatures associated with the return flow from various water users, encompassing WWTW at power stations. Hence, a network of nodes focused on water quality is established in parallel with the Pywr node structure as presented in Figure 4.3.

This water quality network autonomously simulates comprehensive aspects of water quality dynamics. The interconnection between the water quality network and the Pywr network is dynamic at each time-step, Pywr transmits the flow and reservoir storage data for each node to the water quality network. Subsequently, the water quality network employs these Pywr-derived flows as input data to conduct simulations on water quality. Notably, Pywr possesses the capacity to assess the water quality status at a specific node before making critical allocation decisions, such as reservoir abstraction. However, this capability was not explored in any detail in this study. Data descriptions of nodes are presented in Appendix A.

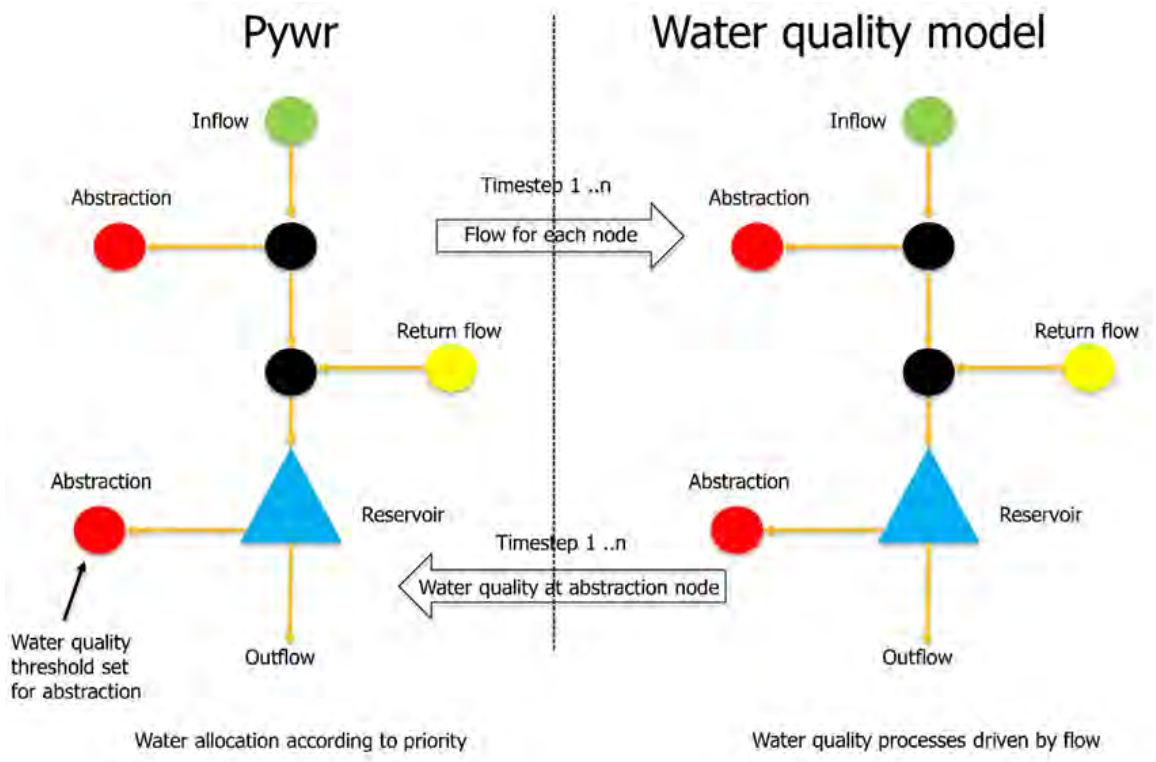

Figure 4.3: The dynamic interaction between the Pywr model and the water quality model. The model's integration resulted in the Pywr-WQ model.

4.2.2 Disaggregation of incremental flow into surface water flow, interflow, and groundwater flow

The baseflow separation component, as outlined by Hughes et al. (2003), was applied. For the modelling process, input data were employed from the Pywr model, comprising datasets related to incremental flow. The baseflow separation method divides the incremental flow into three categories namely, surface water flow, interflow, and groundwater flow (Figure 4.4). The baseflow separation method requires two parameters, denoted as α_{SF} and α_{BF}. However, establishing suitable values for these parameters in hydrological studies presents challenges attributed to various factors. These challenges, as highlighted by Kapangaziwiri et al. (2011), encompass the restricted availability of water quantity and quality data, uncertainties in surface-groundwater interactions complicating the identification of the primary source of low flows, the intricate nature of hydrological processes involving near-surface and saturated groundwater storage, and limitations in resources that impede comprehensive field investigations. In the interest of simplicity, uniform and scientifically justified default values were assigned, drawing upon previous research conducted by Hughes et al. (2003). These values are as follows:

$\alpha_{SF} = 0.95$ and $\alpha_{BF} = 0.92$

where: α_{SF} corresponds to the alpha parameter governing the distinction between surface flow and subsurface flow, and α_{BF} pertains to the parameter demarcating interflow from groundwater flow within the subsurface flow.

As shown in Figure 4.4, the baseflow separation method demonstrates a slightly delayed response compared to interflow and groundwater flow. This delay aligns with the concept that groundwater reacts more slowly to rainfall and drought, showing less variation than surface flow and interflow.

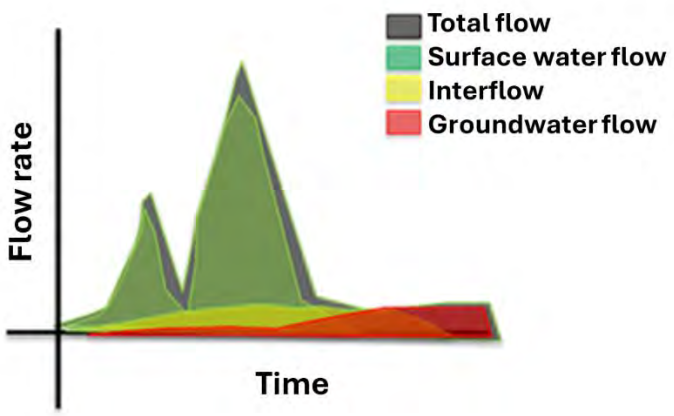

Figure 4.4: Categorization of incremental flow using the baseflow separation method into surface water flow, interflow, and groundwater flow.

4.2.3 Transmission of water quality loads among nodes

The Pywr-WQ model representation of the water system within the Grootdraai Dam Catchment consists of nodes and edges (links). Water quality processes are simulated within designated nodes in the model. Nodes corresponding to areas with agricultural or urban land in the catchment may be identified as recipients of non-point sources of nutrients or salts. Additionally, certain nodes are configured to simulate return flows from WWTW at industrial sources (e.g., ESKOM). Figure 4.5 conceptually illustrates diverse pollution sources within the Grootdraai Dam Catchment, including both point and non-point sources.

In-stream processes are implemented within the links nodes (black), such as the chemical processes affecting nitrogen (i.e., nitrification/denitrification), sedimentation of nutrients, and uptake of nutrients by flora and evaporation. In the simulation of water quality processes within in-stream nodes, ammonification and nitrification are considered, using first-order reaction equations (Chapra, 2008). The water quality mechanisms adopted in the Pywr-WQ model are based on those from the WQSAM, as indicated by Slaughter et al. (2012).

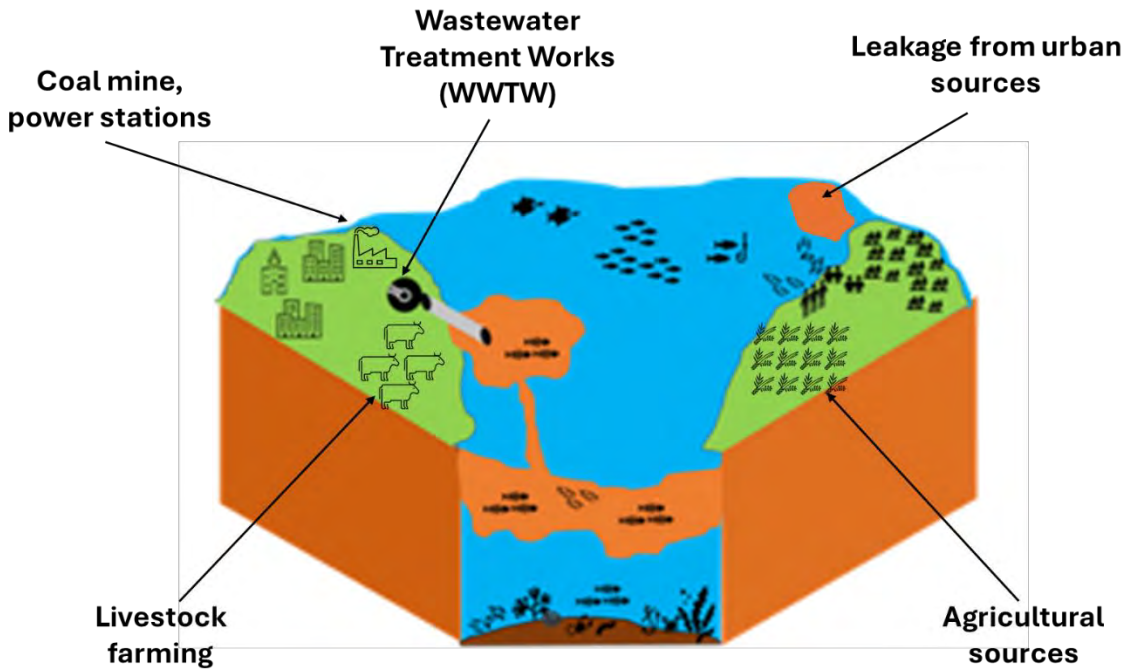

Figure 4.5: Conceptual model of the various identified sources of pollution in the Grootdraai Dam Catchment.

The in-stream processes occur at all nodes and operate on all water quality loads, whether they originate from point or non-point sources. The in-stream processes for reservoirs may be more complex than this for run-of-river nodes as they may include settling of loads to the reservoir bottom as well as re-suspension. Water quality variable loads are directed from nodes upstream to nodes downstream through shared links of nodes and edges.

The incorporation of water quality considerations into the system requires careful attention to essential variables and processes. Key water quality variables, such as water temperature, salts, and nutrients, were integral to the implementation. Simultaneously, various processes have been introduced to augment the model's comprehensiveness. These processes encompass catchment flow separation, mass-balance calculations, nitrification-denitrification dynamics, and reservoir settling/re-suspension (Figure 4.6). Moreover, the modelling of reservoirs assumes complete mixing, enhancing the representation of water quality dynamics within the system. The complete mixing assumption simplifies the mixing process in reservoirs by largely disregarding depth as a factor, despite its influence on water quality, which varies seasonally in lakes/reservoirs (Lima Neto, 2023; Pal et al., 2020). Hence, eliminating these depth-related gradients, the complete mixing offers a simplified representation of the system's dynamics.

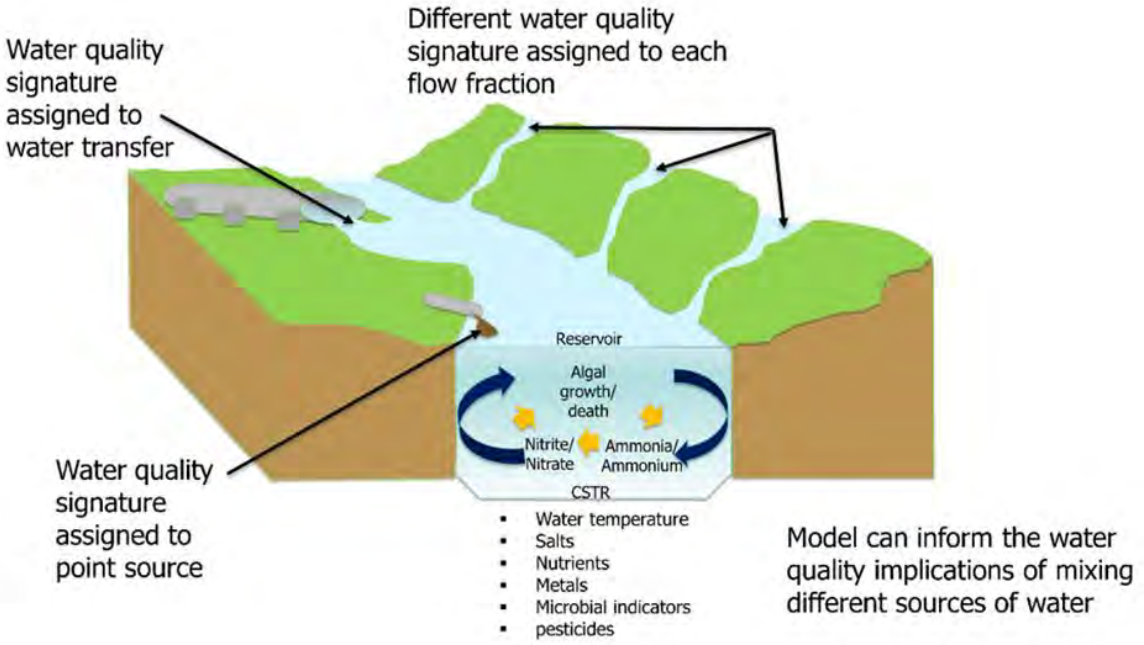

Figure 4.6: Reservoir settling and re-suspension processes within the Pywr-WQ model.

4.2.4 Simulation of non-point, point sources, and reservoirs of water quality variables

Previous studies have observed that nutrients originating from non-point sources exhibit an upward concentration trend with increasing flow, as documented by Jordan et al. (1997) and Ovalle et al. (2013). In contrast, nutrients stemming from point sources demonstrate a decreasing concentration pattern as flow escalates (Bowes et al., 2008). Nutrients derived from non-point sources are mobilised by runoff from the catchment (Lloyd et al., 2019). Consequently, their in-stream concentration rises with increasing flow, as emphasised by Hughes & van Ginkel (1994). However, nutrients originating from relatively stable point sources experience dilution due to the augmented natural flow within the stream (Carey & Migliaccio, 2009; Haggard et al., 2005). Thus, the modelling approach for nutrients and salts (conservative and non-conservative water quality variables) employed in this study followed a node-by-node modelling (Slaughter et al., 2012), starting from the upstream node and progressing towards the downstream node.

4.2.4.1 Salts modelling

The salts that have been incorporated into the Pywr-WQ model include chloride (Cl), calcium (Ca), potassium (K), magnesium (Mg), fluoride (F), sodium (Na), and sulphate (SO_4). The Pywr-WQ model offers flexibility in modifying input parameters for both non-point and point sources. The adjustment of salt signatures was carried out for surface water flow, interflow, and groundwater flow in non-point sources, as well as the signature for return flow in point sources.

The model allows for customisation and refinement of the model inputs, ensuring an accurate representation of water characteristics.

Modelling conservative water quality variables (i.e., Total Dissolved Solids (TDS)), and other water quality variables (i.e., salts and nutrients) simultaneously has facilitated the running of the water quality model and brought less complication as different input parameters can be adjusted for the same node (point sources or non-point sources). The determination of TDS concentrations relied on the unique signatures associated with each water flow component, including incremental flows representing natural flows, as well as the contributions from return flows.

4.2.4.2 Nutrients modelling

The Pywr-WQ model incorporates several nutrients including nitrate plus nitrite (NO_2-N+NO_3-N), ammonium (NH_4-N), and phosphate (PO_4-P) for comprehensive water quality modelling. Similar to the TDS modelling approach (section 4.2.4.1), the nutrient modelling followed a sequential procedure starting from the upstream node and considering the influence of parameter adjustments at each node on the downstream nodes along the water-flow direction. This sequential approach ensures an accurate representation of nutrient dynamics within the system. Integrating nutrient modelling within the shared frame of other water quality variables, such as TDS, enables comprehensive nutrient modelling at both point sources and non-point source nodes.

Nutrients exhibit non-conservative behaviour in water quality, undergoing chemical transformations such as ammonia conversion to nitrates through nitrification and uptake by algae (Slaughter et al., 2012). Consequently, simulating nutrients in the Pywr-WQ model involves more complex processes than those for salts. Furthermore, water temperature influences the rates of these nutrient-related processes. In the Pywr-WQ model, water temperature was represented using a seasonal profile consisting of 12 values, each corresponding to a month.

4.2.5 Present water quality monitoring system in the Grootdraai Dam Catchment

System monitoring plays a crucial role in assessing the significance of system parameters and their temporal variations. It provides valuable insights for adaptive management and decision-making processes (Mantel & Slaughter, 2014). In this study, water quality data were sourced from the Department of Water and Sanitation (DWS) [https://www.dws.gov.za/iwqs/wms/data/C_reg_WMS_nobor.htm].

Following a comprehensive examination of the data, a matching process was undertaken to establish the correspondence between each water quality gauge and its corresponding node in the

Pywr-WQ model, based on their geographical locations. Appendix B outlines the linkages between water quality monitoring points and their respective nodes in the Pywr-WQ model, including details on gauges for boundary conditions, such as transfers from Heyshope and Zaaihoek Dams.

4.2.6 Executing the Pywr-WQ model

The execution of the Pywr-WQ model involves an iterative process to simulate water quality dynamics within the interconnected network of nodes in the Grootdraai Dam Catchment. Initially, the model user loads the water quality model in a locale environment, laying the foundation for subsequent operations. The Pywr-WQ model contains crucial water quality parameters for various nodes, including catchment nodes, return flow nodes, and transfer nodes. These parameters encompass surface water flow, interflow, and groundwater flow signatures, playing a vital role in simulating water quality behaviour within the interconnected network. The water quality variables such as TDS, NO_3-N + NO_2-N, NH_4-N, PO_4-P, SO_4, K, F, Ca, Mg, Cl, and Na were simulated.

The initial phase entails a crucial step, which involves defining nodes, edges, and simulation days, and creating a list of "WaterQualityNode" objects to store water quality data throughout the simulation. Upon completion of the initial phase, the model enters the primary simulation loop. It starts by updating the water quality parameters for each node, distinctively handling output nodes based on flow time series and upstream contributions. For precipitation or evaporation nodes, all water quality parameters are set to zero since they are not involved in water quality calculations. Link nodes can implement in-stream water quality processes. However, these nodes do not have any point or non-point inputs. During the simulation process, the Pywr-WQ model continuously iterates and updates the water quality variables. This iterative updating occurs whenever the model user runs the model, triggering the recalculation of daily loads. After each simulation run, the model user can perform a calibration exercise to assess the accuracy of the simulation results by comparing the model's output with observed time series data and frequency simulations.

4.2.7 Calibrating the Pywr-WQ model

Within the context of water quality modelling, the intricate interplay of key variables is central to constructing accurate and insightful simulations. Firstly, the proportions of surface water flow, interflow, and groundwater flow to total flow form a foundational aspect. Assigning specific water quality signatures to each flow fraction allows for a nuanced representation, and their temporal variations can be determined through observed data. Secondly, the observed in-stream

and in-reservoir water temperature emerges as a critical factor regulating processes that influence nutrient behaviour. The Pywr-WQ model's flexibility in incorporating explicit temperature modelling based on air temperature enables a more accurate portrayal of water quality dynamics. However, we adopted a simplified approach of a seasonal water temperature profile (i.e., 12 values, with each value corresponding to a specific month). Subsequently, another pivotal dimension in water quality modelling involves nutrient concentrations in natural inflows. Observed data for nutrients and salts in runoff and groundwater play a crucial role in calibrating the model, offering essential insights into in-stream water quality. The catchment's land-use pattern also holds significant importance in identifying and characterising non-point sources of nutrients in natural inflows. Equally critical are observed data for nutrients from point sources and transfers, which refine model simulations to align them with in-stream water quality dynamics. Iterative adjustments are made to the water quality parameters, involving incremental changes, model re-runs, and comparisons with observed data (Figure 4.7). This iterative process continues until a satisfactory level of accuracy is achieved, ensuring alignment between the model's outputs and the observed data.

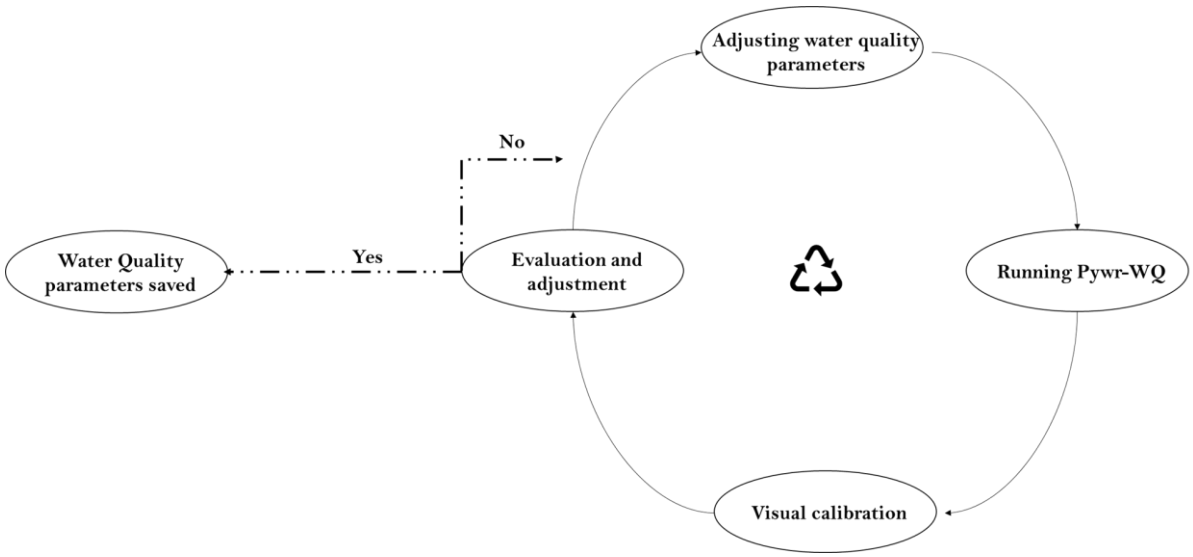

Figure 4.7: Calibration of Pywr-WQ model procedure.

4.2.8 Model evaluation and performance

Water quality models undergo evaluation to validate their output and ensure their accuracy, reliability, and precision (Ebert, 1972; Moriasi et al., 2012). To assess model performance, both graphical and statistical tests were employed. Graphical tests are used during the calibration process to establish agreement between observed and simulated data. A statistical test is conducted to evaluate model performance, employing one of the previously established

performance metrics discussed in Chapter 3. The metric includes the NSE (Nash & Sutcliffe, 1970).

4.3 Results

All figures presented in this section pertain specifically to the Grootdraai Dam.

4.3.1 Total dissolved solids (TDS)

The simulations of TDS demonstrated a relatively accurate representation of observed data, as evidenced by an NSE value reaching 0.89.

The calibrations for groundwater TDS signatures, associated with incremental flow, varied from 279 to 2600 mg.l^{-1}. Conversely, the TDS signatures designated for interflow and surface water flow were notably modest, ranging approximately from 50 to 450 mg.l^{-1}, and from 7 to 50 mg.l^{-1}, respectively. Figure 4.8 shows the frequency distribution graph of observed versus simulated TDS for the Grootdraai Dam node over the full simulation period from 1920 to 2010.

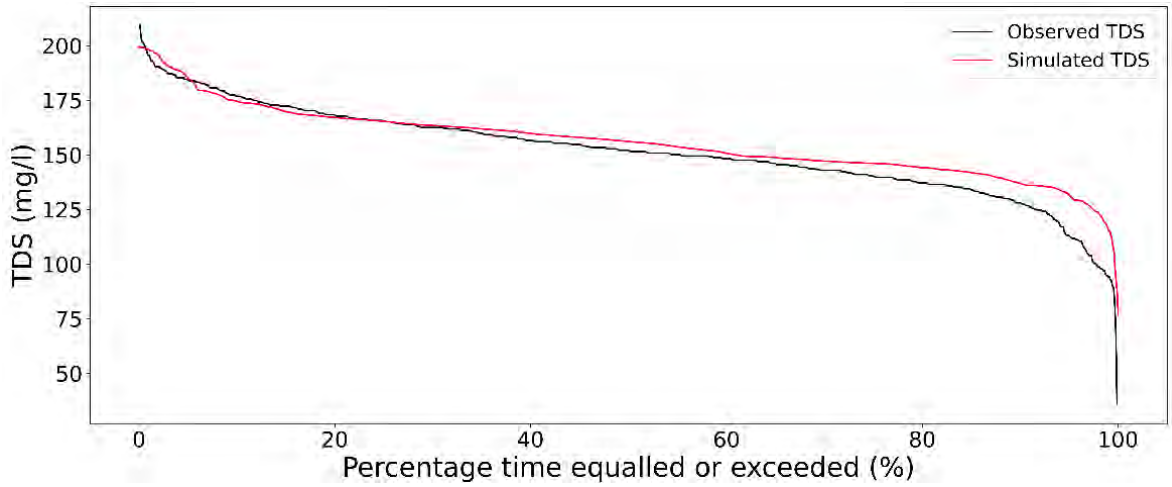

Figure 4.8: Comparison of observed TDS indicating salinity and daily simulated TDS produced by the Pywr-WQ model for the Grootdraai Dam node in the Upper Vaal River Catchment, South Africa, presented as frequency distribution graph for the full simulation period (1920–2010).

The signatures assigned to surface water flow, interflow, and groundwater flow in the catchment nodes upstream of Grootdraai Dam are higher than those assigned to catchment nodes downstream. The calibration of existing water quality data primarily guided the assignment of these signatures.

4.3.2 Nitrate plus nitrite

The signatures assigned to the surface water flow, interflow, and groundwater flow fractions had a significant effect on model simulations. For the catchment nodes from the southwest of

Grootdraai Dam, the signatures assigned to surface water flow, interflow, and groundwater flow ranged from 0.1 to 0.2 mg.l^{-1}, 0.11 to 0.33 mg.l^{-1} and 0.15 to 0.62 mg.l^{-1}, respectively. For the catchment nodes in the southeast of Grootdraai Dam, the signatures assigned to surface flow, interflow, and groundwater flow ranged from 0.01 to 0.15 mg.l^{-1}, 0.025 to 0.25 mg.l^{-1} and 0.05 to 0.95 mg.l^{-1}, respectively. Figure 4.9 shows the frequency distribution graph of observed versus simulated nitrate plus nitrite for the Grootdraai Dam node over the full simulation period ranging from 1920 to 2010.

While the simulations of nitrate plus nitrite demonstrated representativeness with observed data, indicated by an NSE value of 0.88, the model exhibits a duration curve closely resembling the observed data for concentrations below 0.8 mg.l^{-1}. However, at higher concentrations, the model fails to reach the observed high concentrations. This discrepancy may be attributed to the simulations struggling to capture the few points in the observed data with high concentrations, even though lower concentrations prevailing over the majority of the record were reasonably well represented. It is also possible that there were a few abnormally high observed points contributing to the frequency distribution.

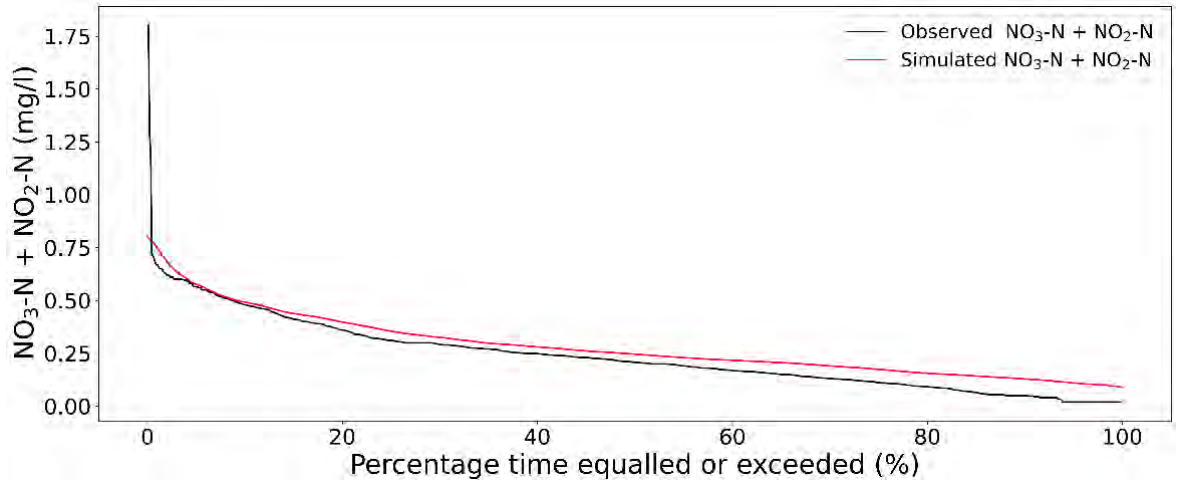

Figure 4.9: Comparison of observed nitrate plus nitrite to that simulated by the Pywr-WQ model for the Grootdraai Dam node in the Upper Vaal River Catchment, South Africa, presented as a frequency distribution graph over the entire period (1920–2010).

4.3.3 Ammonium

Similar to the case of nitrate plus nitrite, the signatures of incremental flow fractions had the most significant impact on the model simulations of ammonium. In the catchment nodes to the southwest of Grootdraai Dam, the signatures for surface water flow, interflow, and groundwater flow ranged from 0.5 to 2.5 mg.l^{-1}, 0.45 to 6.7 mg.l^{-1}, and 1.6 to 12 mg.l^{-1}, respectively. Conversely, for catchment nodes to the southeast of Grootdraai Dam, these signatures were set at

different ranges: 0.07 to 1.1 mg.l^{-1} for surface water flow, 0.23 to 3 mg.l^{-1} for interflow, and 0.45 to 3.5 mg.l^{-1} for groundwater flow. Figure 4.10 shows a frequency distribution graph of observed versus simulated ammonium for the Grootdraai Dam node over the full simulation period from 1920 to 2010. While the simulations for ammonium showcased alignment with observed data, evident through an NSE value of 0.83, the model closely mirrors the duration curve of observed data for concentrations below 0.4 mg.l^{-1}. Nevertheless, when it comes to higher concentrations, the model does not quite reach the observed peaks. This deviation might stem from the simulations struggling to encompass the occasional data points with exceptionally high concentrations, even though the model adequately represented the more common lower concentrations found throughout the majority of the dataset.

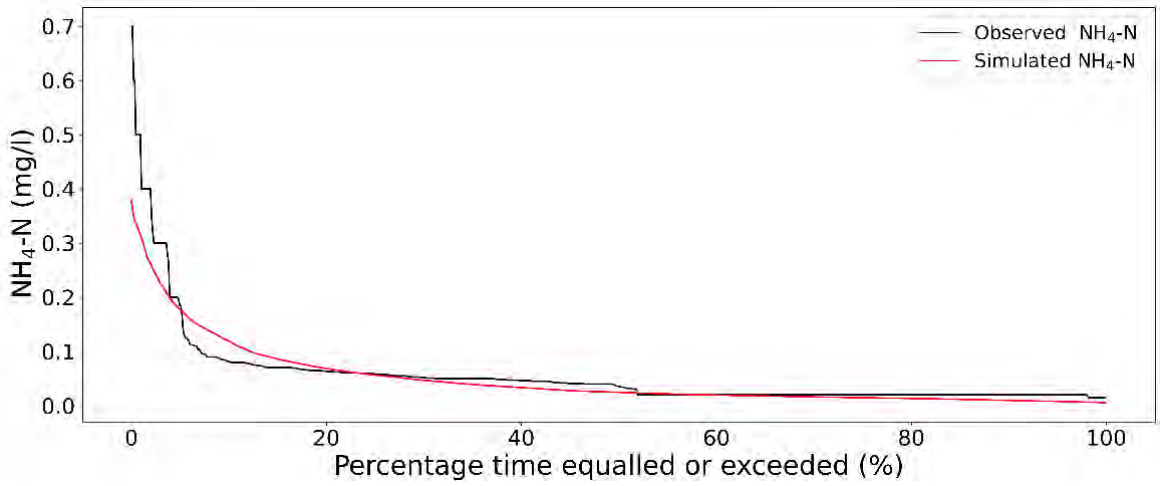

Figure 4.10: Comparison of observed ammonium to that simulated by the Pywr-WQ model for the Grootdraai Dam node in the Upper Vaal River Catchment, South Africa, presented as a frequency distribution graph over the entire period (1920–2010).

4.3.4 Phosphate

As with ammonium and nitrate plus nitrite, the incremental flow fraction signatures exerted a pronounced influence on the model simulations of phosphate.

Calibration efforts aligning with observed phosphate data were deemed effective through the exclusive assignment of concentrations to the fractions associated with surface water flow, interflow, and groundwater flow. For the catchment nodes downstream of Grootdraai Dam, the assigned signatures for surface water flow, interflow, and groundwater flow varied within the ranges of 0.02 to 0.22 mg.l^{-1}, 0.05 to 0.4 mg.l^{-1}, and 0.65 to 1.2 mg.l^{-1}, respectively. Conversely, for the catchment nodes upstream of Grootdraai Dam, the assigned signatures for surface water flow, interflow, and groundwater flow ranged from 0.01 to 0.12 mg.l^{-1}, 0.05 to 0.3 mg.l^{-1}, and 0.187 to 0.5 mg.l^{-1}, respectively.

Figure 4.11 depicts a frequency distribution graph comparing observed versus simulated phosphate for the Grootdraai Dam node over the entire simulation period from 1920 to 2010. The simulations for phosphate showcased a satisfactory alignment with observed data, evident through an NSE value of 0.65. Figure 4.11 demonstrates an overestimation of phosphate concentrations at low frequency levels, with this overestimation persisting across all but the highest frequency levels.

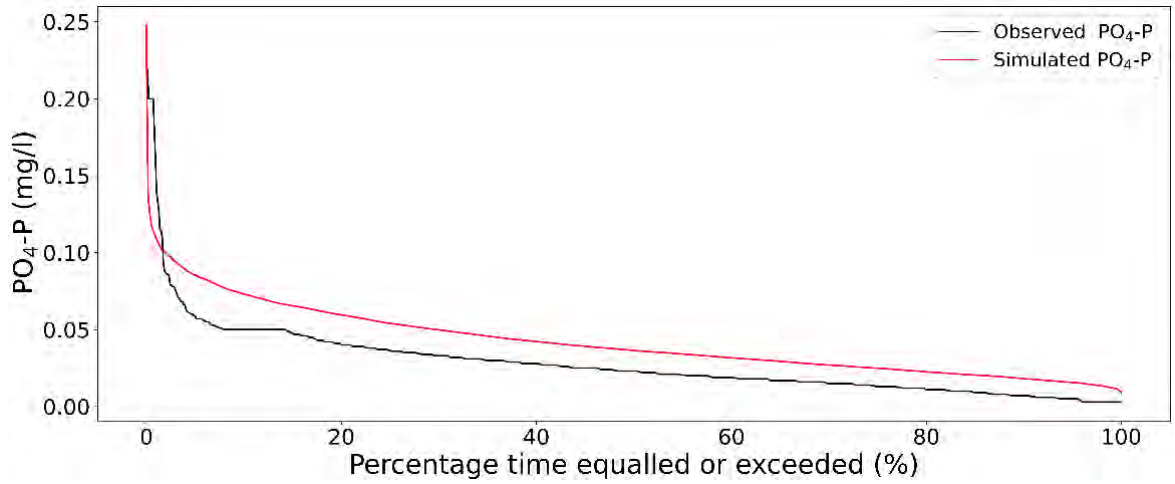

Figure 4.11: Comparison of observed phosphate to that simulated by the Pywr-WQ model for the Grootdraai Dam node in the Upper Vaal River Catchment, South Africa, presented as a frequency distribution graph over the entire period (1920–2010).

4.3.5 Salts

The Pywr-WQ model incorporates processes related to various ions, including calcium, fluoride, potassium, chloride, sulphate, magnesium, and sodium. The simulations yielded favourable NSE results, with potassium, calcium, and sodium estimated at 0.83, 0.89, and 0.81, respectively. Figures 4.12 present frequency distribution graphs comparing observed versus simulated concentrations of potassium, calcium, and sodium for the Grootdraai Dam node throughout the entire simulation period from 1920 to 2010. However, the other simulated salts such as fluoride, chloride, magnesium, and sulphate showed different behaviour with fair to good NSE values estimated at 0.62, 0.66, 0.71, and 0.74, respectively.

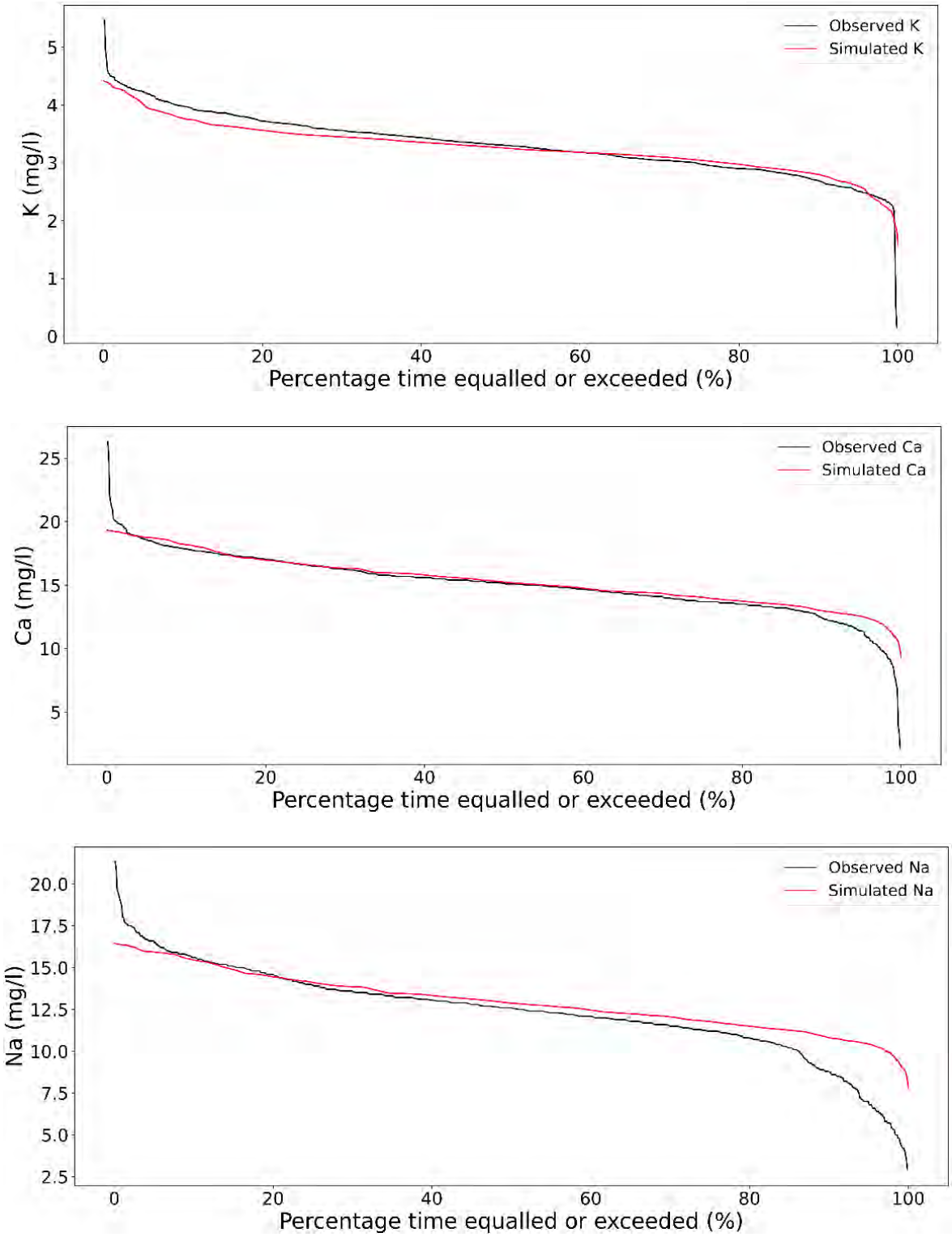

Figure 4.12: Comparison of observed potassium, calcium, and sodium to that simulated by the Pywr-WQ model for the Grootdraai Dam node in the Upper Vaal River Catchment, South Africa, presented as a frequency distribution graph over the entire period (1920–2010).

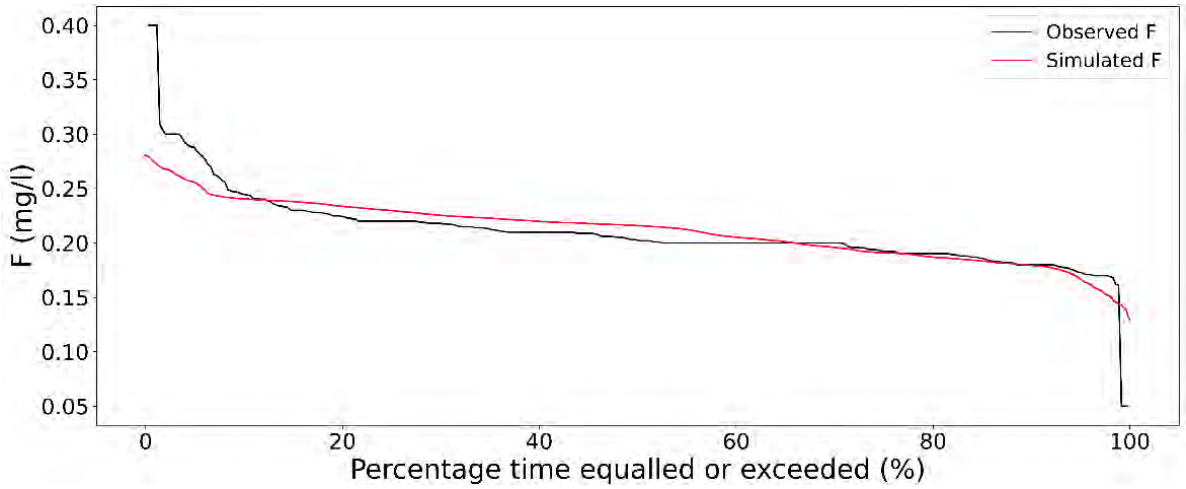

Figure 4.13: Comparison of observed fluoride to that simulated by the Pywr-WQ model for the Grootdraai Dam node in the Upper Vaal River Catchment, South Africa, presented as a frequency distribution graph over the entire period (1920–2010).

Figure 4.13 and Figure 4.14 present frequency distribution graphs comparing observed versus simulated concentrations of fluoride and chloride, magnesium, and sulphate for the Grootdraai Dam node throughout the entire simulation period from 1920 to 2010.

According to Slaughter et al. (2017), the challenge of data scarcity is heightened, particularly concerning water quality data in South Africa. The discrepancies observed in simulated salts, possibly linked to data scarcity at specific nodes within the Grootdraai Dam Catchment, ultimately impacted the calibration at the Dam level. The salt signatures for surface water, interflow, and groundwater flow are presented in Appendix C.

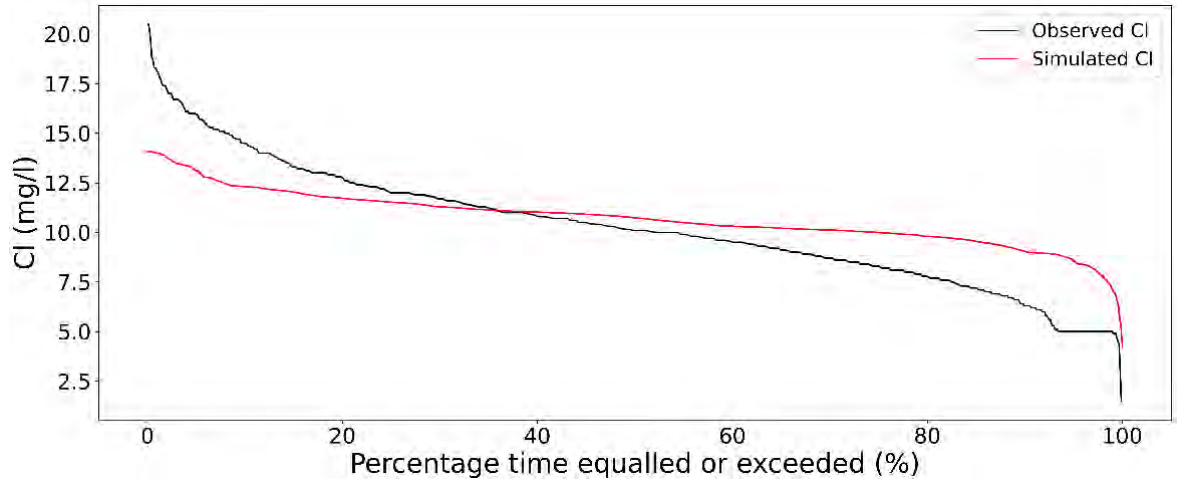

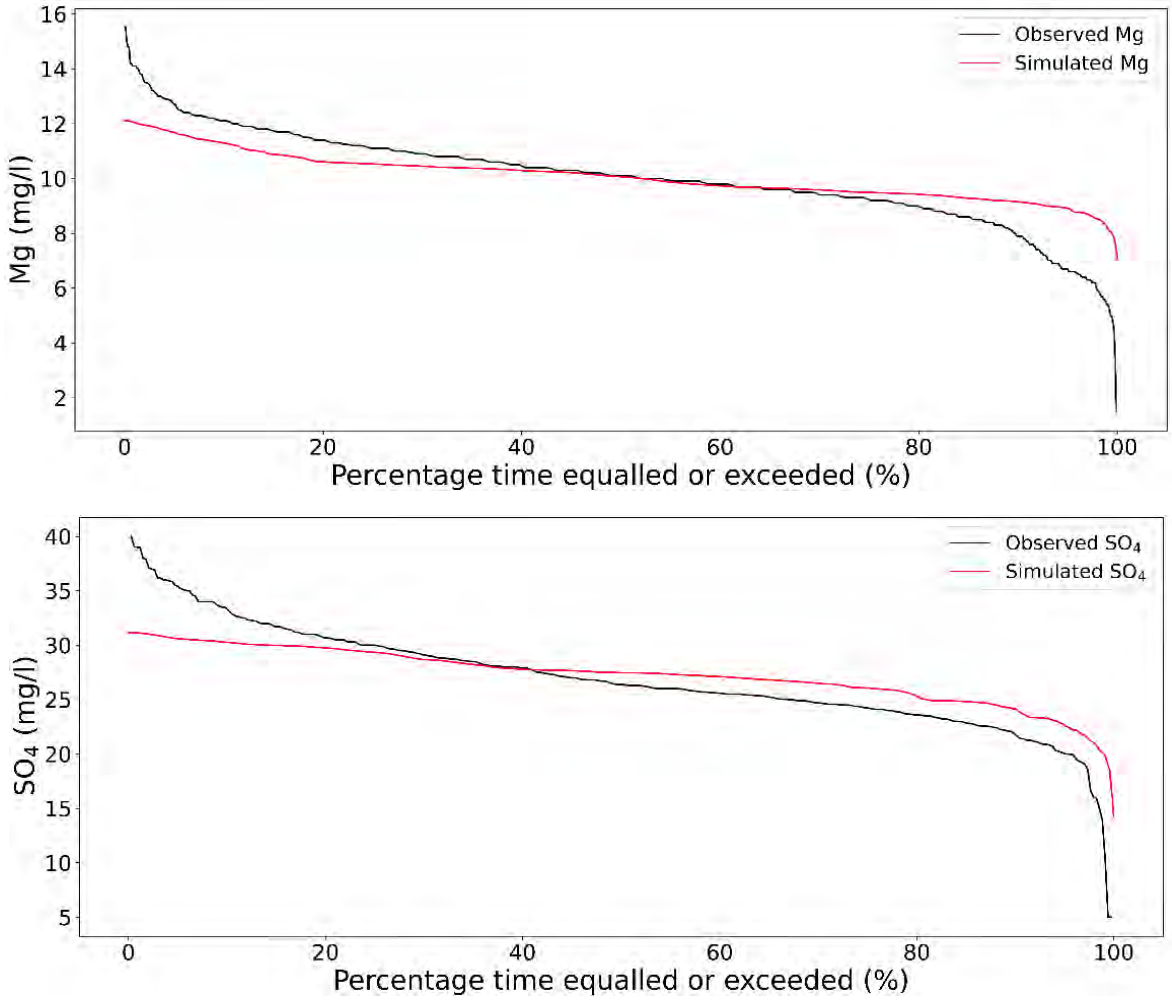

Figure 4.14: A comparison of observed chloride, magnesium, and sulphate to that simulated by the Pywr-WQ model for the Grootdraai Dam node in the Upper Vaal River Catchment in South Africa, presented as a frequency distribution graph over the entire period (1920 – 2010).

4.4 Discussion

4.4.1 Uncertainties within the water quality representation

The Pywr-WQ model relies on incremental flow fraction signatures (i.e., fractions of surface flow, interflow, and groundwater flow) to simulate non-point source loads. These signatures are concentration values assigned to different flow fractions that were determined by calibrating the model against observed data. While land-use exhibits a significant impact on water quality (Kändler et al., 2017), in particular, non-point source loads (Charbonneau & Kondolf, 1993; Cheng et al., 2018), the method of representing non-point sources is considered conceptually sound according to Slaughter et al. (2017). However, a notable uncertainty lies in the absence of observed return flow data in terms of flow, which could potentially affect model accuracy.

This study lacked enough water quality data to perform a split calibration-validation approach. Owing to this limitation, all available water quality data were used exclusively for the calibration exercise. It is worth noting that this approach, criticised by Thomann (1998), questions the logic of neatly dividing datasets into calibration and validation sets, emphasising that new insights continuously emerge with increasing data.

4.4.2 The use of Pywr-WQ within water resource management

The Pywr-WQ model holds significant promise for integration into water quality management practices in South Africa. Being an open-source and free tool, Pywr-WQ offers accessibility to a wide range of users. As demonstrated in Chapter 3, Pywr allows for the spatially distributed representation of catchments at a daily time-step, facilitating water quality modelling. Despite its complexity, the model remains relatively simple, enabling accurate simulations of water quality even with limited observed data. Notably, Pywr-WQ represents water quality as a frequency distribution, facilitating the assessment of how often water quality exceeds certain thresholds, such as Resource Quality Objectives (RQOs). This feature enhances decision-making processes by providing insights into potential water quality issues and aids in evaluating the feasibility of abstraction from specific nodes or reservoirs. To illustrate, Figure 4.16 presents the frequency distribution graphs of TDS, NO_3-N + NO_2-N, and NH_4-N concentrations at Grootdraai Dam. According to Rand Water (2022), water quality guidelines for tributaries within the Grootdraai Dam Catchment (Appendix C) target various classifications, including concentrations under acceptable classification for TDS, NO_3-N + NO_2-N, and NH_4-N of less than or equal to 150, 0.2, and 0.1 $mg.l^{-1}$, respectively.

It becomes apparent from Figure 4.15 that under historical management conditions, these thresholds are exceeded approximately 51%, 70%, and 15% of the time, respectively.

Through scenario analysis and re-execution of the model involving various management interventions, such as the closure of mining areas to reduce mine effluent, the frequency distribution can be recalculated. Subsequently, managers are presented with a revised probability of exceeding this threshold. In addition to its primary functions, the Pywr-WQ model offers water managers a powerful tool for evaluating the influence of water abstraction on water quality within a given catchment.

The Rand water quality guidelines for the Grootdraai Dam are presented in Appendix E.

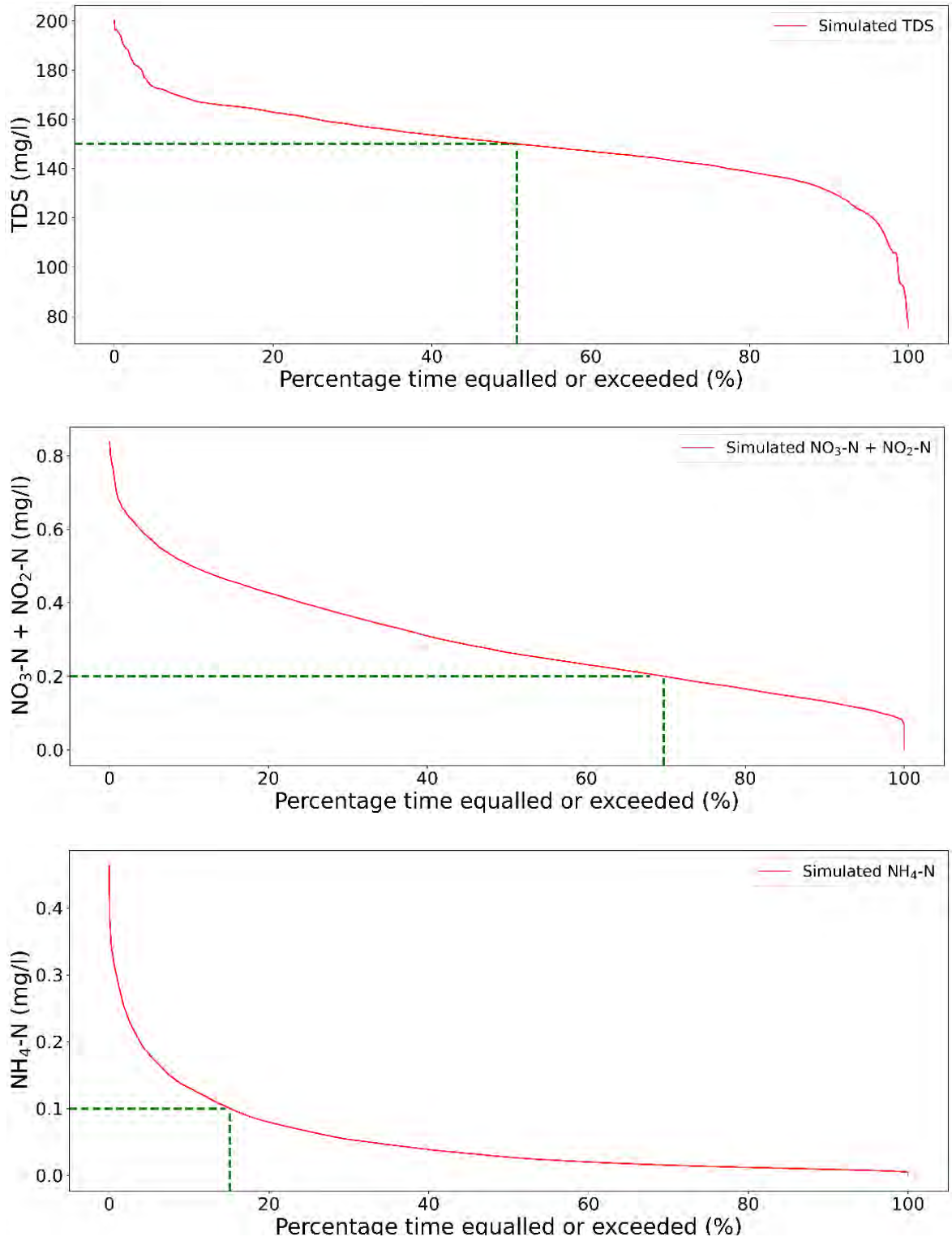

Figure 4.15: Frequency distributions of modelled and observed TDS, nitrite + nitrate, and ammonium for the Grootdraai Dam node in the Upper Vaal River Catchment, South Africa. The green line represents how the frequency distribution of simulated concentrations enables water resource managers to assess the likelihood of surpassing specific management thresholds using the Rand Water (2022) classification.

While Pywr-WQ is designed as a fully dynamic model, it is important to note that this study did not extensively explore the capacity to utilise water quality data for allocation decisions. However, to illustrate this capability briefly, Figures 4.16 and 4.17 provide a glimpse into the potential of Pywr-WQ in integrating water quality considerations into resource allocation strategies. If a specific threshold is exceeded, the model adopts a binary on-off approach to water abstraction from that node, thereby preventing high concentrations and facilitating water quality enhancement by augmenting dilution capacity. However, Pywr-WQ 's flexibility allows for the implementation of more nuanced interactions between water quality and quantity. For instance, instead of a simple binary representation, the model can incorporate complex relationships where the degree of allocation curtailment by water quality follows a curve.

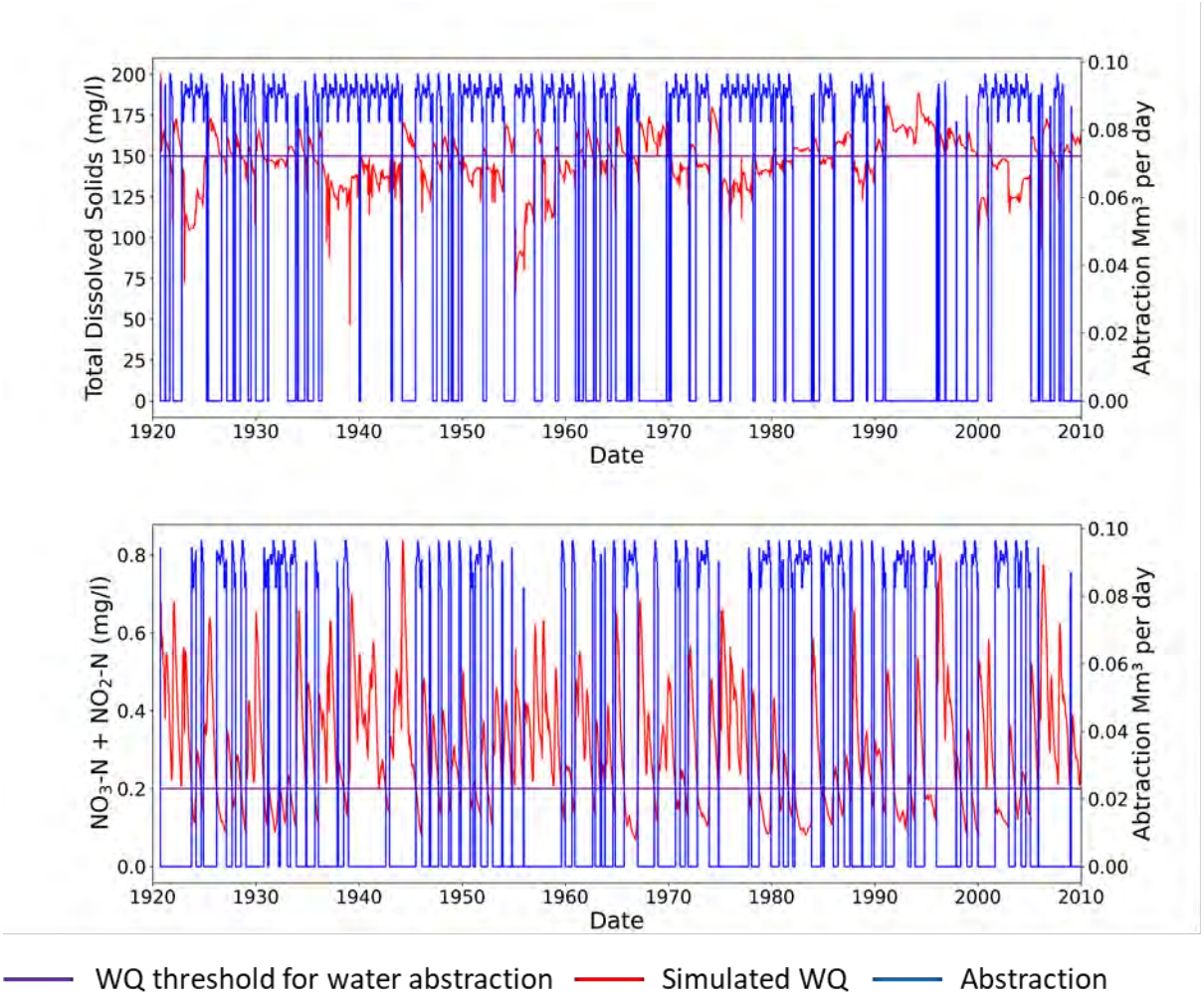

Figure 4.16: Graph showing switching off abstraction at the Grootdraai Dam at thresholds of water quality of total dissolved solids of 150 mg.l^{-1} and NO_3-N + NO_2-N of 0.2 mg.l^{-1}.

Furthermore, Pywr-WQ can dynamically select water from different upstream sources to attain the desired water quality in downstream reservoirs. For example, by selecting different quantities

of water from distinct transfers into the Grootdraai Dam Catchment, each with differing water qualities, Pywr-WQ can adapt to achieve optimal water quality in the dam. Additionally, considerations such as cost reduction objectives can also be factored into the model's decision-making process.

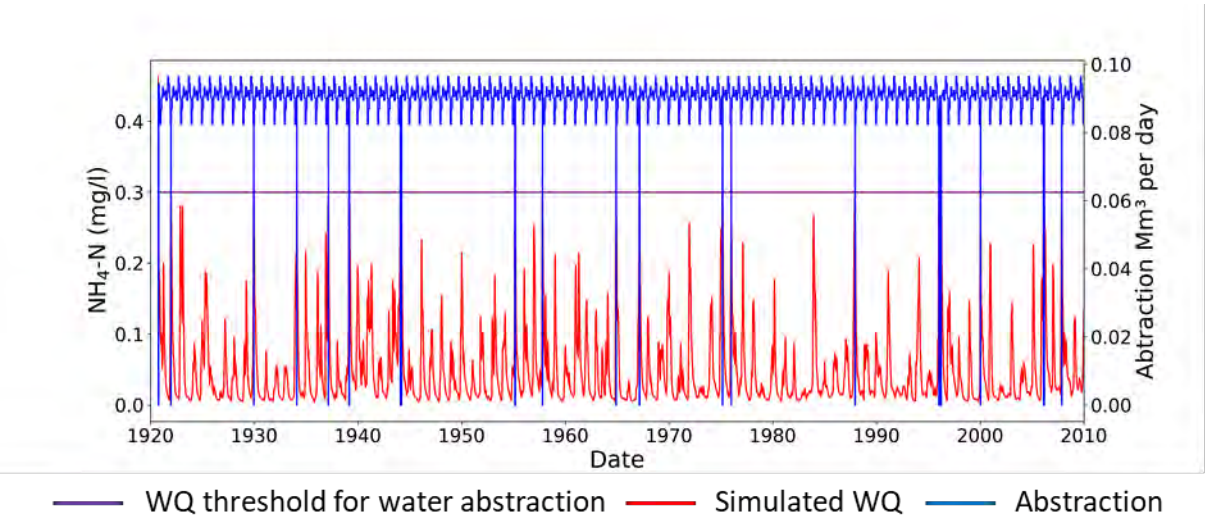

Figure 4.17: Graph showing switching off abstraction at the Grootdraai Dam at thresholds of water quality of ammonium of 0.3 $mg.l^{-1}$.

4.5 Conclusion

This study applies the Pywr-WQ, developed by the Water Research centre (WRc) in the United Kingdom, to the case study catchment. This model is designed for simplicity to necessitate minimal complexity and rely on available historical monitoring data for calibration. The Pywr-WQ model operates on flow data generated by a transparent, open-source, daily system model. This study demonstrates that the Pywr-WQ model can accurately generate daily concentrations of salinity, salts, and nutrients suitable for water quality management. This model holds potential applications in water resource management for various developing countries confronting financial and data constraints. The successful integration observed in this study between the Pywr system model and the water quality model, resulting in the Pywr-WQ mode, suggests a seamless connection that could be replicated in similar contexts

CHAPTER 5: LAND-COVER MODELS TO PREDICT NON-POINT NUTRIENT AND SALT INPUTS FOR THE GROOTDRAAI DAM CATCHMENT, UPPER VAAL, SOUTH AFRICA

5.1 Introduction

Water quality models are used to simulate and forecast the concentrations, spatial distributions, and potential risks associated with chemical pollutants within surface water bodies (Wang et al., 2013), and groundwater flow (Gao & Li, 2015). Water quality models are indispensable for managing water resources; they can offer a detailed understanding of hydrological processes and dynamics, enabling analysis of the impacts of climate change and land-use changes on water quality (Krysanova et al., 1998). Consequently, they can predict the behaviour of water systems and act as decision support systems (DSS) for addressing water management problems (Argent et al., 2009).

In the South African context, the National Water Act (NWA) of 36 of 1998 acknowledges the significance of water quality protection and delineates procedures for establishing resource quality objectives (Makanda et al., 2022). This positions water quality models as valuable contributors to the development of policies and regulations. However, their application within South Africa faces critical challenges. The main constraints limiting the use of these models include the deficiency of essential competencies, a shortage of adequately skilled individuals, and the decrease in observed hydrological data, which raises significant concerns, particularly concerning issues related to water quality (Pitman, 2011). Additional challenges stem from the scarcity of observed data (Slaughter & Mantel, 2017), and limited financial resources, restricting the range of potential models that can be employed in the region (Ngubane et al., 2022).

The Pywr-WQ model showcased the use of a collaborative approach between an open-source, fast, transparent, distributed, daily-step, and user-friendly water simulation model named the Pywr model, according to Tomlinson et al. (2020), and a water quality model. This dynamic integration resulted in the creation of the Pywr-WQ model. The Pywr-WQ model demonstrated its effectiveness in simulating nutrients and salts within the Grootdraai Dam Catchment.

Non-point sources, exemplified by agricultural runoff, urban areas, and atmospheric deposition, pose a considerable challenge to water quality modelling and models in general, as indicated by various studies (León et al., 2001; Rudra et al., 2020; Shen et al., 2012). These sources present challenges due to their diverse and often untraceable origins. Unlike specific point sources isolated to a particular spatial point, and easily monitored (Vaughan & Russell, 1983), non-point

sources, such as nitrogen in the landscape, exhibit spatial variability distributed across landscapes, as evidenced in a study by Zhang & Huang (2011). Moreover, non-point sources are diffusive and are transported primarily by catchment rainfall-runoff and groundwater inputs, as demonstrated in a study by Xie et al. (2019). Incorporating spatial dimensions into water quality assessment, as affirmed by Mouri et al. (2011), enriches our comprehension of spatial patterns, with non-point sources displaying strong positive spatial autocorrelation. Consequently, understanding non-point source loads into water systems may hinge significantly on spatial-temporal scales; however, existing water quality models may inadequately address this challenge (Slaughter & Mantel, 2017). The Pywr-WQ model may also encounter the aforementioned challenges, particularly in the parameterisation of non-point sources (such as flow fraction signatures) during the calibration exercise. This process introduces uncertainty, particularly due to the limited availability of observed water quality data at finer spatial and temporal scales in the region.

Previous studies in South Africa have focused on understanding the correlation between non-point sources of pollutants and distinct land-cover categories. For example, Slaughter & Mantel, (2013) devised a practical model to establish a link between in-stream nutrient concentrations and land-cover categories within a catchment. Nevertheless, their investigation revealed challenges in accurately quantifying non-point nutrient inputs, primarily due to the significant spatial and temporal variations in nutrient inputs. Slaughter & Mantel (2017) conducted a further study introducing a formal model that correlates nutrient signatures of incremental flow with land-cover. However, their research was anchored in the simulation from the WQSAM linked to the WRYM, and the results of the regression model results used in the already calibrated WQSAM. Nonetheless, a challenge arises from the coarse classification of land-cover, contributing to the overall uncertainty in water quality modelling and the estimation of non-point inputs of pollutants into rivers.

In response to the current context and challenges, this study aimed to contribute by examining the relationship between land-cover categories and the loads from non-point sources. The objectives of this study include: (1) creating land-cover models for the quaternary catchments within the study area; (2) examining the links between land cover and water quality signatures of incremental flow; and (3) evaluating land-use scenarios to understand their medium and long term effects on water quality in the Grootdraai Dam Catchment.

5.2 Methods and Materials

5.2.1 Study catchment

The Grootdraai Dam Catchment comprises 11 quaternary catchments, with each receiving incremental flow. Within the model representation, an inflow node is positioned within each quaternary catchment. Figure 5.1 illustrates the incremental nodes within the study area, denoted by the prefix "Inflow_X", where "X" ranges from 1 to 11, distributed across the study area (refer to Chapter 3, Section 3.2.3, for a detailed explanation of the model representation of the catchment).

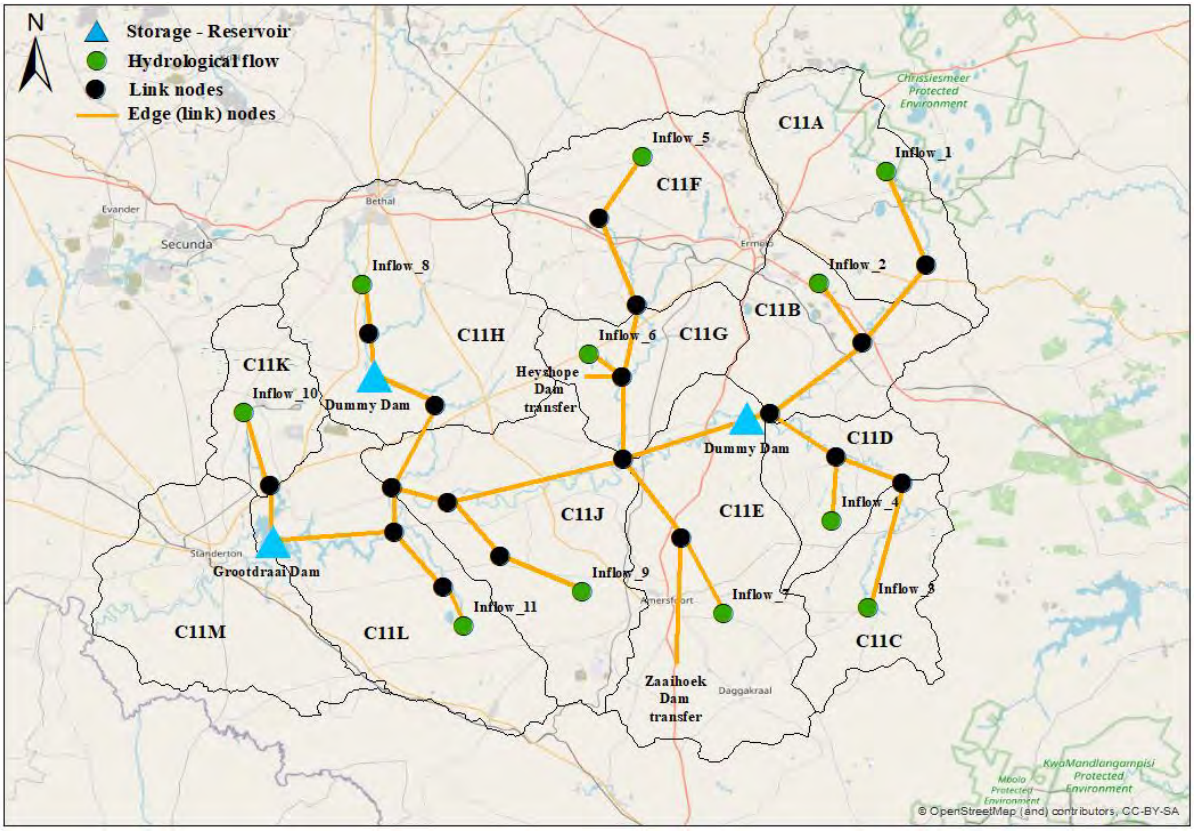

Figure 5.1: Representation of the Grootdraai Dam Catchment within the broader Upper Vaal catchment, South Africa. The map shows the quaternary catchments and provides geospatial coordinates for the inflow nodes incorporated in the Pywr-WQ model.

The water quality of Grootdraai Dam is influenced by multiple quaternary catchments situated upstream of the reservoir. These catchments undergo various water quality processes, encompassing non-point loads, point source loads, and in-stream processes. It proves challenging to isolate non-point source loads; consequently, the selection process involved choosing each quaternary catchment that receives incremental flow, recognising that some of these catchments may be located within landscapes containing informal settlements, towns, or cities that could influence non-point source loads in river streams. Further, it was assumed that these selected

quaternary catchments experience sufficient rainfall-runoff, facilitating the mobilisation of non-point source loads. As a presupposition, it is expected that the chosen quaternary catchments possess an adequate quantity of complete daily flow records and a substantial volume of available water quality data.

Based on these assumptions, 11 quaternary catchments were identified as receivers of incremental flow and deemed suitable for the objectives of this study. Table 5.1 provides a list of the identified quaternary catchments, while Figure 5.2 presents the land-cover and land-use characteristics of the quaternary catchments corresponding to the designated nodes.

Table 5.1: Properties of the incremental flow nodes in the study area.

Node name	Node coordinates		Quat.
	Long	Lat	
Inflow_1	30.17	−26.41	C11A
Inflow_2	30.07	−26.57	C11B
Inflow_3	30.14	−27.01	C11C
Inflow_4	30.09	−26.89	C11D
Inflow_5	29.83	−26.99	C11F
Inflow_6	29.92	−26.66	C11G
Inflow_7	29.94	−27.02	C11E
Inflow_8	29.44	−26.57	C11H
Inflow_9	29.75	−26.99	C11J
Inflow_10	29.28	−26.74	C11K
Inflow_11	29.58	−27.04	C11L

5.2.2 Data

The simulated daily flow datasets were generated for each incremental node within the period from 1920 to 2010. These datasets were acquired utilising the Pywr model, a water simulation model previously employed for the Grootdraai Dam Catchment (Chapter 3: Section 3.2.3.3). Concurrently, water quality data corresponding to each inflow node, sourced from the DWS monitoring data, were examined within the same temporal framework (Chapter 4). The focal point of this investigation revolved around nutrients and salts, with a specific emphasis on nitrate plus nitrite, ammonium, phosphate, TDS, sulphate, and calcium. These particular water quality variables were chosen owing to their prevalent association with non-point source loads

originating from urban areas, cultivated regions, mining areas, and potential undetected leakages from wastewater pipes. Recognised as key variables, they hold substantial significance in contributing to the eutrophication process (Payen et al., 2021; Yan et al., 2021), and to salinity and acidification contamination (Hintz et al., 2022; Hobbs et al., 2008). Land-cover data was obtained from the Landsat images provided by the Southern African National Land-cover (SANLC) [GIS Data Downloads | EGIS (environment.gov.za)] for the years 2013 and 2020. Land cover and land use for the Grootdraai Dam Catchment for 2020 are illustrated in Figure 5.2.

The land-cover dataset was clipped by the positioned inflow node, and quaternary catchment's shapefile, for each catchment, and ArcMap 10.8 functions were utilised to compute the areas under each land-cover class in the catchment. The original dataset contained 42 land-cover classes which were grouped into eight categories for the present study (Table 5.2). The classification was done to avoid any uncertainty that could be imposed by the large number of land-cover classes on statistical analysis, such as multiple regression. Hence, land-cover classes that were similar were grouped, such as temporary crops, fallow land, and old fields. This study investigated the relationship between land-cover and non-point source loads considering all land-cover within quaternary catchments.

Table 5.2: Grouping land-cover categories from the South African National Land-cover Dataset (NLC 2013–2020) into more representative land-cover categories for the current study.

Code	Param	Grouped land-cover category	Original land-cover classes
A	α	Barren land	Barren land (natural, rock surfaces); barren land (dry pans); barren land (eroded lands); barren land (bare riverbed materials); barren land (other bare).
B	β	Urban/ Built-Up	Urban/built-up (residential, formal tree); urban/built-up (residential, formal bush); urban/built-up (residential, formal low vegetation); urban/built-up (residential, formal bare); urban/built-up (residential formal, grass combination); urban/built-up (industrial); urban/built-up (roads and rails).
C	γ	Cultivated land	Cultivated land (commercial, permanent orchards); cultivated land (commercial, annual crops, pivot irrigated); cultivated land (commercial, annual crops, non-pivot

Code	Param	Grouped land-cover category	Original land-cover classes
			irrigated); cultivated land (commercial, annual crops, rain-fed / dryland); cultivated land (fallow land and old field; e.g., trees, bush, grass, bare).
D	δ	Forested land	Forested land (contiguous forest); forested land (dense forest and woodland); forested land (open plantation forest); forested land (temporary unplanted forest).
E	ε	Grassland	Grassland (natural grassland).
F	ζ	Mines and Quarries	Mines and quarries (mines, extraction pits)
G	η	Waterbodies	Waterbodies (natural rivers); waterbodies (natural pans); waterbodies (artificial dams).
H	θ	Wetlands	Wetlands (herbaceous wetlands)

5.2.3 Pywr-WQ model calibration

The Pywr-WQ model setup was created for the Grootdraai Dam Catchment encompassing those quaternary catchments. The generated period of daily flow datasets for each quaternary catchment was used as flow data in the Pywr-WQ model to drive water quality simulations. Hence, the baseflow separation part (Hughes et al., 2003) is applied to the utilised flow datasets. The baseflow separation method separates incremental flow into three flow fractions: surface water flow, interflow, and groundwater flow, and the method requires the setting of two parameter values: α_{SF} and α_{BF} (Chapter 4). In this study, the investigation centred exclusively on establishing correlations between surface water flow, groundwater flow concentrations, and land-cover. While the relationships between land-cover and subsurface flow fractions are less certain and operate on distinct spatial and temporal scales compared to surface water (Slaughter & Mantel, 2017), this study addresses and delves into this challenging aspect.

The Pywr-WQ model was utilised, and adjustments were made solely to parameters associated with the surface flow, groundwater flow fraction nutrient (SF_N), and salts (GWF_S) signatures. In the Pywr-WQ model, configuring the various flow signatures primarily constitutes a calibration exercise. This is essential to accurately represent the highly temporally variable water quality measures observed in the data. Adjustments to the surface flow nutrient signature (SF_N) and

groundwater flow (GWF_S) signatures enable the simulation to mirror these variations. After the calibration process with observed data concluded, the water quality signatures assigned to the surface water flow fraction in each catchment were gathered for subsequent analyses. The process of calibration is thoroughly explained in Chapter 4, specifically in Section 4.2.7.

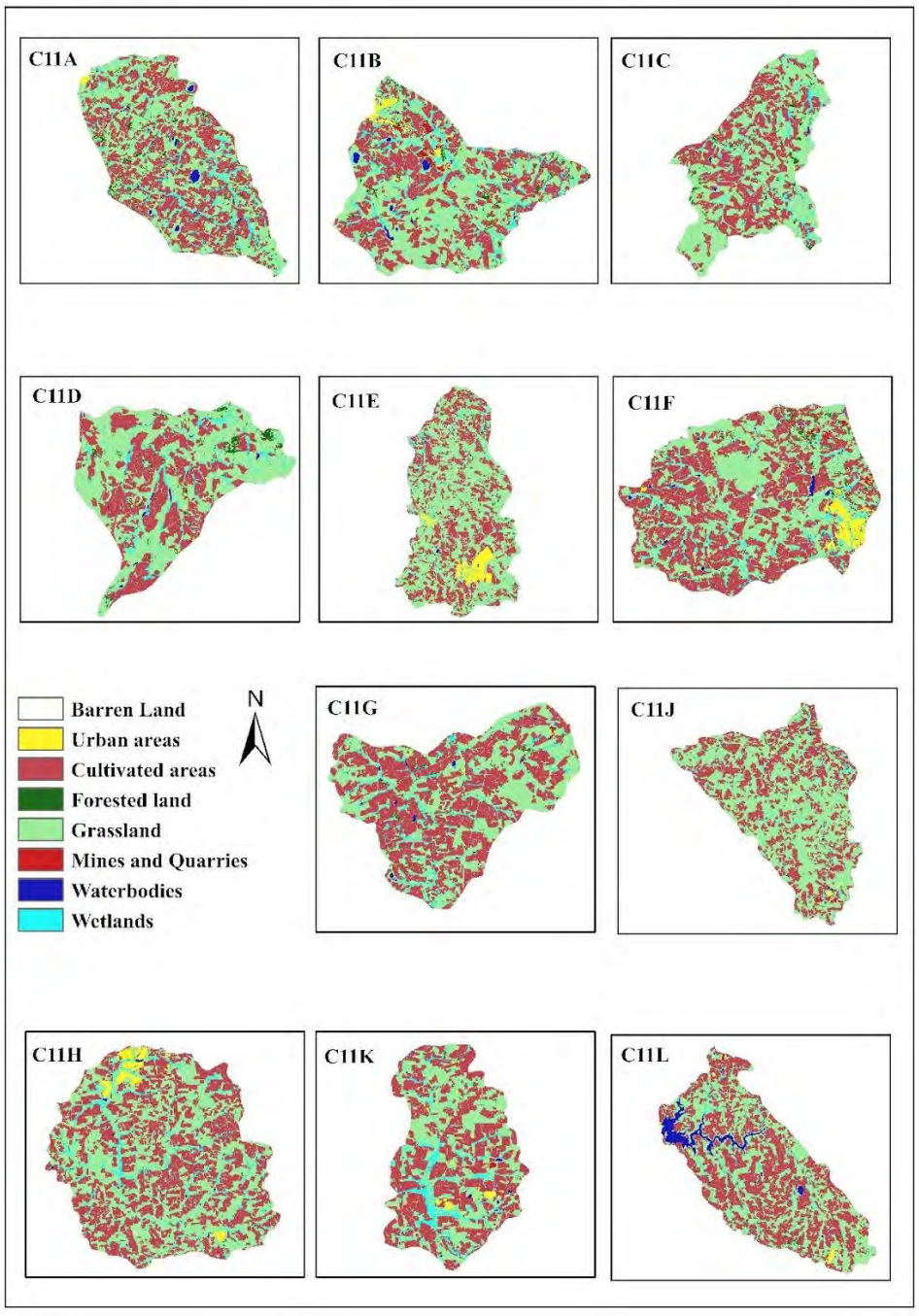

Figure 5.2: Land-cover and land-use of quaternary catchments within the study area.

5.2.4 Multiple regression model development

Multiple regression was employed to investigate the intricate relationships between surface flow (SF_N) (Eq 5.1), groundwater flow (GWF_S) (Eq 5.2) water quality signatures, and land-cover components associated with nutrient and salt content. The distribution of land-cover types within each quaternary catchment was investigated in terms of their proportional representation concerning the total area. This approach aligns with previous studies, such as the work by Slaughter & Mantel (2017). The multiple regression models were conducted using regression equations with the general form of:

$$SF_N = \alpha \times A + \beta \times B + \gamma \times C + \delta \times D + \varepsilon \times E + \zeta \times F + \eta \times G + \theta \times H \quad (5.1)$$

$$GWF_s = \alpha \times A + \beta \times B + \gamma \times C + \delta \times D + \varepsilon \times E + \zeta \times F + \eta \times G + \theta \times H \quad (5.2)$$

where: A-H represents the land-cover categories mentioned earlier, as fractions of the total area (see Table 5.1), α-θ represents the regression parameters applied to respective land-cover categories. The Chi-square statistic, serving as an evaluative metric for the goodness-of-fit of each regression, was employed.

Equation 5.1 was employed to construct nutrient land-cover models for every quaternary catchment, while equation 5.2 was exclusively utilised to create salt land-cover models for specific quaternary catchments, namely C11A, C11B, C11F, and C11K. This selection was driven by the substantial prevalence of mining areas in these regions and the identified high groundwater flow signatures for TDS, sulphate, and calcium observed in these specific areas.

5.2.5 Land-cover and land-use scenarios

In the present study, the examination of land-cover scenarios centred on three primary drivers, as suggested by the catchment stakeholders. These drivers encompass (i) population growth, (ii) expansion of cultivated areas and (iii) intensive mining areas. Figure 5.3 illustrates the scenarios, pressure, state, and potential implications on water quality.

Investigating various scenarios delineated in Figure 5.3, this study recognises distinctive stressors associated with each scenario. These stressors encompass escalated sewage levels, augmented mobilisation of fertilisers through runoff attributed to potentially unsupervised, illegal irrigation practices, and the spread of heavy metals through soil-water mobilisation stemming from acid mine drainage from coal mines within the study area. The identified stressors have direct ramifications for water quality, precipitating substantial influxes of nutrients, TDS,

and salts into the water. These phenomena engender challenges such as eutrophication, the excess of algal and plant growth, potential biodiversity loss, and other associated ecological damage.

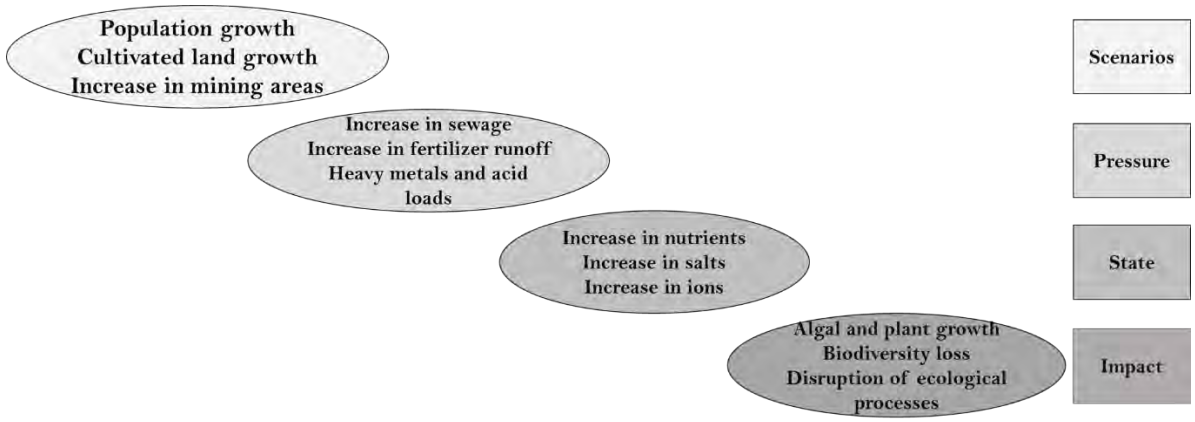

Figure 5.3: Analytical framework for land-cover model scenarios investigation.

The proposed adjustments for each pertinent land-cover type were determined by meticulously comparing the earlier 2013 land-cover data with the most recent 2020 data. This enabled quantifying the potential range of growth that could be justified. Specific percentage values were then allocated to distinct land-cover categories (e.g., urban, mines, and cultivated) based on this assessment.

Table 5.3: Scenario definitions and corresponding water quality variables.

Scenario	Scenario code	Characteristics	Investigated Water Quality Variables
Urban increase	A	High population density. Intensive infrastructure.	NO_3-N+NO_2-N, NH_4-N, PO_4-P TDS, SO_4, Ca
Cultivated increase	B	Agricultural land-use.	NO_3-N+NO_2-N, NH_4-N, PO_4-P
Mining increase	C	Industry activities rely on coal mines.	NO_3-N+NO_2-N, NH_4-N, PO_4-P TDS, SO_4, Ca

To compute the growth rate of individual land-cover categories, a growth rate formula was employed. This formula involved subtracting the land-cover percentage of 2013 from that of 2020 and dividing the resultant difference by the intervening seven years. The modelled growth is an expansion of observed growth rates from 2013 to 2020. Thus, Table 5.3 shows the investigated scenarios and their characteristics, and the investigated water quality variables in each scenario.

It is important to emphasise that when a specific land-cover class among the investigated scenarios experienced an increase, the other investigated land-cover classes remain unchanged, maintaining their 2020 percentages. For example, if there is an increase in the urban area by a certain percentage, the percentages for mining and cultivated land-cover classes will remain at their 2020 levels. This decision was made to prevent any conflicts in scenario investigations. Noteworthy changes will be more pronounced in other land-cover classes, such as forested land, barren land, wetlands, and water bodies.

To illustrate, Table 5.4 shows an example of what has been already explained for all quaternary catchments located at the Grootdraai Dam Catchment.

Table 5.4: Predictions of land-cover classes in the event of a certain rate growth %/year increase in urban (built-up), cultivated land, and mining land-cover within the quaternary catchments in the study area.

Land-cover classes	**Average change rate per year (%)**	**Current situation**	**Medium term**	**Long term**
		2020 (%)	**Horizon 2050 (%)**	**Horizon 2099 (%)**
		C11A		
		Scenario A		
Urban (built-up)	**0.04**	**0.64**	**1.84**	**3.80**
Cultivated land	-	42.44	42.44	42.44
Mines	-	0.33	0.33	0.33
Forested land	-	3.73	3.65	3.52
Grassland	-	44.93	43.98	42.42
Wetland	-	6.51	6.37	6.15
Water bodies	-	1.42	1.39	1.34
		Scenario B		
Urban (built-up)	-	0.64	0.64	0.64
Cultivated land	**0.42**	**42.44**	**55.04**	**75.62**
Mines	-	0.33	0.33	0.33
Forested land	-	3.73	2.90	1.54
Grassland	-	44.93	34.93	18.59
Wetland	-	6.51	5.06	2.69
Water bodies	-	1.42	1.10	0.59
		Scenario C		
Urban (built-up)	-	0.64	0.64	0.64
Cultivated land	-	42.44	42.44	42.44
Mines	**0.03**	**0.33**	**1.23**	**2.70**
Forested land	-	3.73	3.67	3.57
Grassland	-	44.93	44.22	43.05
Wetland	-	6.51	6.41	6.24
Water bodies	-	1.42	1.40	1.36
		C11B		
		Scenario A		

Land-cover classes	Average change rate per year (%)	Current situation	Medium term	Long term
		2020 (%)	Horizon 2050 (%)	Horizon 2099 (%)
Urban (built-up)	**0.03**	**1.58**	**2.48**	**3.59**
Cultivated land	-	36.77	36.77	36.77
Mines	-	1.82	1.82	1.82
Forested land	-	2.56	2.52	2.47
Grassland	-	48.46	47.73	46.83
Wetland	-	7.44	7.33	7.19
Water bodies	-	1.16	1.14	1.12
Barren land	-	0.21	0.21	0.20
		Scenario B		
Urban (built-up)	-	1.58	1.58	1.58
Cultivated land	**0.4**	**36.77**	**48.77**	**68.7**
Mines	-	1.82	1.82	1.82
Forested land	-	2.56	2.05	1.19
Grassland	-	48.46	38.74	22.60
Wetland	-	7.44	5.95	3.47
Water bodies	-	1.16	0.93	0.54
Barren land		0.21	0.17	0.10
		Scenario C		
Urban (built-up)	-	1.58	1.58	1.58
Cultivated land	-	36.77	36.77	36.77
Mines	**0.001**	**1.82**	**1.85**	**1.90**
Forested land	-	2.56	2.56	2.56
Grassland	-	48.46	48.44	48.40
Wetland	-	7.44	7.44	7.43
Water bodies		1.16	1.16	1.16
Barren land	-	0.21	0.21	0.21
		C11C		
		Scenario A		
Urban (built-up)	**0.02**	**0.18**	**0.78**	**1.76**
Cultivated land	-	38.35	38.35	38.35
Mines	-	0.033	0.033	0.033
Forested land	-	2.48	2.46	2.42
Grassland	-	52.75	52.23	51.39
Wetland	-	5.75	5.69	5.60
Water bodies	-	0.28	0.28	0.27
Barren land	-	0.177	0.18	0.17
		Scenario B		
Urban (built-up)	-	0.18	0.18	0.18
Cultivated land	**0.5**	**38.35**	**53.35**	**77.85**
Mines	-	0.033	0.033	0.033
Forested land	-	2.48	1.87	0.89
Grassland	-	52.75	39.87	18.84
Wetland	-	5.75	4.35	2.05
Water bodies	-	0.28	0.21	0.10

Land-cover classes	Average change rate per year (%)	Current situation	Medium term	Long term
		2020 (%)	Horizon 2050 (%)	Horizon 2099 (%)
Barren land		0.177	0.13	0.06
		Scenario C		
Urban (built-up)	-	0.18	0.18	0.18
Cultivated land	-	38.35	38.35	38.35
Mines	**0.001**	**0.033**	**0.06**	**0.11**
Forested land	-	2.48	2.48	2.48
Grassland	-	52.75	52.73	52.68
Wetland	-	5.75	5.75	5.74
Water bodies		0.28	0.28	0.28
Barren land	-	0.177	0.18	0.18
		C11D		
		Scenario A		
Urban (built-up)	**0.02**	**0.24**	**0.84**	**1.82**
Cultivated land	-	36.55	36.55	36.55
Mines	-	0	0	0
Forested land	-	2.85	2.82	2.78
Grassland	-	54.33	53.81	52.97
Wetland	-	5.42	5.37	5.28
Water bodies	-	0.47	0.47	0.46
Barren land	-	0.14	0.14	0.14
		Scenario B		
Urban (built-up)	-	0.24	0.24	0.24
Cultivated land	**0.46**	**36.55**	**50.35**	**72.89**
Mines	-	0	0	0
Forested land	-	2.85	2.23	1.21
Grassland	-	54.33	42.47	23.10
Wetland	-	5.42	4.24	2.30
Water bodies	-	0.47	0.37	0.20
Barren land		0.14	0.11	0.06
		Scenario C		
Urban (built-up)	-	0.24	0.24	0.24
Cultivated land	-	36.55	36.55	36.55
Mines	**0.001**	**0**	**0.03**	**0.079**
Forested land	-	2.85	2.85	2.85
Grassland	-	54.33	54.30	54.26
Wetland	-	5.42	5.42	5.41
Water bodies		0.47	0.47	0.47
Barren land	-	0.14	0.14	0.14
		C11F		
		Scenario A		
Urban (built-up)	**0.1**	**3.0**	**6.0**	**10.9**
Cultivated land	-	44.59	44.59	44.59
Mines	-	0.92	0.92	0.92
Forested land	-	2.37	2.23	2.01

Land-cover classes	Average change rate per year (%)	Current situation	Medium term	Long term
		2020 (%)	Horizon 2050 (%)	Horizon 2099 (%)
Grassland	-	42.81	40.32	36.24
Wetland	-	5.13	4.83	4.34
Water bodies	-	0.9	0.85	0.76
Barren land	-	0.28	0.26	0.24
		Scenario B		
Urban (built-up)	-	3	3	3
Cultivated land	**0.4**	**44.59**	**56.59**	**76.19**
Mines	-	0.92	0.92	0.92
Forested land	-	2.37	1.82	0.92
Grassland	-	42.81	32.83	16.54
Wetland	-	5.13	3.93	1.98
Water bodies	-	0.9	0.69	0.35
Barren land		0.28	0.21	0.11
		Scenario C		
Urban (built-up)	-	3	3	3
Cultivated land	-	44.59	44.59	44.59
Mines	**0.05**	**0.92**	**2.42**	**4.87**
Forested land	-	2.37	2.30	2.19
Grassland	-	42.81	41.56	39.53
Wetland	-	5.13	4.98	4.74
Water bodies		0.9	0.87	0.83
Barren land	-	0.28	0.27	0.26
		C11G		
		Scenario A		
Urban (built-up)	**0.03**	**0.42**	**1.32**	**2.79**
Cultivated land	-	50.65	50.65	50.65
Mines	-	0.132	0.132	0.132
Forested land	-	1.22	1.20	1.16
Grassland	-	41.21	40.45	39.21
Wetland	-	5.53	5.43	5.26
Water bodies	-	0.59	0.58	0.56
Barren land	-	0.248	0.24	0.24
		Scenario B		
Urban (built-up)	-	0.42	0.42	0.42
Cultivated land	**0.5**	**50.65**	**65.65**	**90.15**
Mines	-	0.132	0.132	0.132
Forested land	-	1.22	0.84	0.23
Grassland	-	41.21	28.54	7.85
Wetland	-	5.53	3.83	1.05
Water bodies	-	0.59	0.41	0.11
Barren land		0.248	0.17	0.05
		Scenario C		
Urban (built-up)	-	0.42	0.42	0.42
Cultivated land	-	50.65	50.65	50.65

Land-cover classes	Average change rate per year (%)	Current situation	Medium term	Long term
		2020 (%)	Horizon 2050 (%)	Horizon 2099 (%)
Mines	**0.001**	**0.132**	**2.42**	**4.87**
Forested land	-	1.22	1.16	1.10
Grassland	-	41.21	39.28	37.21
Wetland	-	5.53	5.27	4.99
Water bodies		0.59	0.56	0.53
Barren land	-	0.248	0.24	0.22
		C11E		
		Scenario A		
Urban (built-up)	**0.1**	**4.0**	**7.0**	**11.9**
Cultivated land	-	34.25	34.25	34.25
Mines	-	0.031	0.031	0.031
Forested land	-	1.088	1.04	0.95
Grassland	-	57.13	54.35	49.814
Wetland	-	2.87	2.73	2.50
Water bodies	-	0.356	0.34	0.31
Barren land	-	0.275	0.26	0.24
		Scenario B		
Urban (built-up)	-	4.0	4.0	4.0
Cultivated land	**0.3**	**34.25**	**43.25**	**57.95**
Mines	-	0.031	0.031	0.031
Forested land	-	1.088	0.93	0.67
Grassland	-	57.13	48.80	35.19
Wetland	-	2.87	2.45	1.77
Water bodies	-	0.356	0.30	0.22
Barren land		0.275	0.23	0.17
		Scenario C		
Urban (built-up)	-	4.0	4.0	4.0
Cultivated land	-	34.25	34.25	34.25
Mines	**0.01**	**0.031**	**0.33**	**0.82**
Forested land	-	1.088	1.08	1.07
Grassland	-	57.13	56.85	56.40
Wetland	-	2.87	2.86	2.83
Water bodies		0.356	0.35	0.35
Barren land	-	0.275	0.27	0.27
		C11H		
		Scenario A		
Urban (built-up)	**0.1**	**2.45**	**5.45**	**10.35**
Cultivated land	-	45.23	45.23	45.23
Mines	-	0.011	0.011	0.011
Forested land	-	0.48	0.45	0.41
Grassland	-	45.15	42.56	38.33
Wetland	-	6.02	5.67	5.11
Water bodies	-	0.457	0.43	0.39
Barren land	-	0.202	0.19	0.17

Land-cover classes	Average change rate per year (%)	Current situation	Medium term	Long term
		2020 (%)	Horizon 2050 (%)	Horizon 2099 (%)
		Scenario B		
Urban (built-up)	-	2.45	2.45	2.45
Cultivated land	**0.3**	**45.23**	**54.23**	**68.93**
Mines	-	0.011	0.011	0.011
Forested land	-	0.48	0.40	0.26
Grassland	-	45.15	37.38	24.69
Wetland	-	6.02	4.98	3.29
Water bodies	-	0.457	0.38	0.25
Barren land		0.18	0.17	0.11
		Scenario C		
Urban (built-up)	-	2.45	2.45	2.45
Cultivated land	-	45.23	45.23	45.23
Mines	**0.01**	**0.011**	**0.31**	**0.80**
Forested land	-	0.48	0.48	0.47
Grassland	-	45.15	44.89	44.47
Wetland	-	6.02	5.99	5.93
Water bodies		0.457	0.45	0.45
Barren land	-	0.18	0.20	0.20
		C11L		
		Scenario A		
Urban (built-up)	**0.04**	**0.75**	**1.95**	**3.91**
Cultivated land	-	47.66	47.66	47.66
Mines	-	0.186	0.186	0.186
Forested land	-	0.87	0.85	0.82
Grassland	-	42.11	41.13	39.52
Wetland	-	3.59	3.51	3.37
Water bodies	-	4.63	4.52	4.35
Barren land	-	0.2	0.20	0.19
		Scenario B		
Urban (built-up)	-	0.75	0.75	0.75
Cultivated land	**0.2**	**47.66**	**53.66**	**63.46**
Mines	-	0.186	0.186	0.186
Forested land	-	0.87	0.77	0.60
Grassland	-	42.11	37.19	29.17
Wetland	-	3.59	3.17	2.49
Water bodies	-	4.63	4.09	3.21
Barren land		0.2	0.18	0.14
		Scenario C		
Urban (built-up)	-	0.75	0.75	0.75
Cultivated land	-	47.66	47.66	47.66
Mines	**0.01**	**0.186**	**0.49**	**0.98**
Forested land	-	0.87	0.86	0.86
Grassland	-	42.11	41.86	41.46
Wetland	-	3.59	3.57	3.53

Land-cover classes	Average change rate per year (%)	Current situation	Medium term	Long term
		2020 (%)	Horizon 2050 (%)	Horizon 2099 (%)
Water bodies		4.63	4.60	4.56
Barren land	-	0.2	0.20	0.20
		C11J		
		Scenario A		
Urban (built-up)	**0.02**	**0.4**	**1.0**	**1.98**
Cultivated land	-	36.73	36.73	36.73
Mines	-	0.31	0.31	0.31
Forested land	-	0.56	0.55	0.55
Grassland	-	58.12	57.56	56.65
Wetland	-	3.19	3.16	3.11
Water bodies	-	0.44	0.44	0.43
Barren land	-	0.25	0.25	0.24
		Scenario B		
Urban (built-up)	-	0.4	0.4	0.4
Cultivated land	**0.3**	**36.73**	**45.73**	**60.43**
Mines	-	0.31	0.31	0.31
Forested land	-	0.56	0.48	0.35
Grassland	-	58.12	49.76	36.10
Wetland	-	3.19	2.73	1.98
Water bodies	-	0.44	0.38	0.27
Barren land		0.25	0.21	0.16
		Scenario C		
Urban (built-up)	-	0.4	0.4	0.4
Cultivated land	-	36.73	36.73	36.73
Mines	**0.02**	**0.31**	**0.91**	**1.89**
Forested land	-	0.56	0.55	0.55
Grassland	-	58.12	57.56	56.65
Wetland	-	3.19	3.16	3.11
Water bodies		0.44	0.44	0.43
Barren land	-	0.25	0.25	0.24
		C11K		
		Scenario A		
Urban (built-up)	**0.04**	**1.30**	**2.50**	**4.46**
Cultivated land	-	48.78	48.78	48.78
Mines	-	0.3	0.3	0.3
Forested land	-	0.33	0.32	0.31
Grassland	-	40.25	39.28	37.69
Wetland	-	8.32	8.12	7.79
Water bodies	-	0.58	0.57	0.54
Barren land	-	0.14	0.14	0.13
		Scenario B		
Urban (built-up)	-	1.30	1.30	1.30
Cultivated land	**0.3**	**48.78**	**57.78**	**72.48**

Land-cover classes	Average change rate per year (%)	Current situation	Medium term	Long term
		2020 (%)	Horizon 2050 (%)	Horizon 2099 (%)
Mines	-	0.3	0.3	0.3
Forested land	-	0.33	0.27	0.17
Grassland	-	40.25	32.95	21.03
Wetland	-	8.32	6.81	4.35
Water bodies	-	0.58	0.47	0.30
Barren land		0.14	0.11	0.07
Scenario C				
Urban (built-up)	-	1.3	1.3	1.3
Cultivated land	-	48.78	48.78	48.78
Mines	**0.04**	**0.3**	**1.50**	**3.46**
Forested land	-	0.33	0.32	0.31
Grassland	-	40.25	39.28	37.69
Wetland	-	8.32	8.12	7.79
Water bodies		0.58	0.57	0.54
Barren land	-	0.14	0.14	0.13

Figure 5.4 depicts the methodology used in this chapter, presenting the study phases as a flowchart that depicts the step-by-step approach.

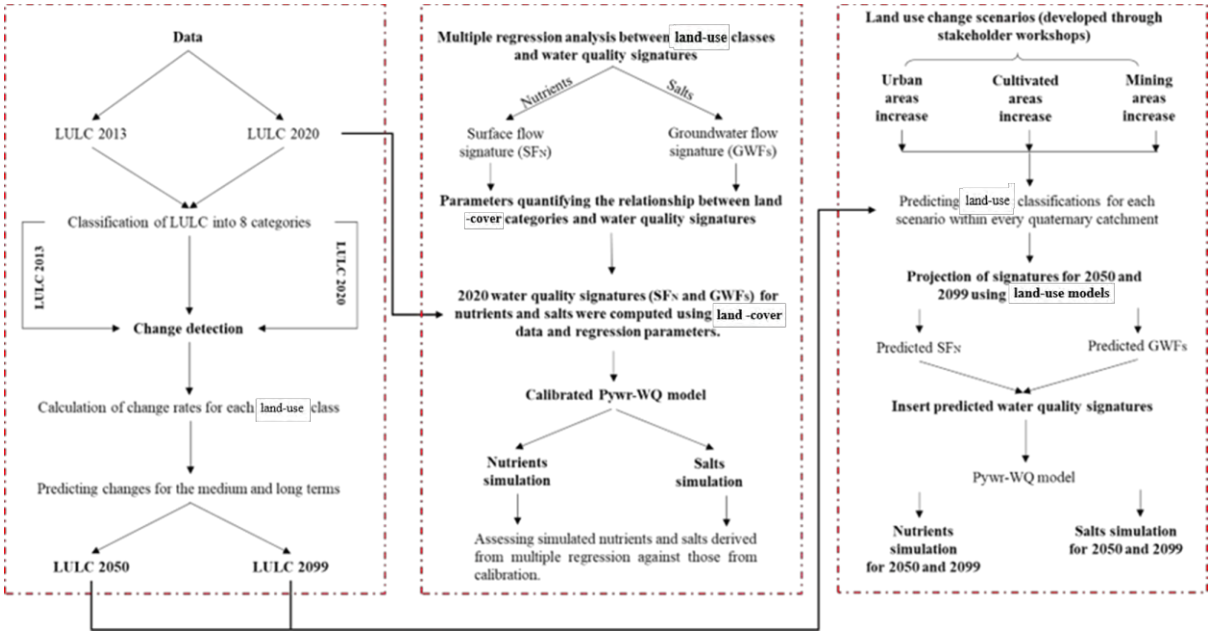

Figure 5.4: Methodology flow chart for linking multiple regression results into the calibrated Pywr-WQ model to assess the impacts of land-use change on water quality in the Grootdraai Dam Catchment.

5.2.6 Land-cover models' performance

The current study assessed the developed land-cover model simulations of the Grootdraai Dam's water quality using the NSE (Nash & Sutcliffe, 1970) performance metric, gauged overall accuracy, with an NSE above 0.9 considered excellent.

5.3 Results

5.3.1 Results of multiple regression

Table 5.5 presents the outcomes of the multiple regression analysis, illustrating the α-θ values corresponding to each incremental flow within every quaternary catchment. To authenticate the findings derived from the multiple regression, the SF_N values obtained from these regressions were cross-referenced with those acquired through the calibration of the Pywr-WQ model (refer to Chapter 4) against observed data.

Table 5.5: Parameter values for the multiple regression equation (see Eq.5.1).

Par.	NO_2-N + NO_3-N	NH_4-N	PO_4-P	Par.	NO_2-N + NO_3-N	NH_4-N	PO_4-P
	C11A: Inflow_1				**C11D: Inflow_4**		
α	0.00	0.00	0.00	α	0.66	3.56	34.72
β	1.05	0.00	0.16	β	0.00	0.00	0.00
γ	5.22	1.72	0.29	γ	0.42	1.78	0.13
δ	0.00	0.00	0.00	δ	0.00	0.00	0.00
ε	0.00	0.00	0.00	ε	0.00	0.00	0.00
ζ	5.56	2.80	7.97	ζ	0.89	5.59	151.51
η	0.00	0.00	0.00	η	0.00	0.00	0.00
θ	0.00	0.00	0.00	θ	0.00	0.00	0.00
	C11B: Inflow_2				**C11F: Inflow_5**		
α	0.00	0.00	0.00	α	0.00	0.00	0.00
β	6.47	9.57	4.70	β	12.79	11.38	2.66
γ	0.00	0.00	0.00	γ	0.00	0.00	0.00

Par.	NO_2-N + NO_3-N	NH_4-N	PO_4-P	Par.	NO_2-N + NO_3-N	NH_4-N	PO_4-P
δ	0.00	0.00	0.00	δ	0.00	0.00	0.00
ε	0.00	0.00	0.00	ε	0.00	0.00	0.00
ζ	2.47	10	5.49	ζ	2.91	8.63	9.56
η	0.00	0.00	0.00	η	0.00	0.00	0.00
θ	6.21	5.18	1.34	θ	3.42	2.40	1.16
	C11C: Inflow_3				**C11G: Inflow_6**		
α	0.00	0.00	0.00	α	0.00	0.00	0.00
β	20.83	0.10	20.83	β	9.76	4.76	11.19
γ	0.14	1.07	0.136	γ	0.15	0.17	0.21
δ	0.00	0.00	0.00	δ	0.00	0.00	0.00
ε	0.00	0.00	0.00	ε	0.00	0.00	0.00
ζ	0.00	0.00	0.00	ζ	0.00	0.00	0.00
η	0.00	0.00	0.00	η	0.00	0.00	0.00
θ	0.00	0.00	0.00	θ	0.00	0.00	0.00
	C11E: Inflow_7				**C11K: Inflow_10**		
α	0.00	0.00	0.00	α	0.00	0.00	0.00
β	7.10	0.00	0.00	β	18.30	25.84	8.35
γ	2.29	0.61	3.1	γ	0.00	0.00	0.00
δ	0.00	0.00	0.00	δ	0.00	0.00	0.00
ε	0.00	0.00	0.00	ε	0.00	0.00	0.00
ζ	2.49	0.56	19.67	ζ	30.80	16.02	14.10
η	0.00	0.00	0.00	η	0.00	0.00	0.00

Par.	NO_2-N + NO_3-N	NH_4-N	PO_4-P	Par.	NO_2-N + NO_3-N	NH_4-N	PO_4-P
θ	0.00	0.00	0.00	θ	0.00	0.00	0.00
	C11H: Inflow_8				**C11L: Inflow_11**		
α	0.00	0.00	0.00	α	0.00	0.00	0.00
β	4.00	23.87	0.40	β	0.00	0.00	0.00
γ	0.00	0.00	0.00	γ	1.05	1.10	0.02
δ	0.00	0.00	0.00	δ	0.00	0.00	0.00
ε	0.00	0.00	0.00	ε	0.00	0.00	0.00
ζ	5.86	4.17	2974.1	ζ	0.00	0.00	0.00
η	0.00	0.00	0.00	η	0.88	1.07	0.25
θ	0.00	0.00	0.00	θ	0.00	0.00	0.00
	C11J: Inflow_9						
α	0.00	0.00	0.00				
β	0.00	0.00	0.00				
γ	0.61	0.61	0.00				
δ	0.00	0.00	0.00		-		
ε	0.00	0.00	0.00				
ζ	0.00	0.00	3.54				
η	0.00	0.00	0.00				
θ	0.56	0.56	0.56				

*Par. refer to multiple regression parameters as described in Equation 5.1.

Figure 5.5 illustrates the comparison of simulated water quality at the Grootdraai Dam. This comparison includes (1) surface flow nutrient concentrations (SF_N) obtained from the Pywr-WQ model calibration against observed data, where the water quality signature for non-point sources in the model was set by calibrating model simulations with observed water quality data; and (2)

surface flow nutrient concentrations derived from multiple regression equations, where the independent data were areas of different land-use. The frequency distribution graphs indicated very good performance, particularly for ammonium and phosphate. The duration curves generated by the land-cover simulation closely resembled those from the calibrated Pywr-WQ simulation. High NSE values, ranging from 0.96 for ammonium to 0.98 for phosphate, underscored the accuracy of the model. However, some disparities were observed for nitrate plus nitrite between the two duration curves, with the NSE estimated at 0.9.

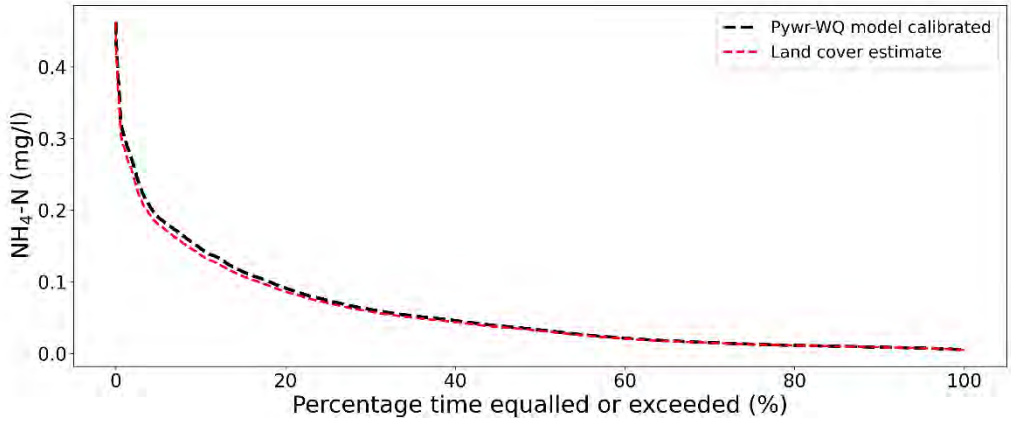

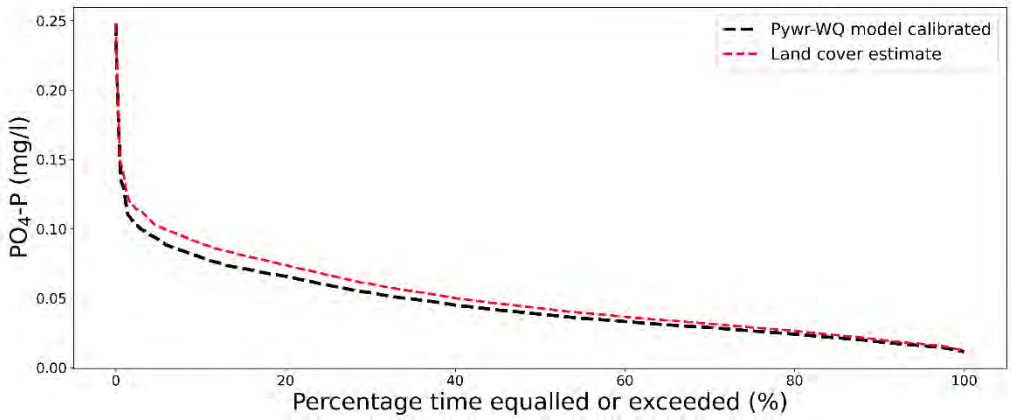

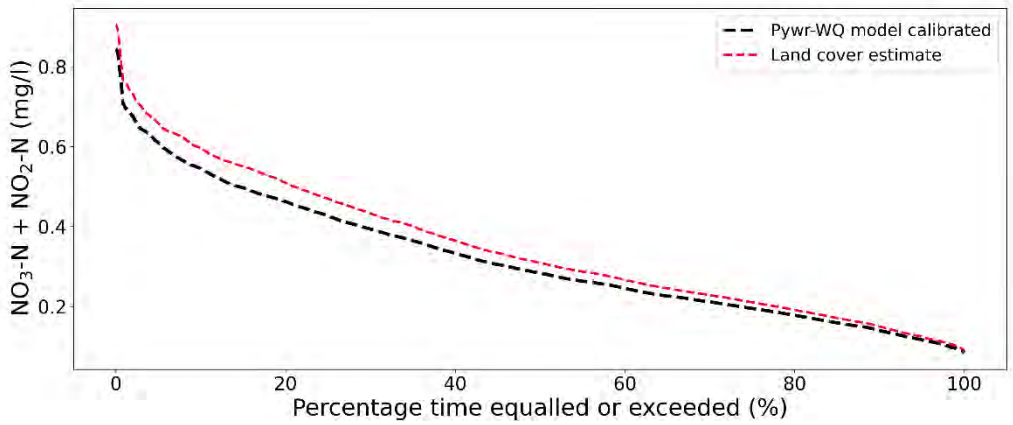

Figure 5.5: The values of surface flow nutrient concentrations (SF_N) as estimated through multiple regression and showing the corresponding SF_N values estimated by calibration of the Pywr-WQ model at the Grootdraai Dam to observed data, used as input into the Pywr-WQ model setups for the quaternary catchments. Shown are the simulations by the Pywr-WQ model for the calibration against observed data, as well as the simulation obtained when the SF_N value obtained through multiple regression was used as the parameter value instead. The comparisons are shown as frequency distributions.

Table 5.6 presents the outcomes of the multiple regression analysis, illustrating the α-θ values corresponding to each incremental flow within every quaternary catchment. To authenticate the findings derived from the multiple regression, the GWF_S values obtained from these regressions were cross-referenced with those acquired through the calibration of the Pywr-WQ model (refer to Chapter 4) against observed data.

Table 5.6: Parameter values for the multiple regression equation (see Eq.5.2).

Par.	**TDS**	**SO_4**	**Ca**	**Par.**	**TDS**	**SO_4**	**Ca**
	C11A: Inflow_1				**C11F: Inflow_5**		
α	0.00	0.00	0.00	α	0.00	0.00	0.00
β	200.61	58.50	35.00	β	14300.00	1800.00	420.00
γ	689.20	120.00	80.00	γ	0.00	0.00	0.00
δ	0.00	0.00	0.00	δ	0.00	0.00	0.00
ε	0.00	0.00	0.00	ε	0.00	0.00	0.00
ζ	17514.97	400.00	988.02	ζ	70000.00	6000.00	1119.56
η	0.00	0.00	0.00	η	0.00	0.00	0.00

Par.	TDS	SO_4	Ca	Par.	TDS	SO_4	Ca
θ	0.00	0.00	0.00	θ	6376.00	1400.00	600.00
	C11B: Inflow_2				**C11K: Inflow_10**		
α	0.00	0.00	0.00	α	0.00	0.00	0.00
β	49638.00	45000.00	330.00	β	15500.00	4500.00	560.76
γ	0.00	0.00	0.00	γ	0.00	0.00	0.00
δ	0.00	0.00	0.00	δ	0.00	0.00	0.00
ε	0.00	0.00	0.00	ε	0.00	0.00	0.00
ζ	27000.00	15000.00	500.00	ζ	45833.34	10000.00	2432.04
η	0.00	0.00	0.00	η	0.00	0.00	0.00
θ	17800.00	13000.00	850.00	θ	0.00	0.00	0.00

*Par. refer to multiple regression parameters as described in Equation 5.2.

Figure 5.6 and Figure 5.7 illustrate the comparison between groundwater flow TDS, sulphate, and calcium concentrations (GWF_S) obtained from multiple regression and those derived from the Pywr-WQ model calibration at the Grootdraai Dam against observed data. The frequency distribution graphs demonstrated excellent performance, especially for TDS and sulphate. The duration curves derived from the land-cover simulation closely mirrored those produced by the calibrated Pywr-WQ simulation. The model's accuracy was supported by high NSE values, reaching 0.99 for TDS and sulphate, and 0.95 for calcium. Multiple regression analysis was conducted to assess the relationship between water quality variables (nutrients, TDS, sulphate, and calcium) and land-use classes (refer to Table 5.5 and Table 5.6).

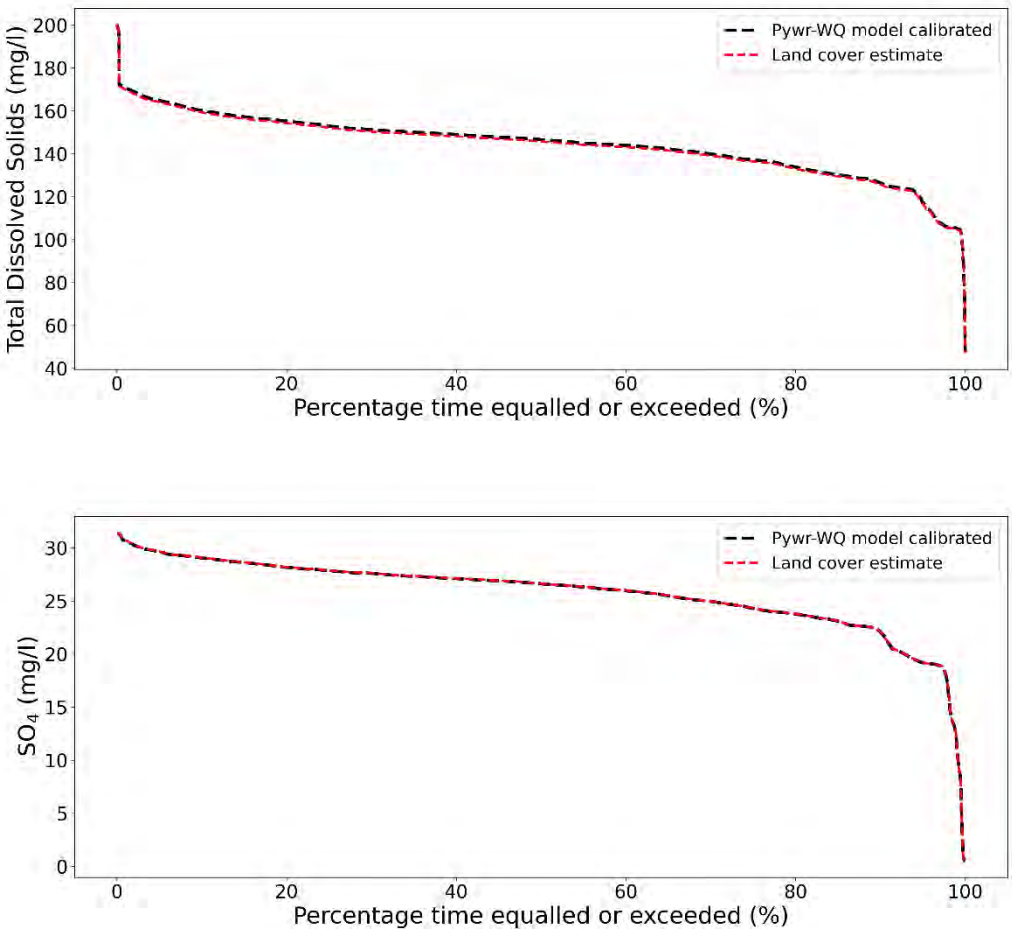

Figure 5.6: The values of groundwater flow TDS and sulphate concentrations (GWF_S) as estimated through multiple regression and showing the corresponding GWF_S values estimated by calibration of the Pywr-WQ model at the Grootdraai Dam to observed data, were used as input into the Pywr-WQ model setups for the quaternary catchments. Shown are the simulations by the Pywr-WQ model for the calibration against observed data, as well as the simulation obtained when the GWF_S value obtained through multiple regression was used as the parameter value instead. The comparisons are shown as frequency distributions.

The objective was to ascertain the significance of their influence on water quality and employ the developed models for scenario analysis.

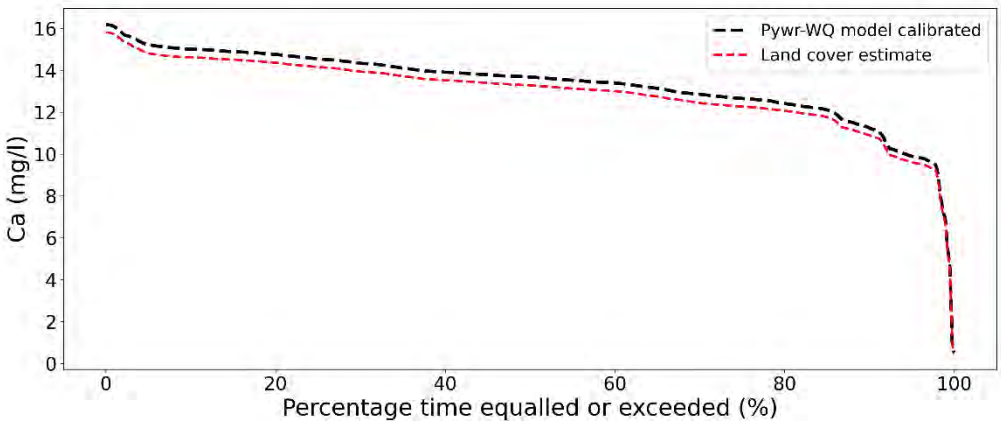

Figure 5.7: The values of groundwater flow calcium concentrations (GWF_S) as estimated through multiple regression and showing the corresponding GWF_S values estimated by calibration of the Pywr-WQ model at the Grootdraai Dam to observed data, were used as input into the Pywr-WQ model setups for the quaternary catchments. Shown are the simulations by the Pywr-WQ model for the calibration against observed data, as well as the simulation obtained when the GWF_S value obtained through multiple regression was used as the parameter value instead. The comparisons are shown as frequency distributions.

This study's findings highlight the dominant impact of land-cover classes on water quality variables. Each parameter ($\alpha, \beta, \gamma, \delta, \varepsilon, \zeta, \eta$, and θ) contributes to the overall SF_N and GWF_S values. Higher values indicate a substantial contribution to surface flow nutrient signatures or groundwater flow signatures. In addition, parameters may have zero values, indicating no influence between a water quality variable and a land-use class. Specifically, concerning nutrients, certain parameters consistently demonstrate high magnitudes across quaternary catchments. Notably, ζ (mines and quarries) exhibits the highest magnitude, followed by β (urban areas), and γ (cultivated areas). These consistently high magnitudes suggest a significant impact on SF_N. However, this order may differ from one quaternary catchment to another. For instance, in C11F, urban areas have a significant impact on nitrate plus nitrite, compared to C11K, where mines and quarries have a substantial impact on ammonium. Mines and quarries demonstrate a predominant influence on TDS, sulphate, and calcium in quaternary catchments, with urban areas following suit, possibly attributed to intense mining activities and potential sewage impacts. These results align with observed groundwater flow salt signatures during calibration.

5.3.2 Land-cover scenarios

In scenarios A, B, and C, the heightened impact on water quality variables is explored in urban, cultivated, and mining areas. The percentage increase varies among quaternary catchments, determined by the average observed increase in each class through a comparison of land-cover between 2013 and 2020.

5.3.2.1 Scenario A: increase in urban areas

Scenario A (the increase in urban areas) explores urban area increases with a distinguished percentage impact on water quality at the Grootdraai Dam Catchment. Figure 5.8 illustrates the duration curve of ammonium for Scenario A at Grootdraai Dam, closely resembling the baseline simulation. The slight increase in pollutant levels at high frequencies suggests some impact from urban expansion at Grootdraai Dam. However, the similarities between baseline and Scenario A duration curves at moderate to lower frequencies indicate effective dilution capabilities within the dam. The duration curves of nitrate plus nitrite in Scenario A at Grootdraai Dam exhibited higher values than those in the baseline simulation at lower frequencies and a closer alignment at higher frequencies. This divergence could be attributed to urban development, or potential alterations linked to the rise in urban areas, possibly leading to increased mobilisation of pollutants through runoff. Furthermore, the duration curve for phosphate in Scenario A (increase in urban areas) at Grootdraai Dam exhibited higher values than the baseline simulation at both low and high frequencies. The concentration of phosphate may be affected by the nutrient signature carried by surface flow, potentially arising from urban expansion, which could result in sewage drainage and wastewater leakage. It is crucial to acknowledge that, when assessing the impact of increased urban areas on water quality, other land-use categories are also considered. These factors may contribute to the elevated phosphate levels observed at Grootdraai Dam.

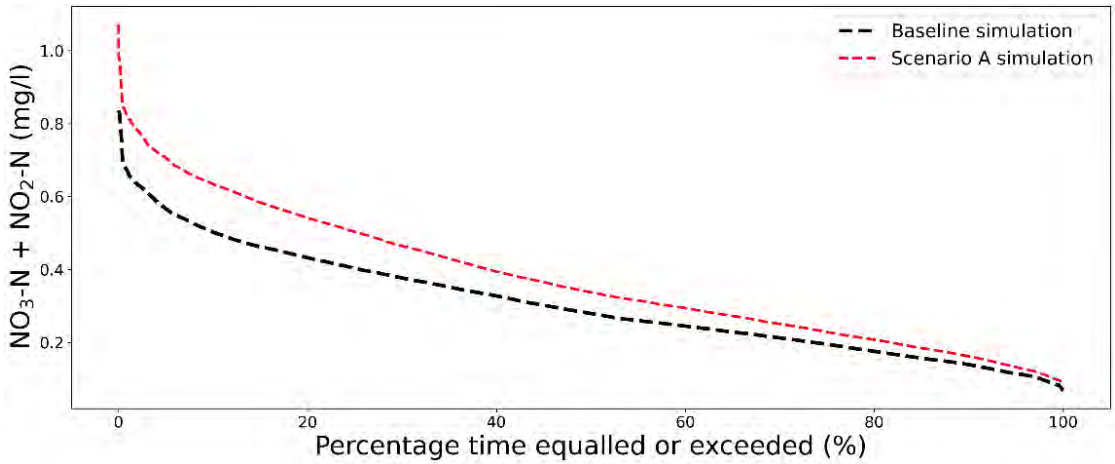

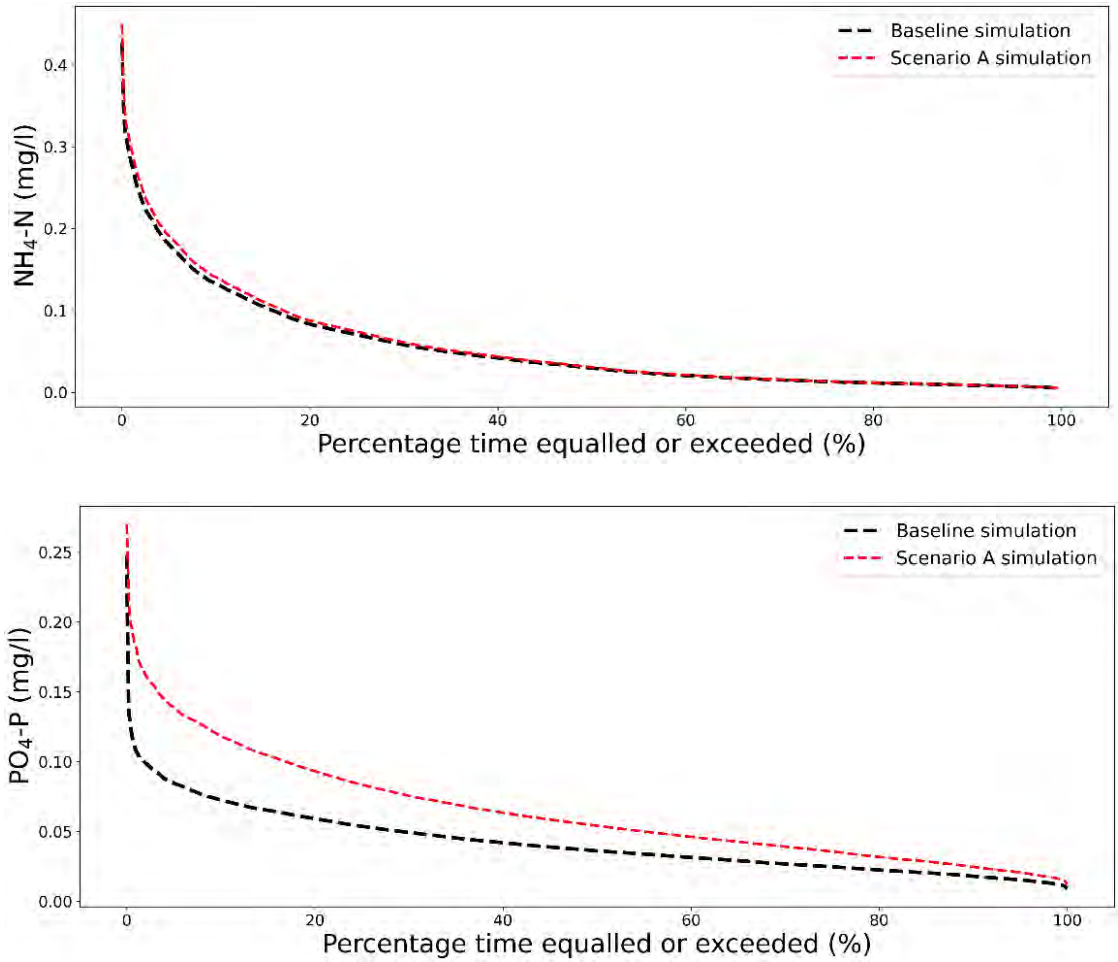

Figure 5.8: The surface flow nutrient concentrations (SF_N) were estimated using multiple regression prediction under Scenario A (referring to the increase in urban areas). These estimated SF_N values, along with corresponding SF_N values obtained by calibrating the Pywr-WQ model to observed data, were utilised as input for the Pywr-WQ model in the respective quaternary catchments. The comparisons are presented as frequency distributions for the Grootdraai Dam over the long term.

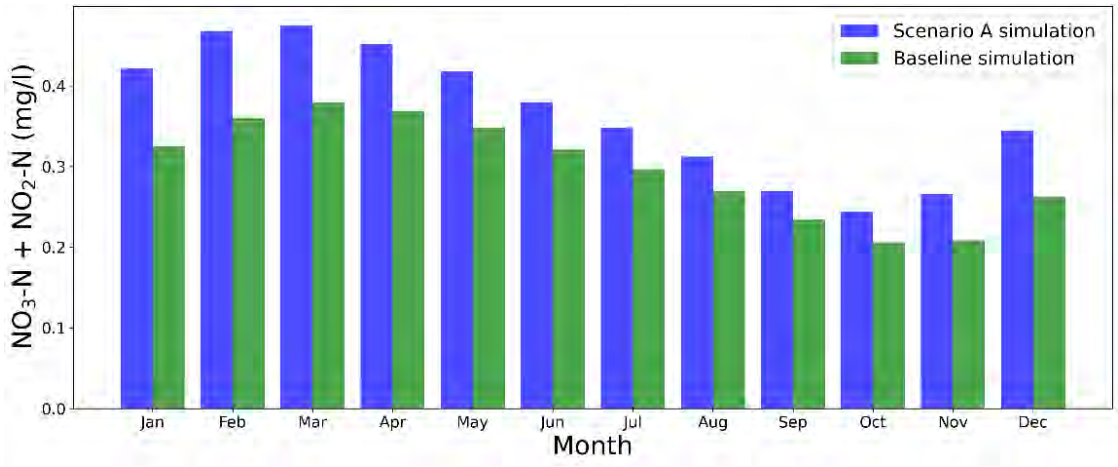

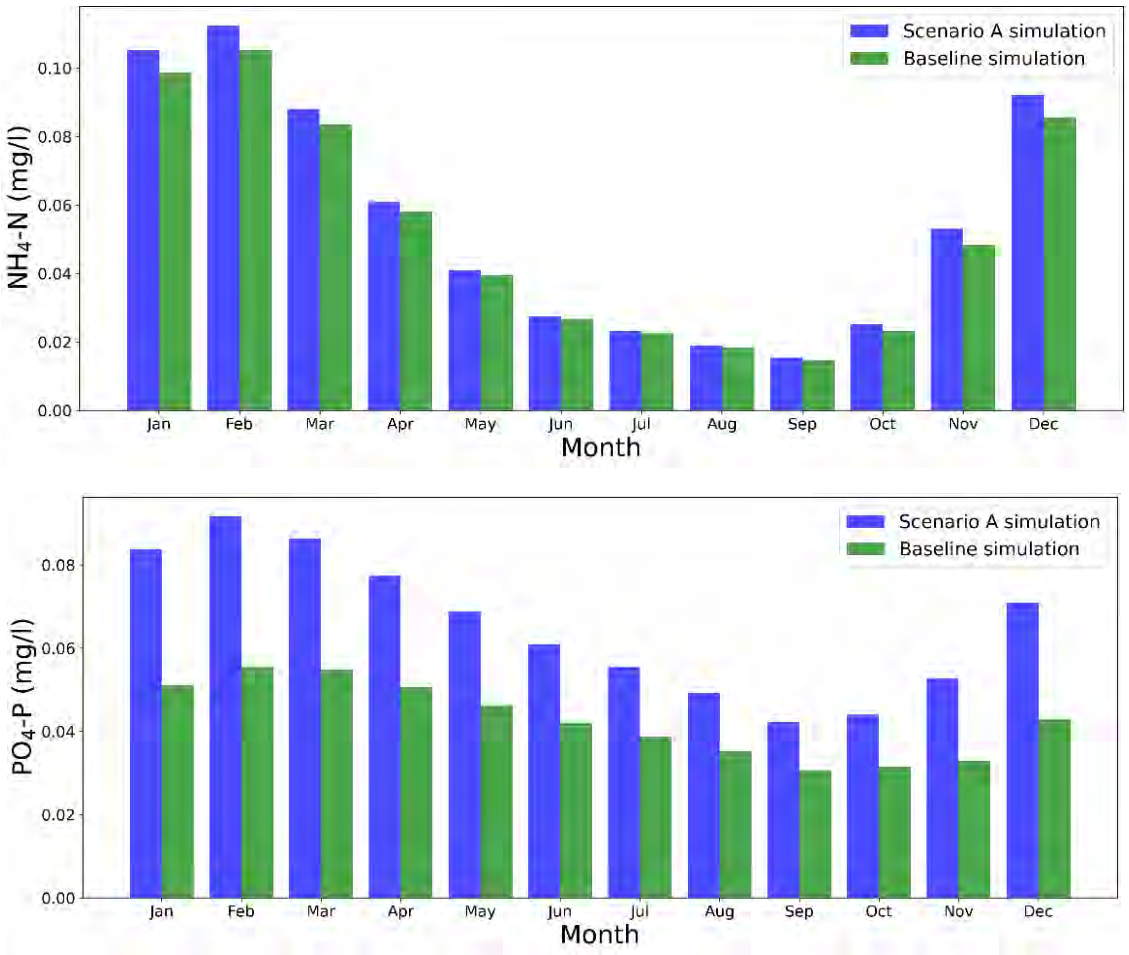

Figure 5.9: Monthly averaged simulated nitrate plus nitrite, ammonium, and phosphate for the Grootdraai Dam under baseline conditions (1920-2010) and under Scenario A (increase in urban areas) (2020-2099).

Figure 5.9 illustrates the seasonal fluctuations in nitrate plus nitrite, ammonium, and phosphate concentrations within the baseline (1920–2010) and Scenario A (referring to the increase in urban areas) (2020–2099) contexts for the Grootdraai Dam. The data highlights that nitrate plus nitrite concentrations reach their peak during the months (October – Mars), followed by a decline from April to September, and then commence an upward trend in October. Similarly, phosphate exhibits a comparable seasonal pattern, with a notable increase in monthly variation when compared to the Scenario A simulation. Conversely, a substantial reduction in ammonium concentration is evident from April to September, indicating a significant and closely aligned variation between baseline and Scenario A simulations. The peak levels of nitrate plus nitrite, ammonium, and phosphate are observed between February and March. This seasonal fluctuation is primarily attributed to variations in surface water flow, as the model parameters remain static. Conversely, the lowest values are recorded in September. These patterns can be attributed to diverse factors, one of which is the surface nutrient signature assigned to each node upstream of

the Grootdraai Dam as a consequence of the predicted land-cover model. For instance, the dataset for nitrate plus nitrite concentrations under Scenario A reveals notable extremes. The highest concentration occurs in February 2075, reaching 1.07 $mg.l^{-1}$. In contrast, the lowest concentration is recorded in October 2066, measuring 0.08 $mg.l^{-1}$. The consistent low values across months in 2066 suggest a sustained trend, as presented in Figure 5.10.

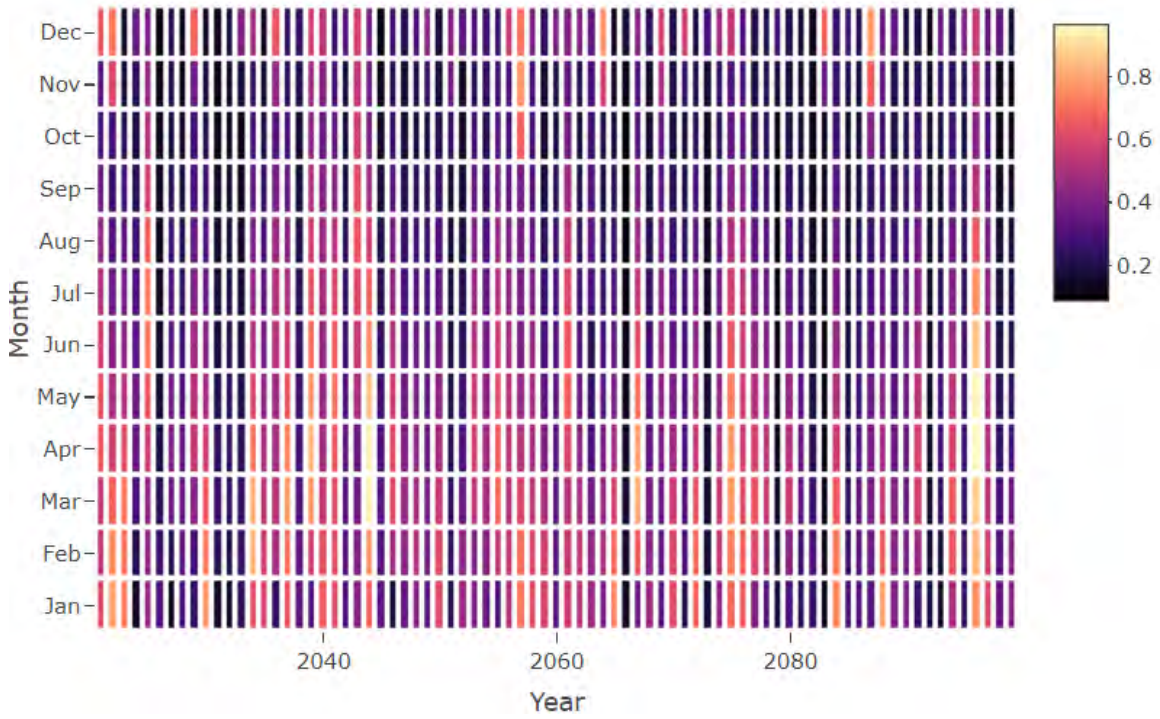

Figure 5.10: Nitrate plus nitrite monthly variation under Scenario A (increase in urban areas) at the Grootdraai Dam over the long term (2020–2099), shown as a heatmap.

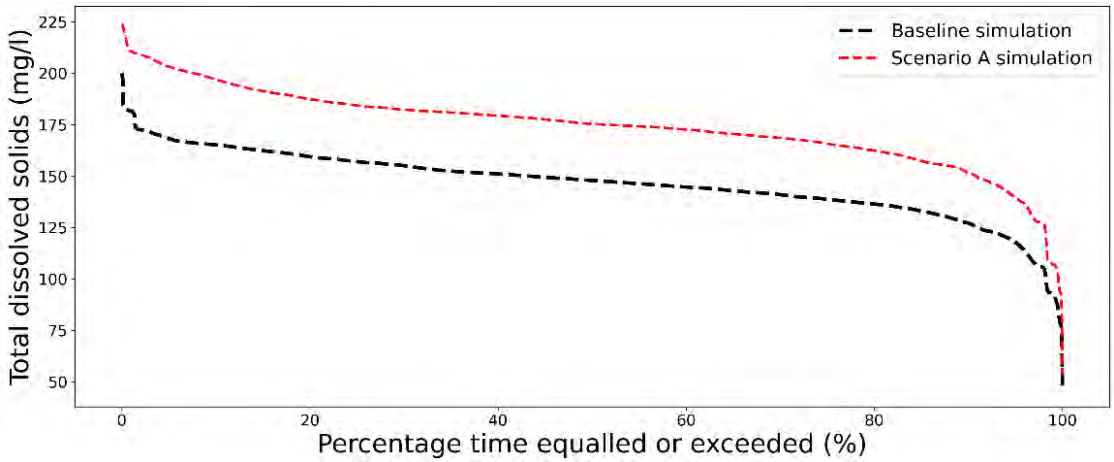

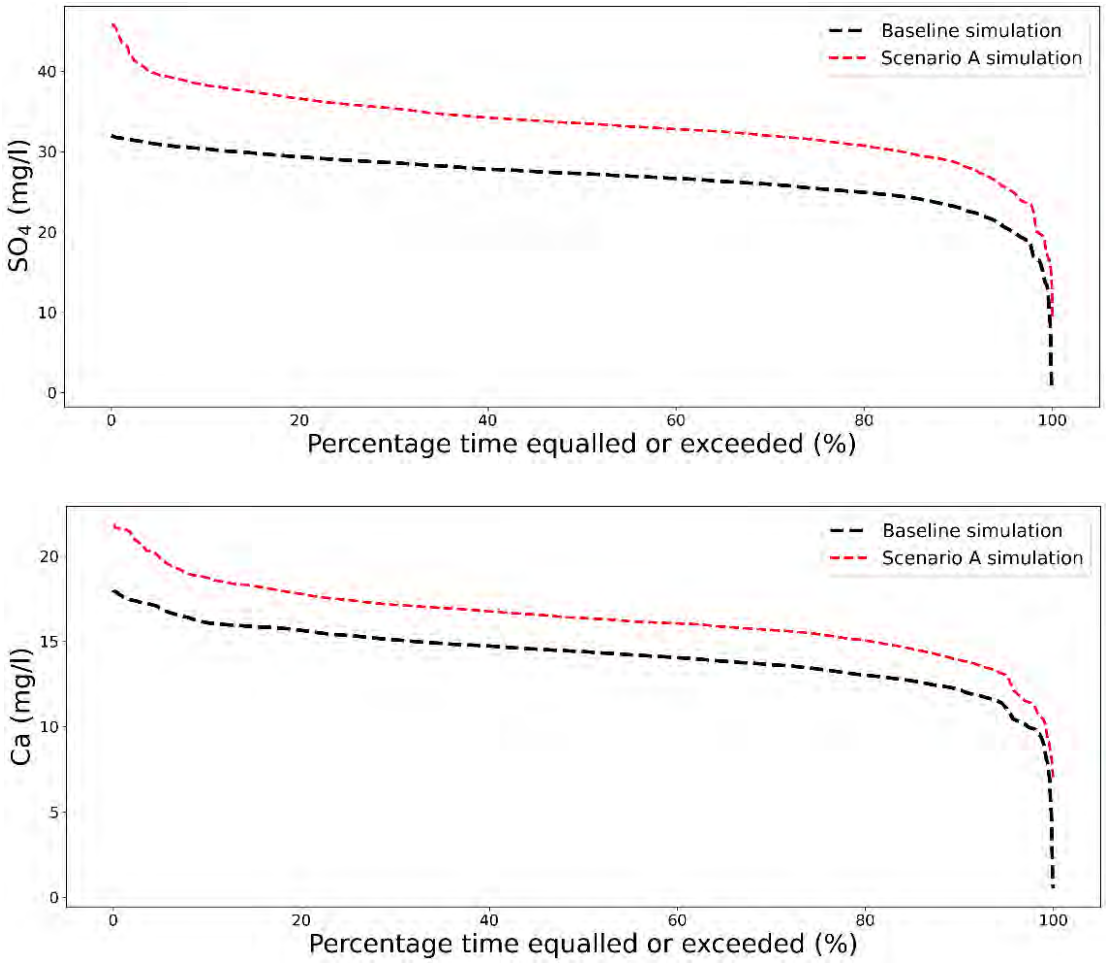

Figure 5.11: The groundwater flow salts concentrations (GWF_S) were estimated using multiple regression prediction under Scenario A (increase in urban areas). These estimated GWF_S values, along with corresponding GWF_S values obtained by calibrating the Pywr-WQ model to observed data, were utilised as input for the Pywr-WQ model in the respective quaternary catchments. The comparisons are presented as frequency distributions for the Grootdraai Dam over the long term.

Figure 5.11 illustrates the duration curve of TDS, sulphate, and calcium for Scenario A (increase in urban areas) at Grootdraai Dam, showing values higher than those in the baseline simulation across identical values across very high frequencies.

The graphs highlight a notable influence of increased urban areas on these salts, possibly correlated with the coefficients assigned to urban areas, where it ranks as the second land-use class with high β values. It is essential to note that while the rise in urban areas may contribute to the elevated levels of salts, it does not necessarily imply that urban areas are the sole factor influencing these concentrations. Although other land-use types may not be experiencing an increase, they could still contribute to the elevated levels, highlighting the complex nature of these influences.

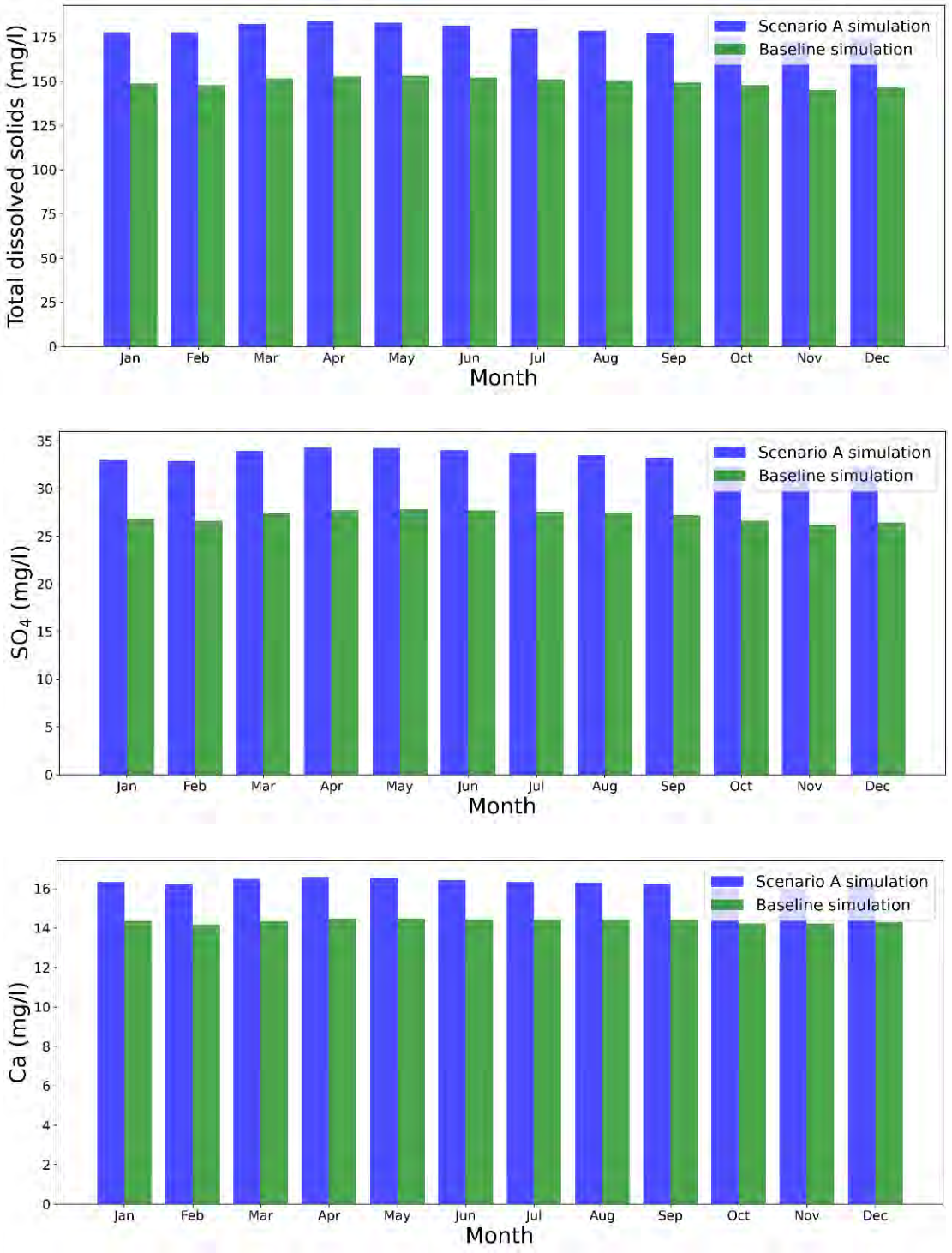

Figure 5.12: Monthly averaged simulated TDS, sulphate, and calcium for the Grootdraai Dam under baseline conditions (1920–2010) and Scenario A (increase in urban areas) (2020–2099).

Figure 5.12 illustrates the seasonal fluctuations in TDS, sulphate, and calcium concentrations within the baseline (1920–2010) and Scenario A (increase in urban areas) (2020–2099) contexts for the Grootdraai Dam. The graphs depict minimal variation or, in some cases, no visible change across the months for the salts. This limited variation can be attributed to the reduced seasonal variation in groundwater flow. For instance, there is a marginal increase in salts observed from

April to May, followed by a slight decrease until November, after which they begin to rise once more.

The TDS monthly variation shown in Figure 5.13, reveals that the monthly variations in Scenario A exhibit notable extremes. The highest concentration occurs in May 2094, reaching 241.8 mg.l^{-1}. In contrast, the lowest concentration is in February 2039, measuring 53.4 mg.l^{-1}. The consistently low values across months in 2055 suggest a sustained trend.

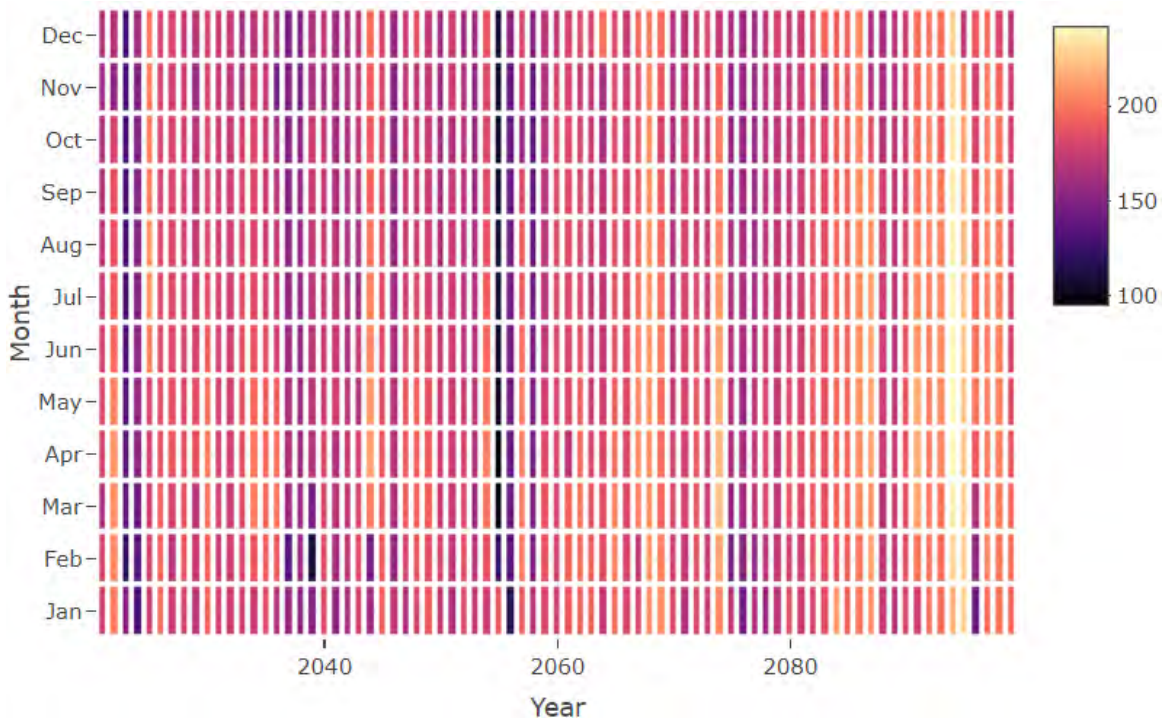

Figure 5.13: TDS monthly variation under Scenario A (increase in urban areas) at the Grootdraai Dam over the long term (2020–2099), shown as a heatmap.

5.3.2.2 Scenario B: increase in cultivated areas

Scenario B (increase in cultivated areas) examines an increase in cultivated areas with a distinguished percentage impact on water quality in the Grootdraai Dam Catchment. Figure 5.14 illustrates the duration curves of nitrate plus nitrite, ammonium, and phosphate for scenario B at Grootdraai Dam.

Figure 5.14, which illustrates nitrate plus nitrite concentrations under Scenario B, reveals heightened values compared to the baseline simulation, particularly at lower frequencies, while exhibiting minimal differences at higher frequencies. This observation can be attributed to the influence of increased cultivated areas, associated with the intensified application of fertilisers and agricultural products, contributing to the observed increase.

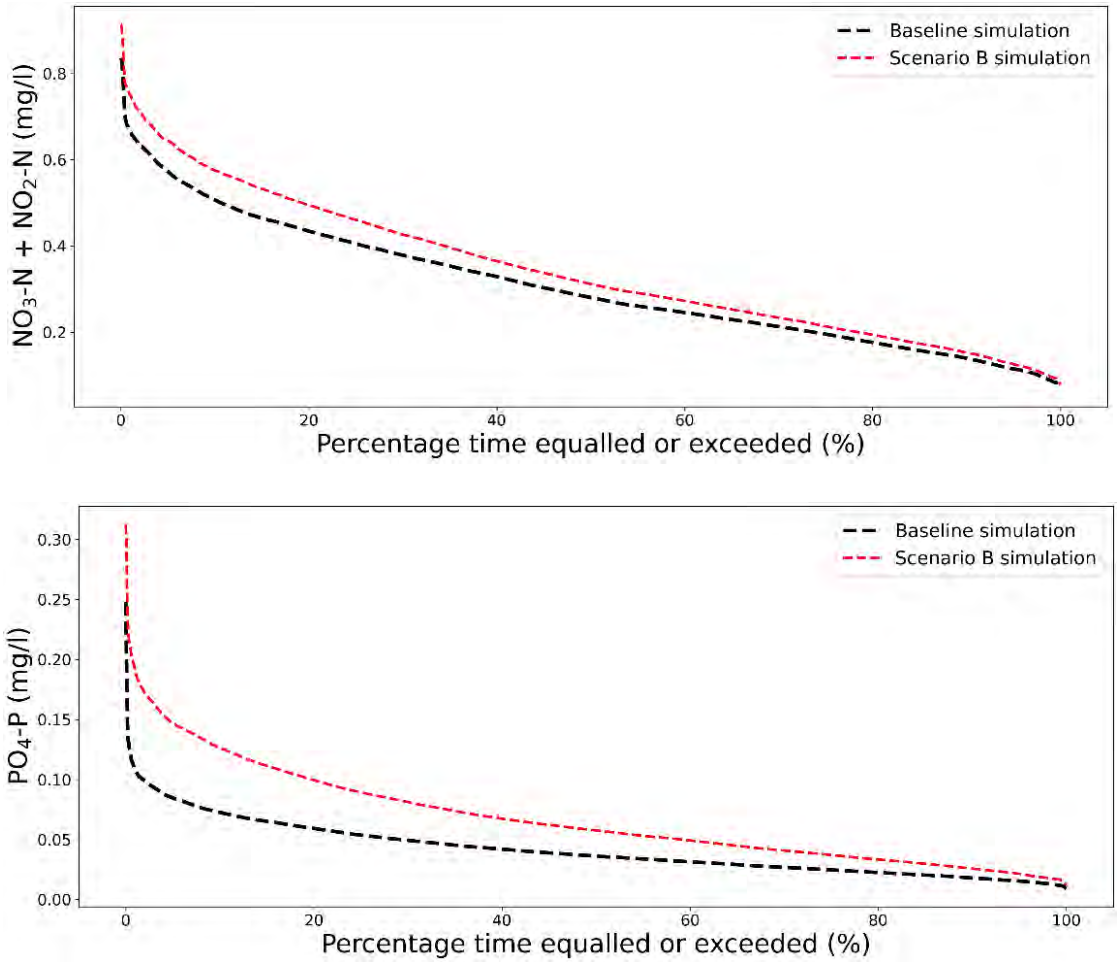

Figure 5.14: The surface flow nutrient concentrations (SF_N) were estimated using multiple regression prediction under Scenario B (referring to the increase in cultivated areas). These estimated SF_N values, along with corresponding SF_N values obtained by calibrating the Pywr-WQ model to observed data, were utilised as input for the Pywr-WQ model in the respective quaternary catchments. The comparisons are presented as frequency distributions for the Grootdraai Dam over the long term. No comparison for ammonium is shown as there was a 0% discrepancy between the baseline simulation and Scenario B simulation.

Furthermore, runoff could potentially facilitate the mobilisation of these contaminants through the soil-water interface, potentially further contributing to the likelihood of elevated concentrations. In addition, the phosphate duration curve under Scenario B demonstrated simulation patterns that are high at both lower and higher frequencies, with significant elevations observed in the intermediate frequency range.

Figure 5.15 presents the monthly average distribution of nitrate plus nitrite and phosphate concentrations in the Grootdraai Dam under Scenario B (increase in cultivated areas) over the long term. Nitrate plus nitrite exhibited elevated values in March, contrasting with lower values observed in October. Conversely, phosphate demonstrated heightened concentrations in February and diminished levels in October. Figure 5.15 highlights February as the month

characterised by a significant difference between the baseline and simulated Scenario B, while September exhibits the minimum difference.

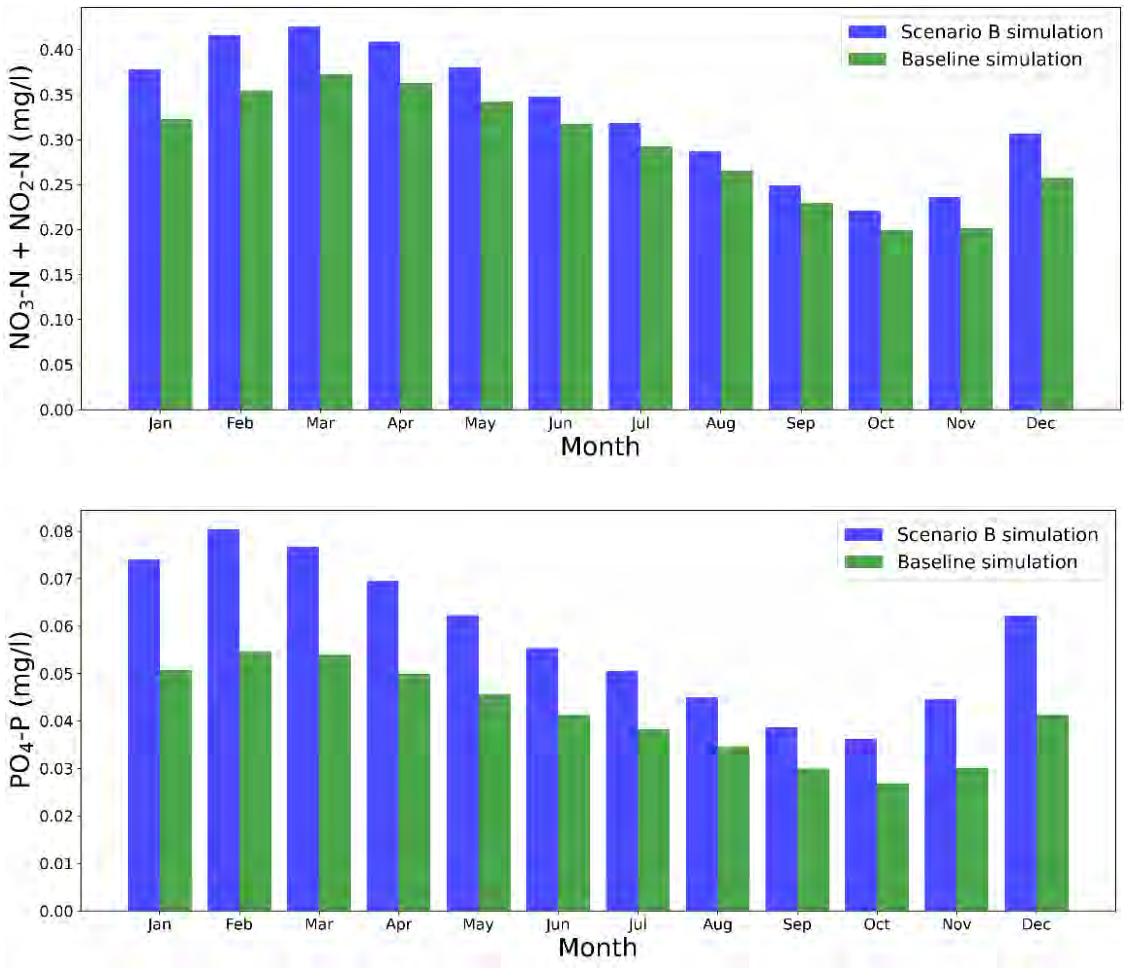

Figure 5.15: Monthly averaged simulated nitrate plus nitrite and phosphate for the Grootdraai Dam under baseline conditions (1920–2010) and under Scenario B (increase in cultivated areas) (2020–2099).

Figure 5.16 illustrates the monthly variation in nitrate plus nitrite concentrations under Scenario B through a heatmap, revealing distinct extremes. The peak concentration was observed in April 2044, reaching 0.9 $mg.l^{-1}$. Conversely, the lowest concentration occurred in October 2066, measuring 0.07 $mg.l^{-1}$. The sustained low values throughout the months of 2066 indicate a persistent trend.

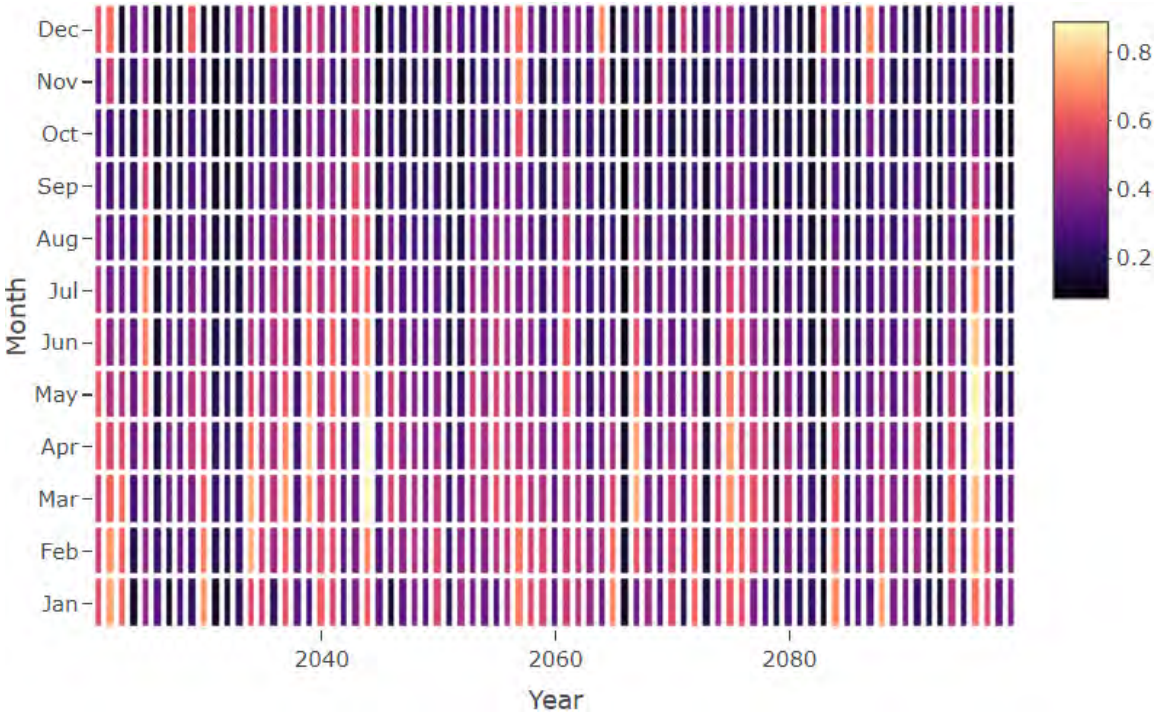

Figure 5.16: Nitrate plus nitrite monthly variation under Scenario B (increase in cultivated areas) at the Grootdraai Dam over the long term (2020–2099), shown as a heatmap.

5.3.2.3 Scenario C: increase in mining areas

Scenario C (increase in mining areas) examines the impact of increased mining activities on water quality in the Grootdraai Dam Catchment. Figure 5.17 shows duration curves for nitrate plus nitrite, ammonium, and phosphate in Scenario C for the Grootdraai Dam. Nitrate plus nitrite concentrations closely align with the baseline at higher frequencies but exhibit higher levels at moderate to lower frequencies. This variation may be attributed to the influence of related land-cover classes, such as cultivated areas, which vary from 34% to more than 50% of the Grootdraai Dam Catchment. Despite the minimal expansion of mines, the persistent influence of cultivated areas remains significant. Phosphate levels in Scenario C closely resemble the baseline, showing slight increases at very low frequencies. The marginal impact of mines on phosphate, indicated by coefficients, explains the similarities between simulated phosphate under Scenario C and the baseline simulation.

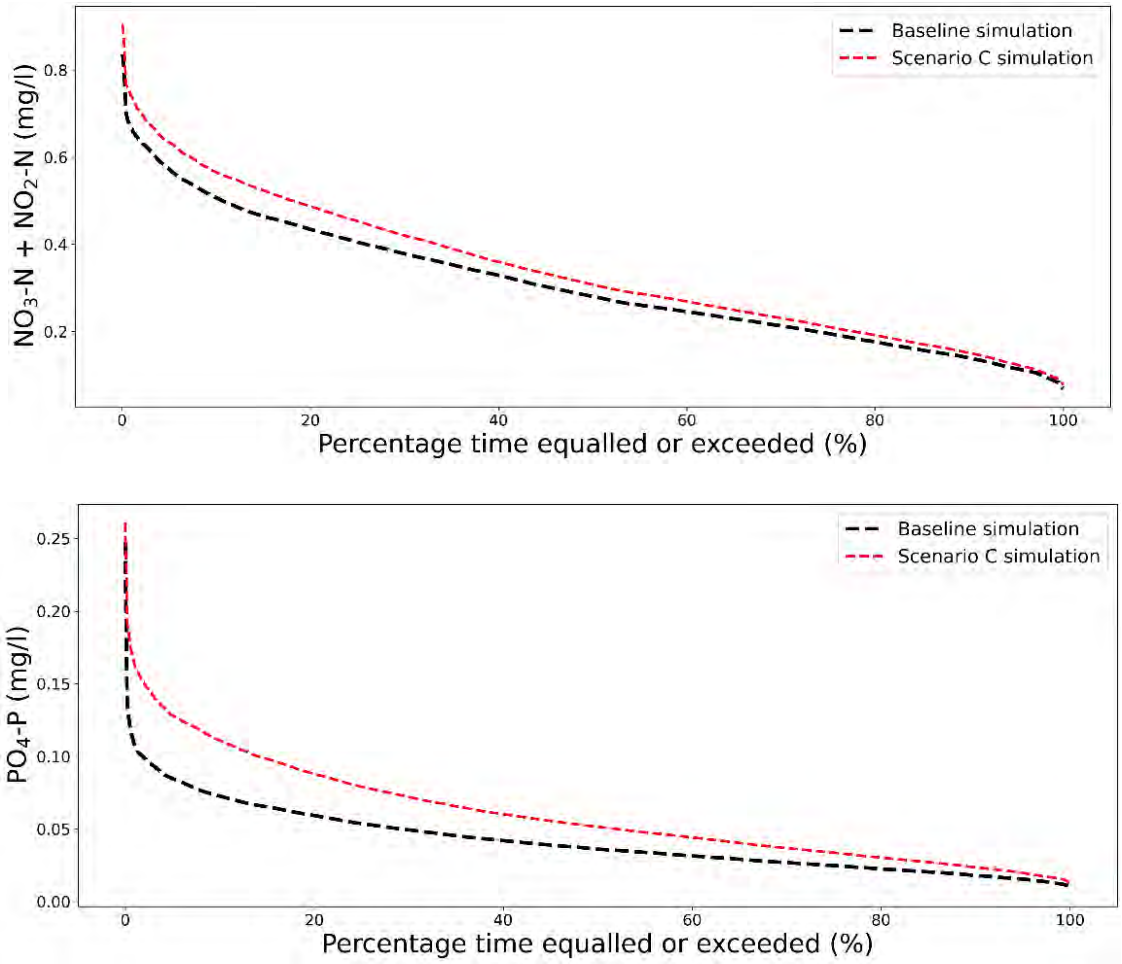

Figure 5.17: The surface flow nutrient concentrations (SF_N) were estimated using multiple regression prediction under Scenario C (increase in mining areas). These estimated SF_N values, along with corresponding SF_N values obtained by calibrating the Pywr-WQ model to observed data, were used as input for the Pywr-WQ model in the respective quaternary catchments. The comparisons are presented as frequency distributions for the Grootdraai Dam over the long term. No comparison for ammonium is shown as there was a 0% discrepancy between the baseline simulation and Scenario C simulation.

Figure 5.18 illustrates the long term monthly average distribution of nitrate plus nitrite and phosphate concentrations in the Grootdraai Dam in Scenario C (increase in mining areas). Higher values for phosphate and nitrate plus nitrite are evident, particularly in February and March. This observed seasonal variation might be attributed to a potential increase in runoff during flood episodes, potentially facilitating the mobilisation of contaminants from soil to water. Conversely, in October, there appears to be a tendency towards very low concentrations, suggesting the possibility of the Grootdraai Dam exhibiting a capacity for dilution. Furthermore, the low concentrations may be attributed to algae and other organisms, which assist with removing nutrients.

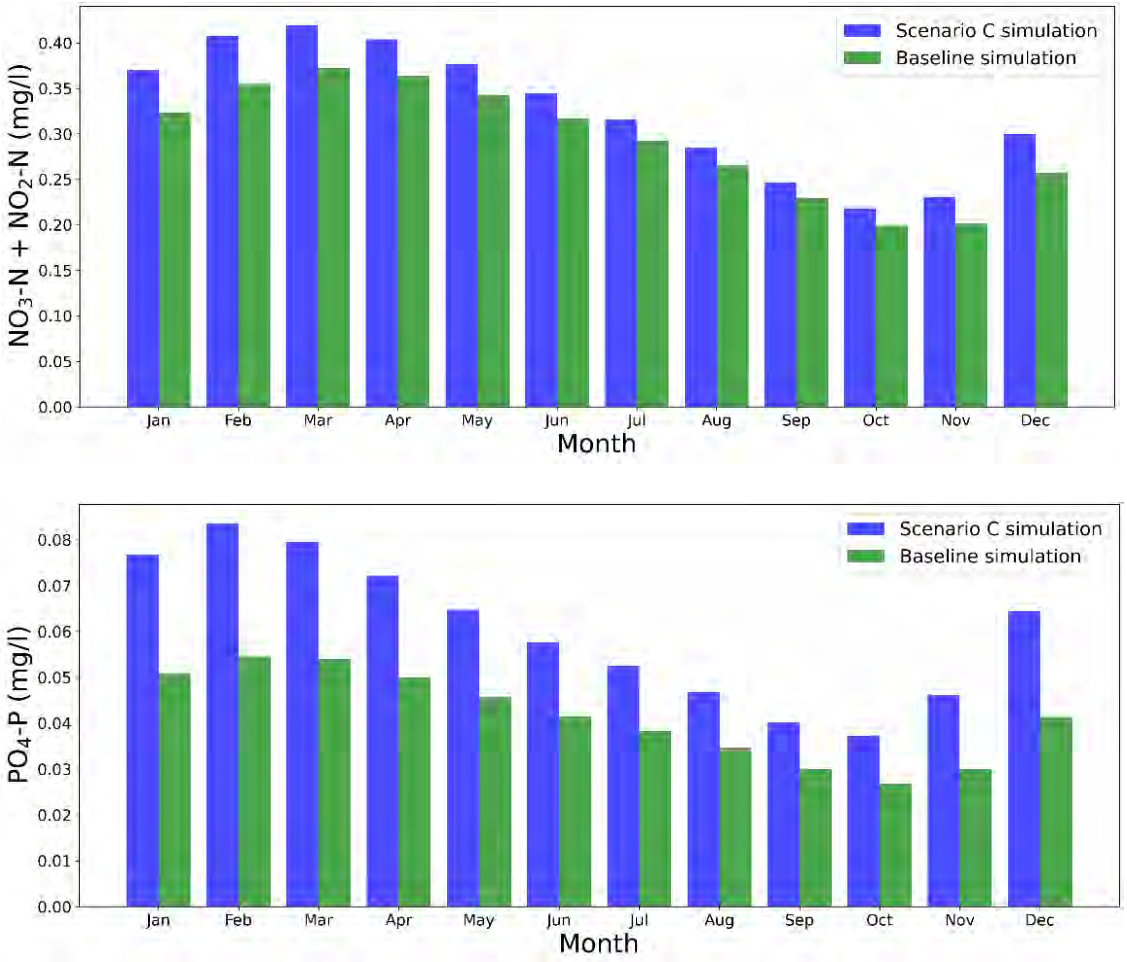

Figure 5.18: Monthly averaged simulated nitrate plus nitrite and phosphate for the Grootdraai Dam under baseline conditions (1920–2010) and in Scenario C (2020–2099).

Figure 5.19 illustrates the duration curves of TDS, sulphate, and calcium for Scenario C (increase in mining areas) at Grootdraai Dam compared to the baseline scenario over the long term. The concentrations in Scenario C surpass those in the baseline simulation and remain consistently elevated, especially at very high frequencies. Notably, TDS concentration exceeds 300 $mg.l^{-1}$, a level not observed in Scenario A. Sulphate concentration also exceeds 50 $mg.l^{-1}$ at low frequencies, contrasting with Scenario A. Calcium exhibits considerable variations, diverging from both the baseline simulation and Scenario A. The elevated levels of TDS, sulphate, and calcium in Scenario C might be associated with the expansion of mining areas. Various factors may contribute to the release of these salts, including potential changes in geological formations. Moreover, the breakdown of pyrite in the presence of water and oxygen results in elevated sulphate levels, known as Acid Mine Drainage (AMD), and lime treatment of AMD leads to an increase in calcium levels. The impact of AMD from mining activities could be a significant factor, as runoff from these areas may transport contaminants through sediments, potentially leading to an increase in salt concentrations at the Dam.

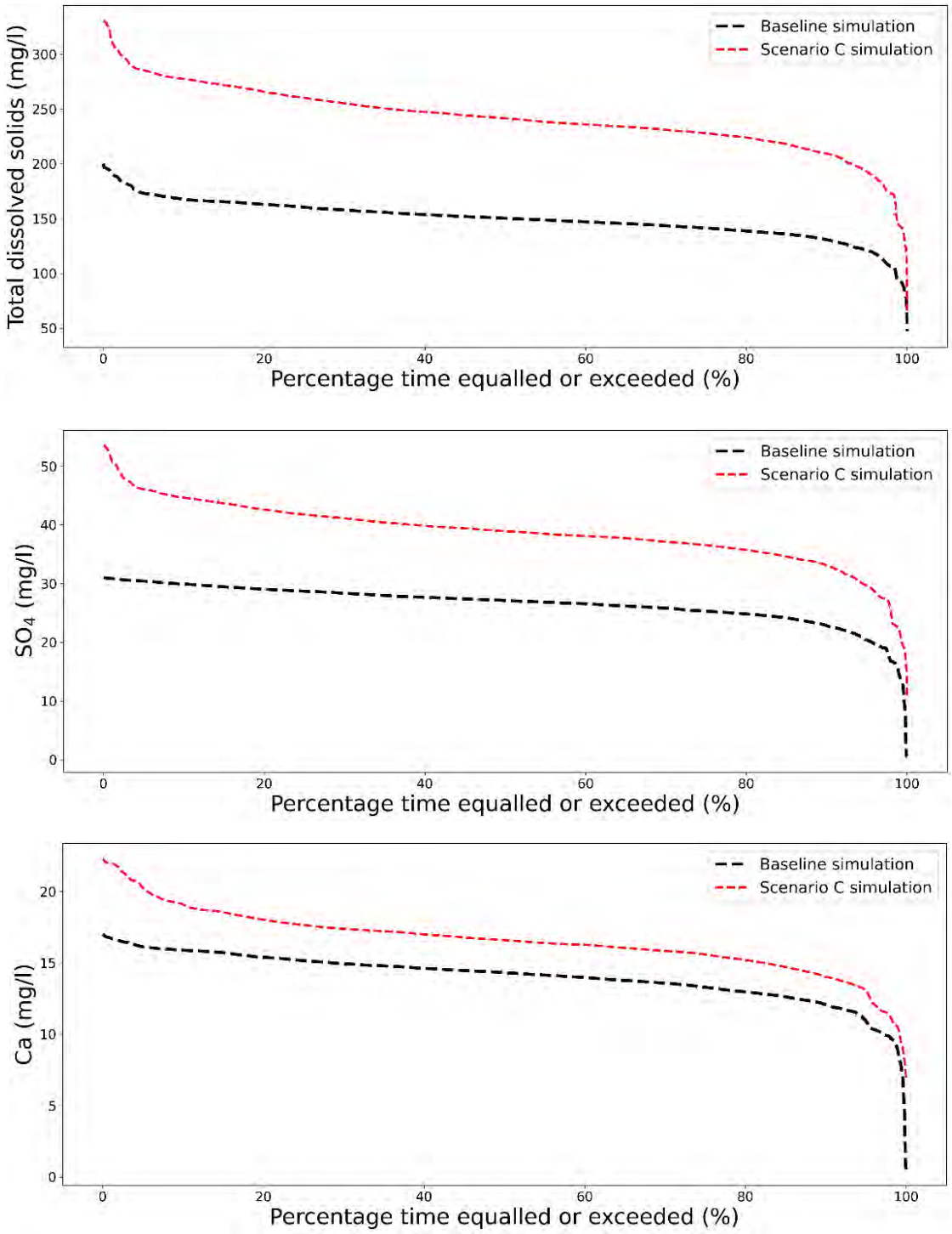

Figure 5.19: The groundwater flow salts concentrations (GWF_S) were estimated using multiple regression prediction under Scenario C (increase in mining areas). These estimated GWF_S values, along with corresponding GWF_S values obtained by calibrating the Pywr-WQ model to observed data, were used as input for the Pywr-WQ model in the respective quaternary catchments. The comparisons are presented as frequency distributions for the Grootdraai Dam over the long term.

Figures 5.20 and 5.21 depict the monthly variations of TDS and sulphate in Scenario C for Grootdraai Dam over the long term.

The peak TDS value occurred in May 2094, reaching a value of 330.5 $mg.l^{-1}$, while the lowest values were recorded in February 2039, with a value of 65 $mg.l^{-1}$. The year 2055 appears to exhibit the least variability in TDS concentrations.

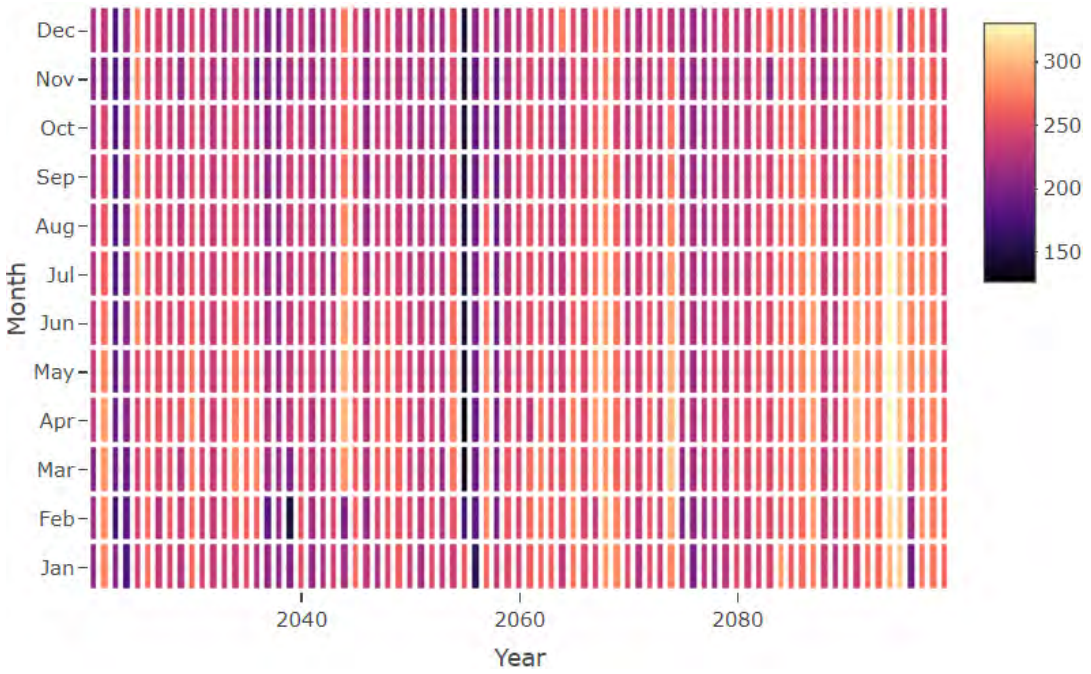

Figure 5.20: TDS monthly variation in Scenario C (increase in mining areas) at the Grootdraai Dam over the long term (2020–2099), shown as a heatmap.

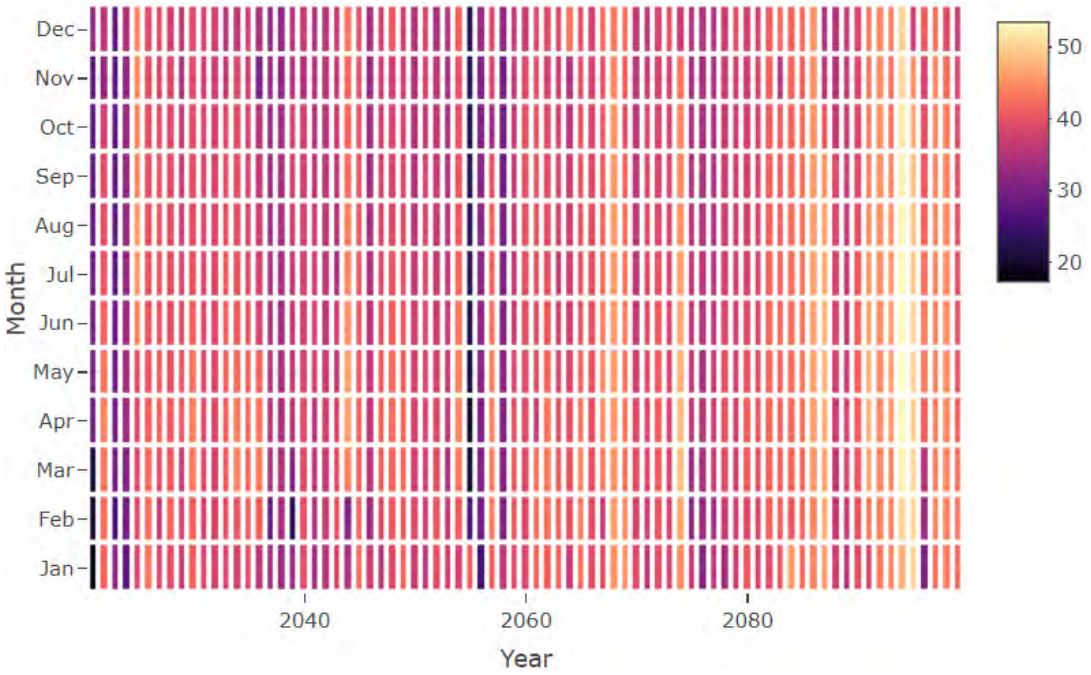

Figure 5.21: Sulphate monthly variation in Scenario C (increase in mining areas) at the Grootdraai Dam over the long term (2020–2099), shown as a heatmap.

High TDS values occurring at the beginning of the dry season may reflect the lack of dilution capacity, which can be impacted by the reservoir volume accumulation. In May 2094, the sulphate concentration was predicted to peak at 53.5 $mg.l^{-1}$, whereas the lowest values, recorded in February 2039, predicted 10.3 $mg.l^{-1}$. Interestingly, the year 2055 displays minimal variability in sulphate concentrations. The synchronicity between the variations in sulphate and TDS implies a potential correlation between these two variables. The reasons for these extreme values may align with those identified in the TDS variation, emphasising common contributing factors.

5.3.3 Land-cover scenarios - water quality implications in the short term

Table 5.6 (section 5.2.1) displays the water quality status for the Grootdraai Dam node located downstream of the catchment over the next 5, 10, and 20 years for each scenario, starting from the year 2020. The categorisation of water quality data in each scenario adheres to the criteria outlined in the Grootdraai Dam Catchment-specific water quality guidelines established by Rand Water (2022). It is important to note that these guidelines can differ among rivers within the Grootdraai Dam Catchment. To ensure accurate guideline selection, certain conditions were taken into account. Firstly, the selected node should not receive any return flows to prevent potential alterations and disturbances to the variation. Secondly, the node should be close to the rivers specified in the water quality guidelines. Water quality guidelines from Rand Water encompass various water quality variables, including TDS, sulphate, nitrate plus nitrite, ammonium, phosphate, chloride, and fluoride. This study specifically focused on the water quality variables listed in Table 5.3 for each investigated scenario. The classification of calcium concentration was constrained by the availability of water quality guidelines, which limited the visualization options.

Table 5.7 illustrates diverse trends in nitrate plus nitrite, ammonium, phosphate, TDS, and sulphate compliance percentages across investigated scenarios over the upcoming 5, 10, and 20 years, starting from the year 2020. In Scenario A (increase in urban areas), nitrate plus nitrite compliance percentages depict a general increase with fluctuations beneath the acceptable level. Scenario B (increase in cultivated areas) shows an upward trajectory in acceptable and tolerable levels, along with a decrease in unacceptable concentrations. Scenario C mirrors B, presenting a notable drop in unacceptable levels at the 20-year scale. Ammonium compliance percentages in Scenario A display a general upward trend with temporal fluctuations below the acceptable level. Conversely, Scenario B showcases escalating acceptable and tolerable levels, coupled with a reduction in unacceptable concentrations.

Table 5.7: Water quality compliance percentages under different classifications for the Grootdraai Dam node over the next 5, 10, and 20 years. Each colour corresponds to a specific classification type: red indicates an unacceptable level, yellow indicates a tolerable level, green indicates an acceptable level, and blue indicates an ideal level.

Water Quality Status													
Nodes	**Year**	**NO_3-N + NO_2-N (%)**			**NH_4-N (%)**			**PO_4-P (%)**	**TDS (%)**			**SO_4 (%)**	
Scenario A													
Grootdraai Dam	5	13.7	41.1	45.2	31.7	68.3	48.8	51.2	78	22	20.6	73.8	5.6
	10	28.5	42.3	29.2	42.4	57.6	45.3	54.7	85.2	14.8	22.1	75	2.9
	20	33.07	38.4	28.5	40	60	43.1	56.9	89.6	10.4	17.9	80.6	1.5
Scenario B													
Grootdraai Dam	5	17.1	44.3	38.6	32.4	67.6	50.1	49.9	-				
	10	33.3	42.9	23.8	43.5	56.5	46.7	53.3					
	20	38.4	39.8	22	41	59	43.5	56.5					
Scenario C													
Grootdraai Dam	5	18.2	44.4	37.4	32.2	67.8	46.1	53.9	27.5	72.5	38.3	56.8	4.9
	10	34.4	42.7	22.9	43.1	56.9	41.6	58.4	14.4	85.6	67.3	29.9	2.5
	20	39.3	39.6	21.1	40.7	59.4	36.7	63.3	8.7	91.3	71.3	27.4	1.3

Notably, Scenario C (increase in mining areas) mirrors the trends observed in Scenario B, highlighting a significant decrease in unacceptable levels at the 20-year scale. Furthermore, phosphate compliance percentages in Scenario A exhibit a decline, Scenario B maintains stabilised levels around the acceptable range, while Scenario C consistently decreases.

The TDS compliance trends in Scenarios A, B, and C over 5, 10, and 20 years from 2020 reveal that Scenario A exhibits a gradual increase, reaching a peak at 20 years within acceptable limits. In Scenario C, a decline in acceptable levels is evident, accompanied by a significant increase in tolerable levels. Hence, sulphate compliance trends in Scenarios A, B, and C over 5, 10, and 20 years from 2020 reveal that Scenario A's levels fluctuate within tolerable, acceptable, and ideal limits. Meanwhile, in Scenario C, a notable decrease in acceptable and ideal levels is evident, yet there is a significant increase in tolerable levels.

5.3.4 Water quality assessment under land-use changes

The assessment of nitrate plus nitrite concentrations under the urban area increase scenario (referred to as Scenario A) uses water quality guidelines (acceptable classification) established by Rand Water (2022) for the Grootdraai Dam, as illustrated in Figure 5.22.

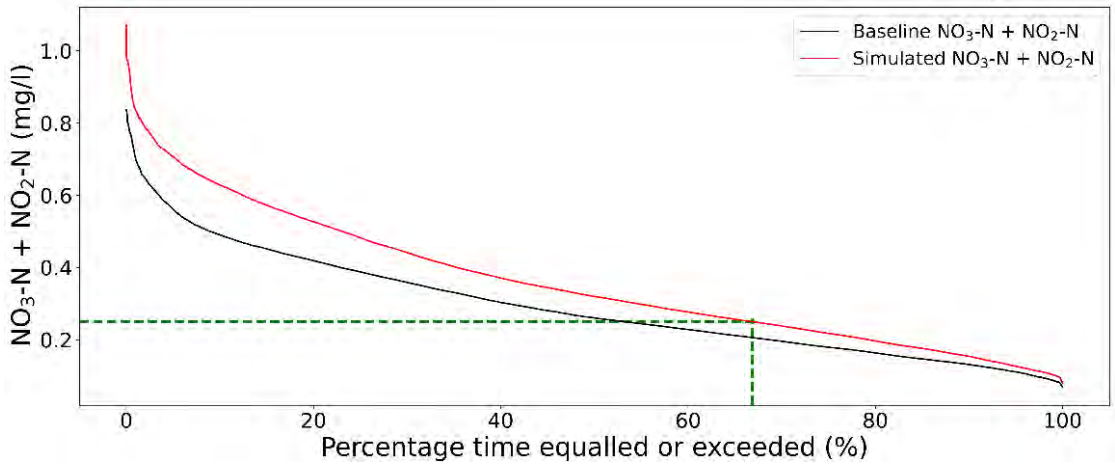

Figure 5.22: The Pywr-WQ model simulated nitrate plus nitrite at the Grootdraai Dam node under urban areas increase scenario (Scenario A) alongside the baseline simulation, which is depicted through frequency distributions. These distributions are juxtaposed with the numerical limits established at the Grootdraai Dam node (Rand Water, 2022). The threshold for the acceptable level is denoted by green lines.

The plot reveals that simulated nitrate plus nitrite levels in Scenario A surpass the numerical limit considered acceptable 66.9% of the time, compared to 53.3% under the baseline scenario. Figure 5.23 shows that ammonium concentration Scenario A surpasses the numerical limit considered acceptable (0.1 $mg.l^{-1}$) for 15.7% of the time, compared to 14.6% under the baseline scenario.

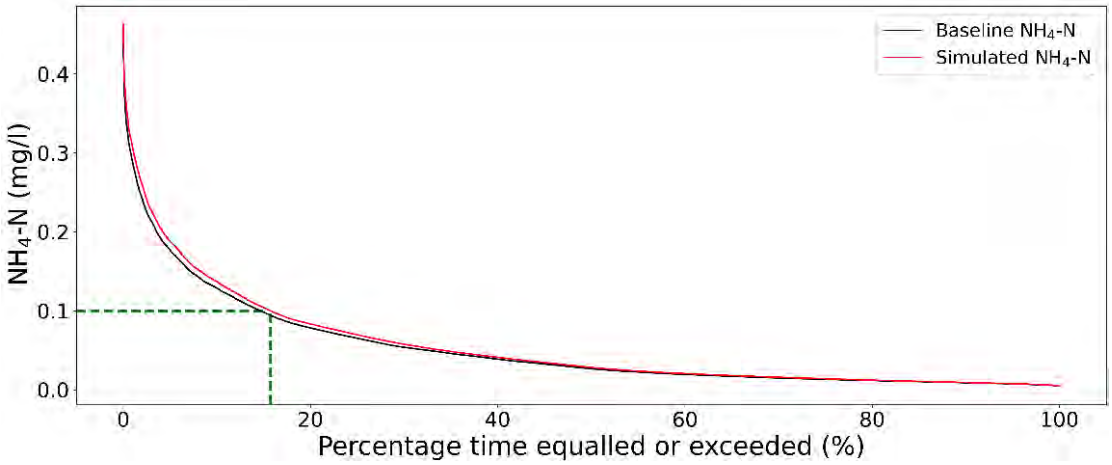

Figure 5.23: The Pywr-WQ model simulated ammonium at the Grootdraai Dam node under urban areas increase scenario (Scenario A) alongside the baseline simulation, is depicted through frequency distributions. These distributions are juxtaposed with the numerical limits established at the Grootdraai Dam node (Rand Water, 2022). The threshold for the acceptable level is denoted by green lines.

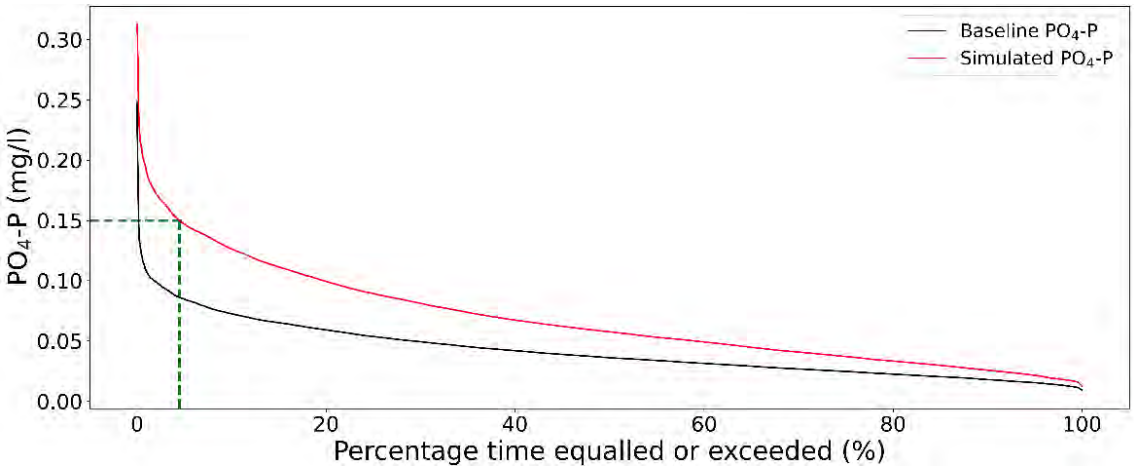

Figure 5.24: Pywr-WQ model simulated phosphate at the Grootdraai Dam node under cultivated areas increase scenario (Scenario B) alongside the baseline simulation, is depicted through frequency distributions. These distributions are juxtaposed with the numerical limits established at the Grootdraai Dam node (Rand Water, 2022). The threshold for the acceptable level is denoted by green lines.

Phosphate concentrations escalate under cultivated areas increase (referred to as Scenario B), exceeding the numerical limit deemed acceptable (0.15 $mg.l^{-1}$) for 4.5% of the time, compared to 0.17% under the baseline scenario (Figure 5.24). Furthermore, phosphate concentrations in

Scenario B surpass the numerical limit considered ideal (0.04 $mg.l^{-1}$) 71.1% of the time, compared to 43% in the baseline scenario (Figure 5.25).

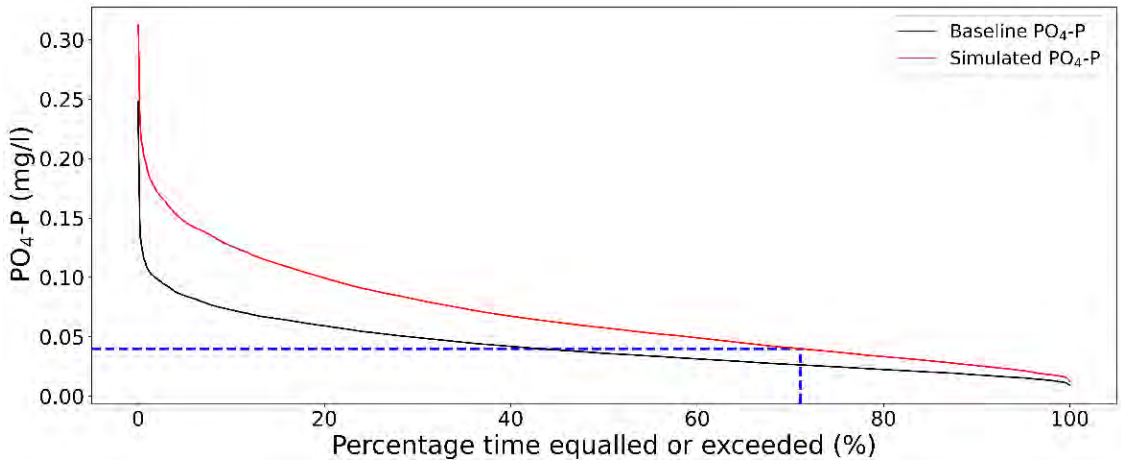

Figure 5.25: Pywr-WQ model simulated phosphate at the Grootdraai Dam node under cultivated areas increase scenario (Scenario B) alongside the baseline simulation, is depicted through frequency distributions. These distributions are juxtaposed with the numerical limits established at the Grootdraai Dam node (Rand Water, 2022). The threshold for the ideal level is denoted by blue lines.

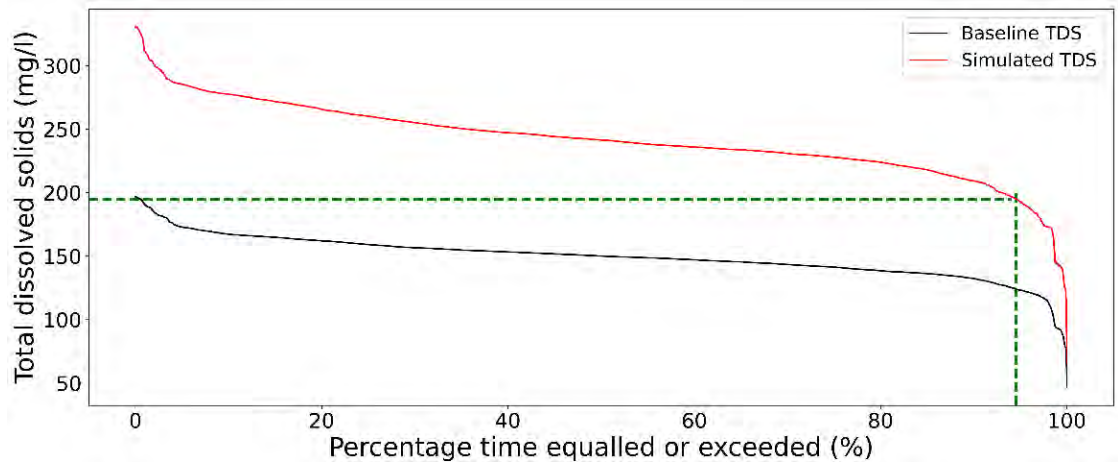

Figure 5.26: The Pywr-WQ model simulated TDS at the Grootdraai Dam node under mining areas increase (Scenario C) alongside the baseline simulation, which is depicted through frequency distributions. These distributions are juxtaposed with the numerical limits established at the Grootdraai Dam node (Rand Water, 2022). The threshold for the acceptable level is denoted by green lines.

The TDS concentrations increase as mining areas expand (referred to as Scenario C), exceeding the numerical limit deemed acceptable (195 $mg.l^{-1}$) 94.5% of the time, compared to 0.54% under the baseline scenario (Figure 5.26).

Sulphate concentrations, too, escalate under mining areas increase, exceeding the numerical limit deemed acceptable (25 mg.l^{-1}) for 98% of the time, compared to 80.7% under the baseline scenario (Figure 5.27).

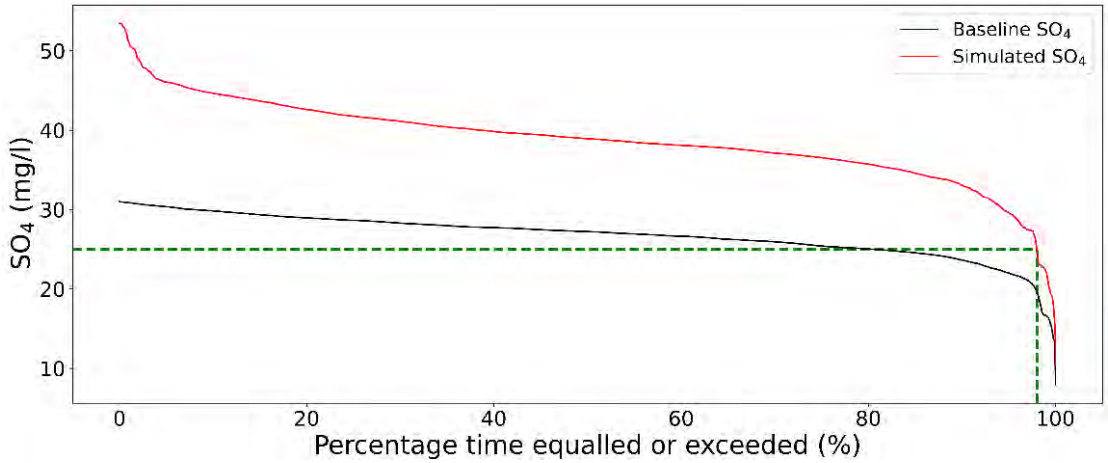

Figure 5.27: The Pywr-WQ model simulated sulphate at the Grootdraai Dam node under mining areas increase (Scenario C) alongside the baseline simulation, which is depicted through frequency distributions. These distributions are juxtaposed with the numerical limits established at the Grootdraai Dam node (Rand Water, 2022). The threshold for the acceptable level is denoted by green lines.

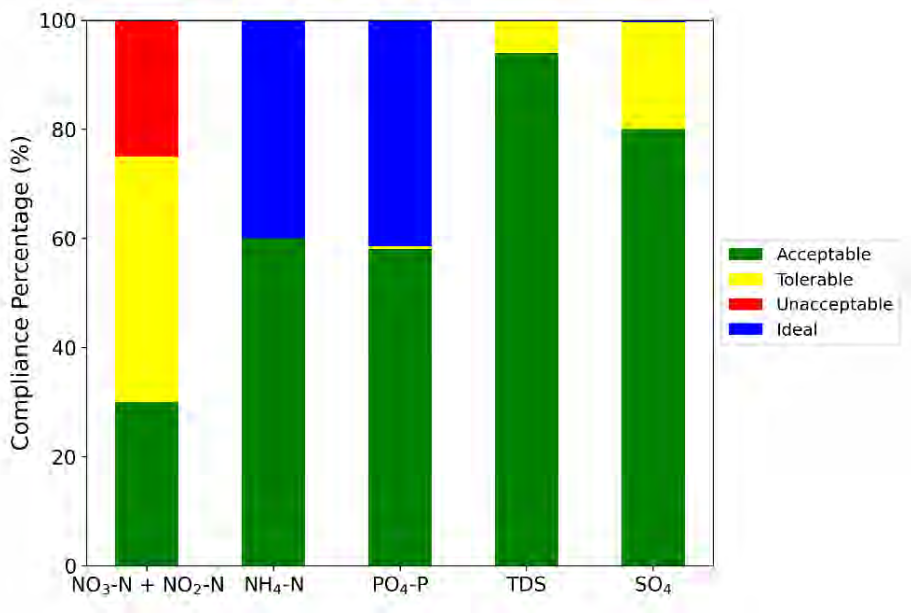

Figure 5.28: Compliance percentages for nitrate plus nitrite, ammonium, phosphate, TDS, and sulphate were evaluated across various classifications at the Grootdraai Dam node over the short term (2010–2050), in the urban increase scenario.

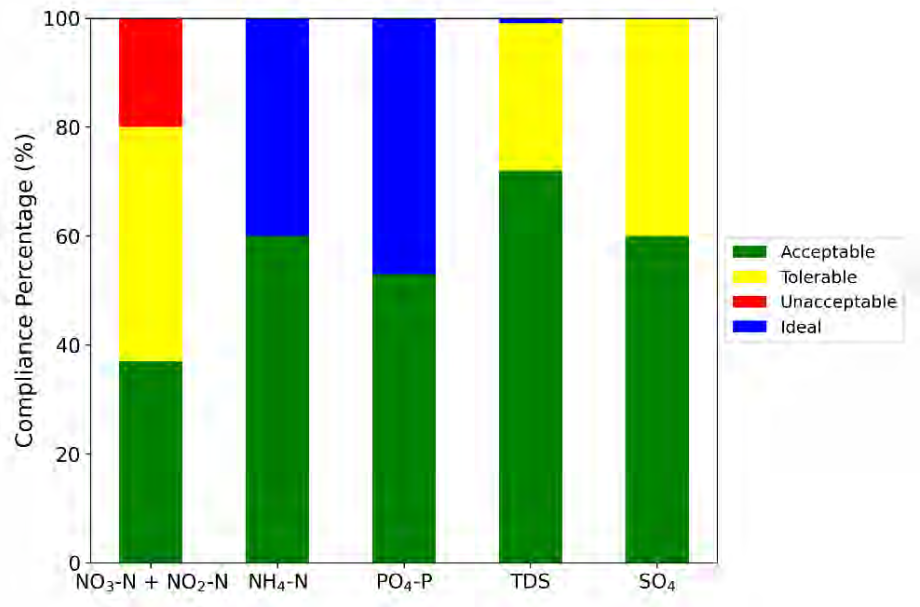

Figure 5.29: Compliance percentages for nitrate plus nitrite, ammonium, phosphate, TDS, and sulphate were evaluated across various classifications at the Grootdraai Dam node over the long term (2050–2099), in the urban increase scenario.

Figures 5.28 and 5.29 illustrate compliance percentages for nitrate plus nitrite, ammonium, phosphate, TDS, and sulphate over short and long term periods in the urban increase scenario (referred to as Scenario A). The graphs indicate an increase in tolerable levels and a decrease in unacceptable levels of nitrate plus nitrite over the long term compared to the short term. Conversely, TDS and sulphate exhibit high tolerable levels and a decrease in acceptable levels over the long term compared to the short term. These findings indicate a potential deterioration in water quality standards for TDS and sulphate, alongside a potential improvement for nitrate plus nitrite, ammonium, and phosphate in the long term in the urban increase scenario.

Figures 5.30 and 5.31 illustrate compliance percentages for nitrate plus nitrite, ammonium, and phosphate over short and long term periods, respectively, in the cultivated increase scenario (referred to as Scenario B). The graphs show a rise in tolerable levels and a decline in unacceptable levels of nitrate plus nitrite over the long term compared to the short term. Conversely, phosphate shows a fraction of tolerable levels in the short term and an increase in ideal levels in the long term. These trends suggest potential improvements in water quality conditions over time, particularly for nitrate plus nitrite and phosphate.

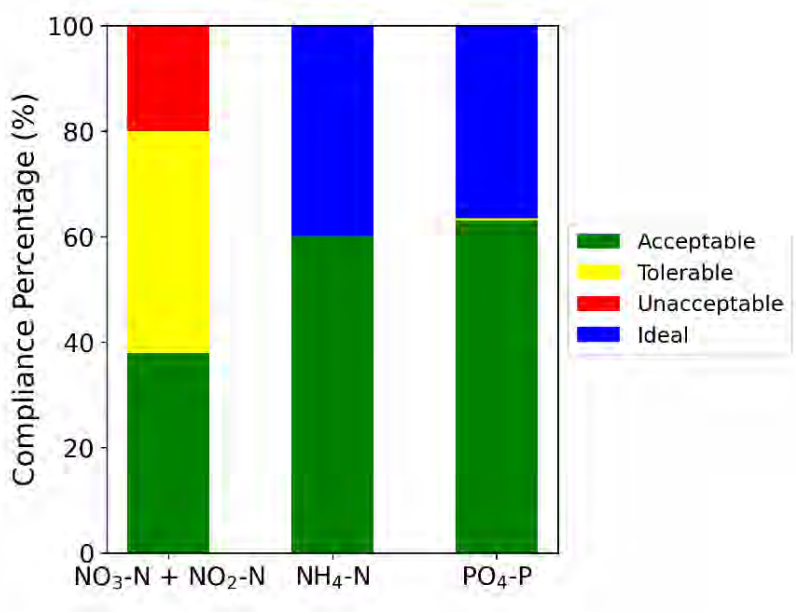

Figure 5.30: Compliance percentages for nitrate plus nitrite, ammonium, and phosphate were evaluated across various classifications at the Grootdraai Dam node over the short-term (2010–2050), in the cultivated increase scenario.

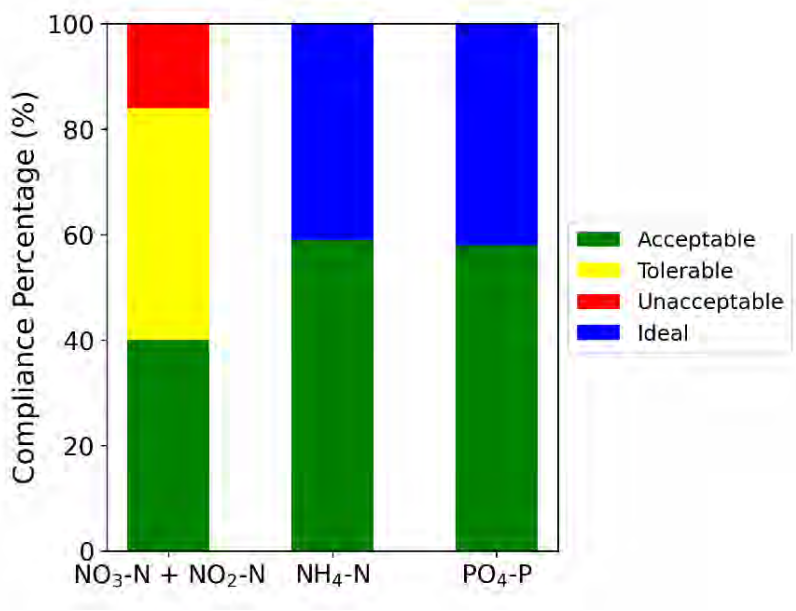

Figure 5.31: Compliance percentages for nitrate plus nitrite, ammonium, and phosphate were evaluated across various classifications at the Grootdraai Dam node over the long term (2010–2099), in the cultivated increase scenario.

Figures 5.32 and 5.33 depict compliance percentages for nitrate plus nitrite, ammonium, phosphate, TDS, and sulphate over short and long term periods, respectively, in the mining increase scenario (referred to as Scenario C). The graphs indicate degradation in TDS and sulphate concentrations over the long term, with unacceptable levels emerging which were not

observed in the short term. Additionally, there are differences in nutrient concentrations between the short and long term; for example, unacceptable levels of nitrate plus nitrite appear to be higher in the short term than in the long term.

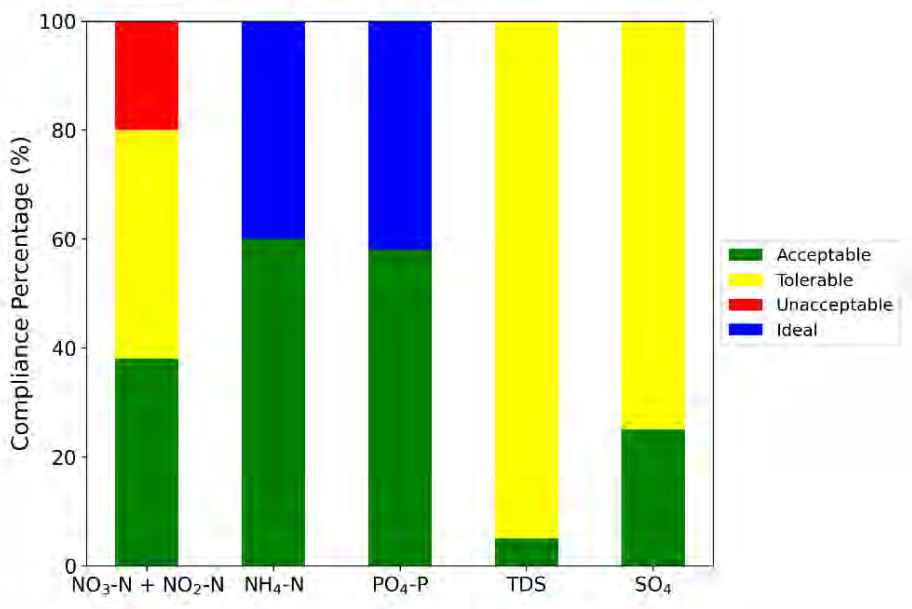

Figure 5.32: Compliance percentages for nitrate plus nitrite, ammonium, phosphate, TDS, and sulphate were evaluated across various classifications at the Grootdraai Dam node over the short term (2010–2050), in the mining increase scenario.

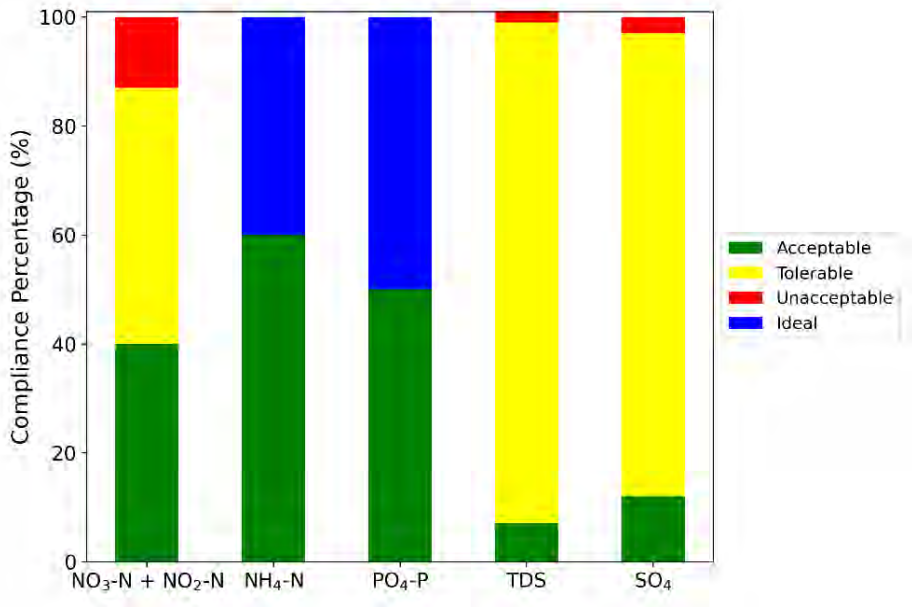

Figure 5.33: Compliance percentages for nitrate plus nitrite, ammonium, phosphate, TDS, and sulphate were evaluated across various classifications at the Grootdraai Dam node over the long term (2050–2099), in the mining increase scenario.

5.4 Discussion

This section delves into the implications of the study's findings, focusing on how land-cover changes within the Grootdraai Dam Catchment affect water quality. This section explores the relationships between various land-cover categories such as urban areas, cultivated lands, and mining activities, and their impact on specific water quality parameters.

5.4.1 Land-cover model parameterisation

The land-cover models were developed for the Grootdraai Dam Catchment using a multiple regression approach. Each quaternary catchment produced various coefficients linked to specific land-cover classes, as shown in Tables 5.5 and 5.6. Across different inflows within quaternary catchments, certain parameters consistently showed higher values, particularly in and of downstream urban, cultivated, and mining areas. Among all inflow nodes, major land-cover categories influencing water quality in terms of nitrate plus nitrite included urban areas, cultivated areas, barren lands, wetlands, and mining areas. For ammonium, cultivated areas and mining were influential, followed by urban areas, wetlands, and barren lands. In the case of phosphate, urban and mining areas were most influential, followed by cultivated areas. Although mining areas had a high influence, their land-cover percentages were not as significant as other land-cover classes. In addition, salts such as TDS, sulphate, and calcium appeared to be dominated by mining and urban areas in a few selected quaternary catchments. For salts, these relationships make conceptual sense, as most of these land-cover categories are traditionally associated with non-point input of salts. Therefore, certain challenges arise in connection with nutrient inputs. For instance, the seemingly unusually predominant association of phosphate input with mining areas poses a notable consideration.

Prior investigations in South Africa have deemed mining areas as plausible contributors to phosphate levels, as well as wastewater treatment (Ashton & Dabrowski, 2010; Griffin et al., 2014). However, a significant phosphate load was identified, primarily from detergents, especially washing powders (Quayle et al., 2010). As a result of phosphate enrichment, eutrophication may occur, leading to the excessive growth of microscopic green plants, algae, and cyanobacteria, which pose a toxic threat to aquatic life and human water users (DEAT, 2006).

5.4.2 Land-cover scenarios and water quality implications

This study provides long term water quality variation predictions built on land-cover changes in the Grootdraai Dam Catchment located in the Upper Vaal in South Africa. This study looked at

water quality impacts, particularly in terms of changes that might be anticipated in response to changes in likely land-cover and land-use classes.

Increased urban areas scenario, showed high nitrate plus nitrite, ammonium, and a marginal increase in phosphate levels compared to the baseline scenario at the Grootdraai Dam. Nitrogen sources in South Africa are potentially related to agriculture, wastewater, and domestic water (Schoeman & Steyn, 2003). Within the Upper and Middle Vaal regions where industries, agriculture, and urban areas are present, nutrient levels were notably higher, as indicated by Ntshalintshali (2019). Similarly, an investigation conducted by Chen et al. (2020) revealed that rapid urbanisation has caused substantial alterations in nitrogen transport within the northern Taihu Basin in China from 1990 to 2017. The predictions indicate a high likelihood of nitrate plus nitrite levels remaining unacceptable over the next 5 to 20 years. Conversely, ammonium exhibits a relatively stable distribution, maintaining a balance between acceptable and ideal water quality classifications. The change in inorganic nitrogen loads to the Grootdraai Dam results in the possibility of promoting the growth of blooms of blue-green algae and other aquatic plants resulting in eutrophication. These algal blooms may include species that are toxic to humans, livestock, and wildlife (DWAF, 1996). Elevated nutrient levels may also cause ecological damage including loss in fish population, morphological modifications in both fish and invertebrate fauna, shifts in faunal composition, and an overall decline in biodiversity (Camargo et al., 2005; Idris et al., 2016; Odume & Muller, 2011; van Ginkel, 2011).

Scenario B, regarding an increase in cultivated areas over the long term, showed high concentrations of phosphate compared to the baseline simulations. Phosphate sources in South Africa can be related to different potential sources such as agricultural activities (Villiers & Thiart, 2007). A recent study suggests that the intensification of agriculture may lead to an elevated concentration of phosphorus in water bodies (Mng'ong'o et al., 2022). Hence, agricultural non-point source pollution can damage water quality status within reservoirs, such as is the case of the Miyun Reservoir in China (Xie et al., 2019). Phosphates are used in the processing and preservation of agricultural products (Soceanu et al., 2009), which could be a reason for the high concentration in the Grootdraai Dam, linked to the expansion of irrigated areas. The enrichment of phosphates is frequently (though not always) responsible for freshwater eutrophication (Griffin, 2017). As a result, an increase in phosphate concentrations may contribute to the production of eutrophication, leading to changes in the aquatic environment and potential loss of biodiversity.

The increase in mining areas in certain quaternary catchments over the long term showed troubling results for both TDS and sulphate. Compliance percentages for TDS and sulphate in Scenario C show a rising trend within tolerable levels at Grootdraai Dam over the next 5, 10, and 20 years while reaching unacceptable levels upstream of the Grootdraai Dam, potentially due to dense mining activities. As per the predictions, the expansion of mining areas produces disquieting variations in sulphate and TDS concentrations, ranging from 12 to 650 $mg.l^{-1}$ for the mean value upstream to downstream and from 242 to 2720 $mg.l^{-1}$, respectively. Mining activities are expected to increase the input of TDS and sulphate in groundwater, which may threaten aquatic life and ecosystem habitats, and cause potential damage to biodiversity within river systems. The TDS and sulphate can be impacted by cultivated areas as this category has been also observed in the developed land-cover model for TDS and sulphate, along urban areas and waterbody categories. du Plessis et al. (2015) confirmed that the expansion of mining areas is anticipated to increase sulphate and EC concentrations within the Grootdraai Dam Catchment.

5.5 Conclusion

South Africa, as a developing country, faces constraints in water resources. The Grootdraai Dam, situated in the Upper Vaal region, plays a pivotal role in supporting various water users, including industrial, agricultural, domestic, and others, to meet their water requirements. The water quality status within the Grootdraai Dam Catchment, especially the reservoir, is of principal importance. The quality of water directly impacts the availability of water resource, influencing the needs of diverse water users. The quantification of non-point inputs within the Pywr-WQ model is linked to flow fraction signatures, encompassing both surface water and sub-surface water (including groundwater and interflow) signatures. However, the parameters defining these signatures may exhibit variability based on the knowledge and expertise of the model user. In response to this challenge, the current study aimed to establish relationships between land-cover categories and water quality variables. Specifically, the investigation concentrates on nitrate plus nitrite, ammonium, phosphate, sulphate, calcium, and TDS. These developed relationships facilitate the estimation of changes in water quality in response to variations in specific land cover classes, whether increasing or decreasing. Hence, future conditions of water quality can be predicted through the employment of the developed multiple regression model equations based on land-cover changes.

With the expansion of mining areas, the Grootdraai Dam is projected to experience high levels of sulphate, TDS, and calcium within the acceptable to ideal range in the reservoir. However, unacceptable values will be concentrated both upstream and in certain parts of the downstream

area of the catchment. While this study examined the effects of expanded mining areas, it is worth noting that coal mining is expected to decline as part of the Just Energy Transition Project (JETP) in response to climate change. The likelihood of increased mining is diminishing (World Bank, 2023).

In the scenario of urban area expansion, the Grootdraai Dam is expected to encounter high levels of nitrate plus nitrite and ammonium ranging from unacceptable to ideal standards. Additionally, an increase in cultivated areas is likely to lead to elevated phosphate values, ranging from acceptable to ideal standards, in the Grootdraai Dam.

Future studies could investigate the inclusion of additional variables in land-cover models, such as precipitation, irrigation, and the frequency of fertiliser application. These variables have the potential to influence the hydrological characteristics of the catchment, potentially resulting in modifications or alterations in water quality and the mobilisation of pesticides. Ultimately, such changes can impact the health of soil-water, aquatic life, ecosystem habitats, and the overall biodiversity of the river system within the catchment.

CHAPTER 6: POTENTIAL FUTURE SCENARIO FOR THE GROOTDRAAI DAM CATCHMENT

6.1 Introduction

South Africa is considered the leading country in Africa in terms of mining production (Stilwell et al., 2000). The country faces a critical decision: adopt a circular economy for sustainable development aligned with SDGs or opt for short-term economic stability reliant on high-risk energy sources, like mining, endangering both the environment and human well-being. The South African government's steadfast commitment to coal mining presents a significant hurdle, with many South Africans perceiving coal combustion as a conventional practice (Chiumia, 2021). Mining areas situated in the Grootdraai Dam Catchment area play a substantial role in the deterioration of water quality (du Plessis et al., 2015; Naidoo, 2017). Power generation and the Sasol-Secunda (coal-to-liquid) plant consume coal, and many coal mines are present in the catchment. Beyond the potential risks of acidification, salinisation, and increased metal solubility attributed to coal-related acid mine drainage and discharge, the combustion or gasification of coal within the catchment area may introduce additional challenges to water quality. These include rain acidification (Munawer, 2018) and the potential for heavy metal contamination (CSIR, 2010). In this regard, coal combustion in South Africa is a significant source of mercury in freshwater systems (Dabrowski et al., 2008). Considering the limited availability of water quality data in South Africa (Slaughter et al., 2017), investigating heavy metal decomposition within river systems presents a substantial challenge.

There has been a notable rise in water demand since the dam's commissioning, and there are projections of further increases in water consumption by Sasol-Secunda (DWS, 2018). South Africa's dual challenges of coal-related environmental risks and its pursuit of sustainable development underscore the urgent need for robust water quality models. The coal industry in South Africa is identified as a major driver of environmental inequality and injustice, which goes against the principles of the Paris Agreement, according to Cock (2019). Eskom is responsible for electricity production in South Africa, with coal-fired plants being the predominant source of electricity (Votteler & Brent, 2016). Eskom failed to capitalise on the potential transition to green energy. Instead, it allegedly employed delaying tactics, leveraged information asymmetry and exploited its monopoly status to obstruct the signing of power purchase agreements with renewable energy developers (Ting & Byrne, 2020). According to Akinbami et al. (2021), South

Africa is progressively advancing its renewable energy sector to reduce CO_2 emissions, with a particular emphasis on developing biomass, wind, and solar energy industries. Moreover, South Africa showed favourable behaviour in addressing the transition from coal to renewable energy. For instance, Eskom's JETP, a project funded by the World Bank approved in 2022 with a $497 million budget at the request of the Government of South Africa (World Bank, 2023). The project supports the transition to a low-carbon, resilient economy by 2050, as outlined in the Just Transition Framework (JTF) and the Integrated Resource Plan (IRP) 2019 (DMRE, 2019). In addition, it is consistent with the country's updated Nationally Determined Commitments (NDCs) to mitigate carbon emissions (PCC, 2021). Hence, Eskom is considering a potential shift from coal-based power stations to green energy sources like solar power within the Upper Vaal region, which includes the study area.

This current study employed the Pywr-WQ model to investigate the combined impacts on water quality of climate change, mining closure, and escalating water demand. This chapter delves into an examination of the combined impacts of various environmental changes, including the closure of mining activities, on water quality. It aims to evaluate the feasibility of adapting to these changes as part of a sustainable, long term strategy for improving water quality in the study area. This evaluation considers evolving climate conditions and the growing pressure on water resource, presenting a plausible scenario for the future.

6.2 Methods and Materials

This study explores two potential future scenarios for the Grootdraai Dam Catchment, each reflecting different levels of water abstraction under the influence of climate change and mining closures. These scenarios, referred to as "low abstraction" and "high abstraction" are developed to understand the long term impacts on water quality in the catchment.

6.2.1 Investigated scenarios

The investigation into these scenarios stemmed from several factors: a projected rise in Sasol-Secunda water abstraction (DWS, 2018), climate change, and the close of mining areas due to a transition from coal-based to renewable power generation sources.

This chapter explored two potential future scenarios for the Grootdraai Dam Catchment, denoted as low and high abstraction. Both scenarios shared two common factors: the closure of mining areas and the utilisation of climate change flow datasets. In addition, the Pywr model, originally calibrated for historical conditions, now incorporates climate change inflows. The sole distinction between low and high abstraction lies in the applied increased percentage of water

abstraction. Specifically, the study considered two different increased water abstraction percentages: a 5% increase, representing a scenario highly probable to occur in the long term, and a 70% increase in water abstraction, deemed highly improbable over the long term to assess the effects of extreme levels of abstraction.

Table 6.1 depicts the scenarios explored in this study, which are connected to the potential future of the Grootdraai Dam Catchment over the long term.

Table 6.1: Scenario definitions and corresponding water quality variables.

Scenario code	Scenario	Investigated WQ variables
Low abstraction	Climate change dataset Mining closure 5% increase in water abstraction	NO_2-N + NO_3-N, NH_4-N PO_4-P, TDS, SO_4, Ca, K, Cl, F, Na, Mg
High abstraction	Climate change Mining closure 70% increase in water abstraction	NO_2-N + NO_3-N, NH_4-N PO_4-P, TDS, SO_4, Ca, K, Cl, F, Na, Mg

6.2.1.1 Climate change datasets

The climate change flow datasets used in this study originated from a prior project conducted in the Vaal Dam Catchment, which examined the effects of climate change on water quality in the area (Aurecon, 2020). These datasets, aimed at understanding the alterations in water quality patterns due to climate change, were derived from the application of the Pitman hydrological model (1973) in conjunction with downscaled projected climate models. The study utilised one of the generated flow datasets under a climate change scenario as it is; no changes were executed on those flow datasets for the Grootdraai Dam Catchment.

The climate change datasets were available for every incremental node (natural flow input) located in the Grootdraai Dam Catchment. The new Pywr-WQ model incorporated these datasets as input to assess changes in water quality variables amid shifting climate conditions. These incremental flow datasets were separated into three distinct flow fractions: surface water flow, interflow, and groundwater flow (refer to Chapter 4; Section 4.2.2). Each flow fraction was associated with a specific water quality signature, including a surface flow signature for nutrients and salts (SF_N and SF_{salts}), an interflow signature for nutrients and salts (IF_N and IF_{salts}), and a groundwater flow signature for nutrients and salts (GWF_N and GWF_{salts}). Notably, the signatures assigned to nutrients and salts such as magnesium, potassium, fluoride, chloride, and sodium remained consistent with those derived during the calibration process (refer to Chapter 4; Section

4.2.7). This decision was driven by the study's focus on the impact of mine closure on selected water quality variables including TDS, sulphate, and calcium while maintaining the signatures of other water quality variables as observed in the calibration exercise. Hence, the climate change datasets encompassed only incremental flows. It was assumed that the maximum and minimum air temperatures remained consistent with historical data, as variations in these temperatures can impact water temperature, which was presumed to remain unchanged under changing climate conditions. The present study operates under the assumption that in the event of climate change, there will be no alteration in the percentages of land-cover classes, implying that the land-cover will remain consistent compared to the baseline scenario.

Statistical tests were employed to assess and characterise the climate change flow datasets concerning the baseline flow datasets including the Seasonal Kendall Test (Helsel & Frans, 2006; Hirsch et al., 1982) and a paired Prentice-Wilcoxon test for paired data (O'Brien & Fleming, 1987). The Seasonal Kendall Test was employed to examine potential trends, whether increasing or decreasing, within the climate change datasets, under the null hypothesis of no significant monotonic trend in the data. The flow datasets from each incremental flow node within the quaternary catchments of the Grootdraai Dam Catchment were collected into two distinct seasons: wet and dry. In the Mpumalanga Province, the wet season primarily occurs from October to March, while the dry season extends from April to September (Rusere et al., 2023). In addition, the Seasonal Kendall Test was employed on the simulated water quality datasets generated by the Pywr-WQ model under changing climate conditions. The water quality datasets for the Grootdraai Dam node for each water quality variable under low and high abstraction scenarios were collected across two primary seasons: wet and dry seasons. The analysis aimed to assess whether there were significant seasonal trends in water quality variables between the low and high abstraction scenarios during both wet and dry seasons. The null hypothesis posits that there exists no statistically significant seasonal trend of water quality variables in the low and high abstraction scenarios throughout both wet and dry seasons.

The paired Prentice-Wilcoxon test was used to determine whether significant differences existed between the average monthly climate change flow datasets and the corresponding baseline average monthly flow datasets for the incremental nodes in the Grootdraai Dam Catchment. The paired Prentice-Wilcoxon test was conducted on the water quality simulations generated under both high and low abstraction scenarios. This test aimed to determine whether there was a significant difference between the monthly baseline scenario (1920–2010) simulation datasets

and the simulated water quality variables datasets over the long term (2010–2099) for the Grootdraai Dam node.

6.2.1.2 Water abstraction increase scenario

Insufficient data regarding the potential long term increase percentage in Sasol-Secunda water abstraction prompted this study to consider two distinct escalation scenarios that may or may not occur in the future. The 70% increase scenario, while unlikely and extreme, functions as a worst-case scenario for modelling, capturing the range of uncertainties. In contrast, the 5% increase in water abstraction represents a more probable scenario. These percentages were chosen to simulate water quality responses under diverse scenarios, spanning from the more plausible to the least probable occurrences. Sasol-Secunda's water abstraction operates based on a rule outlined by Stone (2009), stipulating that Sasol-Secunda abstracts water only when the Dam reaches 90% of its full capacity. However, recent discussions with Sasol partners have confirmed a change in the rule, allowing Sasol to abstract water when the Dam is at only 75% of its full capacity. Therefore, the model integrated the new rule as a parameter, setting forth that abstraction would occur if the dam reached 75% of its capacity; otherwise, no abstraction would take place, thus taking advantage of the dynamic integration between water quantity and quality in Pywr-WQ model.

6.2.1.3 Mining closure scenario

The mining closure scenario is built on the attribution of salt groundwater flow signature to quaternary catchments located in the study area. According to Mulopo (2015), mining effluent is associated with high TDS, sulphate, and heavy metals, as well as the release of mining industry effluents, known for their elevated calcium concentrations (Motaung et al., 2008). To explore the effects of mining closure, the study aimed to identify groundwater signatures representing relatively unimpacted catchments within the Grootdraai Dam Catchment. These signatures, characterised by minimum TDS, sulphate, and calcium concentrations, were presumed to reflect catchments less affected by mining activities. Specifically, the study focused on quaternary catchments C11A, C11B, C11K, and C11F, which exhibited elevated groundwater signatures during the calibration phase (see Chapter 4). It is anticipated that the closure of mines will lead to the long term recovery of groundwater to levels resembling those of unimpacted catchments.

6.2.2 Statistical analysis of investigated scenarios

To assess potential annual and monthly trends and differences in water quality between simulated scenarios and baseline data, several analyses were employed. These analyses included the Mann-

Kendall trend test (McLeod, 2005) and a paired Prentice-Wilcoxon test for paired data (O'Brien & Fleming, 1987). The Mann-Kendall test was used to investigate potential trends either increasing or decreasing within the daily water quality dataset (2010–2099), assuming a null hypothesis of no monotonic trend in the data. The paired Prentice-Wilcoxon test was used to determine whether significant differences existed between the average monthly concentrations of water quality data and their corresponding baseline averages.

6.3 Results

This section presents the key findings of this study, highlighting the impact of future scenarios on water quality within the context of climate change.

6.3.1 Annual and seasonal climate change's flow dataset variation

Table 6.2 shows the average flow and the standard deviation for each incremental flow located in different quaternary catchments in the study area.

Table 6.2: Comparison of the average flow and standard deviation between climate change spanning 2010 to 2099 and the baseline datasets covering the years 1920 to 2010, for quaternary catchments within the Grootdraai Dam Catchment, Upper Vaal, South Africa.

Node	Quat.	Baseline dataset		Climate change dataset	
		mean (Mm^3/day)	std	mean (Mm^3/day)	std
Inflow_1	C11A	0.092	0.366	0.078	0.321
Inflow_2	C11B	0.068	0.272	0.048	0.196
Inflow_3	C11C	0.057	0.228	0.094	0.388
Inflow_4	C11D	0.048	0.189	0.033	0.134
Inflow_5	C11F	0.138	0.548	0.167	0.687
Inflow_6	C11G	0.064	0.255	0.060	0.248
Inflow_7	C11E	0.171	0.681	0.199	0.817
Inflow_8	C11H	0.156	0.620	0.148	0.610
Inflow_9	C11J	0.147	0.586	0.099	0.406
Inflow_10	C11K	0.050	0.197	0.041	0.168
Inflow_11	C11L	0.138	0.550	0.109	0.448
Grootdraai Dam Catchment		0.102	0.408	0.097	0.402

*Quat. refers to the quaternary catchment.

Table 6.2 presents the mean and standard deviation values for various nodes under both the baseline and climate change datasets. It is apparent that, across most nodes, the mean values in the climate change dataset are slightly lower than those in the baseline dataset.

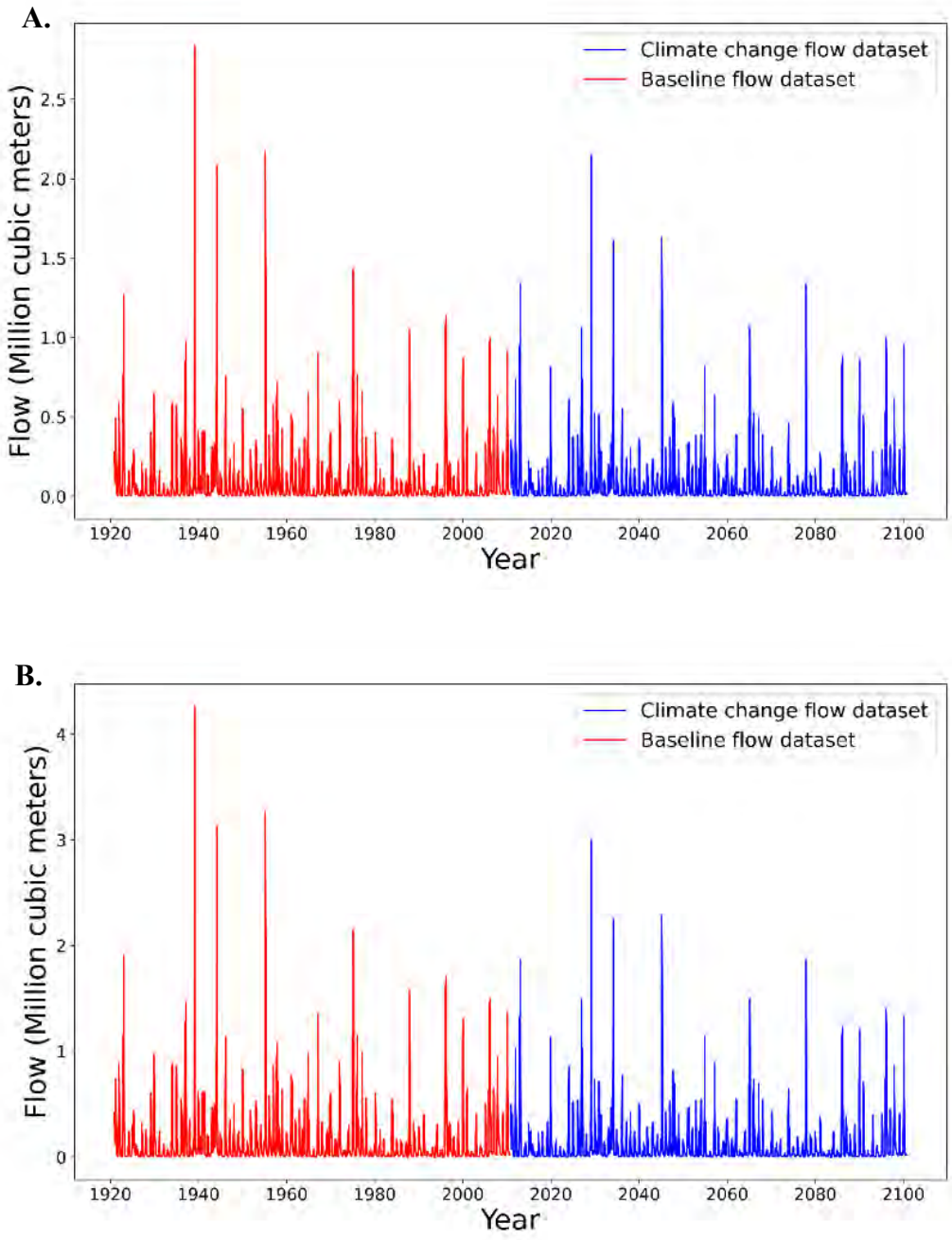

Figure 6.1: The variation in annual average flow within the Grootdraai Dam Catchment was plotted against time (2010–2099). (A) illustrates the annual average flow variation at quaternary catchment C11A, situated in the upstream area, while (B) depicts the annual average flow variation at quaternary catchment C11L, positioned in the downstream area of the Grootdraai Dam Catchment.

Furthermore, the standard deviation indicates that the baseline dataset tends to exhibit higher variability than the climate dataset. In specific cases, such as Inflow_3 (C11C) and Inflow_7 (C11E), the standard deviation values in the climate change dataset are noticeably higher than those in the baseline dataset.

For instance, Figure 6.1 illustrates a disparity between the annual average climate change and baseline flow datasets in both quaternary catchments C11A and C11L, situated upstream and downstream of the Grootdraai Dam Catchment, respectively. Pairwise comparison supports this observation, as there is a significant difference between the climate dataset and the baseline dataset ($p < 0.001$) for C11A and C11L, and for the remaining quaternary catchments that were tested as well. The Seasonal Kendall Test was applied to the daily climate change flow dataset for all quaternary catchments, examining trends separately for the winter and summer seasons. The results consistently revealed a negative trend in the climate change data during the wet season ($p<0.001$), contrasting with a positive trend observed during the dry season ($p<0.001$).

6.3.2 Water abstraction increase scenarios

Figure 6.2 demonstrates the behaviour of the Pywr-WQ model when the 75% threshold for water abstraction is considered. The model considers the enforced rule, where if the available volume in the dam equals or exceeds 262.5 Mm^3, there will be abstraction from the dam.

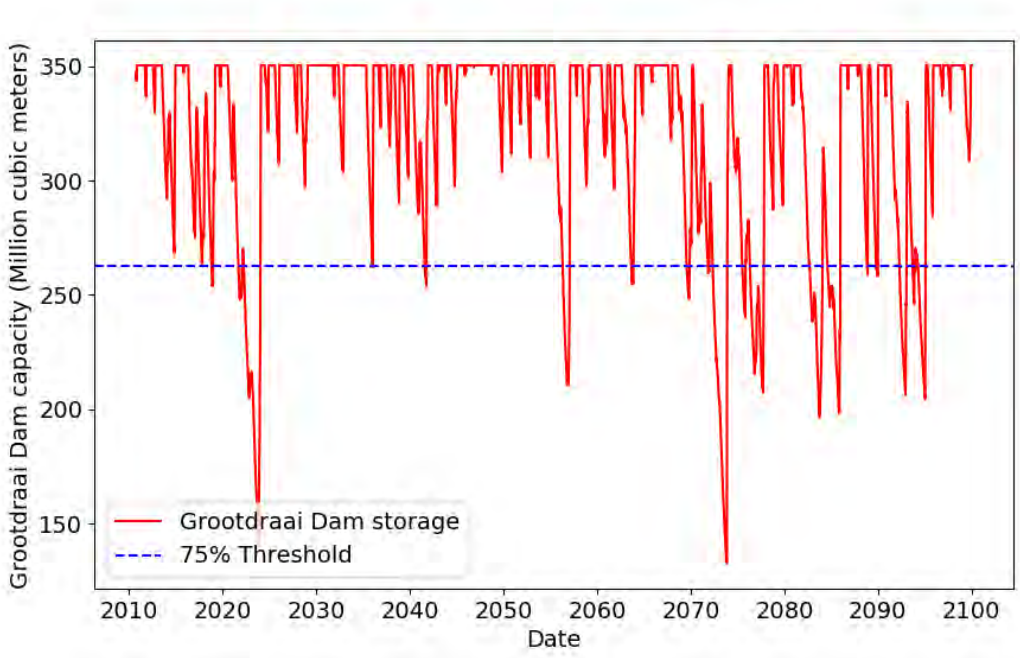

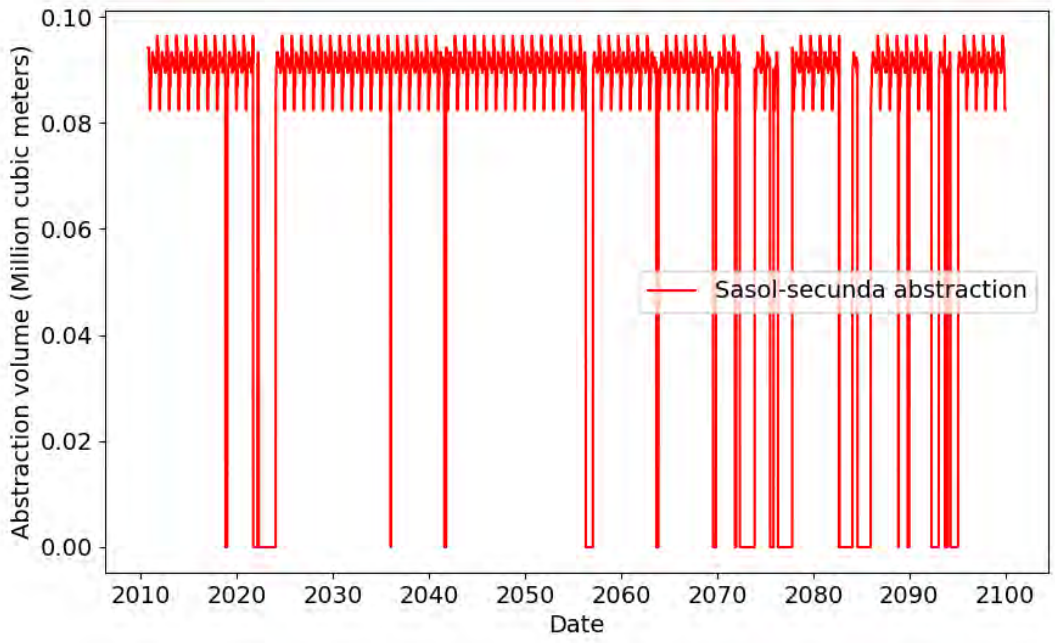

Figure 6.2: Sasol-Secunda abstraction volumes, contingent on adherence to the 75% operating rule. According to this rule, abstraction occurs when the dam's capacity reaches or exceeds 75% of its full capacity. If the storage falls below 262.5 Mm^3, abstraction ceases, exhibiting varying volumes depending on the abstraction.

However, if the current available volume in the Dam surpasses 262.5 Mm^3 (approximately 75% of the full Dam capacity), there will be no abstraction from the Grootdraai Dam.

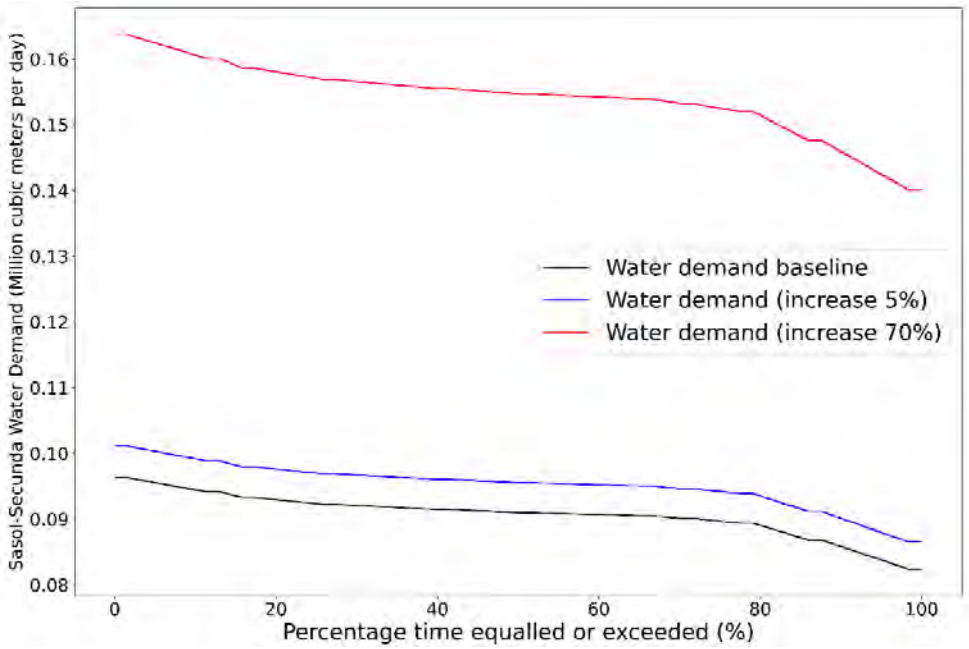

Figure 6.3: Sasol-Secunda water demand is shown as frequency distributions across varied increase rates of 5% and 70% over the long term (2010–2099).

Two distinct increase percentages were applied to the abstraction node at the Grootdraai Dam level to depict two scenarios: one representing a scenario highly likely to occur with an increasing percentage of 5%, and the other representing a scenario unlikely to occur with a 70% increase over the long term. Figure 6.3 illustrates the abstracted volume from Sasol-Secunda under these applied scenarios.

6.3.3 Future scenarios and water quality implications

6.3.3.1 Nutrients

Figure 6.4 presents the daily variation of nitrate plus nitrite levels over the long term within the Grootdraai Dam. It shows the time series distribution and compares future scenario simulations with baseline simulations using frequency distributions.

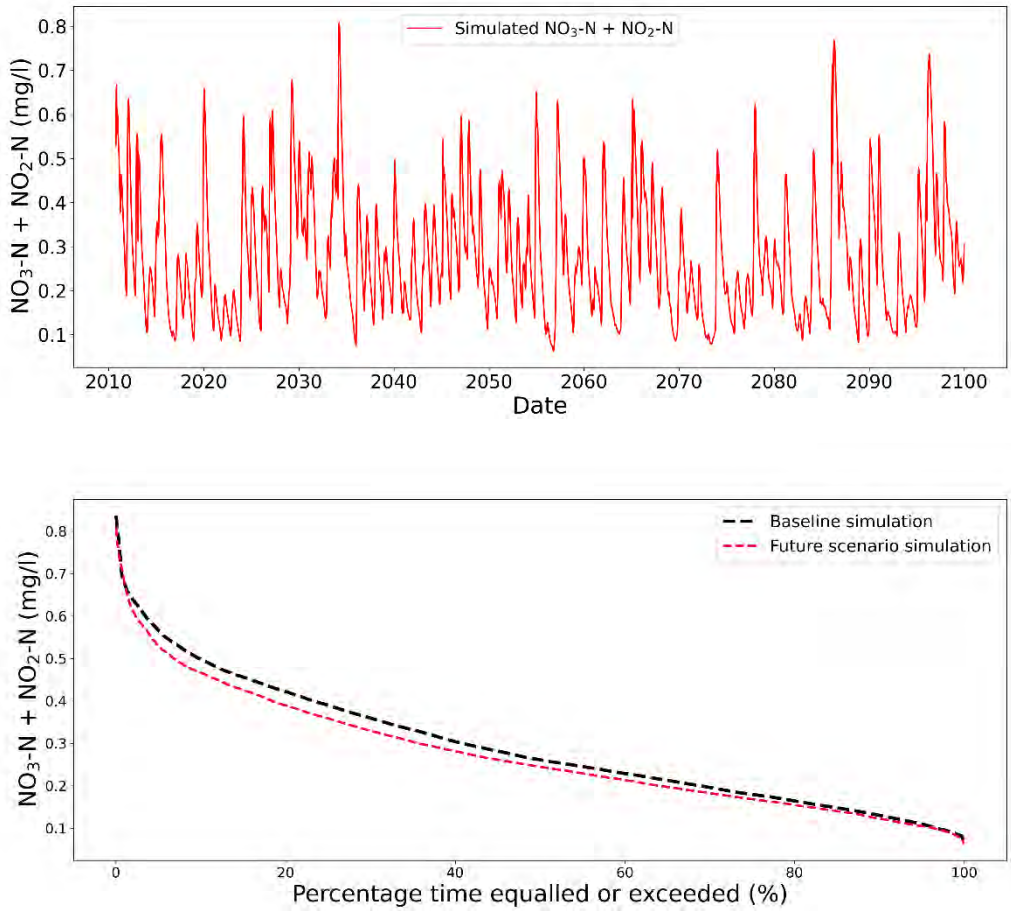

Figure 6.4: The daily variation of nitrate plus nitrite is depicted in the future scenario simulation, presented as a time series distribution over the long term (2010–2099). A comparison between the future scenario simulation and baseline simulation is illustrated through frequency distributions for the Grootdraai Dam. There was no distinction observed between the nitrate plus nitrite outputs under low and high abstraction scenarios, as they yielded identical simulations.

Simulations under low and high abstraction scenarios yielded similar outputs, indicating no variation in nitrate plus nitrite levels between the two simulations. The Seasonal Kendall Test revealed a significant decreasing trend ($p < 0.001$) in nitrate plus nitrite levels across both wet and dry seasons throughout the entire simulation period (2010–2099). The duration curve closely resembles the baseline curve, particularly at both low and high frequencies, indicating a nearly identical pattern across the dataset.

Figure 6.5 presents the daily variation of ammonium levels over the long term within the Grootdraai Dam. It displays the time series distribution and compares future scenario simulations with baseline simulations using frequency distributions.

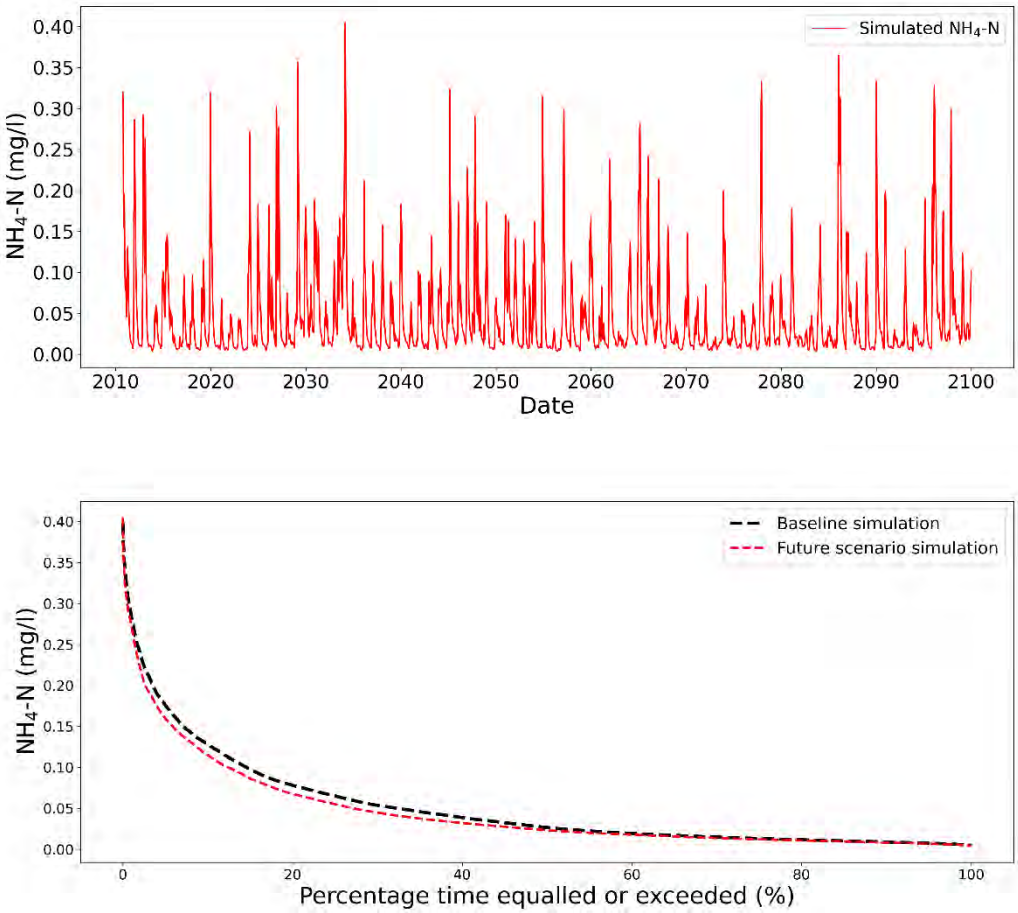

Figure 6.5: The daily variation of ammonium in the future scenario simulation, presented as a time series distribution over the long term (2010–2099). A comparison between the future scenario simulation and baseline simulation is illustrated through frequency distributions for the Grootdraai Dam. There was no distinction observed between the ammonium outputs under low and high abstraction scenarios, as they yielded identical simulations.

The simulations conducted under low and high abstraction scenarios resulted in similar outcomes, implying a consistent pattern in ammonium levels across both simulation scenarios.

The model incorporates nitrification, a process of converting ammonia to nitrate. This suggests that ammonia levels might persist at low levels across scenarios, owing to the conversion of ammonia to nitrate through nitrification. The Seasonal Kendall Test indicated that ammonium demonstrates a decreasing trend ($p < 0.001$) across both wet and dry seasons over the entire simulation period (2010–2099) under low and high abstraction scenarios. A comparison of the duration curves between the simulated and baseline datasets shows a remarkably similar pattern at both low and high frequencies. Figure 6.6 presents the daily variation of phosphate levels over the long term within the Grootdraai Dam. It gives the time series distribution and compares future scenario simulations with baseline simulations using frequency distributions.

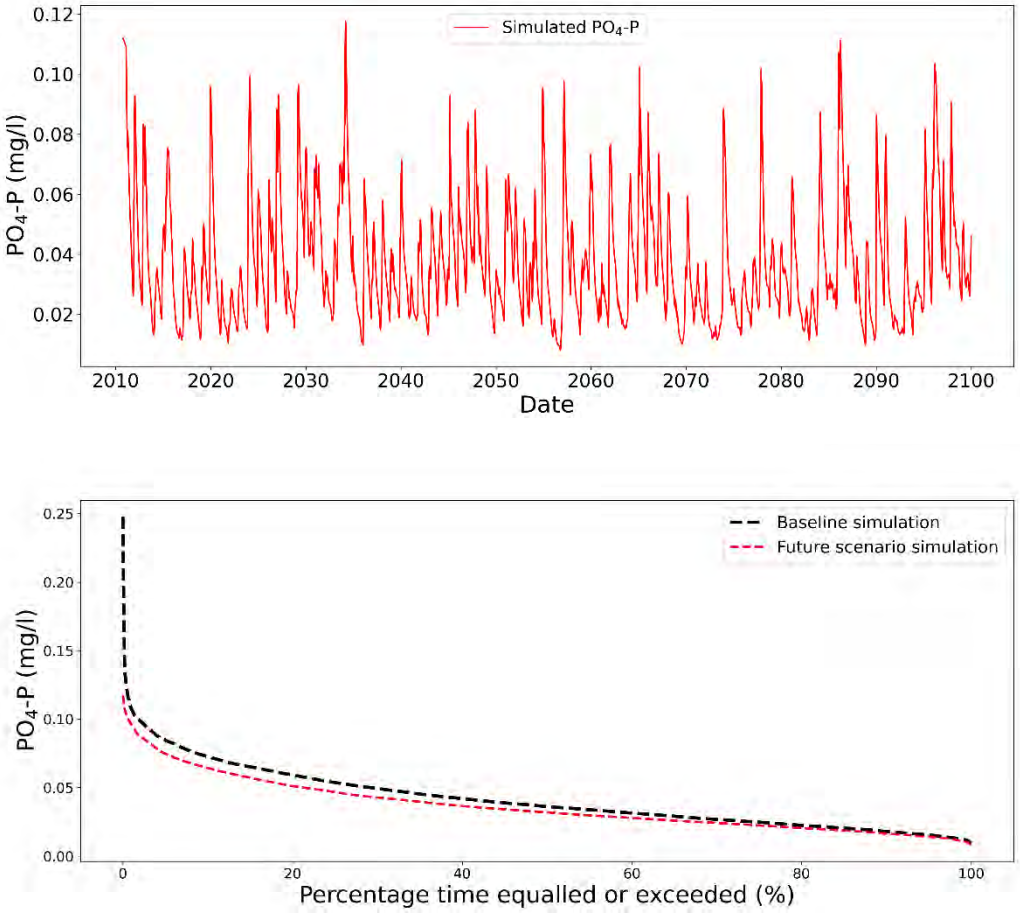

Figure 6.6: The daily variation of phosphate depicted in the future scenario simulation, presented as a time series distribution over the long term (2010–2099). A comparison between the future scenario simulation and baseline simulation is illustrated through frequency distributions for the Grootdraai Dam. There was no distinction observed between the phosphate outputs under low and high abstraction scenarios, as they yielded identical simulations.

The simulations conducted under low and high abstraction scenarios exhibited identical outcomes, suggesting a lack of variance in phosphate levels between the two scenarios. Similar to

the trend observed in nitrate plus nitrite, the Seasonal Kendall Test revealed a decreasing trend within the simulated phosphate dataset under low and high abstraction scenarios ($p < 0.001$) across both wet and dry seasons over the full simulation period (2010–2099). The pairwise test uncovered a significant disparity between the distributions of the two datasets ($p < 0.001$), and the simulated data exhibited a lower mean value than the baseline dataset, with values of 0.03 $mg.l^{-1}$ and 0.04 $mg.l^{-1}$, respectively.

6.3.3.2 Salts

Simulations conducted under low and high abstraction scenarios produced identical outputs, suggesting a lack of variation in the levels of potassium, sodium, fluoride, chloride, and magnesium between the two simulations.

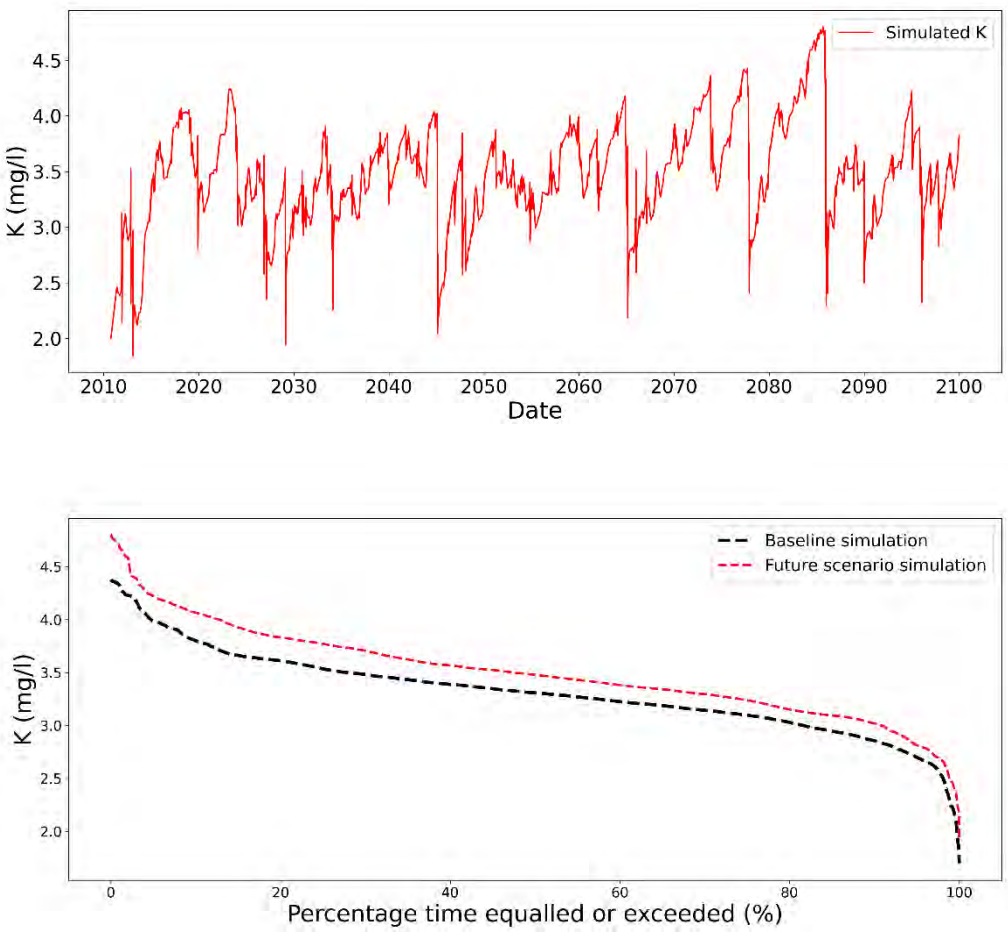

Figure 6.7: The daily variation of potassium over the long term in the future scenario simulation, presented as a time series distribution (2010–2099). A comparison between the future scenario simulation and baseline simulation is illustrated through frequency distributions for the Grootdraai Dam.

Figure 6.7 illustrates the daily variation of potassium levels over the long term within the Grootdraai Dam. It displays the time series distribution and compares future scenario simulations with baseline simulations using frequency distributions. The Seasonal Kendall Test indicates a weak increasing trend in potassium simulated data under low and high abstraction scenarios ($p < 0.001$) across both wet and dry seasons over the full simulation period (2010–2099). The pairwise simulation shows a significant difference between simulated and baseline potassium datasets with mean values of 3.5 and 3.3 $mg.l^{-1}$, respectively.

Figure 6.8 presents the daily variation of sodium levels over the long term within the Grootdraai Dam. It shows the time series distribution and compares future scenario simulations with baseline simulations using frequency distributions. The Seasonal Kendall Test indicates a subtle but significant uptrend in the simulated sodium data across both wet and dry seasons under both low and high abstraction simulation scenarios ($p < 0.001$).

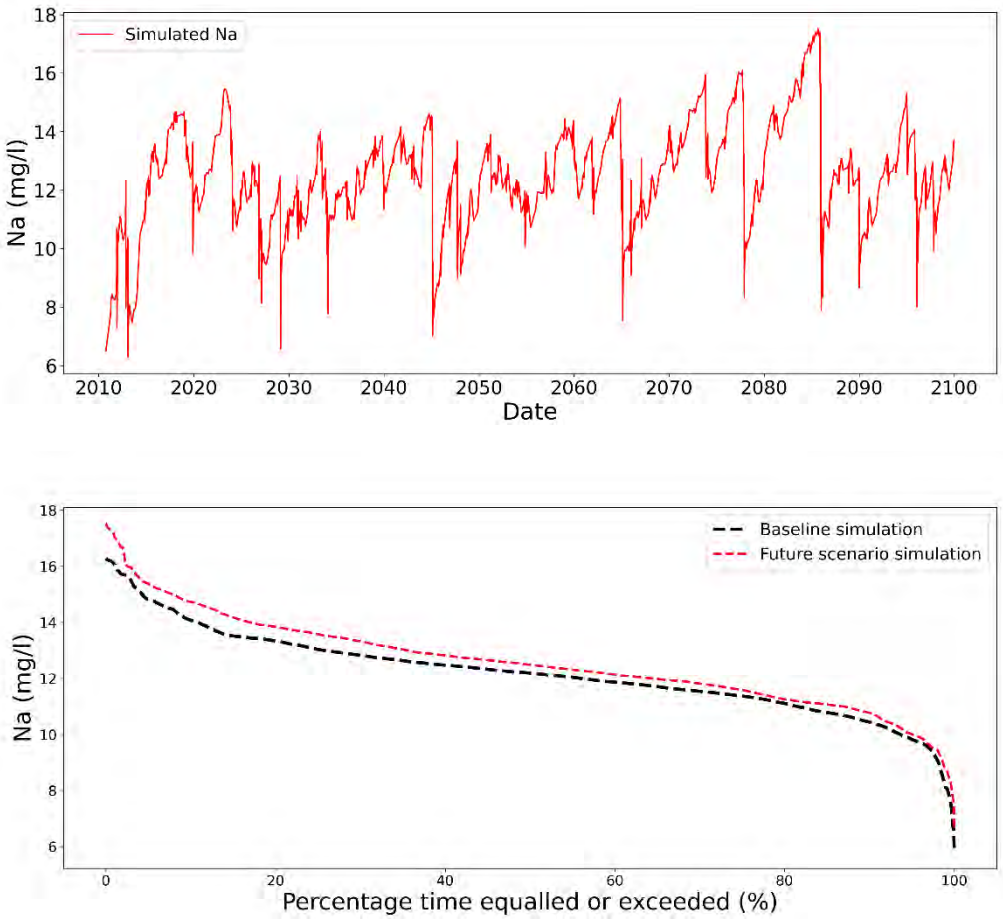

Figure 6.8: The daily variation of sodium over the long term is depicted in the future scenario simulation, presented as a time series distribution (2010–2099). A comparison between the future scenario simulation and baseline simulation is illustrated through frequency distributions for the Grootdraai Dam.

This trend persists throughout the entire simulation period (2010–2099). The distribution curves exhibit a close alignment at low frequencies and are virtually identical at very high frequencies.

Figure 6.9 presents the daily variation of fluoride levels over the long term within the Grootdraai Dam. It displays the time series distribution and compares future scenario simulations with baseline simulations using frequency distributions. The Seasonal Kendall Test reveals a weak increasing trend in fluoride simulated data under low and high abstraction scenarios simulations ($p < 0.001$) across both wet and dry seasons. The average simulated fluoride concentration was calculated to be 0.25 $mg.l^{-1}$, surpassing the baseline value of 0.21 $mg.l^{-1}$. It is noteworthy that in 2045, there was minimal variation observed in calcium concentration.

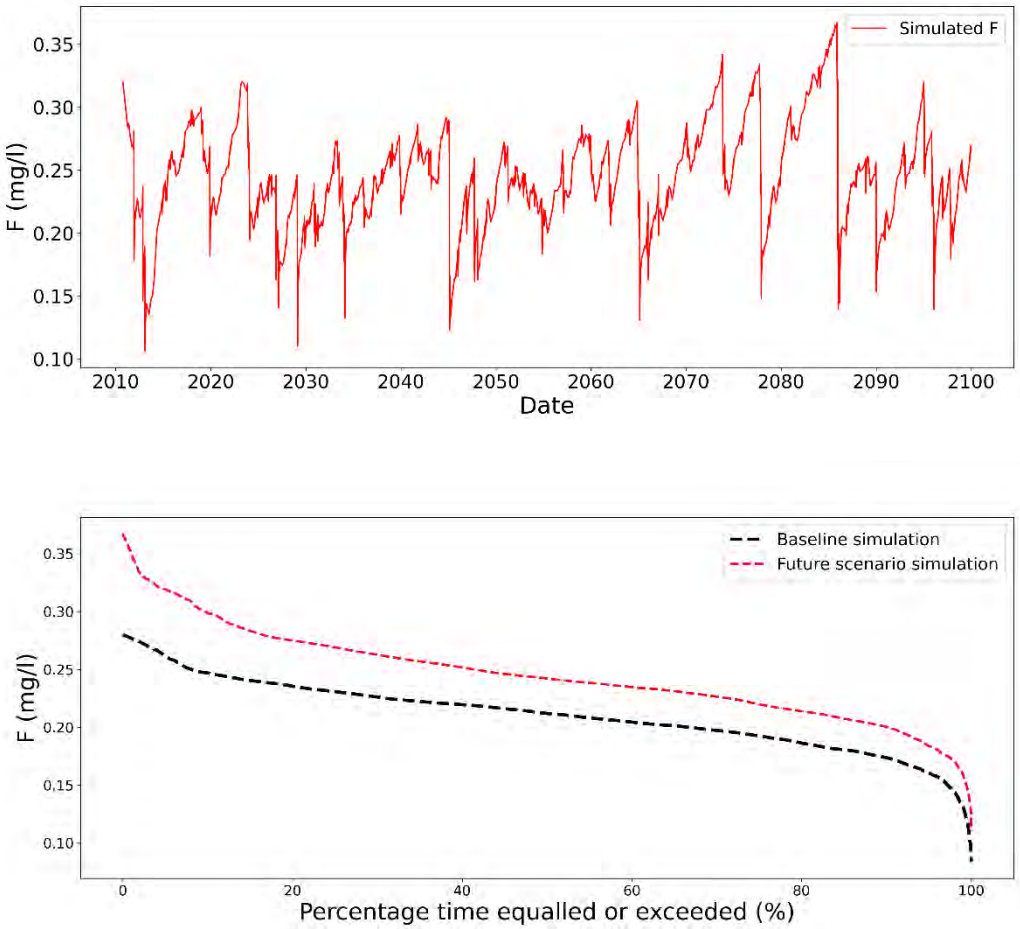

Figure 6.9: The daily variation of fluoride over the long term is depicted in the future scenario simulation, presented as a time series distribution (2010–2099). A comparison between the future scenario simulation and baseline simulation is illustrated through frequency distributions for the Grootdraai Dam.

Figure 6.10 presents the daily variation of chloride levels over the long term within the Grootdraai Dam. It displays the time series distribution and compares future scenario simulations with baseline simulations using frequency distributions. The Seasonal Kendall Test reveals a slight upward trend ($p < 0.001$) in chloride concentrations under both low and high abstraction scenarios across both wet and dry seasons throughout the entire simulation period (2010-2099). Furthermore, the pairwise test indicates a significant difference between the two datasets ($p < 0.001$), characterised by a baseline dataset mean value of 10.2 $mg.l^{-1}$ compared to a simulated mean value of 9.1 $mg.l^{-1}$. In May 2084, the chloride concentration is estimated to have peaked at 13.5 $mg.l^{-1}$, whereas the lowest level of 2.28 $mg.l^{-1}$ was recorded in February 2029.

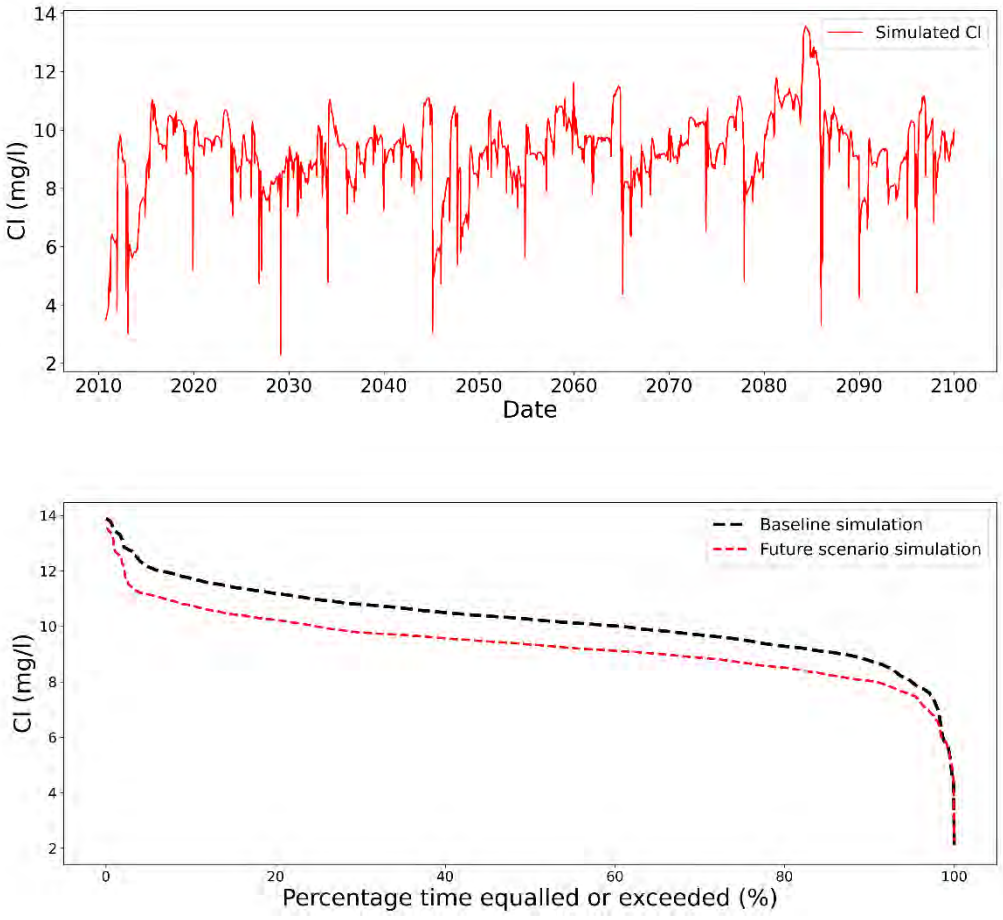

Figure 6.10: The daily variation of chloride over the long term is depicted in the future scenario simulation, presented as a time series distribution. A comparison between the future scenario simulation and baseline simulation is illustrated through frequency distributions.

Figure 6.11 presents the daily variation of magnesium levels over the long term within the Grootdraai Dam. It displays the time series distribution and compares future scenario simulations with baseline simulations using frequency distributions. The Seasonal Kendall Test suggests a rising trend in simulated magnesium concentrations under both low and high abstraction

scenarios ($p < 0.001$) during both wet and dry seasons. However, it is worth noting that the baseline dataset generally shows higher mean values than the simulated dataset, estimated at 10.1 $mg.l^{-1}$ and 8.7 $mg.l^{-1}$, respectively.

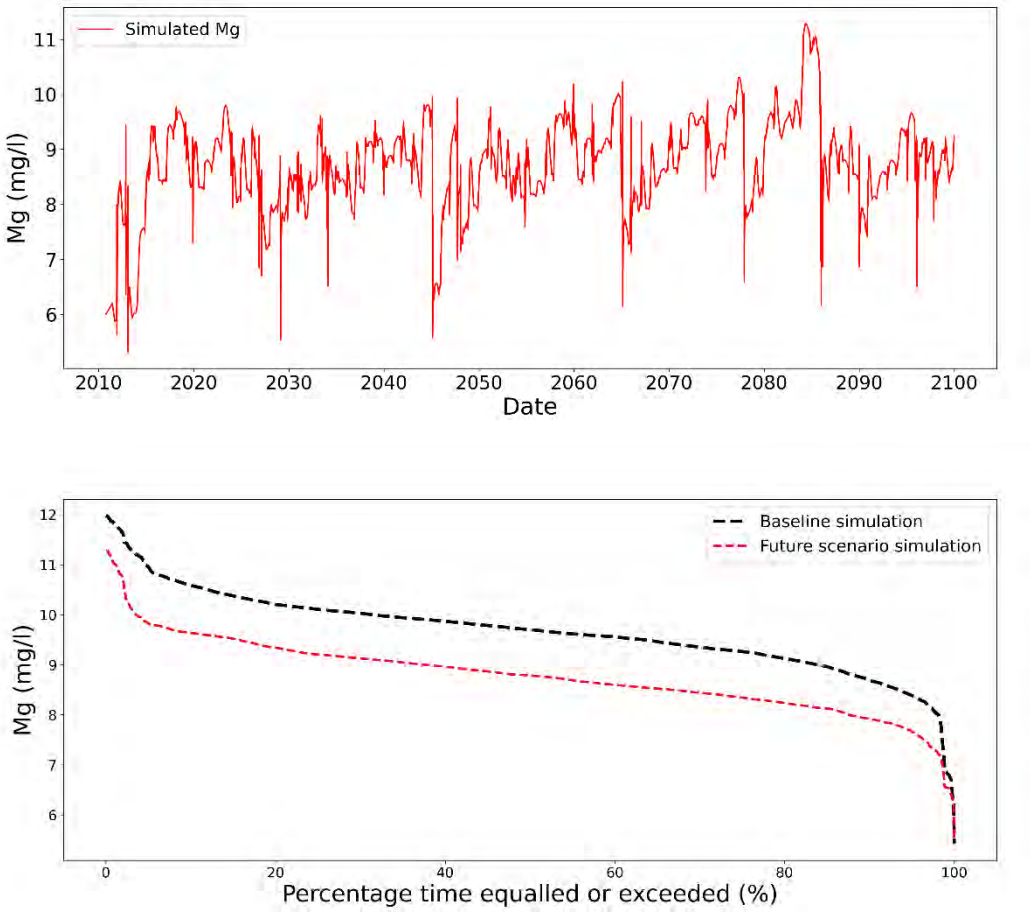

Figure 6.11: The daily variation of magnesium over the long term is depicted in the future scenario simulation, presented as a time series distribution (2010–2099). A comparison between the future scenario simulation and baseline simulation is illustrated through frequency distributions for the Grootdraai Dam.

The salts (i.e., potassium, sodium, fluoride, chloride, and magnesium) simulation presented in the above sections revealed no distinction between low and high abstraction scenarios, likely attributable to several factors. Both scenarios employed identical flow fraction signatures, including surface water flow, interflow, and groundwater flow to the signatures identified through the calibration exercise (see Chapter 4). The absence of variation in these parameter values may have influenced the observed behaviour. Notably, the only salts exhibiting differences between low and high abstraction scenario simulations were TDS, sulphate, and calcium. These specific variables had their signatures changed to explore the effects of mining closure on water quality under changing climate and certain abstraction increases.

Figure 6.12 presents the daily variation of sulphate levels over the long term (2010–2099) within the Grootdraai Dam in a low abstraction scenario. It displays the time series distribution and compares low abstraction scenario simulations with baseline simulations using frequency distributions. The Seasonal Kendall Test showed a weak increasing trend ($p < 0.001$) in sulphate concentrations in the low abstraction scenario across both wet and dry seasons. The pairwise test showed a significant difference between baseline and simulated sulphate ($p < 0.001$). Specifically, the mean of the baseline dataset estimated to be 27.15 $mg.l^{-1}$ is notably higher than the simulated sulphate, which has a mean value of 17.7 $mg.l^{-1}$. Figure 6.12 shows that simulated sulphate in the low abstraction scenario closely resembles the baseline simulation, particularly in very high frequencies.

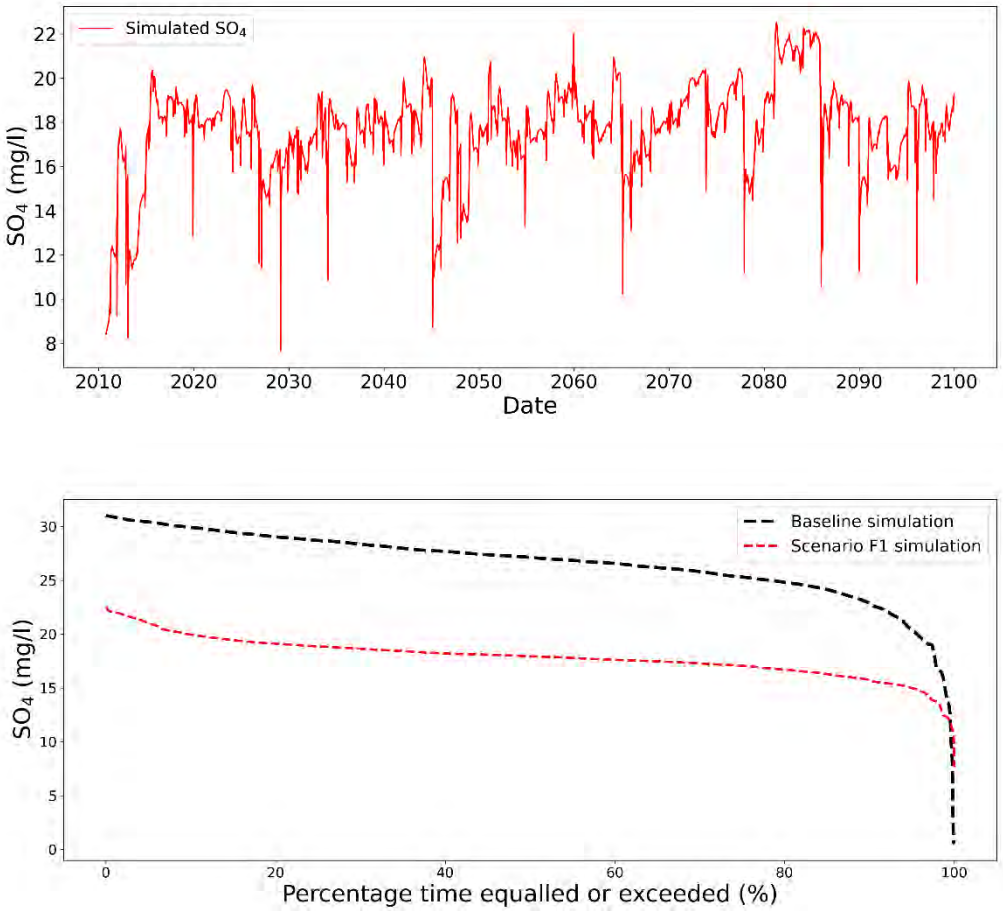

Figure 6.12: The daily variation of sulphate over the long term is depicted in the low abstraction (F_1) scenario simulation, presented as a time series distribution (2010–2099). A comparison between the low abstraction scenario simulation and the baseline simulation is illustrated through frequency distributions for the Grootdraai Dam.

Figure 6.13 presents the daily variation of calcium levels over the long term (2010–2099) within the Grootdraai Dam in a low abstraction scenario. It shows the time series distribution and

compares the low abstraction scenario simulations with the baseline simulations using frequency distributions. The Seasonal Kendall Test showed a weak increase trend ($p < 0.001$) in calcium concentration in the low abstraction scenario across both wet and dry seasons. The pairwise test showed a significant difference between baseline and simulated calcium ($p < 0.001$). Specifically, the mean of the baseline dataset estimated to be 14.4 $mg.l^{-1}$ is notably higher than the simulated calcium, which has a mean value of 10.09 $mg.l^{-1}$.

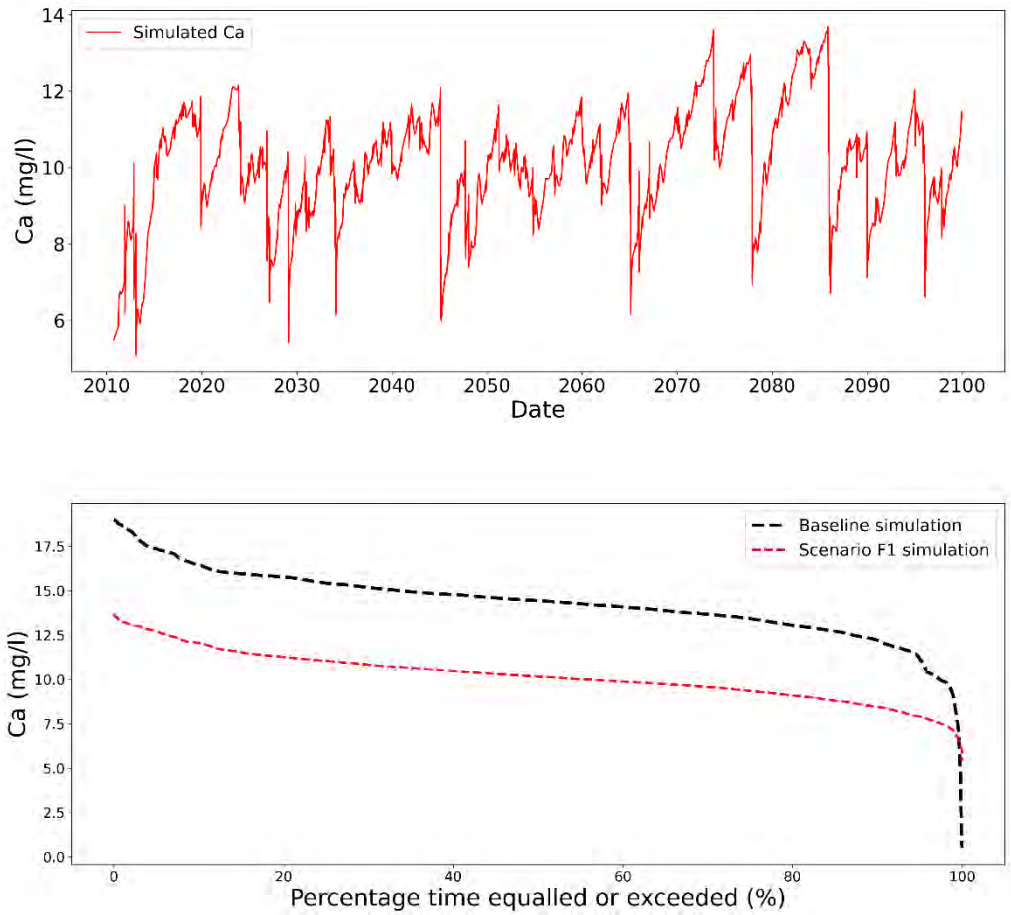

Figure 6.13: The daily variation of calcium over the long term is depicted in the low abstraction (F_1) scenario simulation, presented as a time series distribution (2010–2099). A comparison between the low abstraction scenario simulation and the baseline simulation is illustrated through frequency distributions for the Grootdraai Dam.

Figure 6.14 presents the daily variation of TDS levels over the long term (2010–2099) within the Grootdraai Dam in the low abstraction scenario. It displays the time series distribution and compares the low abstraction scenario simulations with the baseline simulations using frequency distributions. The Seasonal Kendall Test showed a weak increase trend ($p < 0.001$) in TDS concentration in the low abstraction scenario across both wet and dry seasons. The pairwise test showed a significant difference between baseline and simulated calcium ($p < 0.001$). Between

2080 and 2090, the peak TDS value is estimated to have reached 125.16 mg.l^{-1}. The estimated peak TDS concentration of 125.6 mg.l^{-1} occurred in April 2081, while the lowest TDS level of 33.63 mg.l^{-1} occurred in February 2029.

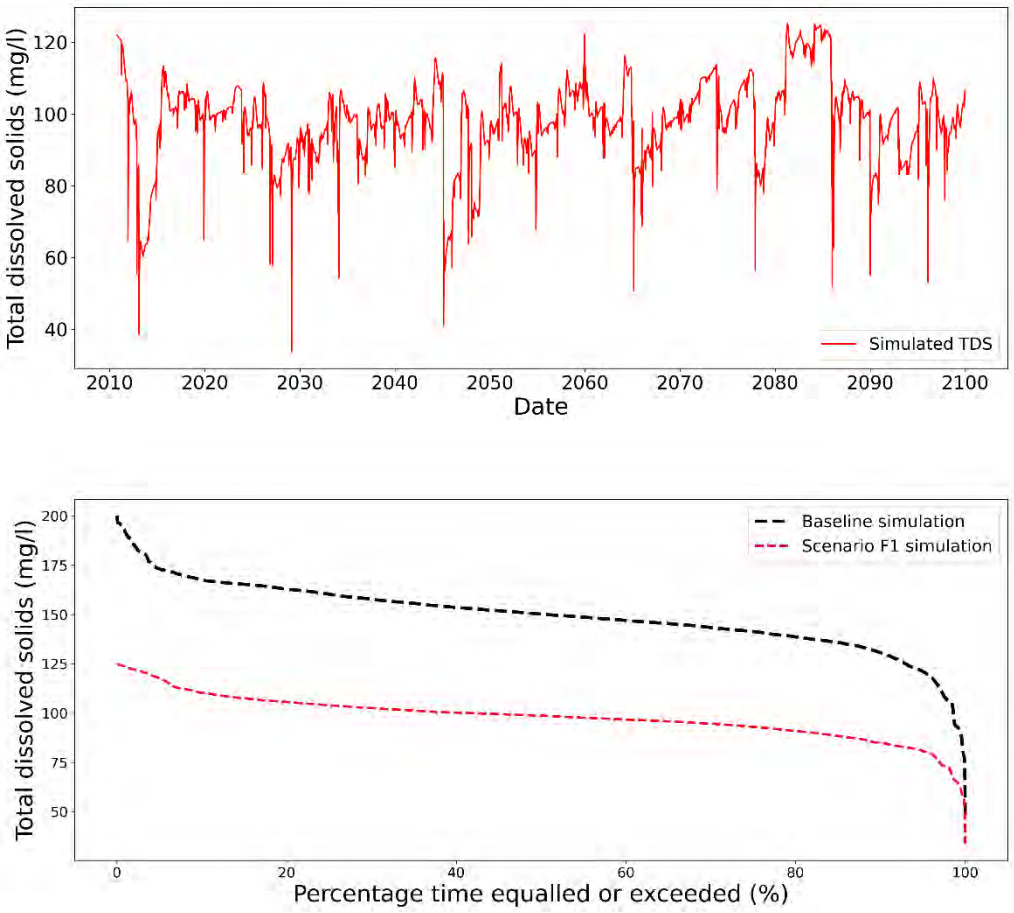

Figure 6.14: The daily variation of TDS over the long term is depicted in the low abstraction (F_1) scenario simulation, presented as a time series distribution (2010–2099). A comparison between the low abstraction scenario simulation and the baseline simulation is illustrated through frequency distributions for the Grootdraai Dam.

Figure 6.15 presents a comparison between simulated TDS, calcium, and sulphate in a high abstraction scenario and the baseline scenario over the long term (2010–2099) for the Grootdraai Dam. The Seasonal Kendall Test showed an increasing trend within TDS, calcium, and sulphate concentrations in the high abstraction scenario ($p < 0.001$) at the Grootdraai Dam level across both wet and dry seasons. The pairwise test showed a significant difference between simulated data in the high abstraction scenario and the baseline ($p < 0.001$). There is a significant difference in the mean and standard deviation of simulated TDS, calcium, and sulphate in the high abstraction scenario compared to the baseline scenario. Specifically, in the high abstraction scenario, the mean values are estimated at 100.4 (TDS), 10.3 (calcium), and 18.1 mg.l^{-1}

(sulphate). In contrast, the baseline scenario shows higher mean values of 149.6 (TDS), 10.09 (calcium), and 27.15 mg.l^{-1} (sulphate). The highest concentrations of TDS and sulphate occurred in September and June of 2084, reaching peak values of 136.83 and 24.41 mg.l^{-1}, respectively. The maximum calcium concentration was estimated to reach 14.8 mg.l^{-1} in November 2085.

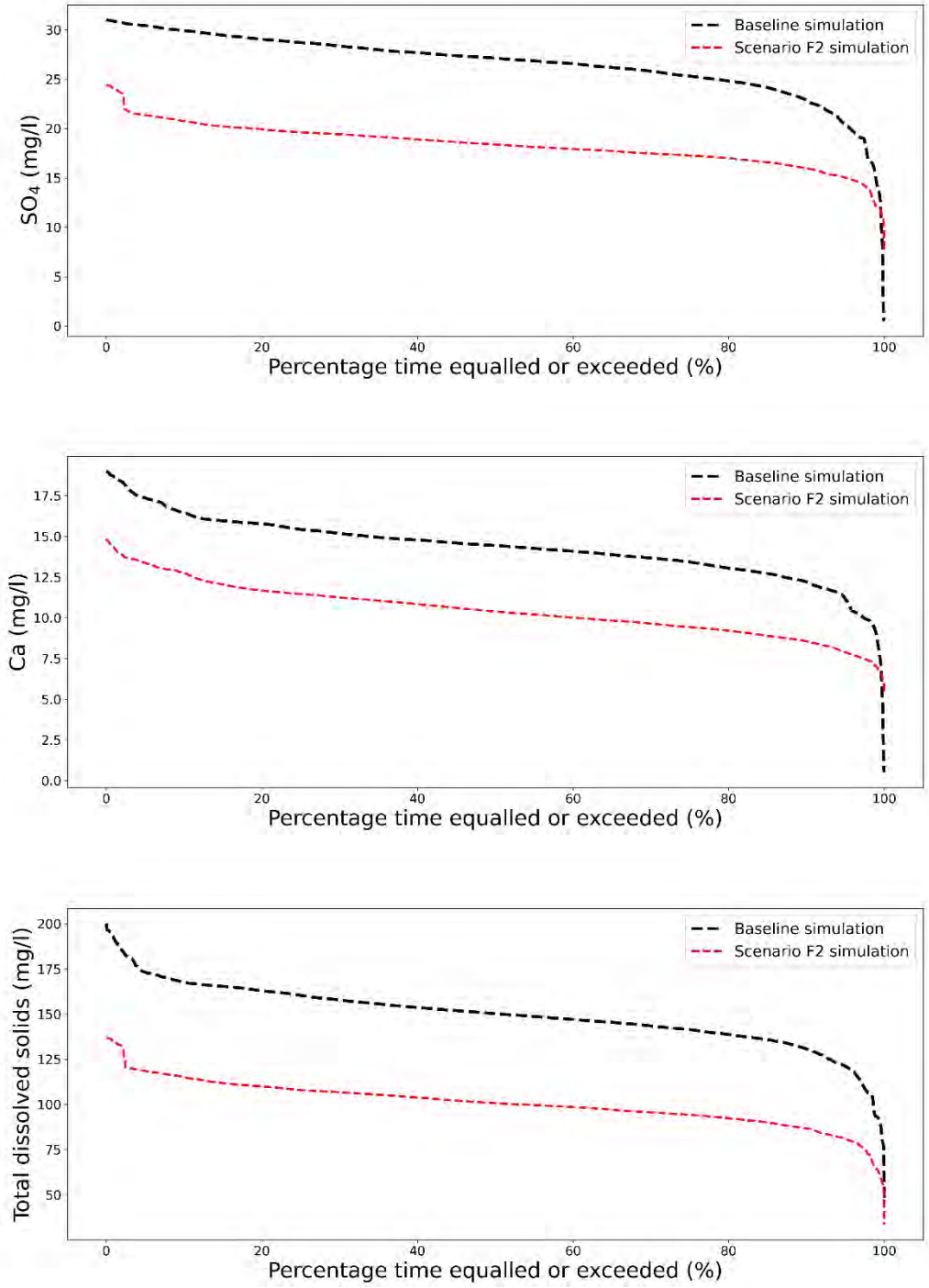

Figure 6.15: Comparison of the high abstraction (F_2) scenario simulation and the baseline simulation shown as frequency distributions of sulphate, calcium, and TDS over the long term (2010–2099) for the Grootdraai Dam.

6.3.4 Classification of mixed scenarios: short, medium, and long term perspectives

6.3.4.1 Water quality implication

The study utilised the Rand Water (2022) water quality guidelines tailored for the Grootdraai Dam. These guidelines specifically address TDS, sulphate, calcium, nitrate plus nitrite, ammonium, phosphate, fluoride, and chloride. Each water quality variable is categorised into four levels: ideal, acceptable, tolerable, and unacceptable. The numerical thresholds for these classifications vary between levels. The same numerical thresholds were applied for classifying the simulated nutrients and salts in both low and high abstraction scenarios. It is important to note that nitrate plus nitrite, ammonium, phosphate, chloride, and fluoride exhibited consistent behaviour across low and high abstraction simulations, displaying no discernible differences. These water quality variables maintained similar patterns throughout the simulations conducted for the Grootdraai Dam node over the long term (2010–2099). This may be attributed to the absence of consideration for potential increases in wastewater release linked to heightened abstractions. The return flows are assumed to remain at baseline levels, even if abstractions are increased. If the abstractions are for domestic water demand, there will likely be increased releases of domestic wastewater, which would then impact nutrients. This aspect could be attributed to the model's assumption regarding constant return flows, regardless of variations in abstractions.

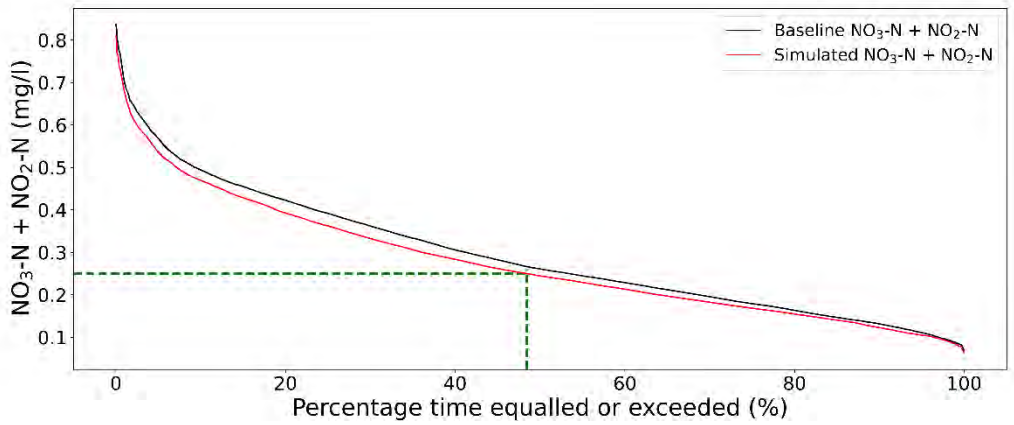

Figure 6.16: The Pywr-WQ model simulated nitrate plus nitrite at the Grootdraai Dam node in future scenarios (low and high abstraction), alongside the baseline simulation, is depicted through frequency distributions. These distributions are juxtaposed with the numerical limits established at the Grootdraai Dam node (Rand Water, 2022). The threshold for the acceptable level is denoted by green lines.

However, TDS, calcium, and sulphate demonstrated varying behaviours between low and high abstraction scenarios simulations. In Figure 6.16, the frequency distributions for nitrate plus

nitrite at Grootdraai Dam illustrate the established numerical limits at Leeuspruit, the location of this node. The plot indicates that simulated water quality exceeds the numerical limit under acceptable levels 48.4% of the time. Additionally, it surpasses the tolerable and unacceptable levels for 7% and 1% of the time, respectively. In comparison, the baseline scenario indicates these levels for 53%, 9%, and 2% of the time, respectively.

In Figure 6.17, the frequency distributions for ammonium at Grootdraai Dam depict the established numerical limits at Leeuspruit, where this node is situated. The plot reveals that the simulated water quality exceeds the numerical limit in the ideal level for 56% of the time, compared to the baseline scenario, which accounts for 59% of the time.

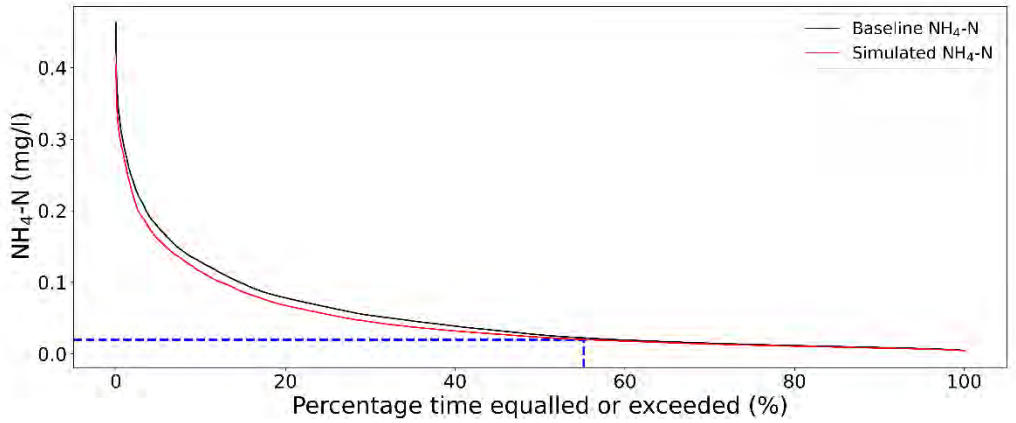

Figure 6.17: The Pywr-WQ model simulated ammonium at the Grootdraai Dam node in future scenarios (low and high abstraction), alongside the baseline simulation, is depicted through frequency distributions. These distributions are juxtaposed with the numerical limits established at the Grootdraai Dam node (Rand Water, 2022). The threshold for the ideal level is denoted by blue lines.

In Figure 6.18, the frequency distributions for phosphate at Grootdraai Dam depict the established numerical limits at Leeuspruit, where this node is situated. The plot reveals that the simulated water quality exceeds the numerical limit in the ideal level for 21% of the time, compared to the baseline scenario, which accounts for 30% of the time.

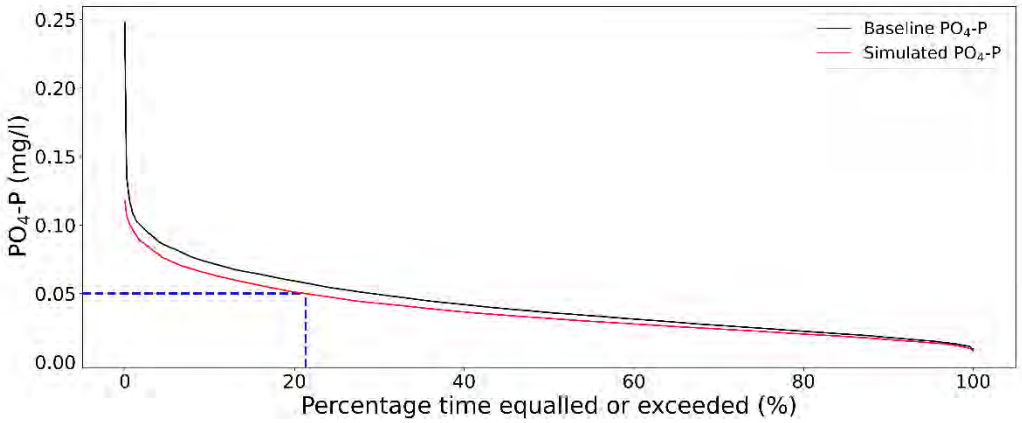

Figure 6.18: The Pywr-WQ model simulated phosphate at the Grootdraai Dam node in future scenarios (low and high abstraction), alongside the baseline simulation, is depicted through frequency distributions. These distributions are juxtaposed with the numerical limits established at the Grootdraai Dam node (Rand Water, 2022). The threshold for the ideal level is denoted by blue lines.

In Figure 6.19, the frequency distributions for fluoride at Grootdraai Dam depict the established numerical limits at Leeuspruit, where this node is situated. The plot reveals that the simulated water quality exceeds the numerical limit at the acceptable level for 90% of the time.

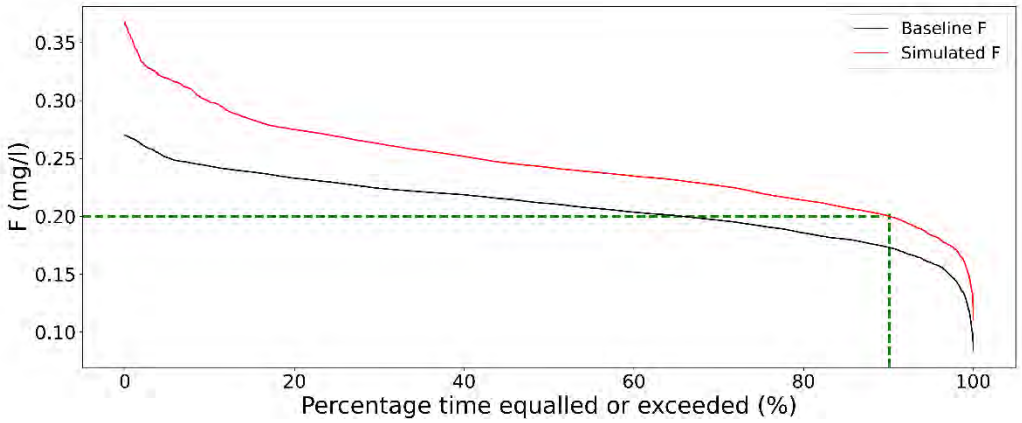

Figure 6.19: The Pywr-WQ model simulated fluoride at the Grootdraai Dam node in future scenarios (low and high abstraction), alongside the baseline simulation, is depicted through frequency distributions. These distributions are juxtaposed with the numerical limits established at the Grootdraai Dam node (Rand Water, 2022). The threshold for the acceptable level is denoted by green lines.

In Figure 6.20, the frequency distributions for chloride at Grootdraai Dam depict the established numerical limits at Leeuspruit, where this node is situated. The plot reveals that the simulated water quality exceeds the numerical limit at the ideal level for 25% of the time.

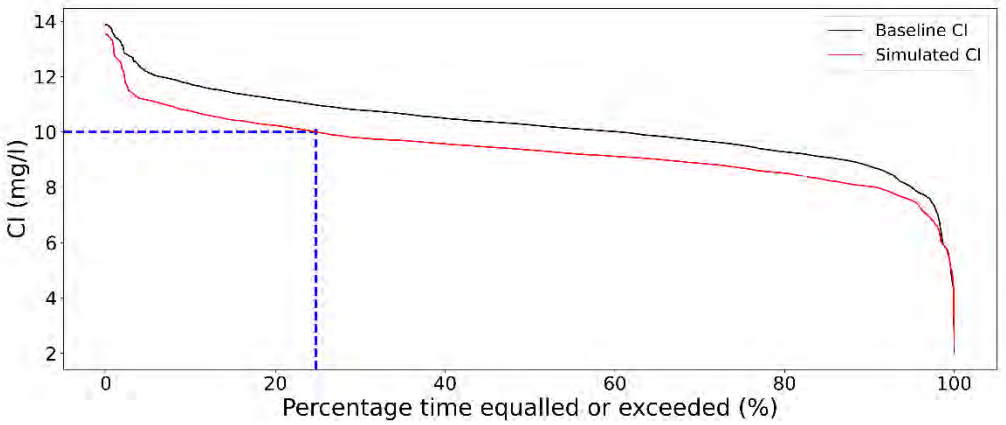

Figure 6.20: The Pywr-WQ model simulated chloride at the Grootdraai Dam node in future scenarios (low and high abstraction), alongside the baseline simulation, is depicted through frequency distributions. These distributions are juxtaposed with the numerical limits established at the Grootdraai Dam node (Rand Water, 2022). The threshold for the ideal level is denoted by blue lines.

Figure 6.21 illustrates the frequency distributions of TDS in low and high abstraction scenario simulations, respectively, at Grootdraai Dam, showcasing the designated numerical limits at Leeuspruit, the node's location. The graphs show that the simulated water quality surpasses the numerical limit set for the ideal level, accounting for 56% and 64% of the time, compared to the baseline scenario, which accounts for 99% of the time.

In Figure 6.22, the frequency distributions of sulphate in low and high abstraction scenarios simulations are presented at Grootdraai Dam, showcasing the designated numerical limits at Leeuspruit, the node's location. The graphs reveal that the simulated water quality surpasses the numerical limit set for the ideal level, accounting for 95% and 96% of the time, respectively, compared to the baselines, which account for 99% of the time. Even though there is a significant drop in sulphate under the low and high abstraction scenarios, the concentrations remain above the ideal threshold.

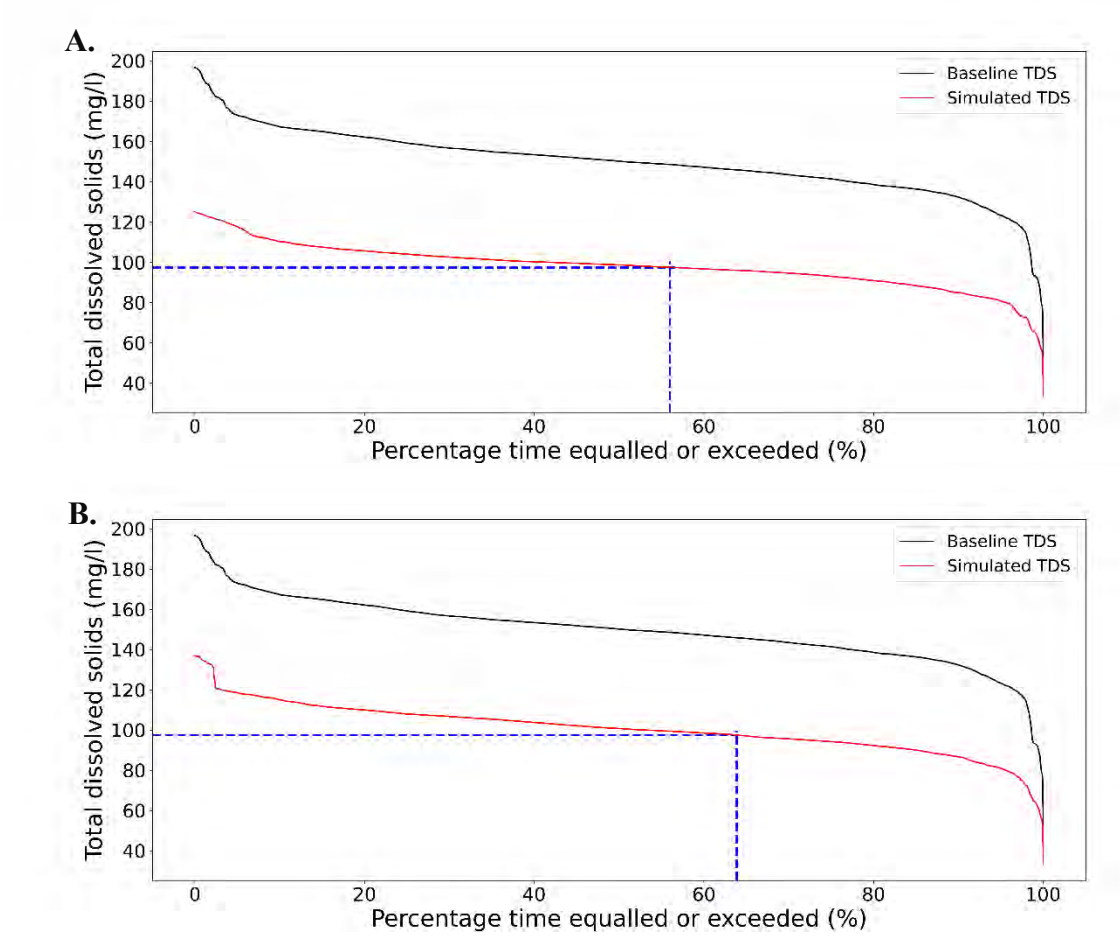

Figure 6.21: The Pywr-WQ model simulated TDS at the Grootdraai Dam node under future scenarios, alongside the baseline simulation, are illustrated through frequency distributions. Graph A showcases the simulated TDS levels in the low abstraction scenario simulation, while graph B illustrates TDS levels in the high abstraction scenario simulations. These distributions are contrasted with the numerical limits established at the Grootdraai Dam node (Rand Water, 2022). The threshold for the ideal level is denoted by blue lines.

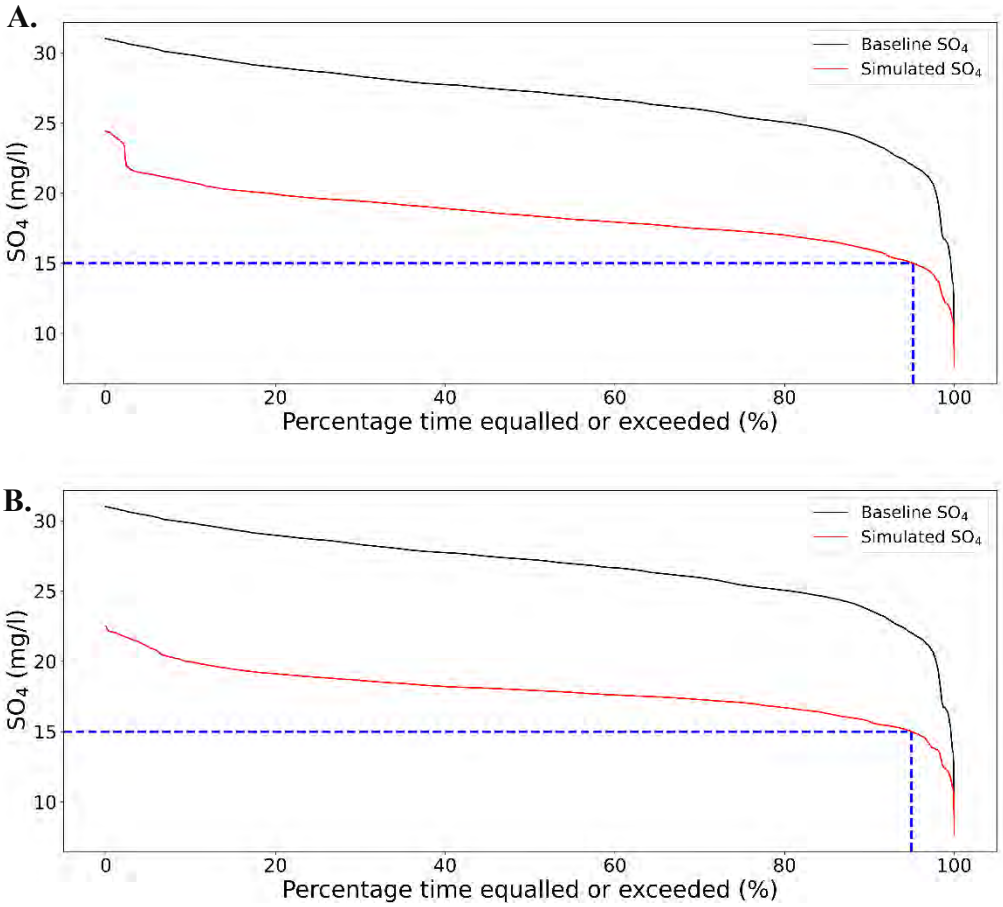

Figure 6.22: The Pywr-WQ model simulated sulphate at the Grootdraai Dam node in future scenarios, alongside the baseline simulation, are illustrated through frequency distributions. Graph A showcases the simulated sulphate levels under the low abstraction scenario simulation, while graph B illustrates sulphate levels under the high abstraction scenario simulations. These distributions are contrasted with the numerical limits established at the Grootdraai Dam node (Rand Water, 2022). The threshold for the ideal level is denoted by blue lines.

6.3.4.2 Focus on short term trends

Figure 6.23 depicts the categorisation of nitrate plus nitrite, ammonium, and phosphate concentrations in future scenarios (low and high abstraction) for the Grootdraai Dam, projected over the next 10, 20, and 30 years starting from 2010, using the Rand Water (2022) water quality guidelines. There were no discernible differences observed in the simulation of nutrients between the low and high abstraction scenarios.

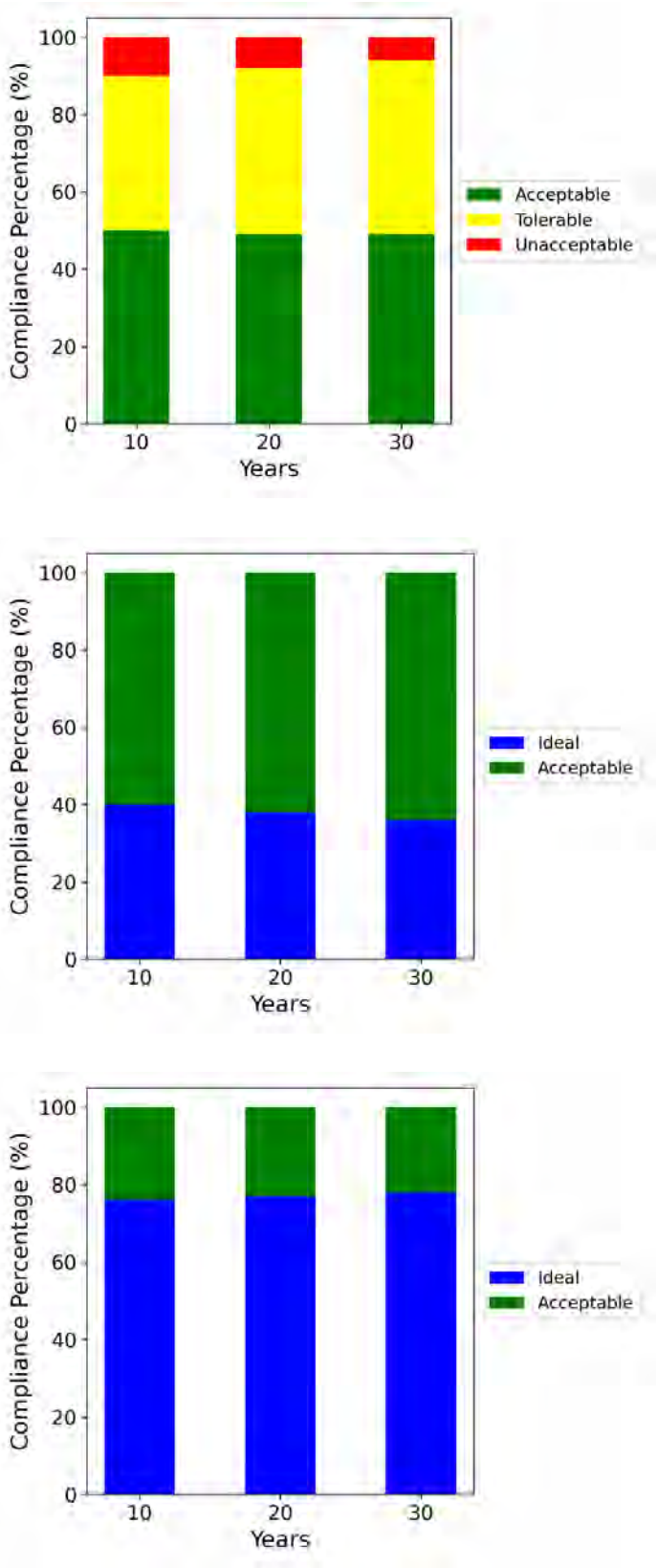

Figure 6.23: Compliance percentages for nitrate plus nitrite, ammonium, and phosphate are assessed across different classifications at the Grootdraai Dam node over the next 10, 20, and 30 years, beginning in 2010, in future scenarios (low and high abstraction). There are no disparities observed in the simulation of nutrients between low and high abstraction scenarios.

In response to climate change, increased water abstraction (5%–70%), and the scenario of decreased mining activity, nitrate plus nitrite exhibits a transition from unacceptable levels to tolerable and acceptable levels. However, the percentage of tolerable levels shows a gradual increase over time. Compliance percentages for ammonium demonstrate a smooth transition from ideal levels to acceptable levels. Conversely, phosphate indicates a decreasing trend in acceptable levels and an increasing trend in ideal levels. It is noteworthy that the short term classification influenced by the modelling assumptions did not account for the potential influence of increased return flows, a factor that could significantly affect the observed trends in nitrate plus nitrite, ammonium, and phosphate levels.

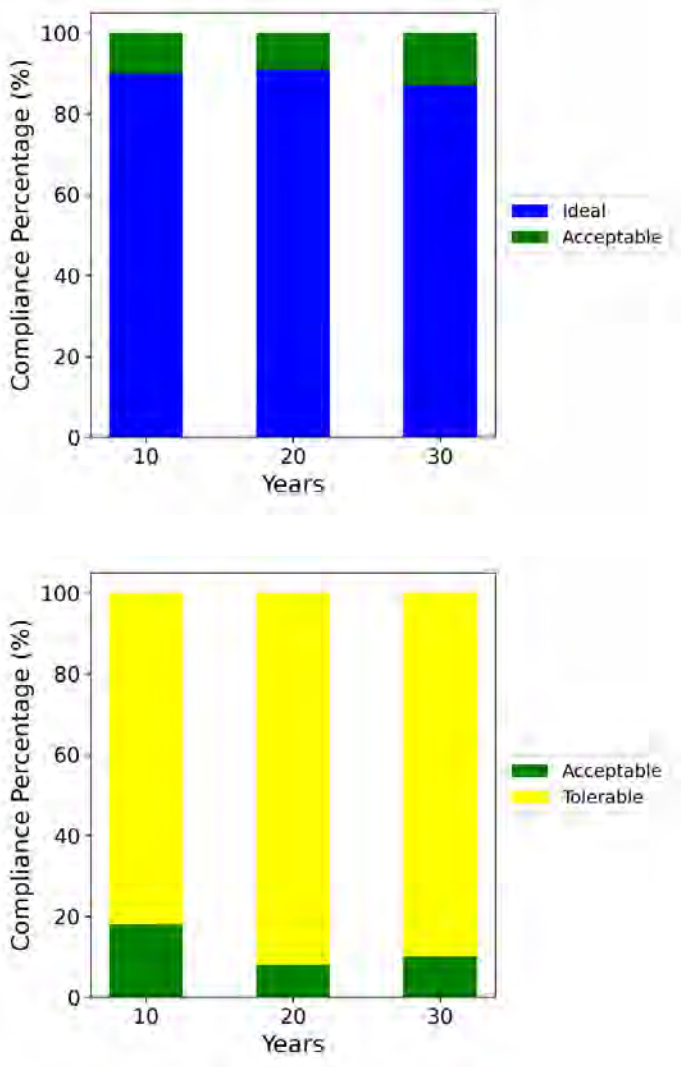

Figure 6.24: Compliance percentages for chloride and fluoride are assessed across different classifications at the Grootdraai Dam node over the next 10, 20, and 30 years, beginning in 2010, in future scenarios (low and high abstraction). There are no disparities observed in the simulation of nutrients between low and high abstraction scenarios.

Figure 6.24 presents the categorisation of chloride and fluoride concentrations in future scenarios (low and high abstraction) for the Grootdraai Dam projected over the next 10, 20, and 30 years starting from 2010, based on the Rand Water (2022) water quality guidelines. The simulation results for chloride and fluoride exhibited no disparity between the low and high abstraction scenarios. The compliance percentages for fluoride exhibit an increasing trend in tolerable levels and a decreasing trend in acceptable levels, indicating a shift from acceptable to tolerable levels over the next 30 years. Conversely, chloride displays a positive trajectory, with ideal levels showing an increasing trend and acceptable levels showing a decreasing trend, suggesting a transition from acceptable to ideal levels.

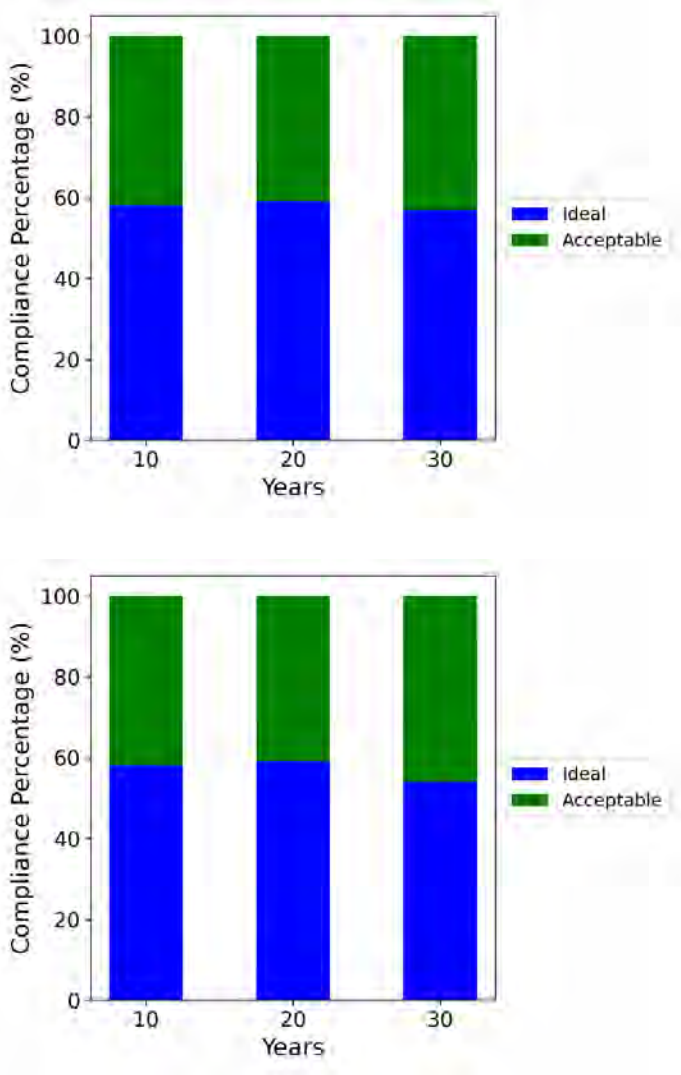

Figure 6.25: Compliance percentages for TDS were evaluated across various classifications at the Grootdraai Dam node over the next 10, 20, and 30 years, starting in 2010, in the low abstraction and the high abstraction scenarios.

Figure 6.25 presents the categorisation of TDS concentrations in future scenarios (low and high abstraction) for the Grootdraai Dam projected over the next 10, 20, and 30 years starting from 2010, based on the Rand Water (2022) water quality guidelines. The compliance percentages for TDS indicate that ideal levels in the high abstraction scenario are higher than those in the low abstraction scenario, with ideal percentages showing an increasing trend while acceptable levels show a decreasing trend, suggesting a potential transition from acceptable to ideal levels. Similar observations were made in the high abstraction scenario, except that ideal percentages are marginally higher than those observed in the low abstraction scenario. Figure 6.26 illustrates the categorisation of sulphate concentrations in future scenarios (F_1 and F_2) for the Grootdraai Dam projected over the next 10, 20, and 30 years starting from 2010, based on the Rand Water (2022) water quality guidelines.

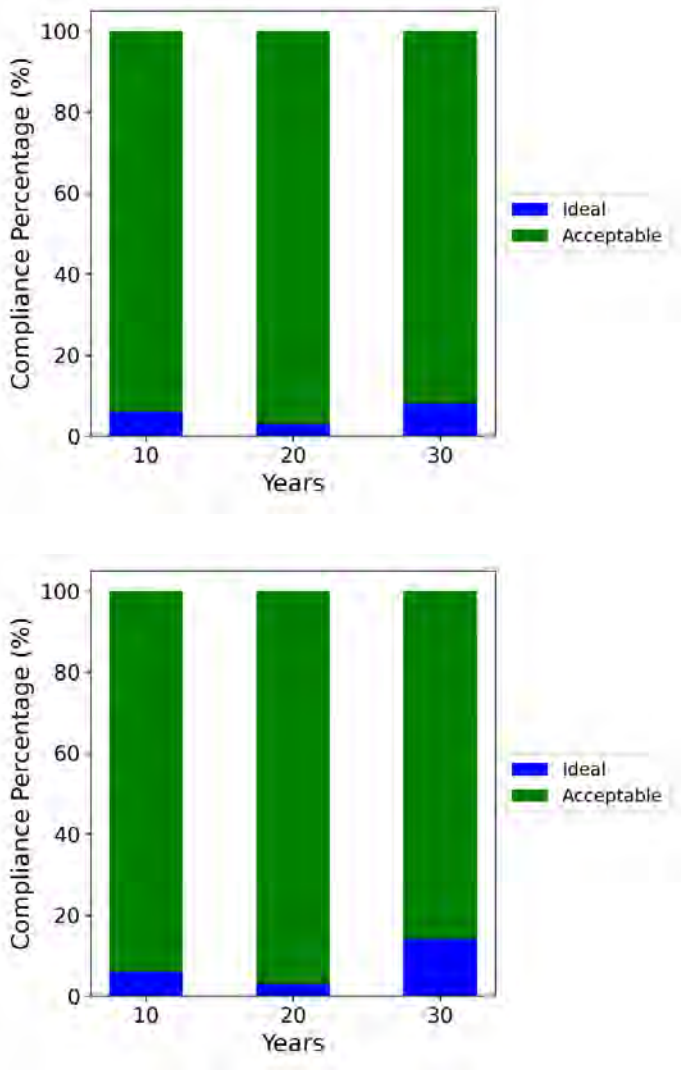

Figure 6.26: Compliance percentages for sulphate were evaluated across various classifications at the Grootdraai Dam node over the next 10, 20, and 30 years, starting in 2010, in low and high abstraction scenarios.

Sulphate compliance percentages show that in both low and high abstraction scenarios, acceptable levels seem to dominate the simulation, as the highest percentages are at the acceptable level, compared to the ideal level. Sulphate exhibits a similar compliance percentage distribution between the low and high abstraction scenarios, with fluctuations within acceptable levels. Ideal levels decrease followed by an increase in the subsequent period.

6.3.4.3 Focus on medium and long term trends

Figure 6.27 illustrates compliance percentages for nitrate plus nitrite, ammonium, phosphate, fluoride, and chloride over the short term (2010–2050) in future simulation scenarios (low and high abstraction). The graph illustrates significant occurrences within the tolerable classification for fluoride, alongside prominent chloride variations, with over 80% of the data exceeding the ideal level. Fluoride, conversely, registers over 85% of the data falling within the tolerable level. In Figure 6.28, the compliance percentages for nitrate plus nitrite, ammonium, phosphate, fluoride, and chloride are illustrated for the long term period (2050–2099) in the future simulation scenarios (low and high abstraction). The data indicate that fluoride consistently maintains compliance levels exceeding 90%, remaining within tolerable limits throughout the simulation period. Conversely, chloride demonstrates a lower compliance percentage, approximately 67%, in comparison to the short term results. Moreover, there are notable positive changes observed in nutrients such as nitrate plus nitrite, ammonium, and phosphate, with more data falling under acceptable and ideal levels compared to the short term results. The results indicate a positive trend towards enhanced compliance with water quality standards over the long term, especially for specific nutrient components. However, the situation differs for fluoride, where the trend towards improved compliance is not as pronounced.

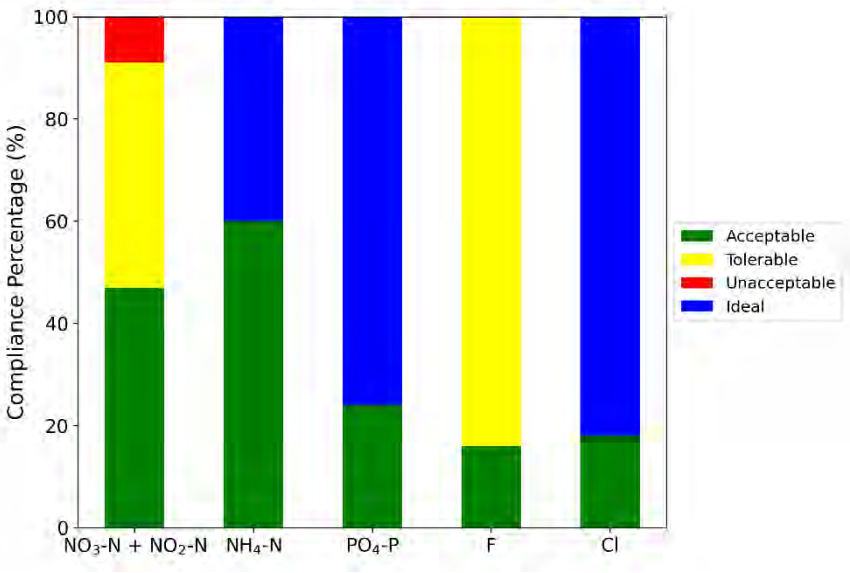

Figure 6.27: Compliance percentages for nitrate plus nitrite, ammonium, phosphate, fluoride, and chloride were evaluated across various classifications at the Grootdraai Dam node over the short term (2010–2050), in the future simulation scenario (low and high abstraction).

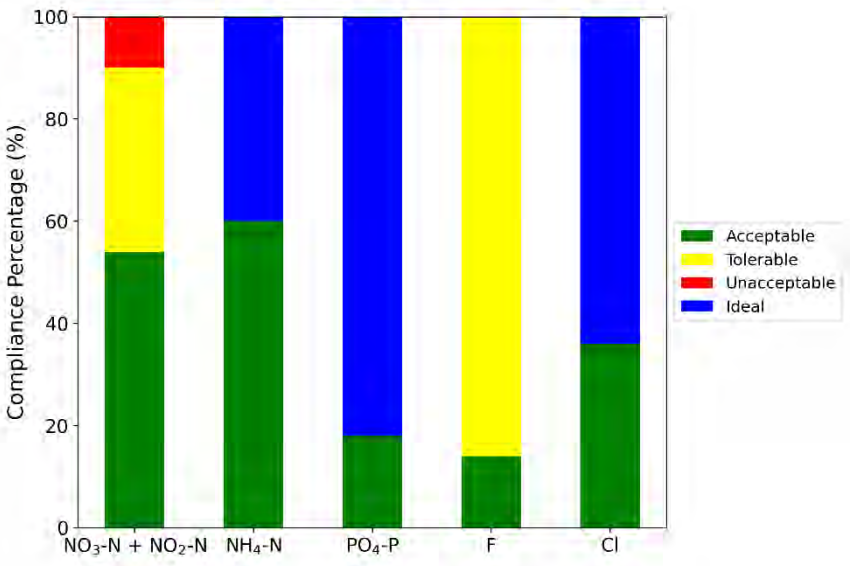

Figure 6.28: Compliance percentages for nitrate plus nitrite, ammonium, phosphate, fluoride, and chloride were evaluated across various classifications at the Grootdraai Dam node over the long term (2050–2099), in the future simulation scenario (low and high abstraction).

Figure 6.29 and Figure 6.30 illustrate compliance percentages for TDS and sulphate at the Grootdraai Dam in the short term (2010–2050) and long term (2050–2099) periods, in low and high abstraction scenarios. The graphs reveal that TDS exhibits high acceptable levels and low ideal levels in both low and high abstraction scenarios in the long term compared to the short term, which presents a contrasting pattern. However, high abstraction appears to be the scenario with high acceptable levels and low ideal levels in both the short and long term. These findings suggest that mine closure has a significant effect on TDS and sulphate, while water abstraction can also

influence these levels, especially in the long term where simulations indicate a high level of acceptability.

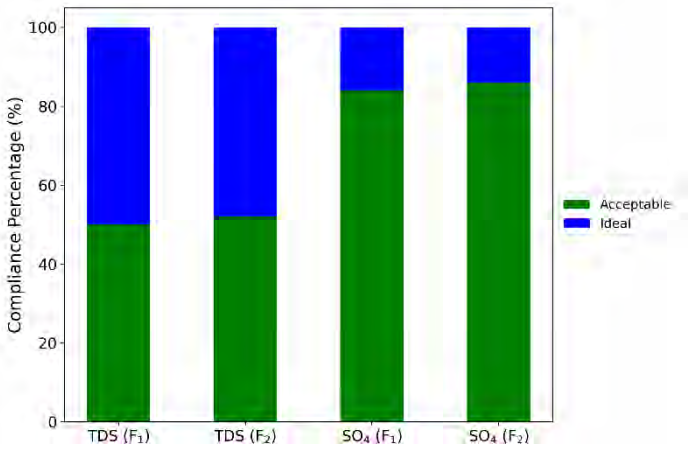

Figure 6.29: Compliance percentages for TDS and sulphate were evaluated across various classifications at the Grootdraai Dam node over the short term (2010–2050), in the future simulation scenario (low and high abstraction).

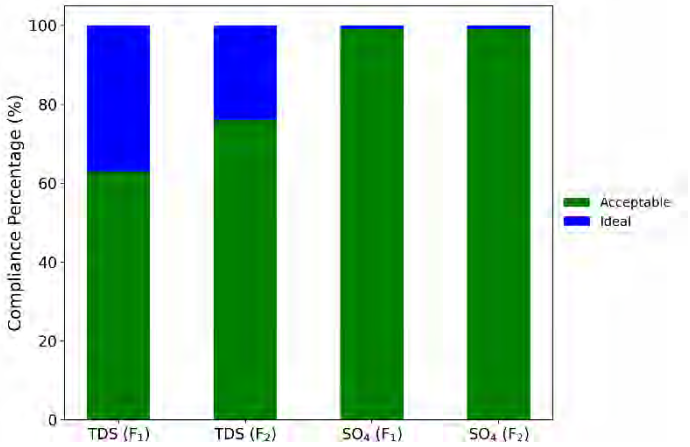

Figure 6.30: Compliance percentages for TDS and sulphate were evaluated across various classifications at the Grootdraai Dam node over the long term (2050–2099), in the future simulation scenario (low and high abstraction).

6.4 Discussion

The present chapter aimed to investigate two primary scenarios referred to as low and high abstraction. Low abstraction entails a combination of climate change data, mining closure, and a 5% increase in water abstraction, which is highly likely to occur in the future. Conversely, high abstraction comprises climate change data, mining closure, and a 70% increase in water abstraction, which is less likely to happen in the future, but allows some measure of uncertainty to be considered in the modelling. The chapter relies on the Pywr-WQ model to assess the impact of these scenarios on water quality fluctuations over the long term.

The simulation output revealed no discernible difference in nutrient behaviour, including nitrate plus nitrite, ammonium, and phosphate, between simulations of low and high abstraction. This lack of variation may stem from various factors, including the consistent calibration of flow fraction signatures for these water quality variables; the dilution capacity of the dam, influenced by varying abstraction levels, which likely played a role; and the unchanged signatures of return flows from WWTW within the study area. The model assumes constant return flows at baseline levels, regardless of increased water abstractions, not acknowledging potential impacts on nutrient levels from increased releases of domestic wastewater. This limitation stems from uncertainties regarding future advancements in water treatment technology, making it challenging to predict the exact effects of increased wastewater return flows on nutrient levels. Addressing this limitation in future studies would provide a more comprehensive understanding of how changes in wastewater management practices could influence water quality dynamics.

The consistent similarities observed in nutrient levels and several salts (e.g., potassium, magnesium, sodium, chloride, fluoride) during simulations of both low- and high-water abstraction scenarios prompted an inquiry into the reliability of the Pywr-WQ model's outputs.

Consequently, an additional abstraction threshold was applied to the Grootdraai Dam to assess the behaviour of these water quality variables under this improbable abstraction condition. The simulations revealed minimal changes in nutrient levels and salts, notwithstanding the implementation of a highly unusual 90% abstraction increase percentage. Despite the unconventional nature of this increase, the response of these water quality variables remained relatively insignificant. Thus, these findings suggest that the simulations of water quality variables, including nutrients and select salts, under a 70% abstraction increase are adequately justified. According to Salimi et al. (2021), changes in precipitation patterns and hydrology can influence the release of nutrients, potentially leading to nutrient enrichment in surface water. In addition, warmer conditions can lead to higher microbial activity and increased nitrification and denitrification rates, resulting in higher nitrous oxide emissions (Huang et al., 2013). Yet, the study utilised a climate change flow dataset, while keeping water temperature consistent with historical conditions. This might account for the similar patterns seen in simulated nitrate plus nitrite and ammonium levels between the baseline and future scenarios (i.e., low and high abstraction scenarios), which could be regarded as a limitation of the study.

Furthermore, the output of fluoride simulation in future scenarios (i.e., low and high abstraction) indicates that over 85% of the simulated fluoride falls within the tolerable level. South Africa is one of the countries in sub-Saharan Africa where high fluoride levels in groundwater have been

reported (Kut et al., 2016). Elevated fluoride levels can promote algae growth, influenced by factors such as concentration and exposure time, while also posing a significant toxicity risk to fish (Camargo, 2003).

TDS, sulphate, and calcium exhibited a significant decrease over the long term, primarily attributable to mining closure. This reduction is linked to the assignment of very low groundwater flow signatures to the quaternary catchments, which release the high TDS, sulphate, and calcium signatures observed during the calibration process. Although the salts demonstrated a notable decrease compared to the baseline scenario, differences between low and high abstraction scenarios were apparent. This disparity may stem from the applied increase in abstraction levels, with higher abstraction levels (high abstraction, featuring a 70% increase) resulting in elevated concentrations of these salts, while lower abstraction levels (low abstraction, with a 5% increase) led to dilution and salt conservatism. The assumption utilised may be deemed unrealistic since mining closure does not necessarily imply low TDS, sulphate, and calcium signatures. For instance, in the case of the Pebble Mine Project in Alaska, the closure of the mine could have substantial negative impacts on the environment. These consequences encompass the potential dissolution of secondary minerals, the leaching of wall rock and pyritic acid-generating waste, and the cumulative effects of multiple metals on fish toxicity (Maest et al., 2020). According to Ndaguba & Marais (2023), the ecological and social effects of mining, encompassing closure, persist beyond the operational phase of mining activities. Post-closure of mines can lead to various environmental threats according to Ochieng et al. (2010), such as the decline in valued recreational fish species, contamination of drinking water and agricultural lands, as well as disrupted growth and reproduction of aquatic plants and animals if left untreated. In South Africa, mining activities can have detrimental impacts on water quality, presenting a substantial risk to water resources (DWAF, 2008a). Therefore, adopting effective management practices to prevent or mitigate water pollution is essential for ensuring the sustainability of mining operations. Moreover, DWAF (2008b) reported that the successful closure of mines necessitates a multifaceted strategy that includes (1) implementing a risk-based approach with contingency measures; (2) prioritising pollution prevention throughout the mine's life-cycle; and (3) conducting risk assessments and involving stakeholders in risk management. In the context of long term environmental management, the anticipation typically revolves around the reversion of environmental conditions to their pre-disturbance state after the cessation of mining activities. However, a limitation within the scope of this study pertains to the absence of an approach to delineating a gradual reduction in groundwater signatures. The assumption underlying this

limitation posits an immediate amelioration in groundwater salinity levels upon the closure of mining operations, a premise that diverges from the complexities in real-world scenarios. The envisaged trajectory of significant improvement in groundwater quality, while conceptually convenient, disregards the temporal dynamics and intricacies involved in the process. Consequently, it underscores the imperative for forthcoming investigations to adopt a more realistic approach capable of delineating the gradual attenuation of groundwater salinity following mining closure, thereby aligning with the empirical realities of environmental rehabilitation.

According to González-Quirós & Fernández-Álvarez (2019), the effects of mining closure also include groundwater rebound and the restoration of water levels in the mine. Groundwater contamination following mine closure can have implications on surface water, contributing to environmental degradation. A recent study conducted by Alexander & Ndambuki (2023) found that mine closures may lead to unstable and altered groundwater quality, marked by increased acidity levels and concentrations of salts in the vicinity of the mines. Insufficient efforts in post-mining areas can perturb the hydrodynamic equilibrium within groundwater systems, manifesting in uncontrolled outflows and alterations in the positions of spring pools (Potrykus et al., 2022). In addition, the closure of mines can release accumulated pollutants such as heavy metals, according to Liu et al. (2020). However, it is essential to acknowledge a notable limitation within the current study: the non-consideration of potential increases in return flows associated with increased abstraction represents a significant constraint in the study's scope.

6.5 Conclusion

The Pywr-WQ model stands as a crucial tool for water managers, facilitating comprehensive water resource management and quality assessment. It enables the simulation of water quality dynamics across various scenarios, including future climate changes, potential increases in demand such as abstraction volume, and economic-related decisions like mining closure scenarios.

In the current study, the Pywr-WQ model played a pivotal role in evaluating the potential impacts of future climate change, mining closure, and varying degrees of water abstraction increase (i.e., 5% and 70% increase in abstraction). Through simulations provided by the Pywr-WQ model, the study classified water quality variables, including nitrate plus nitrite, ammonium, phosphate, magnesium, potassium, fluoride, chloride, sodium, sulphate, and TDS, into unacceptable, tolerable, acceptable, and ideal levels. Projections for the next 30 years in a worst-case scenario

involving climate change, mining closure, and a 70% increase in water abstraction indicated favourable outcomes for TDS concentrations, with over 50% falling within the ideal classification. Similarly, sulphate levels were predicted to be more than 90% within acceptable levels. However, fluoride presented unsettling findings, with over 85% of simulated fluoride concentrations falling below the tolerable level, in contrast with chloride, where more than 85% of simulated concentrations were deemed ideal. Nutrient levels generally yielded positive outcomes, except for nitrate plus nitrite, which exceeded 5% under unacceptable levels and approximately 45% under tolerable levels. In contrast, phosphate levels show more than 70% within the ideal range.

Future studies should adopt a comprehensive approach to address key assumptions in this study. Firstly, considering the influence of climate change, studies should explore variations in water temperature. Secondly, future studies could delve into the phased closure of mining areas, studying the individual contributions of different mining sites to changes in salt concentrations. Studies could explore the continuous drainage of salts from mining areas over time, considering the gradual reduction of salt levels. Furthermore, future studies should investigate the potential impacts of increased wastewater return flows resulting from escalated abstractions, particularly concerning nutrient levels. Future studies should aim to address the limitations of assuming constant return flows and explore how advancements in water treatment technology may influence these impacts over time.

Hence, a developed version of the Pywr-WQ model that incorporates progressive shifts from initial salt signatures to recommended salt signatures would facilitate a more realistic representation of salt concentration changes over time, and engaging with stakeholders, including power stations, can provide valuable insights and data related to mining closures, post-closure practices, and the broader impact of mining closure on water quality.

CHAPTER 7: DISCUSSION, CONCLUSIONS AND RECOMMENDATIONS

7.1 Introduction

Water quality models encompass descriptions of physical, chemical, and biological mechanisms that influence the fate and transport of pollutants (Cho et al., 2020), and they serve several important purposes in the field of water resource management and environmental protection. These models have various purposes such as assessing and predicting pollutant transport (Huang et al., 2012), investigating the long term quality of surface water and conducting environmental impact assessments in various pollution scenarios, assisting in the standardisation and consistent application of models for regulatory purposes (Wang et al., 2013), and modelling complex processes within aquatic ecosystems (Liu, 2018). According to du Plessis (2019), within the context of South Africa, the 2014 National Water Resource Strategy of the country recognised that the water resources do not receive the necessary attention and recognition they merit, with widespread issues of wastage, pollution, and degradation prevailing. As noted by the DWS (2016), key issues encompassed salinisation, nutrient enrichment due to urban runoff pollution, and microbial contamination. There is considerable focus on point source pollution and its influence on water quality. However, there is a scarcity of studies on non-point source pollution and its environmental impact (Adu & Kumarasamy, 2018; Lu et al., 2023; Xue et al., 2022; Yang et al., 2017).

This study utilised the Pywr model to simulate water dynamics and reflect water quality changes in the Grootdraai Dam Catchment situated within the Upper Vaal region of South Africa. The Pywr-WQ model, in conjunction with multiple regression models, was employed to evaluate the effects of the various scenarios investigated, including land-use and land-cover alterations, climate change, and mining activity closures, as well as increased water abstraction, on water quality variables such as nitrate plus nitrite, ammonium, phosphate, chloride, fluoride, magnesium, potassium, sodium, calcium, and sulphate. This chapter presents an overview of the thesis findings, aligns them with the overarching objectives, draws conclusions from this study and inquiries posed by this study, and offers a comparative analysis of the study's results, their implications, and their significance within the context of water quality modelling in South Africa. Finally, the chapter discusses the limitations of the models and methodologies employed in the study and concludes by suggesting recommendations for future studies.

7.2 Water Quantity Models within Developing Countries

This study introduced a framework (Figure 7.1) to transition from monthly lumped models, specifically the commonly used WRYM in Southern African countries, to an open-source, finely spatially distributed model using the Pywr model. The framework outlines a structured approach for this transition. Initially, a comprehensive understanding of the study area, encompassing physiographical characteristics, is essential, along with grasping the lumped structure of the existing monthly model. This forms the basis for creating an updated, detailed, and distributed version of the operational water system. The current structure comprises hydrological nodes that collect runoff from various quaternary catchments. This study primarily focuses on redistributing the runoff received from different quaternary catchments to multiple nodes rather than consolidating it into one node. Each quaternary catchment is associated with a specific natural inflow node, which receives runoff determined using surface ratio theory. The drained surfaces vary depending on the lumped structure within WRYM (as discussed in Chapter 3). A monthly to daily disaggregation method was applied, followed by a conversion from m^3/s to Mm^3/day, as the new simulation model accepts data in Mm^3 or ML, and follows daily, weekly, or yearly time-steps. The upgraded iteration of the operational water system was then merged with the Pywr environment, forming its foundational topology. The model's typology was acquired in JSON code format from the Waterstrategy.org website. Although Waterstrategy.org provides the option to execute the Pywr model within its interface, this study opted to download the model setup file and conduct simulations locally using the local run-time environment. After obtaining the model setup file code, the updated version, incorporating external data sources like precipitation, evaporation, and natural flow time series, was executed. The model was run for the study area, generating a comprehensive dataset comprising daily flow data, storage levels, transfers, reservoir releases, and abstraction values.

The framework shows potential applications for Water-Energy-Food (WEF) nexus projects. Regarding the WEF application within developing countries, process-making may be delayed, slowed, and interrupted (Mitchell et al., 2015) due to various problems, such as the shortage of data (Purwanto et al., 2021), involvement of many stakeholders (Wichelns, 2017), and the limitations of water simulation models used in the WEF nexus (Soleimanian et al., 2022). The framework illustrated in Figure 7.1 addresses limitations observed in various simulation models, such as the absence of simulation reservoir operation rules and massive required data (Soleimanian et al., 2022) within GSFLOW, C2Vsim, and CWatM models (Alam et al., 2019; Burek et al., 2019; Sun et al., 2018). The SWAT model (Arnold et al., 2012) cannot consider

reservoir operation rule and return flow (Soleimanian et al., 2022), and the WEAP model (Yates et al., 2009) is a licensed model that cannot be used freely by policymakers and stakeholders, limiting their capabilities for such applications. The developed framework serves as a practical tool to address the previously mentioned limitations and contribute to WEF nexus applications in developing countries. The simulation model employed in the framework has been actively employed in case studies within developing countries for WEF nexus purposes, including Ghana (Gonzalez et al., 2021) and a transboundary case involving three East African countries: Egypt, Sudan, and Ethiopia (Basheer et al., 2023). Applying this framework in developing countries, such as those in Southern Africa, facilitates work on WEF nexus applications and contributes to identifying optimised trade-offs within water-energy to enhance water resilience.

The framework developed (Figure 7.1) in this study holds various implications for addressing the challenges highlighted in previous reviews. For example, its potential ability to be integrated with ecosystem services (ES) models. One significant barrier in comprehending the dynamic interactions among multiple ecosystem services is the absence of an accurate water yield model, as pointed out by Agudelo et al. (2020). The current limitations of existing yield models within ES models include their inability to accurately represent complex processes in natural systems, neglecting the impact of land-use change on water availability, and overlooking the effects of climate change on water availability. In response, our framework introduces a more detailed and distributed structure for the water system, considering both current and planned land-use modifications (Agudelo et al., 2020; De Groot et al., 2010; Zheng et al., 2019). Additionally, utilising the Pywr environment incorporated within the framework enables simultaneous scenario simulations with different time-steps, and it contributes to existing research aimed at understanding the resilience of ecosystems and their capacity to consistently provide multiple services over time (e.g., Posner et al., 2016; Zhao et al., 2020).

In the context of contemporary climate change studies (e.g., Leavesley, 1994; Wilby, 2005), particularly within developing countries, various constraints manifest in the models utilised to examine the influence of climate change on water resources. These limitations encompass scale, climate scenario generation, data, and model structures. Moreover, climate change studies are packaged with different uncertainties related to methods of translating global climate changes to regional scales, and uncertainties in water resource models used for climate change impact assessment according to Wilby (2005). Kusangaya et al. (2014) recognised the imperative for additional research to enhance comprehension of the potential ramifications of climate change on water availability, accessibility, and demand within Southern African regions. The established

framework facilitates research in developing countries by employing a more intricate, distributed structure with a finer temporal scale (daily, weekly, and yearly). Notably, the framework is devoid of any limitations pertaining to surface area restrictions in its application; the employed water resources tool used in the framework has significant speed-up characteristics, approaching four times the equivalent single scenario run-time with 160 scenarios (Tomlinson et al., 2020). These characteristics enable the generation of temporal flow data for diverse climate change scenarios in a single run.

The overall conclusion regarding the presented framework relies on its various capabilities, including:

i. The transition from licensed lumped monthly models to daily distributed, open-source models, adopting the actualised structure of the operating water system to reflect the current and planned land-use of the study area.
ii. The ability to seamlessly transition from a broader spatiotemporal scale to a finer resolution.
iii. The potential for use in post-hydrological modelling studies, climate change investigations on water quantity management under changing conditions, and water infrastructure investments.

While the developed framework offers an effective step-by-step methodology to enhance current water quantity management within developing countries, in particular South Africa, there are still potential recommendations, including:

i. Investigating the viability of implementing the framework across all of South Africa's water management areas (WMAs) to shift from the WRYM to the open-source Pywr model and incorporate it as a National-Scale Water Resources Simulation Model.
ii. Exploring the potential use of remote sensing data as input for data-scarce regions, such as rural areas, and assessing the framework's performance with climatic parameters, including precipitation, temperature, and evaporation datasets.

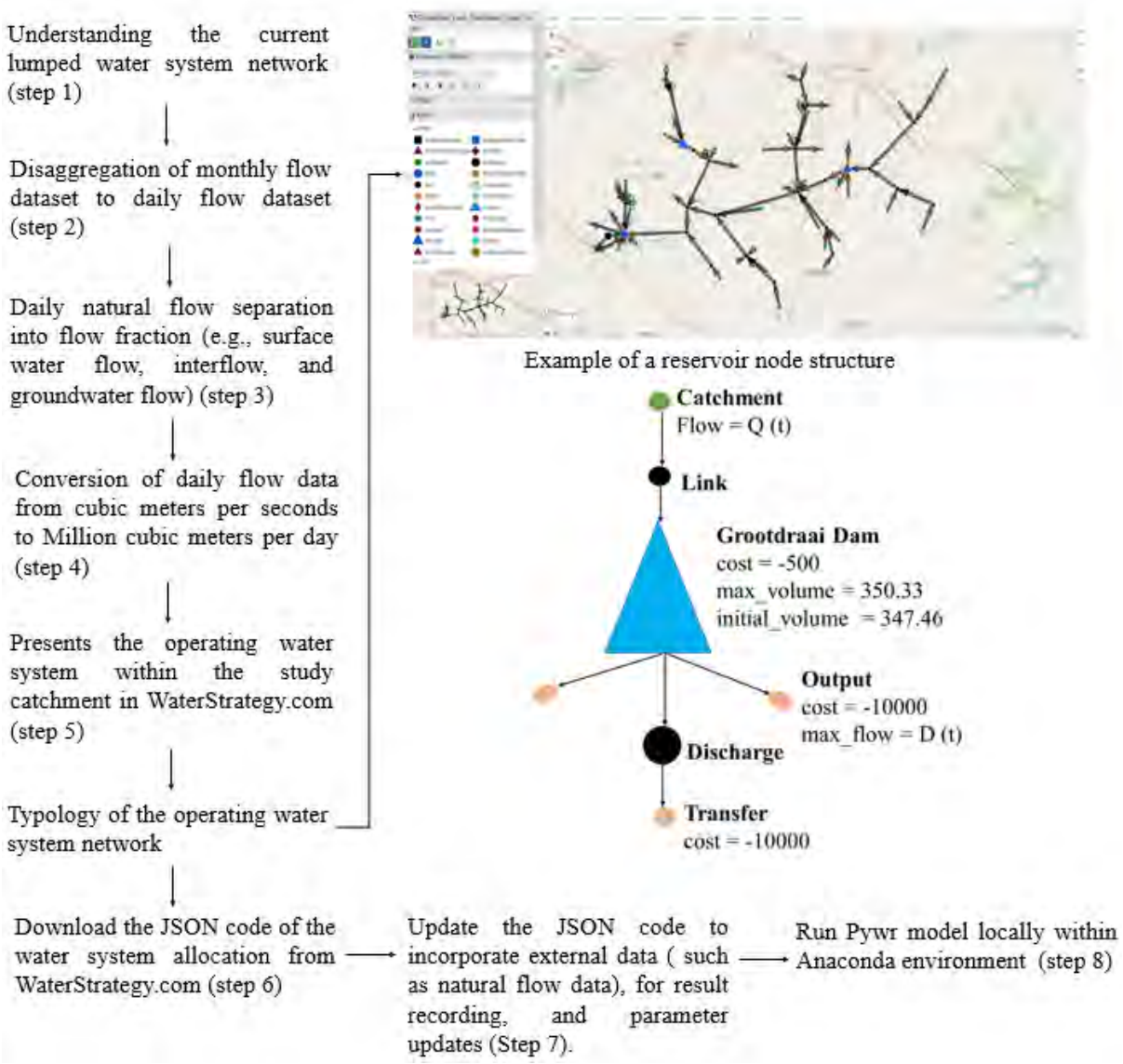

Figure 7.1: A research framework for the application of the Pywr model within a catchment in a developing country, namely the Grootdraai Dam catchment located in Upper Vaal, South Africa. The framework works as a step-by-step guide to shift from a monthly, lumped model to a daily, spatially finer model.

7.3 Application of the Pywr-WQ for Dynamic Integration of Water Quality Systems Assessment within the Grootdraai Dam Catchment

In South Africa, rivers typically receive waste from deficient wastewater infrastructure, mining areas, and agricultural activities (Ngubane et al., 2022). Water scarcity is influenced not only by the quantity of available resources but also by the ongoing degradation of water quality due to urbanisation, industrialisation, and agricultural practices, which limits the availability of freshwater for safe use as noted by Giri (2021). In the context of South Africa, three potential constraints pose challenges within water quality modelling: (i) the scarcity of data and the non-availability of water quantity and quality data in some river catchments; (ii) the lack of

institutional resources, professional skills, and funding necessary to apply widely used models worldwide, even if data are available; and (iii) limitations within current water simulation models linked to water quality models. Chapter 4 introduces the Pywr-WQ model, an implementation of the WQSAM processes into a Pywr environment. The Pywr-WQ model dynamically linked to the Pywr model mirrors the water quantity aspect of the operating water system within the Grootdraai Dam Catchment.

The model serves as a water quantity-quality tool, aiding in the water management process by enabling risk assessment (see Figure 4.15, Chapter 4) and assisting decision-making regarding compliance with water quality guidelines (Figure 4.16, Chapter 4) within specific abstraction nodes in the Grootdraai Dam area. In South Africa, water quality management faces several challenges related to ineffective knowledge and information management due to limited technical capacity, and gaps in monitoring systems according to the National Water Resource Strategy (NWRS-3) formulated by DWS (2021). The present study contributes to enhancing water quality assessment by introducing a tool designed to assist water managers in their monitoring missions within the context of water resource, thereby facilitating effective knowledge production and decision-making.

water quality management regards abstraction as a critical factor in water resource management owing to its impact on both water quantity and quality (DWAF, 2001; DWS, 2017). For instance, abstraction can exacerbate water quality issues by reducing dilution capacity, potentially leading to increased concentrations of pollutants at specific points. Similarly, return flows, which may carry pollutants from various sources, can further contribute to high concentrations and degrade water quality. This shift can cause pollutant levels to transition from ideal to acceptable, tolerable, or even unacceptable levels. By employing the Pywr-WQ model, water managers can prioritise water quality over quantity at specific abstraction points, such as reservoirs, storage facilities, or in-stream river nodes. The knowledge conveyed in the present study (refer to Chapter 4) addresses the gaps outlined in the 6th strategic objective of the NWRS-3. The Pywr-WQ model represents a significant advancement in water quality management by addressing limitations inherent in models such as the WRYM. Unlike traditional approaches that focus solely on determining the usable yield of a catchment for water resource planning, Pywr-WQ takes into account both water quantity and quality considerations. This holistic approach ensures more realistic estimations of usable water, thereby enabling more informed decision-making in water allocation and management.

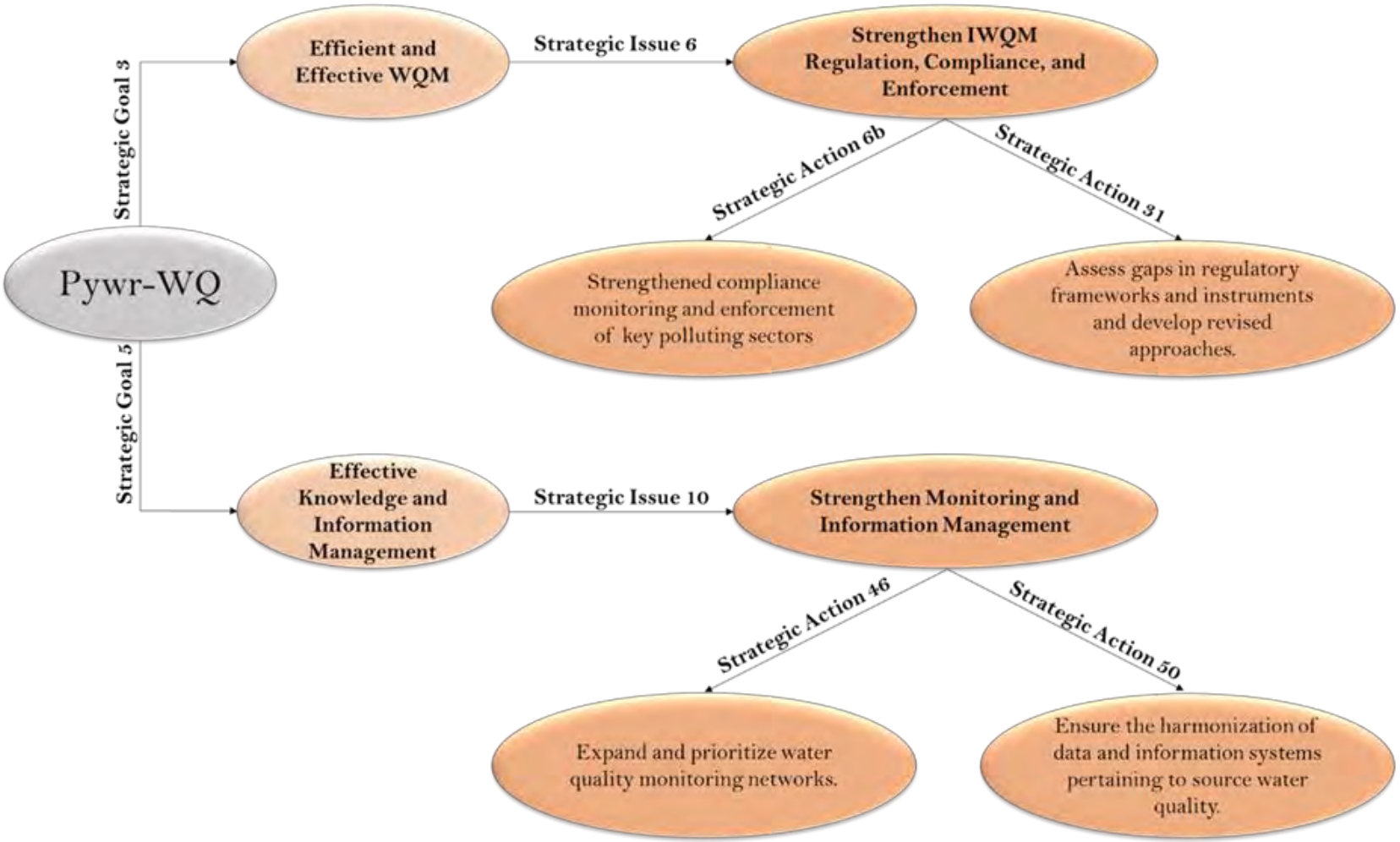

Figure 7.2: This proposal explores the application of the Pywr-WQ model within the framework of Integrated Water Quality Management (IWQM), considering strategic goals, issues, and actions as outlined by DWS (2017) and DWS (2023).

Figure 7.2 depicts the actions and objectives extracted from the Integrated Water Quality Management (IWQM) Strategy report by DWS (2017). It highlights the effective utilisation of the Pywr-WQ model in water quality monitoring, analysis, and management.

One key advantage of Pywr-WQ is its ability to facilitate optimal choices among different water sources to achieve target water quality standards. For instance, in the Grootdraai Catchment, which receives multiple inflowing transfers with varying water quality signatures, Pywr-WQ can inform decision-makers on how much water should be abstracted from each transfer and at what times to achieve desired water quality levels in the Grootdraai Dam. This capability enhances regulation, compliance, and enforcement in water quality management, aligning with the objectives of the NWRS-3 and contributing to the achievement of SDG 6 targets. The Pywr-WQ model exhibits considerable potential, not only aligning with the first objective of the NWRS-3, emphasising sustainable and equitable management, protection, use, development, conservation, and control of water (DWS, 2023), but also contributes to the achievement of SDG 6 targets as outlined in Stats SA (2019).

The Pywr-WQ model can be adopted as a tool for identifying trends and patterns in water quality parameters and facilitating regulatory compliance assessments. Furthermore, the model can assist in refining regulatory frameworks by simulating the effects of diverse water quality guidelines and standards on pollutant variations across finer scales and different timeframes. This support enables policymakers and water managers to make well-informed decisions regarding regulatory adjustments.

7.4 Land-use Changes and Water Quality Implications

While building upon a prior study conducted by Slaughter & Mantel (2017), this study adopted a similar approach to assess both surface water and groundwater quality. It established correlations between surface water quality and nutrient concentrations, and groundwater quality and salts such as TDS, sulphate, and calcium. Sadeghi et al. (2021) discovered no significant relationship between rainfall rates, land-use changes, and groundwater quality, suggesting that alterations in groundwater quality were not solely attributable to these factors. However, past studies have drawn different conclusions, highlighting a strong correlation between land-cover classes and water quality variables. For instance, a study concentrating on eight distinct cities in South and Southeast Asia concludes that the importance of land-use and land-cover change is a significant driver and pressure impacting water quality, and urges its consideration in decision-making processes (Kumar, 2019). A separate study carried out in South Carolina

, particularly in the Waccamaw River at Conway Marina, emphasised that watershed characteristics, such as land-use, play a crucial role in regulating stream water quality indicators (Mishra et al., 2021). When regression analysis techniques were extensively employed to model the relationship between land-use/land-cover and water quality, the analysis revealed significant correlations between land-cover classes such as urban areas, forested land, and others with nutrients, turbidity, and related water quality parameters (e.g., Amiri & Nakane, 2008; Boeder & Chang, 2008; Huang et al., 2013; Paul & Meyer, 2001; Rothenberger et al., 2009; Sliva & Dudley Williams, 2001). Yet, the complex nature of water quality data necessitates novel statistical approaches capable of revealing spatiotemporal variability, as noted by Afed Ullah et al. (2018).

The ongoing processes of urbanisation, industrialisation, and agricultural activities will persist in exerting adverse effects on water quality across various scales (Camara et al., 2019). Land-use alteration may influence the stream ecosystem through different measures and scales, and contribute to ecosystem degradation (Pereira, 2020). For instance, deforestation, urbanisation, and agriculture raise stream sediment levels, harming aquatic life and food webs (Sutherland et al., 2002; Wood & Armitage, 1997). Agricultural activities can lead to nutrient pollution in streams, fostering algae growth and altering species composition toward less native, more resilient types (Delong & Brusven, 1998; Niyogi et al., 2003). Moreover, urban land-use changes can introduce heavy metals, synthetic chemicals, and toxic organics into streams, harming aquatic life with deformities, higher mortality rates, and disruptions in growth and reproduction (Kolpin et al., 2002). The omission of critical factors such as climate change, land-use and cover changes and population growth could have a profound impact on water resources, resulting in exacerbating issues related to water quantity and quality as noted by Zy Harifidy et al. (2022).

The present study (refer to Chapter 5) examines the influence of land-use changes on water quality parameters across varied scenarios within three distinct categories: mining areas, urban areas, and cultivated areas over the long term (2020–2099) under historical climate conditions. Water quality parameters investigated in mining and urban areas encompassed nitrate plus nitrite, ammonium, phosphate, sulphate, calcium, and TDS. Conversely, cultivated areas were examined solely for nutrient levels, including nitrate plus nitrite, ammonium, and phosphate. This study employed the Pywr-WQ model along with multiple regression to investigate the land-use change scenarios. It is important to note that while increasing one land-cover class, other remaining land-cover classes may also impact the simulations. When urban and cultivated areas increased, the simulations showed elevated levels of nitrate plus nitrite at the Grootdraai Dam compared to the mining scenario, surpassing acceptable water quality standards (refer to Chapter 5, Table 5.7).

Ammonium levels remained within acceptable limits in the urban area increase scenario, while phosphate levels remained acceptable in the cultivated area increase scenario. Multiple studies indicate that the substantial nutrient inputs from agricultural and urban areas have significantly degraded the water quality of rivers and streams (Delkash et al., 2018; Foote et al., 2015; Ludwig et al., 2009; Nie et al., 2018), and past research has demonstrated positive correlations between anthropogenic factors such as agriculture and urbanisation, and the concentration of nutrients like nitrogen and phosphorus (Giri & Qiu, 2016; Lintern et al., 2018).

Simulated salts such as TDS and sulphate in mining areas showed very high concentrations classified under tolerable and acceptable levels (refer to Chapter 5, Table 5.7) although mines cover small areas over the quaternary catchments. A study conducted in Brazil observed that mining, despite covering a small percentage of the territory, has a significant impact on water quality, leading to high turbidity, and heavy metals contamination (de Mello et al., 2020). Active coal mining operations exhibit negative impacts on ecosystem services, while some positive impacts were related to restoration activities (Boldy et al., 2021). For instance, mining can harm aquatic organisms by elevating metal and pollutant concentrations, adversely affecting fish, macroinvertebrates, and algae, as noted by Jain & Das (2017).

Chapter 5, referenced from Figure 5.22 to Figure 5.27, illustrates the advantages of employing the Pywr-WQ model to explore scenarios and assess the risk impact on water quality variables. It indicates that the increased urban areas scenario (referred to as Scenario A) poses risks of exceeding acceptable levels for nitrate plus nitrite and ammonium concentrations at the Grootdraai Dam over the long term (2020–2099), with relative increases in exceedance compared to the historical scenario at 25% and 8%, respectively. The elevated phosphate levels in the increased cultivated areas scenario (referred to as Scenario B) exhibit a relative increase in exceedance of phosphate's ideal level compared to the historical scenario, estimated at 65%. The relative increase in exceedance of acceptable levels for sulphate in Scenario C (referred to as mining areas increase) compared to the historical scenario is estimated at 21%. In contrast, the relative increase in exceedance of acceptable levels for TDS in Scenario C compared to the historical scenario exceeds 100%, revealing the alarming impact of increased mining activities on TDS concentrations due to multiple regression parameters for groundwater signatures and applied increase percentages per quaternary catchment. Previous studies have demonstrated that nitrate concentration typically displays a statistically significant positive correlation with urban density (Krause et al., 2008). Moreover, urban land-use contributes to nutrient loads of surface water runoff through wash-off (Lee et al., 2009). du Plessis & van Veelen (1991), Liu et al. (2014),

and Villiers & Thiart (2007) indicated that phosphates sourced mainly from agricultural activities and agricultural land-use strongly influence phosphorus.

While Chapter 5 did not explore heavy metals dynamics owing to limited datasets, it aligns with the National Water Resources Strategy-2 outlined in DWS (2013). This study highlights the impact of various factors, including mining operations (resulting in elevated TDS, sulphate, and calcium levels), urban expansion (leading to increased salinity, nitrate plus nitrite, and ammonium levels), and agricultural expansion (potentially causing sediment accumulation and elevated phosphate runoff) and agrees with the resulting issues from these land-use changes as outlined in NWRS-2 and NWRS-3.

The junction between the Pywr-WQ model and regression models aimed to address the knowledge gap in understanding the impact of specific land-use changes on water quality within the South African context. Integrating the Pywr-WQ model with statistical approaches like multiple regression, we demonstrated the capability of the Pywr-WQ model to complement and simulate the outputs of statistical models. However, the heterogeneity and diversity of the landscape pose challenges and can significantly impact the output of regression models. Recently highlighted the challenge of understanding the spatial and temporal patterns of water quality variables concerning land-use and land-cover in Beijing, China (Chen et al., 2016).

The current study fails to introduce and consider the effect of the expansion of urban areas on hydrological dynamics, which could ultimately affect water quality. For instance, changes in slopes, elevations, soils, and vegetation coverage alter how rainfall is captured, stored, and released within hydrological systems (McGrane, 2016). These modifications may influence runoff production and result in the mobilisation of contaminants across the river system within the study area. Study conducted by Miller & Hutchins (2017) in the United Kingdom revealed that urbanisation can lead to changes in the temperature of receiving watercourses. This aspect can be considered as another limitation of the study, as the current study assumes historical climate conditions without accounting for changes in water temperature.

7.5 Enhancing Water Quality amid Uncertain Futures

Chapter 6 of the study outlined the future outlook for water quality within the Grootdraai Dam, taking into account several influential factors. These factors included climate change, potential increases in abstraction volume from Grootdraai Dam, and the closure of mines in the area, all of which are relevant to the potential transition toward sustainable energy sources, such as solar power, for power generation purposes. This study examined the impact of mine closures on

specific quaternary catchments within the Grootdraai Dam Catchment. These quaternary catchments were chosen due to their high levels of TDS, sulphate, and calcium found during the calibration process.

Analysis indicated that under the improbable 70% increase in water abstraction from the Grootdraai Dam by Sasol-Secunda, concentrations of TDS and sulphate were notably elevated compared to the more plausible scenario, which entailed a 5% increase in water abstraction. Nevertheless, visible differences between the two simulated datasets were not observed in the short term (2010–2050). In the subsequent 30-year period (starting from 2020), TDS levels in both the scenarios of a 5% and 70% increase in abstraction volume depicted a respective 54% and 51% decrease in the acceptable level fraction compared to the baseline simulation. Additionally, there was a significant rise in the fraction of simulated data falling under the ideal level. These findings underscore an enhancement in water quality in the mines closure scenario, attributable to the decrease in groundwater signatures exerting a noticeable influence on this favourable trend. Even in the event of the worst-case scenario (70% increase), the levels exhibit visible improvements in TDS levels. However, sulphate demonstrated only a marginal relative decrease in the acceptable fraction, estimated at 10% for both scenarios, in contrast to the significant change observed in TDS levels.

The current study linked the closure of mines to a reduction in TDS, sulphate, and calcium groundwater signatures. However, Alexander & Ndambuki (2023) highlight that the magnitude and extent of the impact of mine closure on water resources, particularly groundwater, remain poorly defined. In addition, their study found that after mine closure in the Westrand Basin (WRB) in South Africa, the natural groundwater neutralising processes were overwhelmed, leading to the release of large quantities of acidified water from mineral deposits into the groundwater system. Yet, DWAF (2008a, 2008b) stated that after the mine closure phase, third-party entities are tasked with executing post-closure monitoring and maintenance programmes, and this phase will persist until the remaining impact of the mine reaches acceptable levels. This highlights the necessity of ensuring that following mine rehabilitation, mine effluents conform to acceptable levels of particular pollutants, notably TDS and sulphate, given that their pronounced concentrations within specific quaternary catchments include mine operations. The study findings align with the statement by the DWAF (2008b), as TDS and sulphate levels fall predominantly within the ideal and acceptable ranges.

This part of the study is limited by the use of the same historical water temperature data under climate change conditions. By keeping water temperature constant and only altering flow datasets, the direction of the model's outputs may be affected. Moreover, the scenarios of low and high abstractions did not account for increased return flows, particularly from domestic wastewater, which could have impacted nutrients. This omission could have led to deceptive results regarding the minimal impact of nutrients observed in the study. Additionally, assigning low groundwater signatures may not accurately reflect real-world conditions, as mine closure and rehabilitation processes take time, and mine closures in the study area are unlikely to occur simultaneously. The assumption that mine closure would result in an immediate improvement in groundwater salts is unrealistic. In reality, it may take decades for groundwater quality to return to pre-mining levels. As a result, the short term and long term trends in the simulations presented in the study are probably unrealistic.

Addressing these limitations could be a focus of future studies. For instance, in the climate change scenario, water temperature could be computed based on the corresponding air temperature projections. Furthermore, engaging stakeholders from Eskom could facilitate discussions on the mine closure process, enabling more accurate reflection in the modelling aspect.

7.6 Limitations and Future Studies

The present study encountered several challenges, which may be considered limitations, and uncertainties regarding the generated predictions for water quality variables in the medium and long term. For instance, certain quaternary catchments lacked water quality datasets, affecting the simulation of specific salts and resulting in unsatisfactory NSE values. In other quaternary catchments, peak values in the observed dataset may be attributed to potential instrument errors influencing the simulations. Furthermore, the climate change datasets utilised in the study were only available in terms of flow datasets, while air temperature datasets, which impact water temperature and subsequently the simulations, were not available. Additionally, return flows are assumed to remain at baseline levels, even if abstractions are increased. The study acknowledges a limitation concerning the implementation of a graded decrease in groundwater signatures. It assumed that mine closure would lead to an immediate improvement in groundwater salt signatures, which is unrealistic, as mine closure requires time for rehabilitation and is contingent upon the adopted policy and arrangement for closure.

Future studies could explore several paths based on the findings and limitations highlighted in the current study:

i. The prospective application of developed methodologies to establish relationships between land-use categories and water quality signatures, while considering additional influential factors such as fertiliser application rates, precipitation intensity and frequency, and irrigation duration.
ii. Conducting hydrological study (preliminary water quality investigation) to produce climate change runoff datasets utilising projected climate change models (e.g., the business-as-usual scenario). This includes considering anticipated alterations in air temperature, which may impact both water temperature and subsequent variations in water quality.
iii. Focus on the impacts of increased wastewater return flows resulting from assumed abstractions for domestic water demand. Specifically, investigate how advancements in water treatment technology might influence these impacts, as this aspect was not fully considered in the current study.
iv. Implement a graded decrease in groundwater signatures to better reflect the realistic process of mine closure and its impact on groundwater quality.
v. Incorporate advanced functionalities of the Pywr-WQ model to serve as a standalone water quantity-quality model. For example, if the water quality of a transfer is deemed low (e.g., ranging from tolerable to unacceptable), the model can implement a condition preventing the transfer from occurring either to or from the Grootdraai Dam. Additionally, the model can trigger alerts or actions if specific thresholds for water quality variables are exceeded.
vi. Apply the Pywr-WQ model in managing water quality in complex river systems with multiple upstream sources of varying quality. For instance, consider a scenario where a downstream dam receives water from five upstream dams through pipes, each with dramatically different water quality. The Pywr-WQ model could be employed to optimise the selection and blending of water from these upstream sources. By regulating the opening and closing of pipes from each dam, the Pywr-WQ model could determine the optimal combination of upstream water sources, the quantity of water to extract from each source, and the timing of withdrawals to attain a specific water quality target in the downstream dam. This capability could prove invaluable in ensuring the availability of safe and suitable water for various downstream uses, such as drinking water supply, agriculture, and environmental conservation.

7.7 Conclusions

This study addresses a notable gap in current water allocation models utilised in South Africa and water quality research. This study has developed a framework that can assist and support water managers and researchers in transitioning from monthly lumped models like WRYM to more efficient, open-source, rapid, spatially distributed, and transparent models. Moreover, it facilitates stronger connections between industry partners, policymakers, and scientific panels by fostering trust, engagement, and collaboration. This study presents significant benefits, notably in terms of time and cost savings. The Pywr-WQ model demonstrates significant efficacy in tackling water quality issues within South Africa, including risk assessment and abstraction management, ensuring that water quantity considerations do not overshadow concerns related to water quality. The study established a connection between the Pywr-WQ model and land-use models to explore the impact of land-use changes on water quality. While the Pywr-WQ model dynamically incorporates changes in water quantity that affect water quality, the integration with land-use models involved examining predetermined land-use scenarios and generating corresponding water quality parameter sets for the Pywr-WQ model. It is important to note that the Pywr-WQ model, in its current state, does not have the capability to inform land-use changes in real-time to achieve specific management objectives. It showed the classification of water quality variables under varying land-use conditions based on water quality guidelines, facilitating the visualisation of how specific water quality variables behave within different land-use changes.

The investigation indicates that water quality within the Grootdraai Dam Catchment, located in South Africa's Upper Vaal region, is declining owing to a variety of factors. These factors include dominant land-use classes, which display diverse impacts on the water quality variables examined in the study. This study examined the increased water abstraction from the Grootdraai Dam and mine closure, which is anticipated due to the potential transition from coal to green energy as a source of power generation under changing climate conditions. The scenarios investigated suggest that urban area expansion may have a significant impact on nitrate plus nitrite and ammonium levels, while phosphate levels are more sensitive to cultivated area expansion. Conversely, the expansion of mines appears to have a significant influence on sulphate, calcium, and TDS levels. This study emphasises the long term impact of mine closures on water quality variables. Across both scenarios of increased abstraction percentages, there was a notably positive change in the levels of TDS, calcium, and sulphate, with reduced variability compared to the baseline scenario. However, the scenarios underline that at very high abstraction

percentages, the levels of TDS, sulphate, and calcium surpass those at low abstraction percentages. This study marks the innovative use of the Pywr model in South Africa, integrating it with a local water quality model to create the dynamic Pywr-WQ model.

REFERENCES

Abbaspour, K. C., Rouholahnejad, E., Vaghefi, S., Srinivasan, R., Yang, H., & Kløve, B. (2015). A continental-scale hydrology and water quality model for Europe: Calibration and uncertainty of a high-resolution large-scale SWAT model. Journal of Hydrology, 524, 733–752. Elsevier.

Adom, R. K., & Simatele, M. D. (2022). The role of stakeholder engagement in sustainable water resource management in South Africa. Natural Resources Forum, 46, 4, 410–427. Blackwell Publishing Ltd.

Adgolign, T. B., Rao, G. S., & Abbulu, Y. (2016). WEAP modelling of surface water resources allocation in Didessa Sub-Basin, West Ethiopia. Sustainable Water Resources Management, 2, 55-70. Springer.

Adu, J. T., & Kumarasamy, M. V. (2018). Assessing non-point source pollution models: A review. Polish Journal of Environmental Studies, 27, 5, 1801-1813. Polish Academy of Sciences.

Afed Ullah, K., Jiang, J., & Wang, P. (2018). Land-use impacts on surface water quality by statistical approaches. Global Journal of Environmental Science and Management, 4, 2, 231–250. https://doi.org/10.22034/gjesm.2018.04.02.010

Agudelo, C. A. R., Bustos, S. L. H., & Moreno, C. A. P. (2020). Modelling interactions among multiple ecosystem services. A critical review. Ecological Modelling, 429, 109103. Elsevier. https://doi.org/10.1016/j.ecolmodel.2020.109103

Akamagwuna, F. C. (2021). Application of Macroinvertebrate-Based Biomonitoring and Stable Isotopes for Assessing the Effects of Agricultural Land-Use on River Ecosystem Structure and Function in the Kat River, Eastern Cape, South Africa (Master's thesis). Rhodes University.

Akhtar, N., Syakir Ishak, M. I., Bhawani, S. A., & Umar, K. (2021). Various natural and anthropogenic factors responsible for water quality degradation: A review. Water, 13, 19, 2660. MDPI. https://doi.org/10.3390/w13192660

Akinbami, O. M., Oke, S. R., & Bodunrin, M. O. (2021). The state of renewable energy development in South Africa: An overview. Alexandria Engineering Journal, 60, 6, 5077–5093. Elsevier. https://doi.org/10.1016/j.aej.2021.03.065

Alam, S., Gebremichael, M., & Li, R. (2019). Remote sensing-based assessment of the crop, energy and water nexus in the Central Valley, California. Remote Sensing, 11, 14, 1701. MDPI.

Alexander, A. C., & Ndambuki, J. M. (2023). Impact of mine closure on groundwater resource: Experience from Westrand Basin-South Africa. Physics and Chemistry of the Earth, Parts A/B/C, 128, 103432. Elsevier.

Alley, W. M. (1984). On the treatment of evapotranspiration, soil moisture accounting, and aquifer recharge in monthly water balance models. Water Resources Research, 20, 8, 1137-1149. American Geophysical Union.

Ali, M. M., Hossain, D., Al-Imran, A., Khan, M. S., Begum, M., & Osman, M. H. (2021). Environmental pollution with heavy metals: A public health concern. Heavy Metals – Their Environmental Impacts and Mitigation, 771–783. Springer.

Amiri, B. J., & Nakane, K. (2008). Entire catchment and buffer zone approaches to modeling linkage between river water quality and land cover—a case study of Yamaguchi Prefecture, Japan. Chinese Geographical Science, 18, 85–92. Springer. https://doi.org/10.1007/s11769-008-0085-6

Andreu, J., Capilla, J., & Sanchís, E. (1996). AQUATOOL, a generalized decision-support system for water-resources planning and operational management. Journal of Hydrology, 177, 3-4, 269-291. Elsevier. https://doi.org/10.1016/0022-1694(95)02963-X

Anokye, N. A. (2013). Stakeholder Participation in Water Resources Management: The Case of Densu Basin in Ghana (PhD-Thesis - Research and graduation internal, Vrije Universiteit Amsterdam).Vu Research Portal.

Argent, R. M., Perraud, J. M., Rahman, J. M., Grayson, R. B., & Podger, G. M. (2009). A new approach to water quality modelling and environmental decision support systems. Environmental Modelling & Software, 24, 7, 809–818. Elsevier. https://doi.org/10.1016/j.envsoft.2008.12.010

Arnold, J. G., Moriasi, D. N., Gassman, P. W., Abbaspour, K. C., White, M. J., Srinivasan, R., Santhi, C., Harmel, R. D., Griensven, A. van, Liew, M. W. Van, Kannan, N., & Jha, M. K. (2012). SWAT: Model use, calibration, and validation. Transactions of the ASABE, 55 , 4, 1491–1508. American Society of Agricultural and Biological Engineers. https://doi.org/10.13031/2013.42256

Arnold, U., & Orlob, G. T. (1989). Decision support for estuarine water quality management. Journal of Water Resources Planning and Management, 115, 6, 775-792. American Society of Civil Engineers.

Artioli, Y., Bendoricchio, G., & Palmeri, L. (2005). Defining and modelling the coastal zone affected by the Po river (Italy). Ecological Modelling, 184, 1, 55–68. Elsevier.

Ashton, P. J., & Dabrowski, J. M. (2010). An overview of surface water quality in the Olifants River catchment. WRC Report No. KV, 293(11). Water Research Commission.

Aurecon (2020). Development and piloting of a water quality model for Vaal Dam reservoir and the contributing catchment: Phase 2 – Model Calibration and Validation. Aurecon Report No. 12169/504672. Rand Water.

Ayana, E. (2019). Determinants of Declining Water Quality. World Bank.

Azevedo, L. G. T. D., Gates, T. K., Fontane, D. G., Labadie, J. W., & Porto, R. L. (2000). Integration of water quantity and quality in strategic river basin planning. Journal of Water Resources Planning and Management, 126, 2, 85-97. American Society of Civil Engineers.

Baisch, J. (2009). Data shortage in Africa. Desalination, 248, 1-3, 524–529. Elsevier.

Basheer, M., Nechifor, V., Calzadilla, A., Gebrechorkos, S., Pritchard, D., Forsythe, N., Gonzalez, J. M., Sheffield, J., Fowler, H. J., & Harou, J. J. (2023). Cooperative adaptive management of the Nile River with climate and socio-economic uncertainties. Nature Climate Change, 13, 1, 48–57. Springer Nature.

Bergström, S. (1992). The HBV model–its structure and applications. Swedish Meteorological and Hydrological Institute (SMHI).

Bharti, R., & Sharma, R. (2022). Effect of heavy metals: An overview. Materials Today: Proceedings, 51, 880–885. Elsevier.

Blanchon, D. (2003). La nouvelle politique de l'eau en Afrique du Sud: vers une gestion environnementale des ressources? Espace Géographique, 32, 1, 21–30. Belin.

Boeder, M., & Chang, H. (2008). Multi-scale analysis of oxygen demand trends in an urbanizing Oregon watershed, USA. Journal of Environmental Management, 87, 4, 567–581. Elsevier. https://doi.org/10.1016/j.jenvman.2007.12.009

Boldy, R., Santini, T., Annandale, M., Erskine, P. D., & Sonter, L. J. (2021). Understanding the impacts of mining on ecosystem services through a systematic review. The Extractive Industries and Society, 8, 1, 457–466. Elsevier. https://doi.org/10.1016/j.exis.2020.12.005

Bongaarts, J. (2009). Human population growth and the demographic transition. Philosophical Transactions of the Royal Society B: Biological Sciences, 364, 1532, 2985–2990. Royal Society Publishing.

Bouleau, G., & Pont, D. (2014). Les conditions de référence de la directive cadre européenne sur l'eau face à la dynamique des hydrosystèmes et des usages. Natures Sciences Sociétés, 22, 1, 3–14. EDP Sciences.

Bowes, M. J., Smith, J. T., Jarvie, H. P., & Neal, C. (2008). Modelling of phosphorus inputs to rivers from diffuse and point sources. Science of the Total Environment, 395, 2-3, 125–138. Elsevier.

Bradford, W. L. (1977). Urban stormwater pollutant loadings: A statistical summary through 1972. Water Pollution Control Federation, 49, 4, 613–622. Water Environment Federation.

Braune, E., & Roger, K. H. (1987). The Vaal River catchment: Problems and research needs. Council for Scientific and Industrial Research (CSIR). https://researchspace.csir.co.za/dspace/handle/10204/2373

Burek, P., Satoh, Y., Kahil, T., Tang, T., Greve, P., Smilovic, M., Guillaumot, L., & Wada, Y. (2019). Development of the Community Water Model (CWatM v1.04): A high-resolution hydrological model for global and regional assessment of integrated water resource management. International Institute for Applied Systems Analysis (IIASA).

Burigato Costa, C. M. D. S., da Silva Marques, L., Almeida, A. K., Leite, I. R., & De Almeida, I. K. (2019). Applicability of water quality models around the world—a review. Environmental Science and Pollution Research, 26, 36, 36141–36162. Springer. https://doi.org/10.1007/s11356-019-06637-2

Can, E. K., & Houck, M. H. (1984). Real-time reservoir operations by goal programming. Journal of Water Resources Planning and Management, 110, 3, 297–309. American Society of Civil Engineers.

Camara, M., Jamil, N. R., & Abdullah, A. F. B. (2019). Impact of land-uses on water quality in Malaysia: A review. Ecological Processes, 8, 1, 1–10. Springer.

Camargo, J. A. (2003). Fluoride toxicity to aquatic organisms: A review. Chemosphere, 50, 3, 251–264. Elsevier.

Camargo, J. A., Alonso, A., & Salamanca, A. (2005). Nitrate toxicity to aquatic animals: A review with new data for freshwater invertebrates. Chemosphere, 58, 9, 1255–1267. Elsevier.

Cañedo-Argüelles, M., Kefford, B. J., Piscart, C., Prat, N., Schäfer, R. B., & Schulz, C. J. (2013). Salinisation of rivers: An urgent ecological issue. Environmental Pollution, 173, 157–167. Elsevier. https://doi.org/10.1016/j.envpol.2012.10.011

Carey, R. O., & Migliaccio, K. W. (2009). Contribution of wastewater treatment plant effluents to nutrient dynamics in aquatic systems: A review. Environmental Management, 44, 205–217. Springer. https://doi.org/10.1007/s00267-009-9309-5

Cariou, A. (2015). L'eau en Asie centrale. Institut Français d'Études sur l'Asie centrale. UMIFRE.

Casey, E., Beaini, S., Pabi, S., Zammit, K., & Amarnath, A. (2017). The triple bottom line for efficiency: Integrating systems within water and energy networks. IEEE Power and Energy Magazine, 15, 1, 34-42. IEEE. https://doi.org/10.1109/MPE.2016.2629741

Cetinkaya, C. P., Fistikoglu, O., Harmancioglu, N. B., & Fedra, K. (2008). Optimization methods applied for sustainable management of water-scarce basins. Journal of Hydroinformatics, 10, 1, 69-95. International Water Association.

Chapman, D. V. (2021). Water quality assessments: A guide to the use of biota, sediments and water in environmental monitoring (3rd ed.). CRC Press. https://iris.who.int/handle/10665/41850

Chapman, R. A., Manders, P. T., Scholes, R. J., & Bosch, J. M. (1995). Who should get the water? Decision support for water resource management. Water Science and Technology, 32, 5-6, 37-43. Elsevier.

Chapman, D. V., World Health Organization, UNESCO, & United Nations Environment Programme. (1996). Water quality assessments: A guide to the use of biota, sediments and water in environmental monitoring (2nd ed.). Taylor & Francis. https://iris.who.int/handle/10665/41850

Chapra, S. C. (2008). Surface water-quality modeling. Waveland Press.

Charbonneau, R., & Kondolf, G. M. (1993). Land-use change in California, USA: Nonpoint source water quality impacts. Environmental Management, 17, 4, 453–460. Springer.

Chen, X., Wang, Y., Cai, Z., Wu, C., & Ye, C. (2020). Effects of land-use and land-cover change on nitrogen transport in northern Taihu Basin, China during 1990–2017. Sustainability, 12, 9, 3895. MDPI. https://doi.org/10.3390/su12093895

Chen, X., Zhou, W., Pickett, S. T., Li, W., & Han, L. (2016). Spatial-temporal variations of water quality and its relationship to land-use and land-cover in Beijing, China. International Journal of Environmental Research and Public Health, 13, 5, 449. MDPI. https://doi.org/10.3390/ijerph13050449

Cheng, P., Meng, F., Wang, Y., Zhang, L., Yang, Q., & Jiang, M. (2018). The impacts of land-use patterns on water quality in a trans-boundary river basin in northeast China based on eco-functional regionalization. International Journal of Environmental Research and Public Health, 15, 9, 1872. MDPI.

Chiumia, S. (2021). Coal-affected but also coal-dependent: Mpumalanga, the coal-mining hotspot – Fossil energy and energy transition in South Africa. Climate Justice Central. https://www.climatejusticecentral.org/posts/coal-affected-but-also-coal-dependent-mpumalanga-the-coal-mining-hotspot

Cho, K. H., Pachepsky, Y., Ligaray, M., Kwon, Y., & Kim, K. H. (2020). Data assimilation in surface water quality modeling: A review. Water Research, 186, 116307. Elsevier https://doi.org/10.1016/j.watres.2020.116307

Chu, T. W., & Shirmohammadi, A. (2004). Evaluation of the SWAT model's hydrology component in the Piedmont physiographic region of Maryland. Transactions of the ASAE, 47, 4, 1057–1073. American Society of Agricultural and Biological Engineers. https://elibrary.asabe.org/abstract.asp?aid=16579

Cock, J. (2019). Resistance to coal inequalities and the possibilities of a just transition in South Africa. Development Southern Africa, 36, 6, 860–873. Taylor & Francis. https://doi.org/10.1080/0376835X.2019.1660859

Coleman, T. J., van Rooyen, P., & Görgens, A. H. M. (2007, September). Framework for future water resource analysis in South Africa. 13th SANCIAHS National Hydrology Symposium, 6–7. SANCIAHS.

Conallin, J. C., Dickens, C., Hearne, D., & Allan, C. (2017). Stakeholder engagement in environmental water management. Water for the Environment, 129–150. Academic Press.

Cortés, U., Sànchez-Marrè, M., R-Roda, I., & Poch, M. (2003). Towards Environmental Decision Support Systems. Springer. https://api.semanticscholar.org/CorpusID:17420852

Cropper, M., & Griffiths, C. (1994). The interaction of population growth and environmental quality. The American Economic Review, 84, 2, 250–254. American Economic Association.

CSIR, A. (2010). A CSIR perspective on water in South Africa. Council for Scientific and Industrial Research (CSIR). www.csir.co.za

Cullis, J. D., Rossouw, N., Du Toit, G., Petrie, D., Wolfaardt, G., De Clercq, W., & Horn, A. (2018). Economic risks due to declining water quality in the Breede River catchment. Water SA, 44, 3, 464–473. Water Research Commission.

Dabrowski, J. M., Ashton, P. J., Murray, K., Leaner, J. J., & Mason, R. P. (2008). Anthropogenic mercury emissions in South Africa: Coal combustion in power plants. Atmospheric Environment, 42, 27, 6620–6626. Elsevier.

Davis, J., O'Grady, A. P., Dale, A., Arthington, A. H., Gell, P. A., Driver, P. D., Bond, N., Casanova, M., Finlayson, M., & Watts, R. J. (2015). When trends intersect: The challenge of protecting freshwater ecosystems under multiple land-use and hydrological intensification scenarios. Science of the Total Environment, 534, 65–78. Elsevier.

de Coning, C. (2006). Overview of the water policy process in South Africa. Water Policy, 8, 6, 505–528. IWA Publishing. https://doi.org/10.2166/wp.2006.039

de Groot, R. S., Alkemade, R., Braat, L., Hein, L., & Willemen, L. (2010). Challenges in integrating the concept of ecosystem services and values in landscape planning, management and decision making. Ecological Complexity, 7, 3, 260–272. Elsevier. https://doi.org/10.1016/j.ecocom.2009.10.006

de Mello, K., Taniwaki, R. H., de Paula, F. R., Valente, R. A., Randhir, T. O., Macedo, D. R., Leal, C. G., Rodrigues, C. B., & Hughes, R. M. (2020). Multiscale land-use impacts on water quality: Assessment, planning, and future perspectives in Brazil. Journal of Environmental Management, 270, 110879. Elsevier. https://doi.org/10.1016/j.jenvman.2020.110879

Delkash, M., Al-Faraj, F. A., & Scholz, M. (2018). Impacts of anthropogenic land-use changes on nutrient concentrations in surface waterbodies: A review. CLEAN–Soil, Air, Water, 46, 5, 1800051. Wiley-VCH.

Delong, M. D., & Brusven, M. A. (1998). Macroinvertebrate community structure along the longitudinal gradient of an agriculturally impacted stream. Environmental Management, 22, 3, 445–457. Springer.

Dickinson, N. M. (2003). Soil degradation and nutrients. N. C. Johnson (Ed.), The Restoration and Management of Derelict Land: Modern Approaches, 50–65. Springer.

Dikio, E. D. (2010). Water quality evaluation of Vaal River, Sharpeville and Bedworth lakes in the Vaal region of South Africa. Research Journal of Applied Sciences, Engineering and Technology, 2, 6, 574–579. Maxwell Scientific Organization.

Dinku, T. (2019). Challenges with availability and quality of climate data in Africa. A. Sharma & C. Singh (Eds.), Extreme Hydrology and Climate Variability, 71–80. Elsevier.

Department of Mineral Resources and Energy (DMRE). (2019). Integrated Resource Plan (IRP2019). Government of South Africa.

Draper, A. J., Munévar, A., Arora, S. K., Reyes, E., Parker, N. L., Chung, F. I., & Peterson, L. E. (2004). CalSim: Generalized model for reservoir system analysis. Journal of Water Resources Planning and Management, 130, 6, 480–489. American Society of Civil Engineers.

du Plessis, A. (2019). South Africa's water reality: Challenges, solutions, actions and a way forward. Water as an Inescapable Risk: Current Global Water Availability, Quality and Risks with a Specific Focus on South Africa, 281–296. Springer. https://doi.org/10.1007/978-3-030-03186-2_12

du Plessis, A. (2017). Freshwater Challenges of South Africa and its Upper Vaal River, 129-151, Berlin, Germany Springer.

du Plessis, A., Harmse, T., & Ahmed, F. (2015). Predicting water quality associated with land cover change in the Grootdraai Dam Catchment, South Africa. The Water Legacies of Conventional Mining, 178–194. Routledge. https://doi.org/10.1080/02508060.2015.1067752

du Plessis, H. M., & van Veelen, M. (1991). Water quality: Salinization and eutrophication time series and trends in South Africa. South African Journal of Science, 87, 1, 11–16. Academy of Science of South Africa.

Durmishyan, A. G. (1974). Compaction of argillaceous rocks. International Geology Review, 16, 6, 650–653. Taylor & Francis. https://doi.org/10.1080/00206817409471815

Department of Cooperative Governance and Traditional Affairs, Mpumalanga Provincial Government (DCOGTA). (2019). Mpumalanga Spatial Development Framework: Executive Summery. Mpumalanga Provincial Government.

Department of Water Affairs (DWA). (2011). Directorate Water Resource Planning Systems: Water Quality Planning. Resource Directed Management of Water Quality. Planning Level Review of Water Quality in South Africa. Sub-series No. WQP 2.0. Pretoria, South Africa.

Department of Water Affairs and Forestry (DWAF). (1996). South African Water Quality Guidelines. Volume 7: Aquatic Ecosystems. Pretoria, South Africa.

Department of Water Affairs & Forestry (DWAF). (1997). Overview of the water resources availability and utilisation in South Africa. Department of Water Affairs and Forestry, Pretoria.

Department of Water Affairs and Forestry (DWAF). (2001). Water Quality Management Series, Sub-Series No. MS 8.2, Edition 1: A Guideline to the Water Quality Management Component of a Catchment Management Strategy. Pretoria. http://www.dwa.gov.za/iwqs/wrmais/other/GUIDELINE_WQ_CMS_V04.pdf

Department of Water Affairs and Forestry, South Africa. (2004). Upper Vaal Water Management Area: Internal Strategic Perspective. Prepared by PDNA, WRP Consulting Engineers (Pty) Ltd, WMB and Kwezi-V3 on behalf of the Directorate: National Water Resource Planning. DWAF Report No P WMA 08/000/00/0304. Pretoria, South Africa. https://docslib.org/doc/366931/upper-vaal-water-management-area-wma-no-8

Department of Water Affairs and Forestry (DWAF). (2006). Resource Directed Management of Water Quality: Volume 2.1: Summary Strategy. Edition 1. Water Resource Planning Systems Series, Sub-series No. WQP 1.5.1. ISBN No. 0-621-36789-3. Pretoria, South Africa.

Department of Water Affairs and Forestry (DWAF). (2008a). Best Practice Guideline G4: Impact Prediction. Pretoria, South Africa.

Department of Water Affairs and Forestry (DWAF). (2008b). Best Practice Guideline G5: Water Management Aspects for Mine Closure. Pretoria, South Africa.

Department of Water Affairs and Forestry (DWAF). (2009). Vaal River system: Large bulk water supply reconciliation strategy: second stage reconciliation strategy. Pretoria, South Africa. https://www.wrc.org.za/wp-content/uploads/mdocs/TT%20446%20Water%20Quality%20Management.pdf

Department of Environmental Affairs and Tourism (DEAT). (2006). South Africa environment outlook: A report on the state of the environment. 371. Pretoria, South Africa.

Department of Water and Sanitation (DWS). (2006). Directorate : Resource Directed Measures Letaba Catchment Reserve Determination Study – Groundwater Report Final. Pretoria, South Africa. https://www.dws.gov.za/rdm/documents/Hydrology%20Support%20&%20Water%20Resources%20Evaluaution.pdf

Department of Water and Sanitation (DWS). (2011). The Groundwater Dictionary. https://www.dws.gov.za/Groundwater/GroundwaterDictionary.aspx

Department of Water and Sanitation (DWS). (2013). National Water Resource Strategy - 2nd edition 2013. Water Resources, Pretoria, South Africa. http://www.dwa.gov.za/documents/Other/Strategic Plan/NWRS2-Final-email-version.pdf

Department of Water and Sanitation (DWS). (2016). Water Quality and Water Quality Management Challenges in South Africa. Pretoria, South Africa. http://www.dwa.gov.za/stories/Water Quality and Water Quality Management Challenges in South Africa.pdf

Department of Water and Sanitation (DWS). (2017). Water Quality Management Policies and Strategies for South Africa. Report No. 3.3 Summary of IWQM Strategy – Edition 2. Water Resource Planning Systems Series, DWS Report No.: 000/00/21715/17. Pretoria, South

Africa. https://www.dws.gov.za/iwrp/iwqms/Documents/Report 3.3 IWQM Strategy Summary_Final.pdf

Department of Water and Sanitation (DWS). (2018). Vaal Reconciliation Strategy Phase 2: Water Requirements. Pretoria, South Africa.

Department of Water and Sanitation (DWS). (2021). National Water Resource Strategy 3. In Water Resources. Pretoria, South Africa.

Department of Water and Sanitation (DWS). (2023). National Water Strategy 3. Pretoria, South Africa. https://www.dws.gov.za/Documents/Gazettes/Approved National Water Resource Strategy Third Edition (NWRS3) 2023.pdf

Ebert, E. (1972). Ein Fall aus Der versicherngsärztlichen Praxis. Lebensversicherungsmedizin, 24, 4, 94–97. Georg Thieme Verlag.

Edokpayi, J. N., Odiyo, J. O., & Durowoju, O. S. (2017). Impact of wastewater on surface water quality in developing countries: A case study of South Africa. Water Quality, 10, 66561, 10–5772. IntechOpen.

Ejigu, M. T. (2021). Overview of water quality modeling. Cogent Engineering, 8, 1, 1891711. Taylor & Francis. https://doi.org/10.1080/23311916.2021.1891711

Fang, X., Zhang, J., Chen, Y., & Xu, X. (2008). QUAL2K model used in the water quality assessment of Qiantang River, China. Water Environment Research, 80, 11, 2125–2133. Water Environment Federation.

Food and Agriculture Organization of the United Nations (FAO). (2006). Guidelines for Soil Description. FAO. https://www.fao.org/land-water/land/land-governance/land-resources-planning-toolbox/category/details/en/c/1236461/

Fleming, G. (1975). Computer Simulation Techniques in Hydrology. Elsevier. https://lccn.loc.gov/74021788

Foote, K. J., Joy, M. K., & Death, R. G. (2015). New Zealand dairy farming: Milking our environment for all its worth. Environmental Management, 56, 3, 709–720. Springer.

Forrester, J. W. (1968). Industrial dynamics – A response to Ansoff and Slevin. Management Science, 14, 9, 601–618. INFORMS.

Gao, L., & Li, D. (2015). A review of hydrological/water-quality models. Frontiers of Agricultural Science and Engineering, 1, 4, 267–276. the Chinese Academy of Engineering (CAE).

Giri, S. (2021). Water quality prospective in the twenty-first century: Status of water quality in major river basins, contemporary strategies, and impediments: A review. Environmental Pollution, 271, 116332. Elsevier. https://doi.org/10.1016/j.envpol.2020.116332

Giri, S., & Qiu, Z. (2016). Understanding the relationship of land-uses and water quality in the twenty-first century: A review. Journal of Environmental Management, 173, 41–48. Elsevier.

González-Quirós, A., & Fernández-Álvarez, J. P. (2019). Conceptualization and finite element groundwater flow modeling of a flooded underground mine reservoir in the Asturian Coal Basin, Spain. Journal of Hydrology, 578, 124036. Elsevier. https://doi.org/10.1016/j.jhydrol.2019.124036

Gonzalez, J. M., Matrosov, E. S., Obuobie, E., Mul, M., Pettinotti, L., Gebrechorkos, S. H., Sheffield, J., Bottacin-Busolin, A., Dalton, J., & Smith, D. M. (2021). Quantifying cooperation benefits for new dams in transboundary water systems without formal operating rules. Frontiers in Environmental Science, 9, 596612. Frontiers.

Griffin, N. J. (2017). The rise and fall of dissolved phosphate in South African rivers. South African Journal of Science, 113, 11-12, 1–7. Academy of Science of South Africa. https://doi.org/10.17159/SAJS.2017/20170020

Griffin, N. J., Palmer, C. G., & Scherman, P. A. (2014). Critical analysis of environmental water quality in South Africa: Historic and current trends. Water Research Commission, 1, 5. Water Research Commission.

Grizzetti, B., Bouraoui, F., Granlund, K., Rekolainen, S., & Bidoglio, G. (2003). Modelling diffuse emission and retention of nutrients in the Vantaanjoki watershed (Finland) using the SWAT model. Ecological Modelling, 169, 1, 25–38. Elsevier.

Guan, Y., Shao, C., & Ju, M. (2014). Heavy metal contamination assessment and partition for industrial and mining gathering areas. International Journal of Environmental Research and Public Health, 11, 7, 7286–7303. MDPI.

Guillot, P. (1981). The "GRADEX" method. La Houille Blanche.

Guillot, P., & Durand, D. (1969). La méthode du GRADEX pour le calcul de la probabilité des crues à partir des pluies. La Houille Blanche.

Guillot, P., & Duband, D. (1980). Fonction de transfert pluie-débit sur les bassins versants de l'ordre de 1000 km². La Houille Blanche, 66, 4-5, 279–290. La Houille Blanche.

Gupta, H. V., Sorooshian, S., & Yapo, P. O. (1999). Status of automatic calibration for hydrologic models: Comparison with multilevel expert calibration. Journal of Hydrologic Engineering, 4, 2, 135–143. American Society of Civil Engineers.

Gwapedza, D., Nyamela, N., Hughes, D. A., Slaughter, A. R., Mantel, S. K., & van der Waal, B. (2020). Prediction of sediment yield of the Inxu River catchment (South Africa) using the MUSLE. International Soil and Water Conservation Research, 8, 4, 494–504. Elsevier.

Haggard, B. E., Stanley, E. H., & Storm, D. E. (2005). Nutrient retention in a point-source-enriched stream. Journal of the North American Benthological Society, 24, 1, 29–47. University of Chicago Press. https://doi.org/10.1899/0887-3593(2005)024%3C0029:nriaps%3E2.0.co;2

Helsel, D. R., & Frans, L. M. (2006). Regional Kendall test for trend. Environmental Science & Technology, 40, 13, 4066–4073. American Chemical Society.

Herman, J. D., Reed, P. M., Zeff, H. B., & Characklis, G. W. (2015). How should robustness be defined for water systems planning under change? Journal of Water Resources Planning and Management, 141, 10, 04015012. American Society of Civil Engineers.

Hintz, W. D., Fay, L., & Relyea, R. A. (2022). Road salts, human safety, and the rising salinity of our fresh waters. Frontiers in Ecology and the Environment, 20, 1, 22–30. Wiley.

Hirsch, R. M., Slack, J. R., & Smith, R. A. (1982). Techniques of trend analysis for monthly water quality data. Water Resources Research, 18, 1, 107–121. American Geophysical Union

Hobbs, P., Oelofse, S. H., & Rascher, J. (2008). Management of environmental impacts from coal mining in the upper Olifants River catchment as a function of age and scale. International Journal of Water Resources Development, 24, 3, 417–431. Taylor & Francis. https://doi.org/10.1080/07900620802127366

Horlitz, T. (2007). The role of model interfaces for participation in water management. Water Resources Management, 21, 7, 1091–1102. Springer.

House, M. A., Ellis, J. B., Herricks, E. E., Hvitved-Jacobsen, T., Seager, J., Lijklema, L., Aalderink, H., & Clifforde, I. T. (1993). Urban drainage-impacts on receiving water quality. Water Science and Technology, 27, 12, 117–158. IWA Publishing.

Huang, J., Zhan, J., Yan, H., Wu, F., & Deng, X. (2013). Evaluation of the impacts of land-use on water quality: A case study in the Chaohu Lake Basin. The Scientific World Journal, 2013. Hindawi . https://doi.org/10.1155/2013/32918

Huang, L., Bai, J., Xiao, R., Gao, H., & Liu, P. (2012). Spatial distribution of Fe, Cu, Mn in the surface water system and their effects on wetland vegetation in the Pearl River Estuary of China. CLEAN–Soil, Air, Water, 40, 10, 1085–1092. Wiley-VCH.

Huang, L., Gao, X., Guo, J., Ma, X., & Liu, M. (2013). A review on the mechanism and affecting factors of nitrous oxide emission in constructed wetlands. Environmental Earth Sciences, 68, 2171–2180. Springer.

Hughes, D. A., Hannart, P., & Watkins, D. (2003). Continuous baseflow separation from time series of daily and monthly streamflow data. Water SA, 29, 1, 43–48. Water Research Commission.

Hughes, D. A., & Slaughter, A. R. (2016). Disaggregating the components of a monthly water resources system model to daily values for use with a water quality model. Environmental Modelling & Software, 80, 122–131. Elsevier.

Hughes, D. A., & Van Ginkel, C. (1994). Nutrient loads from developing urban areas, as simulation approach and identification of information requirements. Water SA, 20, 2, 139–150. Water Research Commission.

Hybinette, M., & Fujimoto, R. M. (2001). Cloning parallel simulations. ACM Transactions on Modelling and Computer Simulation (TOMACS), 11, 4, 378–407. ACM.

Idris, S., Yusuf, A., & Saini, G. (2016). Assessment of surface water quality using Qual2k software: A case study of River Yamuna, India. European Journal of Advances in Engineering and Technology, 3, 7, 16–23. SynchroMind Publishing.

Idris, S., Yusuf, A., & Saini, G. (2016). Assessment of surface water quality using Qual2k software: A case study of River Yamuna, India. European Journal of Advances in Engineering and Technology, 3, 7, 16–23. EJAET.

Ilich, N. (2009). Limitations of network flow algorithms in river basin modelling. Journal of Water Resources Planning and Management, 135, 1, 48-55. American Society of Civil Engineers.

Issaka, S., & Ashraf, M. A. (2017). Impact of soil erosion and degradation on water quality: A review. Geology, Ecology, and Landscapes, 1, 1, 1–11. Taylor & Francis. https://doi.org/10.1080/24749508.2017.1301053

Jacobs, U. (2007). Appendix 24.5–SIMCAT Modelling Assessment of the Operational Phase of the AWPR affecting the River Dee and its Tributaries. Aberdeen Western Peripheral Route, Environmental Statement Appendices. Transport Scotland.

Jain, M. K., & Das, A. (2017). Impact of mine waste leachates on aquatic environment: A review. Current Pollution Reports, 3, 31–37. Springer. https://doi.org/10.1007/s40726-017-0050-z

Jang, D. (2021). Analysis of the Water Quality Improvement in Urban Stream Using MIKE 21 FM. Applied Sciences, 11, 19, 8890. MDPI.

Janus, T., Tomlinson, J., Anghileri, D., Sheffield, J., Kollet, S., & Harou, J. J. (2023). Multicriteria land cover design via coupled hydrologic and multi-sector water management models. Journal of Hydrology, 620, 129294. Elsevier. https://doi.org/10.1016/j.jhydrol.2023.129294

Jha, M. K., & Gupta, A. D. (2003). Application of Mike Basin for water management strategies in a watershed. Water International, 28, 1, 27–35. Taylor & Francis. https://doi.org/10.1080/02508060308691662

Jordan, T. E., Correll, D. L., & Weller, D. E. (1997). Relating nutrient discharges from watersheds to land-use and streamflow variability. Water Resources Research, 33, 11, 2579–2590. American Geophysical Union.

Juizo, D., & Lidén, R. (2010). Modeling for transboundary water resources planning and allocation: The case of Southern Africa. Hydrology and Earth System Sciences, 14, 11, 2343–2354. Copernicus Publications. https://doi.org/10.5194/hess-14-2343-2010

Juízo, D., & Líden, R. (2008). Modeling for transboundary water resources planning and allocation. Hydrology and Earth System Sciences Discussions, 5, 1, 475–509. Copernicus Publications.

Kändler, M., Blechinger, K., Seidler, C., Pavlů, V., Šanda, M., Dostál, T., Krása, J., Vitvar, T., & Štich, M. (2017). Impact of land-use on water quality in the upper Nisa catchment in the Czech Republic and in Germany. Science of the Total Environment, 586, 1316–1325. Elsevier. https://doi.org/10.1016/j.scitotenv.2016.10.221

Kapangaziwiri, E., Hughes, D. A., Tanner, J., & Slaughter, A. (2011). Resolving uncertainties in the source of low flows in South African rivers using conceptual and modelling studies. IAHS-AISH Publication, 345, 127–132. IAHS Press.

Khan, M. N., & Mohammad, F. (2014). Eutrophication: Challenges and solutions. Eutrophication: Causes, Consequences and Control: Volume 2, 1–15. Springer.

Kolpin, D. W., Furlong, E. T., Meyer, M. T., Thurman, E. M., Zaugg, S. D., Barber, L. B., & Buxton, H. T. (2002). Pharmaceuticals, hormones, and other organic wastewater contaminants in US streams, 1999−2000: A national reconnaissance. Environmental Science & Technology, 36, 6, 1202–1211. American Chemical Society.

Krause, S., Jacobs, J., Voss, A., Bronstert, A., & Zehe, E. (2008). Assessing the impact of changes in land-use and management practices on the diffuse pollution and retention of nitrate in a riparian floodplain. Science of the Total Environment, 389, 1, 149–164. Elsevier.

Krysanova, V., Müller-Wohlfeil, D. I., & Becker, A. (1998). Development and test of a spatially distributed hydrological/water quality model for mesoscale watersheds. Ecological Modelling, 106, 2-3, 261–289. Elsevier. https://doi.org/10.1016/S0304-3800(97)00204-4

Kumar, P. (2019). Numerical quantification of current status quo and future prediction of water quality in eight Asian megacities: Challenges and opportunities for sustainable water management. Environmental Monitoring and Assessment, 191, 1–12. Springer. https://doi.org/10.1007/s10661-019-7497-x

Kusangaya, S., Warburton, M. L., Van Garderen, E. A., & Jewitt, G. P. (2014). Impacts of climate change on water resources in southern Africa: A review. Physics and Chemistry of the Earth, Parts A/B/C, 67, 47–54. Elsevier . https://doi.org/10.1016/j.pce.2013.09.014

Kut, K. M. K., Sarswat, A., Srivastava, A., Pittman Jr, C. U., & Mohan, D. (2016). A review of fluoride in African groundwater and local remediation methods. Groundwater for Sustainable Development, 2, 190–212. Elsevier.

Labadie, J. W. (2003). MODSIM River Basin Network Flow Model. Colorado State University.

Leavesley, G. H. (1994). Modeling the effects of climate change on water resources-a review. Climatic Change, 28, 1–2, 159–177. Springer. https://doi.org/10.1007/BF01094105

Lee, S. W., Hwang, S. J., Lee, S. B., Hwang, H. S., & Sung, H. C. (2009). Landscape ecological approach to the relationships of land-use patterns in watersheds to water quality characteristics. Landscape and Urban Planning, 92, 2, 80–89. Elsevier.

Lerotholi, S., Palmer, C. G., & Rowntree, K. (2004, May). Bioassessment of a river in a semiarid, agricultural catchment, Eastern Cape. Proceedings of the 2004 Water Institute of Southern Africa (WISA) Biennial Conference, Cape Town, South Africa, 338–344. WISA.

Lima Neto, I. E. (2023). Modelling water quality in a tropical reservoir using CE-QUAL-W2: Handling data scarcity, urban pollution, and hydroclimatic seasonality. Brazilian Journal of Water Resources, 28, e8. Associação Brasileira de Recursos Hídricos.

Lintern, A., Webb, J. A., Ryu, D., Liu, S., Bende-Michl, U., Waters, D., Leahy, P., Wilson, P., & Western, A. W. (2018). Key factors influencing differences in stream water quality across space. Wiley Interdisciplinary Reviews: Water, 5, 1, e1260. Wiley.

Liu, L. (2018). Application of a hydrodynamic and water quality model for inland surface water systems. Applications in Water Systems Management and Modeling, 10, 58–66. Elsevier.

Liu, R., Wang, J., Shi, J., Chen, Y., Sun, C., Zhang, P., & Shen, Z. (2014). Runoff characteristics and nutrient loss mechanism from plain farmland under simulated rainfall conditions. Science of the Total Environment, 468, 1069–1077. Elsevier.

Liu, W., Liu, S., Tang, C., Qin, W., Pan, H., & Zhang, J. (2020). Evaluation of surface water quality after mine closure in the coal-mining region of Guizhou, China. Environmental Earth Sciences, 79, 1–15. Springer. https://doi.org/10.1007/s12665-020-09167-0

Lloyd, C. E. M., Johnes, P. J., Freer, J. E., Carswell, A. M., Jones, J. I., Stirling, M. W., Hodgkinson, R. A., Richmond, C., & Collins, A. L. (2019). Determining the sources of nutrient flux to water in headwater catchments: Examining the speciation balance to inform the targeting of mitigation measures. Science of the Total Environment, 648, 1179–1200. Elsevier. https://doi.org/10.1016/j.scitotenv.2018.08.190

Loucks, D. P., Stedinger, J. R., & Haith, D. A. (1981). Water Resource Systems Planning and Analysis: Solutions Manual. Prentice-Hall.

Loucks, D. P., & Van Beek, E. (2017). Water Resource Systems Planning and Management: An Introduction to Methods, Models, and Applications. Springer.

Lu, Y., Wang, C., Yang, R., Sun, M., Zhang, L., Zhang, Y., & Li, X. (2023). Research on the progress of agricultural non-point source pollution management in China: A review. Sustainability, 15, 18, 13308. MDPI.

Ludwig, W., Dumont, E., Meybeck, M., & Heussner, S. (2009). River discharges of water and nutrients to the Mediterranean and Black Sea: Major drivers for ecosystem changes during past and future decades? Progress in Oceanography, 80, 3–4, 199–217. Elsevier.

Lynch, S. D. (2004). Development of a raster database of annual, monthly, and daily rainfall for Southern Africa. Water Research Commission Report No. 1156/1/03. Water Research Commission. http://www.wrc.org.za/knowledge%20hub%20documents/researchstudy%20reports/1156-1-04.pdf

Maass, A., Hufschmidt, M. M., Dorfman, R., Thomas, Jr, H. A., Marglin, S. A., & Fair, G. M. (1962). Design of Water-Resource Systems: New Techniques for Relating Economic Objectives, Engineering Analysis, and Governmental Planning. Harvard University Press.

Maass, L. F. (2017). Comparison of Stochastic Streamflow Generators and the Use Thereof within the Water Resources Yield Model and MIKE Hydro Basin (Doctoral dissertation). Stellenbosch University.

Maeda, E. E., Haapasaari, P., Helle, I., Lehikoinen, A., Voinov, A., & Kuikka, S. (2021). Black boxes and the role of modelling in environmental policy making. Frontiers in Environmental Science, 9, 629336. Frontiers.

Maest, A., Prucha, R., & Wobus, C. (2020). Hydrologic and water quality modeling of the Pebble Mine project pit lake and downstream environment after mine closure. Minerals, 10, 8, 727. https://doi.org/10.3390/min10080727 MDPI.

Makanda, K., Nzama, S., & Kanyerere, T. (2022). Assessing the role of water resources protection practice for sustainable water resources management: A review. Water, 14, 19, 3153. MDPI . https://doi.org/10.3390/w14193153

Mallory, S. J. L., Odendaal, P., & Desai, A. (2011). The Water Resources Modelling Platform User's Guide v3.3. Water Resources Consulting.

Mantel, S., & Slaughter, A. (2014). Chapter 8. Current monitoring network. Informing the Responses of Water Service Delivery Institutions to Climate and Development Changes: A Case Study in the Amatole Region, Eastern Cape, 60–77. Water Research Commission.

Mare, H. (2007). Orange River Integrated Water Resources Management Plan. Botswana Department of Water Affairs.

McGrane, S. J. (2016). Impacts of urbanisation on hydrological and water quality dynamics, and urban water management: A review. Hydrological Sciences Journal, 61, 13, 2295–2311. Taylor & Francis. https://doi.org/10.1080/02626667.2015.1128084

McLeod, A. I. (2005). Kendall rank correlation and Mann-Kendall trend test. R Package Kendall, 602, 1–10. The R Foundation.

Megdal, S. B., Eden, S., & Shamir, E. (2017). Water governance, stakeholder engagement, and sustainable water resources management. Water, 9, 3, 190. MDPI.

Miller, J. D., & Hutchins, M. (2017). The impacts of urbanisation and climate change on urban flooding and urban water quality: A review of the evidence concerning the United Kingdom.

Journal of Hydrology: Regional Studies, 12, 345–362. Elsevier. https://doi.org/10.1016/j.ejrh.2017.06.006

Mishra, A., Alnahit, A., & Campbell, B. (2021). Impact of land-uses, drought, flood, wildfire, and cascading events on water quality and microbial communities: A review and analysis. Journal of Hydrology, 596, 125707. Elsevier. https://doi.org/10.1016/j.jhydrol.2020.125707

Mitchell, B., Bellette, K., & Richardson, S. (2015). 'Integrated' approaches to water and natural resources management in South Australia. International Journal of Water Resources Development, 31, 4, 718–731. Taylor & Francis.

Molobela, I. P., & Sinha, P. (2011). Management of water resources in South Africa: A review. African Journal of Environmental Science and Technology, 5, 12, 993–1002. Academic Journals.

Momoh, J. A., El-Hawary, M. E., & Adapa, R. (1999). A review of selected optimal power flow literature to 1993. II. Newton, linear programming and interior point methods. IEEE Transactions on Power Systems, 14, 1, 105–111. IEEE.

Moriasi, D. N., Wilson, B. N., Douglas-Mankin, K. R., Arnold, J. G., & Gowda, P. H. (2012). Hydrologic and water quality models: Use, calibration, and validation. Transactions of the ASABE, 55, 4, 1241–1247. American Society of Agricultural and Biological Engineers.

Motaung, S., Maree, J., De Beer, M., Bologo, L., Theron, D., & Baloyi, J. (2008). Recovery of drinking water and by-products from gold mine effluents. International Journal of Water Resources Development, 24, 3, 433–450. Taylor & Francis.

Mothetho, M. (2018). Assessment of Local Water Distribution Infrastructure Management and Maintenance Challenges (Master's thesis). University of Cape Town.

Mouri, G., Takizawa, S., & Oki, T. (2011). Spatial and temporal variation in nutrient parameters in stream water in a rural-urban catchment, Shikoku, Japan: Effects of land cover and human impact. Journal of Environmental Management, 92, 7, 1837–1848. Elsevier.

Moyen-Orient, B. R., & du Nord, A. (2007). République tunisienne évaluation du coût de la dégradation de l'eau. World Bank Report No. 38856-TN. World Bank.

Mulopo, J. (2015). Continuous pilot scale assessment of the alkaline barium calcium desalination process for acid mine drainage treatment. Journal of Environmental Chemical Engineering, 3, 2, 1295–1302. Elsevier. https://doi.org/10.1016/j.jece.2014.12.001

Munawer, M. E. (2018). Human health and environmental impacts of coal combustion and post-combustion wastes. Journal of Sustainable Mining, 17, 2, 87–96. Elsevier.

Munishi, L. K., & Ndakidemi, P. A. (2022). Increasing agricultural soil phosphate (P) status influences water P levels in paddy farming areas: Their implication on environmental quality. Case Studies in Chemical and Environmental Engineering, 6, 100259. Elsevier. https://doi.org/10.1016/j.cscee.2022.100259

Nabinejad, S., Jamshid Mousavi, S., & Kim, J. H. (2017). Sustainable basin-scale water allocation with hydrologic state-dependent multi-reservoir operation rules. Water Resources Management, 31, 3507–3526. Springer.

Nagelkerke, N. J. (1991). A note on a general definition of the coefficient of determination. Biometrika, 78, 3, 691–692. Biometrika Trust.

Naidoo, S. (2017). Acid mine drainage in South Africa [electronic resource]: Development actors, policy impacts, and broader implications. Springer. https://doi.org/10.1007/978-3-319-44435-2

Nash, J. E., & Sutcliffe, J. V. (1970). River flow forecasting through conceptual models, Part I – A discussion of principles. Journal of Hydrology, 10, 3, 282–290. Elsevier.

Nazari-Sharabian, M., Ahmad, S., & Karakouzian, M. (2018). Climate change and eutrophication: A short review. Engineering, Technology and Applied Science Research, 8, 6, 3668–3672. Engineering, Technology & Applied Science Research.

Ncube, S. (2014). An assessment of the contribution of agricultural non-point source pollution on the water quality of the Vaal River within the Grootdraai Dam Catchment (Master's thesis). University of South Africa. https://uir.unisa.ac.za/handle/10500/18199

Ndaguba, E., & Marais, L. (2023). A scientometric analysis of mine closure research. Environment, Development and Sustainability, 1–17. Springer. https://doi.org/10.1007/s10668-023-03785-x

Neubert, S. (1993). Model construction in MIKE (Model Based and Incremental Knowledge Engineering). International Conference on Knowledge Engineering and Knowledge Management, 200–219. Springer.

Neumann, L., Western, A., & Argent, R. (2007). To split or lump? Influence of spatial representation in flow and water quality response simulation. Proceedings of the International Congress on Modelling and Simulation, 2368–2374. Modelling and Simulation Society of Australia and New Zealand.

Ngcobo, S. I. (2013). Projected impacts of climate change on water quality constituents and implications for adaptive management (Master's thesis). University of KwaZulu-Natal.

Ngubane, Z., Bergion, V., Dzwairo, B., Troell, K., Amoah, I. D., Stenström, T. A., & Sokolova, E. (2022). Water quality modelling and quantitative microbial risk assessment for uMsunduzi River in South Africa. Journal of Water and Health, 20, 4, 641–656. IWA Publishing.

Nie, J., Feng, H., Witherell, B. B., Alebus, M., Mahajan, M. D., Zhang, W., & Yu, L. (2018). Causes, assessment, and treatment of nutrient (N and P) pollution in rivers, estuaries, and coastal waters. Current Pollution Reports, 4, 154–161. Springer.

Niyogi, D. K., Simon, K. S., & Townsend, C. R. (2003). Breakdown of tussock grass in streams along a gradient of agricultural development in New Zealand. Freshwater Biology, 48, 9, 1698–1708. Wiley.

Nkomo, S., & van der Zaag, P. (2004). Equitable water allocation in a heavily committed international catchment area: The case of the Komati Catchment. Physics and Chemistry of the Earth, Parts A/B/C, 29, 15-18, 1309–1317. Elsevier. https://doi.org/10.1016/j.pce.2004.09.022

Nkwonta, O. I., Dzwairo, B., Otieno, F. A. O., & Adeyemo, J. A. (2017). A review on water resources yield model. South African Journal of Chemical Engineering, 23, 1, 107–115. Elsevier. https://doi.org/10.1016/j.sajce.2017.04.002

Ntshalintshali, P. (2019). Nutrient loading in the Vaal River over the past two decades (Master's thesis). Faculty of Science, Department of Environmental and Geographical Science. University of Cape Town. http://hdl.handle.net/11427/30950

O'Brien, P. C., & Fleming, T. R. (1987). A paired Prentice-Wilcoxon test for censored paired data. Biometrics, 43, 1, 169–180. Wiley.

Ochieng, G. M., Seanego, E. S., & Nkwonta, O. I. (2010). Impacts of mining on water resources in South Africa: A review. Scientific Research and Essays, 5, 22, 3351–3357. Academic Journals.

Odume, O. N. (2011). Application of macroinvertebrate-based biomonitoring approaches to assess anthropogenic impacts in the Swartkops River, South Africa (Master's thesis). Rhodes University.

Odume, O. N. (2014). An evaluation of macroinvertebrate-based biomonitoring and ecotoxicological assessments of deteriorating environmental water quality in the Swartkops River, South Africa (Doctoral dissertation). Rhodes University.

Odume, O. N. (2017). Ecosystem approach to managing water quality. Water Quality, 13–34. IntechOpen.

Odume, O. N. (2020). Searching for urban pollution signature and sensitive macroinvertebrate traits and ecological preferences in a river in the Eastern Cape of South Africa. Ecological Indicators, 108, 105759. Elsevier.

Odume, O. N., & Muller, W. J. (2011). Diversity and structure of Chironomidae communities in relation to water quality differences in the Swartkops River. Physics and Chemistry of the Earth, Parts A/B/C, 36, 14-15, 929–938. Elsevier.

Okereafor, U., Makhatha, M., Mekuto, L., Uche-Okereafor, N., Sebola, T., & Mavumengwana, V. (2020). Toxic metal implications on agricultural soils, plants, animals, aquatic life, and human health. International Journal of Environmental Research and Public Health, 17, 7, 2204. MDPI.

Oliveira, B., Bola, J., Quinteiro, P., Nadais, H., & Arroja, L. (2012). Application of Qual2Kw model as a tool for water quality management: Cértima River as a case study. Environmental Monitoring and Assessment, 184, 6197–6210. Springer.

Olowe, K. O., & Kumarasamy, M. V. (2018). Assessment of some existing water quality models. Nature Environment & Pollution Technology, 17, 3, 1023–1033. Technoscience Publications.

Ovalle, A. R. C., Silva, C. F., Rezende, C. D., Gatts, C. E. N., Suzuki, M. S., & Figueiredo, R. O. (2013). Long-term trends in hydrochemistry in the Paraíba do Sul River, southeastern Brazil. Journal of Hydrology, 481, 191–203. Elsevier. https://doi.org/10.1016/j.jhydrol.2012.12.036

Pal, M., Roy, M. B., & Roy, P. K. (2020). Effect of water turbidity on the seasonal variation of modeled mixed layer depth—A case study of Dumboor Reservoir, Tripura. Journal of Scientific Research, 64, 2, 98–110. Institute of Science, Banaras Hindu University, Varanasi, India.

Palma, V. G. J. (2021). Adaptation to climate change in basins within the context of water-energy-food nexus (Master's thesis). Pontificia Universidad Católica de Chile.

Palmer, W. C. (1965). Meteorological drought, 30. U.S. Department of Commerce, Weather Bureau.

Paredes, J., & Lund, J. R. (2006). Refill and drawdown rules for parallel reservoirs: Quantity and quality. Water Resources Management, 20, 359–376. Springer.

Paredes-Arquiola, J., Andreu-Álvarez, J., Martín-Monerris, M., & Solera, A. (2010). Water quantity and quality models applied to the Jucar River Basin, Spain. Water Resources Management, 24, 2759–2779. Springer.

Paul, M. J., & Meyer, J. L. (2001). Streams in the urban landscape. Annual Review of Ecology and Systematics, 32, 1, 333–365. Annual Reviews. https://doi.org/10.1146/annurev.ecolsys.32.081501.114040

Payen, S., Cosme, N., & Elliott, A. H. (2021). Freshwater eutrophication: Spatially explicit fate factors for nitrogen and phosphorus emissions at the global scale. The International Journal of Life Cycle Assessment, 26, 388–401. Springer.

Presidential Climate Commission (PCC). (2021). South Africa's NCD targets for 2025 and 2030, Issue 2. Presidential Climate Commission. https://pccommissionflow.imgix.net/uploads/images/1eb85a_75d745eb859d43c288f461810b336dd3-compressed.pdf

Pereira, P. (2020). Ecosystem services in a changing environment. The Science of the Total Environment, 702, 135008. Elsevier.

Perera, B. J. C., James, B., & Kularathna, M. D. U. (2005). Computer software tool REALM for sustainable water allocation and management. Journal of Environmental Management, 77, 4, 291–300. Elsevier. https://doi.org/10.1016/j.jenvman.2005.06.014

Pinho, J., Sobral, J. L., & Rocha, M. (2013). Parallel evolutionary computation in bioinformatics applications. Computer Methods and Programs in Biomedicine, 110, 2, 183–191. Elsevier. https://doi.org/10.1016/j.cmpb.2012.10.001

Pitman, W. V. (1973). A mathematical model for generating monthly river flows from meteorological data in South Africa. Department of Civil Engineering. University of the Witwatersrand. https://doi.org/LK-https://worldcat.org/title/24136837

Pitman, W. V. (2011). Overview of water resource assessment in South Africa: Current state and future challenges. Water SA, 37,5, 659–664. Water Research Commission.

Pitman, W., Bailey, A., & Beater, A. (2002). Report No: P08000/00/0301 Department of Water Affairs and Forestry: Water resources planning upper Vaal water management area water resources situation assessment main report final: July 2002 compiled by: Sterkfontein Dam outlet with Crump weir Vaal dam. Department of Water Affairs and Forestry.

Pitt, R. (1979). Demonstration of nonpoint pollution abatement through improved street cleaning practices, 1. Environmental Protection Agency, Office of Research and Development, Municipal Environmental Research Laboratory.

Pörtner, H.-O., Scholes, R. J., Agard, J., Archer, E., Arneth, A., Bai, X., Barnes, D., Burrows, M., Chan, L., & Cheung, W. L. (2021). IPBES-IPCC co-sponsored workshop report on biodiversity and climate change. Wageningen University & Research.

Posner, S., Verutes, G., Koh, I., Denu, D., & Ricketts, T. (2016). Global use of ecosystem service models. Ecosystem Services, 17, 131–141. Elsevier.

Potrykus, D., Lidzbarski, M., & Tarnawska, E. (2022). Hydrogeohazards in post-mining areas: The phenomenon of uncontrolled groundwater outflows in wetlands. Geological Quarterly, 66, 3, 1–14. Polish Geological Institute National Research Institute.

Purwanto, A., Sušnik, J., Suryadi, F. X., & de Fraiture, C. (2021). Water-energy-food nexus: Critical review, practical applications, and prospects for future research. Sustainability, 13, 4, 1919. MDPI.

Qi, C., & Grunwald, S. (2005). GIS-based hydrologic modeling in the Sandusky watershed using SWAT. Transactions of the ASAE, 48, 1, 169–180. American Society of Agricultural and Biological Engineers.

Qi, J., Li, S., Li, Q., Xing, Z., Bourque, C. P. A., & Meng, F. R. (2016). A new soil-temperature module for SWAT application in regions with seasonal snow cover. Journal of Hydrology, 538, 863–877. Elsevier.

Quayle, L. M., Dickens, C. W. S., Graham, M., Simpson, D., Goliger, A., Dickens, J. K., Freese, S., & Blignaut, J. (2010). Investigation of the positive and negative consequences associated with the introduction of zero-phosphate detergents into South Africa. WRC Report No. TT 446(10). Water Research Commission.

Rafiee, M., Akhond Ali, A. M., Moazed, H., Lyon, S. W., Jaafarzadeh, N., & Zahraie, B. (2014). A case study of water quality modeling of the Gargar River, Iran. Journal of Hydraulic Structures, 1, 2, 10–22. Bu-Ali Sina University.

Raju, K. S., & Pillai, C. R. S. (1999). Multicriterion decision making in river basin planning and development. European Journal of Operational Research, 112, 2, 249–257. Elsevier.

Rand Water. (2022). Water quality guidelines for the Grootdraai Dam Catchment. Retrieved from https://www.reservoir.co.za/viewtopic.php?t=38

Ricalde, I., Vicuña, S., Melo, O., Tomlinson, J. E., Harou, J. J., & Characklis, G. (2022). Assessing trade-offs in the design of climate change adaptation strategies for water utilities in Chile. Journal of Environmental Management, 302, 114035. Elsevier. https://doi.org/10.1016/j.jenvman.2021.114035

Rizzo, L., Dondio, P., Delany, S. J., & Longo, L. (2016). Modelling mental workload via rule-based expert system: A comparison with NASA-TLX and Workload Profile. Artificial Intelligence Applications and Innovations. AIAI 2016. IFIP Advances in Information and Communication Technology, 475, 179–191. Springer. https://doi.org/10.1007/978-3-319-44944-9_19

Roberts, M. (2003). Simple tools to estimate impacts of development on water quantity, water quality, and riparian processes. Georgia Basin/Puget Sound Research Conference, Vancouver, BC, Mar. https://api.semanticscholar.org/CorpusID:209480055

Rode, M., Arhonditsis, G., Balin, D., Kebede, T., Krysanova, V., Van Griensven, A., & Van der Zee, S. E. (2010). New challenges in integrated water quality modelling. Hydrological Processes, 24, 24, 3447–3461. Wiley. https://doi.org/10.1002/hyp.7766

Rothenberger, M. B., Burkholder, J. M., & Brownie, C. (2009). Long-term effects of changing land-use practices on surface water quality in a coastal river and lagoonal estuary. Environmental Management, 44, 505–523. Springer. https://doi.org/10.1007/s00267-009-9330-8

Rudra, R. P., Mekonnen, B. A., Shukla, R., Shrestha, N. K., Goel, P. K., Daggupati, P., & Biswas, A. (2020). Current status, challenges, and future directions in identifying critical source areas for non-point source pollution in Canadian conditions. Agriculture, 10, 10, 468. MDPI. https://doi.org/10.3390/agriculture10100468

Ruiters, C., & Matji, M. P. (2015). Water institutions and governance models for the funding, financing, and management of water infrastructure in South Africa. Water SA, 41, 5, 660–676. Water Research Commission.

Rusere, F., Hunter, L., Collinson, M., & Twine, W. (2023). Nexus between summer climate variability and household food security in rural Mpumalanga Province, South Africa. Environmental Development, 47, 100892. Elsevier. https://doi.org/10.1016/j.envdev.2023.100892

Sadeghi, A., Galalizadeh, S., Zehtabian, G., & Khosravi, H. (2021). Assessing the change of groundwater quality compared with land-use change and precipitation rate (Zrebar Lake's Basin). Applied Water Science, 11, 1–15. Springer. https://doi.org/10.1007/s13201-021-01508-z

Salimi, S., Almuktar, S. A., & Scholz, M. (2021). Impact of climate change on wetland ecosystems: A critical review of experimental wetlands. Journal of Environmental Management, 286, 112160. Elsevier. https://doi.org/10.1016/j.jenvman.2021.112160

Savenije, H. H., & Van der Zaag, P. (2008). Integrated water resources management: Concepts and issues. Physics and Chemistry of the Earth, Parts A/B/C, 33, 5, 290–297. Elsevier. https://doi.org/10.1016/j.pce.2008.02.003

Schulze, R. E. (2010). Atlas of climate change and the South African agricultural sector: A 2010 perspective. Department of Agriculture, Forestry and Fisheries.

Schoeman, J. J., & Steyn, A. (2003). Nitrate removal with reverse osmosis in a rural area in South Africa. Desalination, 155, 1, 15–26. Elsevier. https://doi.org/10.1016/S0011-9164(03)00235-2

Seong, C., Her, Y., & Benham, B. L. (2015). Automatic calibration tool for hydrologic simulation program-FORTRAN using a shuffled complex evolution algorithm. Water, 7, 2, 503–527. MDPI . https://doi.org/10.3390/W7020503

Shen, Z., Liao, Q., Hong, Q., & Gong, Y. (2012). An overview of research on agricultural non-point source pollution modelling in China. Separation and Purification Technology, 84, 104–111. Elsevier. https://doi.org/10.1016/j.seppur.2011.01.018

Shrestha, B. P., Duckstein, L., & Stakhiv, E. Z. (1996). Fuzzy rule-based modeling of reservoir operation. Journal of Water Resources Planning and Management, 122, 4, 262–269. American Society of Civil Engineers.

Sieber, J., & Purkey, D. (2007). Water evaluation and planning system user guide for WEAP21. Stockholm Environment Institute, U.S. Center.

Sigalla, O. Z., Tumbo, M., & Joseph, J. (2021). Multi-stakeholder platform in water resources management: A critical analysis of stakeholders' participation for sustainable water resources. Sustainability, 13, 16, 9260. MDPI.

Singh, J., Knapp, H. V., Arnold, J. G., & Demissie, M. (2005). Hydrological modeling of the Iroquois River watershed using HSPF and SWAT 1. Journal of the American Water Resources Association, 41, 2, 343–360. Wiley.

Slaughter, A., Gwapedza, D., Mantel, S., Hughes, D., & Griffin, N. (2018). Extending functionality and knowledge transfer of the Water Quality Systems Assessment Model. Water Research Commission (WRC), Report No 2448/1/18. https://www.wrc.org.za/wp-content/uploads/mdocs/2448_final.pdf

Slaughter, A. R., Hughes, D. A., & Mantel, S. K. (2012). The development of a water quality systems assessment model (WQSAM) and its application to the Buffalo River catchment, Eastern Cape, South Africa. International Congress on Environmental Modelling and Software. International Environmental Modelling and Software Society. https://scholarsarchive.byu.edu/iemssconference/2012/Stream-B/198

Slaughter, A. R., & Mantel, S. K. (2018). Water quality modelling of an impacted semi-arid catchment using flow data from the WEAP model. Proceedings of the International Association of Hydrological Sciences, 377, 25–33. Copernicus Publications. https://doi.org/10.5194/PIAHS-377-25-2018

Slaughter, A. R., & Hughes, D. A. (2013). A simple model to separately simulate point and diffuse nutrient signatures in stream flows. Hydrology Research, 44, 3, 538–553. IWA Publishing.

Slaughter, A. R., Hughes, D. A., Retief, D. C. H., & Mantel, S. K. (2017). A management-oriented water quality model for data scarce catchments. Environmental Modelling & Software, 97, 93–111. Elsevier.

Slaughter, A. R., & Mantel, S. K. (2013). A simple and rapid method to relate land cover and river flow rate to river nutrient concentration. Physics and Chemistry of the Earth, Parts A/B/C, 66, 131–138. Elsevier. https://doi.org/10.1016/j.pce.2013.08.001

Slaughter, A. R., & Mantel, S. K. (2017). Land cover models to predict non-point nutrient inputs for selected biomes in South Africa. Water SA, 43, 3, 499–508. Water Research Commission. https://doi.org/10.4314/wsa.v43i3.15

Slaughter, A. R., Mantel, S. K., & Hughes, D. A. (2014). Investigating possible climate change and development effects on water quality within an arid catchment in South Africa: A comparison of two models. International Congress on Environmental Modelling and Software. International Environmental Modelling and Software Society. https://scholarsarchive.byu.edu/iemssconference/2014/Stream-H/13

Slaughter, A. R., Retief, D. C. H., & Hughes, D. A. (2015). A method to disaggregate monthly flows to daily using daily rainfall observations: Model design and testing. Hydrological Sciences Journal, 60, 11, 1896–1910. Taylor & Francis. https://doi.org/10.1080/02626667.2014.993987

Sliva, L., & Williams, D. D. (2001). Buffer zone versus whole catchment approaches to studying land-use impact on river water quality. Water Research, 35, 14, 3462–3472. Elsevier. https://doi.org/10.1016/S0043-1354(01)00062-8

Soceanu, A., Dobrinas, S., Birghila, S., Popescu, V., & Magearu, V. (2009). Levels of phosphorus in citrus fruits. Ovidius University Annals of Chemistry, 20, 87–90. Ovidius University Press.

Soleimanian, E., Afshar, A., & Molajou, A. (2022). A review on water simulation models for the WEF Nexus: Development perspective. Environmental Science and Pollution Research, 29, 53, 79769–79785. Springer. https://doi.org/10.1007/s11356-022-19849-w

Song, X., Zhang, Y., & Yu, Z. (2021). An eco-environmental assessment of harmful algal bloom mitigation using modified clay. Harmful Algae, 107, 102067. Elsevier. https://doi.org/10.1016/j.hal.2021.102067

Stats SA. (2019). Sustainable Development Goals: Country report. Statistics South Africa. https://www.statssa.gov.za/MDG/SDGs_Country_Report_2019_South_Africa.pdf

Stone, T. (2009). Water supply: Thinking strategically: Water and sanitation. IMIESA, 34, 1, 46–54. Sabinet African Journals. https://journals.co.za/doi/epdf/10.10520/EJC44417

Su, C. (2014). A review on heavy metal contamination in the soil worldwide: Situation, impact and remediation techniques. Environmental Skeptics and Critics, 3, 2, 24–38. IAEES.

Sulis, A., & Sechi, G. M. (2013). Comparison of generic simulation models for water resource systems. Environmental Modelling & Software, 40, 214–225. Elsevier. https://doi.org/10.1016/j.envsoft.2012.09.012

Sun, Z., Zheng, Y., Li, X., Tian, Y., Han, F., Zhong, Y., Liu, J., & Zheng, C. (2018). The nexus of water, ecosystems, and agriculture in Endorheic River Basins: A system analysis based on integrated ecohydrological modeling. Water Resources Research, 54, 10, 7534–7556. Wiley.

Sutherland, A. B., Meyer, J. L., & Gardiner, E. P. (2002). Effects of land cover on sediment regime and fish assemblage structure in four southern Appalachian streams. Freshwater Biology, 47, 9, 1791–1805. Wiley.

Tempelhoff, J. W. (2009). Civil society and sanitation hydropolitics: A case study of South Africa's Vaal River Barrage. Physics and Chemistry of the Earth, Parts A/B/C, 34, 3, 164–175. Elsevier.

Thomann, R. V. (1998). The future "golden age" of predictive models for surface water quality and ecosystem management. Journal of Environmental Engineering, 124, 2, 94–103. American Society of Civil Engineers.

Thomas Jr, H. A. (1981). Improved methods for national water assessment, water resources contract: WR15249270. Harvard Water Resources Group.

Thornthwaite, C. W., & Mather, J. R. (1955). The Water Balance. Climatology, 8, 104. Drexel Institute of Technology—Laboratory of Climatology, Publications in Climatology, Centerton.

Ting, M. B., & Byrne, R. (2020). Eskom and the rise of renewables: Regime-resistance, crisis, and the strategy of incumbency in South Africa's electricity system. Energy Research & Social Science, 60, 101333. Elsevier. https://doi.org/10.1016/j.erss.2019.101333

Tomlinson, J. E., Arnott, J. H., & Harou, J. J. (2020). A water resource simulator in Python. Environmental Modelling & Software, 126, 104635. Elsevier. https://doi.org/10.1016/j.envsoft.2020.104635

Uddin, M. K. (2017). A review on the adsorption of heavy metals by clay minerals, with special focus on the past decade. Chemical Engineering Journal, 308, 438–462. Elsevier.

UNEP. (2009). Water sustainability of agribusiness activities in South Africa. UNEP Finance Initiative (Issue October). UNEP. https://www.unepfi.org/fileadmin/publications/water/chief_liquidity1_South_Africa.pdf

Utembe, W., Faustman, E. M., Matatiele, P., & Gulumian, M. (2015). Hazards identified and the need for health risk assessment in the South African mining industry. Human & Experimental Toxicology, 34, 12, 1212–1221. SAGE Publications. https://doi.org/10.1177/0960327115600370

van Ginkel, C. E. (2011). Eutrophication: Present reality and future challenges for South Africa. Water SA, 37, 5, 693–702. Water Research Commission.

Vaughan, W. J., & Russell, C. S. (1983). Monitoring point sources of pollution: Answers and more questions from statistical quality control. The American Statistician, 37, 4b, 476–487. Taylor & Francis.

7.1 Verdier, J., & Viollet, P. L. (2015). Les tensions sur l'eau en Europe et dans le bassin méditerranéen. Des crises de l'eau d'ici 2050. La Houille Blanche, 6, 102–107. la SHF.

Vicuña, S., Ricalde, I., Melo, O., Tomlinson, J., Harou, J. J., & Characklis, G. (2019). Climate change adaptation in regulated water utilities. Geophysical Research Abstracts, 21. European Geosciences Union.

Viljoen, G., & Van der Walt, K. (2018). Suid-Afrika se waterkrisis – 'n interdissiplinêre benadering. Tydskrif vir Geesteswetenskappe, 58, 3, 483–500. Academy of Science of South Africa. https://doi.org/10.17159/2224-7912/2018/v58n3a3

Villiers, S. D., & Thiart, C. (2007). The nutrient status of South African rivers: Concentrations, trends, and fluxes from the 1970s to 2005. South African Journal of Science, 103, 7–8, 343–349. Academy of Science of South Africa.

Votteler, R. G., & Brent, A. C. (2016). A literature review on the potential of renewable electricity sources for mining operations in South Africa. Journal of Energy in Southern Africa, 27, 2, 1–21. Energy Research Centre, University of Cape Town. https://www.scielo.org.za/pdf/jesa/v27n2/01.pdf

Wang, Q., Li, S., Jia, P., Qi, C., & Ding, F. (2013). A review of surface water quality models. The Scientific World Journal. Wiley. https://doi.org/10.1155/2013/231768

Wichelns, D. (2017). The water-energy-food nexus: Is the increasing attention warranted, from either a research or policy perspective? Environmental Science & Policy, 69, 113–123. Elsevier.

Wilby, R. L. (2005). Uncertainty in water resource model parameters used for climate change impact assessment. Hydrological Processes: An International Journal, 19, 16, 3201–3219. Wiley.

Williams, M. L., Palmer, C. G., & Gordon, A. K. (2003). South African riverine macroinvertebrate responses to chlorine and chlorinated sewage effluents: An overview. Proceedings of the 2004 Water Institute of Southern Africa (WISA) Biennial Conference, 2–6. WISA.

Wong, M. H. (2003). Ecological restoration of mine-degraded soils, with emphasis on metal-contaminated soils. Chemosphere, 50, 6, 775–780. Elsevier.

Wood, P. J., & Armitage, P. D. (1997). Biological effects of fine sediment in the lotic environment. Environmental Management, 21, 2, 203–217. Springer.

World Bank. (2023). Factsheet: Eskom Just Energy Transition Project in South Africa. World Bank. https://www.worldbank.org/en/news/factsheet/2023/06/05/factsheet-eskom-just-energy-transition-project-in-afe-south-africa

Wurbs, R. A. (1993). Reservoir-system simulation and optimization models. Journal of Water Resources Planning and Management, 119, 4, 455–472. American Society of Civil Engineers.

Xie, H., Dong, J., Shen, Z., Chen, L., Lai, X., Qiu, J., Wei, G., Peng, Y., & Chen, X. (2019). Intra- and inter-event characteristics and controlling factors of agricultural non-point source pollution under different types of rainfall-runoff events. Catena, 182, 104105. Elsevier. https://doi.org/10.1016/j.catena.2019.104105

Xu, C. Y., & Singh, V. P. (1998). A review on monthly water balance models for water resources investigations. Water Resources Management, 12, 20–50. Springer. https://doi.org/10.1023/A:1007916816469

Xu, C. Y., & Singh, V. P. (2004). Review on regional water resources assessment models under stationary and changing climate. Water Resources Management, 18, 591–612. Springer. https://doi.org/10.1007/s11269-004-9130-0

Xu, M. J., Yu, L., Zhao, Y. W., & Li, M. (2012). The simulation of shallow reservoir eutrophication based on MIKE21: A case study of Douhe Reservoir in North China. Procedia Environmental Sciences, 13, 1975–1988. Elsevier.

Xue, J., Wang, Q., & Zhang, M. (2022). A review of non-point source water pollution modeling for the urban–rural transitional areas of China: Research status and prospect. Science of the Total Environment, 826, 154146. Elsevier. https://doi.org/10.1016/j.scitotenv.2022.154146

Yan, Q., Cheng, T., Song, J., Zhou, J., Hung, C. C., & Cai, Z. (2021). Internal nutrient loading is a potential source of eutrophication in Shenzhen Bay, China. Ecological Indicators, 127, 107736. Elsevier.

Yang, B., Huang, K., Sun, D., & Zhang, Y. (2017). Mapping the scientific research on non-point source pollution: A bibliometric analysis. Environmental Science and Pollution Research, 24, 4352–4366. Springer.

Yates, D., Sieber, J., Purkey, D., & Huber-Lee, A. (2005). WEAP21 – A demand-, priority-, and preference-driven water planning model: Part 1: Model characteristics. Water International, 30, 4, 487–500. Taylor & Francis. https://doi.org/10.1080/02508060508691893

Zhang, H., & Huang, G. H. (2011). Assessment of non-point source pollution using a spatial multicriteria analysis approach. Ecological Modelling, 222, 2, 313–321. Elsevier. https://doi.org/10.1016/j.ecolmodel.2009.12.011

Zhao, R. J. (1992). The Xinanjiang model applied in China. Journal of Hydrology, 135, 1-4, 371-381. Department of Hydrology, Ho-hai University, China. CABI digital library www.cabidigitallibrary.org

Zhao, Y., Liu, Z., & Wu, J. (2020). Grassland ecosystem services: A systematic review of research advances and future directions. Landscape Ecology, 35, 793–814. Springer.

Zheng, W., Ke, X., Zhou, T., & Yang, B. (2019). Trade-offs between cropland quality and ecosystem services of marginal compensated cropland – A case study in Wuhan, China. Ecological Indicators, 105, 613–620. Elsevier.

Zhu, M., Zhu, G., Zhao, L., Yao, X., Zhang, Y., Gao, G., & Qin, B. (2013). Influence of algal bloom degradation on nutrient release at the sediment–water interface in Lake Taihu, China. Environmental Science and Pollution Research, 20, 1803–1811. Springer.

Ziervogel, G., New, M., Archer van Garderen, E., Midgley, G., Taylor, A., Hamann, R., Stuart-Hill, S., Myers, J., & Warburton, M. (2014). Climate change impacts and adaptation in South Africa. Wiley Interdisciplinary Reviews: Climate Change, 5, 5, 605–620. Wiley.

Zy Harifidy, R., Zy Misa Harivelo, R., Hiroshi, I., Jun, M., & Kazuyoshi, S. (2022). A systematic review of water resources assessment at a large river basin scale: Case of the major river basins in Madagascar. Sustainability, 14, 19, 12237. MDPI.

APPENDICES

Appendix A: Node attributes (i.e., inputs data) in the dynamic Pywr-WQ model.

Name	Type	Description
Daily flows	Time Series	Contains daily flows obtained from the Pywr model ($m^3.s^{-1}$).
Daily evaporation	Time Series	Contains daily evaporation obtained from the Pywr model ($m^3.d^{-1}$).
Daily inflows	Time Series	Daily flows into a node obtained from the Pywr model ($m^3.d^{-1}$).
Daily outflows	Time Series	Daily flows out of a node obtained from the Pywr model ($m^3.d^{-1}$).
Daily return flow	Time Series	Daily return flows obtained from the Pywr model ($m^3.d^{-1}$).
Daily storage	Time Series	Daily reservoir storage obtained from the Pywr model ($m^3.d^{-1}$).
Downstream node	Text	The downstream node is linked for routing water quality variables.
Monthly storage	Time Series	The volume (10^6 m^3) is held within nodes which are storage nodes (dummy dams and Grootdraai Dam). Each value represents the storage within a node at the beginning of a month.
Daily incremental flows	Time Series	Daily incremental flows obtained from the Pywr model ($m^3.d^{-1}$).
Node name	Text	Identifier for the nodes.
Quantity parameters	Array	Parameters required by Pywr-WQ to perform water quantity modelling such as baseflow separation.
Reservoir water quality parameters	Array	Water quality parameters for simulation of water quality in reservoirs.
Observed Ca	Time Series	Daily observed calcium concentrations for a particular node ($mg.l^{-1}$).
Observed Cl	Time Series	Daily observed chlorine concentrations for a particular node ($mg.l^{-1}$).
Observed F	Time Series	Daily observed fluorine concentrations for a particular node ($mg.\ l^{-1}$).
Observed K	Time Series	Daily observed potassium concentrations for a particular node ($mg.l^{-1}$).
Observed Mg	Time Series	Daily observed magnesium concentrations for a particular node ($mg.l^{-1}$).
Observed Na	Time Series	Daily observed sodium concentrations for a particular node ($mg.l^{-1}$).
Observed NH_4-N	Time Series	Daily observed ammonium concentrations for a particular node ($mg.\ l^{-1}$).
Observed NO_3-N+NO_2-N	Time Series	Daily observed nitrate concentrations for a particular node ($mg.\ l^{-1}$).
Observed PO_4-P	Time Series	Daily observed phosphate concentrations for a particular node ($mg.l^{-1}$).
Observed TDS	Time Series	Daily observed total dissolved solids concentrations for a particular node ($mg.l^{-1}$).

Name	Type	Description
Boundary condition Ca	Time Series	Daily boundary condition calcium concentrations for a particular node ($mg.l^{-1}$).
Boundary condition Cl	Time Series	Daily boundary condition chlorine concentrations for a particular node ($mg.l^{-1}$).
Boundary condition F	Time Series	Daily boundary condition fluorine concentrations for a particular node ($mg.l^{-1}$).
Boundary condition K	Time Series	Daily boundary condition potassium concentrations for a particular node ($mg.l^{-1}$).
Boundary condition Mg	Time Series	Daily boundary condition magnesium concentrations for a particular node ($mg.l^{-1}$).
Boundary condition Na	Time Series	Daily boundary condition sodium concentrations for a particular node ($mg.l^{-1}$).
Boundary condition NH_4-N	Time Series	Daily boundary condition ammonium concentrations for a particular node ($mg.l^{-1}$).
Boundary condition NO_3-N+NO_2-N	Time Series	Daily boundary condition nitrate concentrations for a particular node ($mg.l^{-1}$).
Boundary condition PO_4-P	Time Series	Daily boundary condition phosphate concentrations for a particular node ($mg.l^{-1}$).
Boundary condition SO_4	Time Series	Daily boundary condition sulphate concentrations for a particular node ($mg.l^{-1}$).
Boundary condition TDS	Time Series	Daily boundary condition salinity concentrations for a particular node ($mg.l^{-1}$).
Observed water temperature	Time Series	Daily observed water temperature for a particular node (°C).
Boundary condition NO_3-N+NO_2-N	Time Series	Daily boundary condition nitrate concentrations for a particular node ($mg.l^{-1}$).
Boundary condition PO_4-P	Time Series	Daily boundary condition phosphate concentrations for a particular node ($mg.l^{-1}$).
Boundary condition SO_4	Time Series	Daily boundary condition sulphate concentrations for a particular node ($mg.l^{-1}$).
Boundary condition TDS	Time Series	Daily boundary condition salinity concentrations for a particular node ($mg.l^{-1}$).
Observed water temperature	Time Series	Daily observed water temperature for a particular node (°C).

Appendix B: Assigning DWS station for different nodes located in the distributed structures within the Pywr-WQ model.

Model Node	Station ID	Sample
Link_4	1-1153	125
Inflow_1	VS1	201
Link_2	VS2	252
Inflow_2	177947	218
Inflow_5	1-1042	197
Link_7	C1H027	1067
Link_9	C1H007	2573
Inflow_8	177956	204
Link_17	C1H006	1947
Link_16	VS2-4	236
Grootdraai_Dam	C1R002	2893
Link_7	W5R003Q01	1067

Appendix C: Salts signatures for flow fractions (i.e., surface water, interflow, and groundwater flow) allocated through calibration exercise within the Pywr-WQ model.

Node	SO_4			Cl			F			K			Mg		
	SF_s	IF_s	GF_s	SF_s	IF_s	GF_s	SFs	IFs	GFs	SF_s	IF_s	GF_s	SF_s	IF_s	GF_s
Inflow 1	3	20	52	3	9	23	0	0.29	0.87	1	3.25	10.5	0	2.75	15
Inflow 2	3.5	20	1950	2.5	21	33.5	0.55	0.6	0.765	6.5	7	9	16	35	220
Inflow 3	1	5	37	0.3	9.6	17	0	0.17	4.25	0.2	2	50	3	5	19
Inflow 4	0.6	3	48	3	13.6	30	0	0.55	1.7	0.25	6.5	20	4	15	20
Inflow 5	1	4	180	0.15	1	82	0.2	0.7	1.45	4	8	18	2.5	9	19
Inflow 6	1.5	8	130	0.3	0.5	69	0	0.55	0.81	7	9	10	12	21	33
Inflow 7	8	11	18.66	0.5	1.5	2.5	0.12	0.33	0.89	1.1	2.1	3.45	4	5.3	8
Inflow 8	9	46.5	165	4	7.5	18	0.12	0.33	0.89	1.5	3.9	10.5	4	15	80
Inflow 9	1.8	10	180	0.4	1.5	59	0.015	0.3	0.5	1.1	2.1	3.45	2	9	13
Inflow 10	0.1	55	90	0.2	1	63	0	0.065	0.1525	0.4	4	7.5	10	20	49
Inflow 11	0.2	65	120	0.1	1	53	0	0.042	0.125	0.34	4	7.5	14	36	69

Appendix D: Salts signatures for flow fractions (i.e., surface water, interflow, and groundwater flow) allocated through calibration exercise within the Pywr-WQ model.

Node	Na			Ca		
	SF_s	**IF_s**	**GF_s**	**SF_s**	**IF_s**	**GF_s**
Inflow 1	6	11	35	7	11	37
Inflow 2	22	24	31	22	24	31
Inflow 3	5	7	176	0.1	8.5	177
Inflow 4	4	22	106	1	23	110
Inflow 5	7	28	63	8	29	64
Inflow 6	24	31	35	25	32	36
Inflow 7	4	7	12	4	7.5	13
Inflow 8	5	13	37	5.5	14	38
Inflow 9	1	10	30	8.5	24	46
Inflow 10	4.5	8	19	0	20	33
Inflow 11	5	11	22	0	23	36

Appendix E: Water quality guidelines for the Grootdraai Dam adopted in this study (Rand Water, 2022).

Variables	Measured as	Ideal catchment background	Acceptable management target	Tolerable interim target	Unacceptable
TDS	mg.l^{-1}	< 97.5	97.5 - 195	195 – 325	> 325
NH_4-N		< 0.02	0.02 – 0.5	0.5 – 1	> 1
NO_3-N + NO_2-N		< 0.05	0.05 – 0.25	0.25 – 0. 5	> 0.5
Cl		< 10	10 - 20	20 - 30	> 30
F		< 0.05	0.05 – 0.2	0.2 – 0.4	> 0.4
PO_4-P		< 0.05	0.05 – 0.25	0.25 – 0.5	> 0.5
SO_4		< 15	15 - 35	35 - 50	> 50

Appendix F: Ethical clearance letter.

RHODES UNIVERSITY
Where leaders learn

Rhodes University Human Research Ethics Committee
Main Admin Building, Drostdy Road, Makhanda, 6139, South Africa
PO Box 94, Makhanda, 6140, South Africa
t: +27 (0) 46 603 7314
e: ethics-committee@ru.ac.za
https://www.ru.ac.za/researchgateway/ethics/
NHREC Registration number: RC-241114-045

22 July 2024

Ms. Sofia Lazar
Institute for Water Research
Rhodes University

Dear Ms. Lazar,

Re: Water quality modeling within the Grootdraai Dam catchment located in Mpumalanga province.

The Rhodes University Human Research Ethics Committee (RU-HREC) has reviewed your request for ethics waiver. Your research involves analysis of open-source datasets and does not involve interaction with human participants. As such it does not require research ethics approval, and your request for ethics waiver has been approved.

Your request for an ethics clearance waiver for this study has been APPROVED.

Ethics Waiver Number: RUHREC-2024-0015

Sincerely,

Sincerely,

Janet Hayward

Dr Janet Hayward
Chair of Rhodes University Human Research Ethics Committee